Supporting Information for

Sterically shielded, stabilized nitrile imine for rapid bioorthogonal protein labeling in live cells

*Peng An,[†] Tracey M. Lewandowski,[†] Tuğçe G. Erbay,[‡] Peng Liu[‡,] and Qing Lin[†,]**

[†]Department of Chemistry, State University of New York at Buffalo, Buffalo, New York 14260-3000, United States [‡]Department of Chemistry, University of Pittsburgh, Pittsburgh, Pennsylvania 15260, United States

Table of Contents

Supplemental Figures and Tables

Table S1. Product distribution after photoirradiating the substituted tetrazoles in the presence of equal molar ratio of acrylamide and glutathione in phosphate buffer/acetonitrile (1:1) [a]

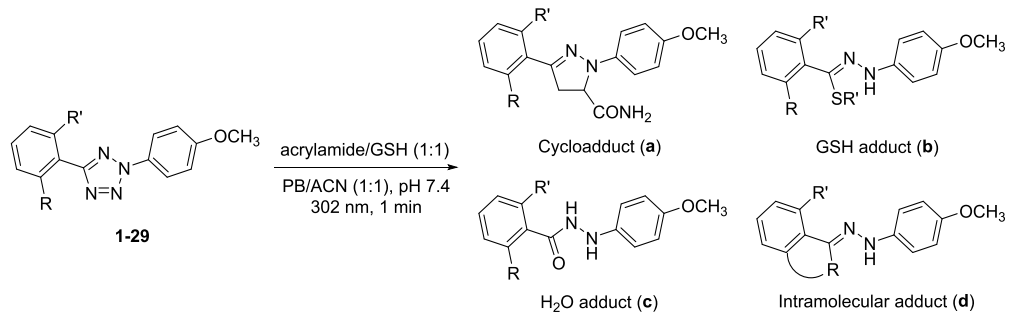

Tetrazole structure		Product distribution (%) [b]			
		a	**b**	**c**	**d**
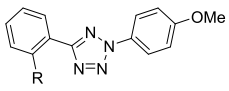 **1-10**	**1:** R = H	47	51	2	0
	2: R = CH_3	50	48	2	0
	3: R = CH_2OH	0	0	0	100
	4: R = COOH	0	0	0	100
	5: R = CH_2CN	38	42	20	0
	6: R = CH_2OCH_3	55	45	0	0
	7: R = CH_2SCH_3	0	70	0	30
	8: R = $CH_2N(CH_3)_2$	0	0	0	100
	9: R = $CH_2CH_2OCH_3$	51	49	0	0
	10: R = $CH(CH_3)OCH_3$	38	42	20	0
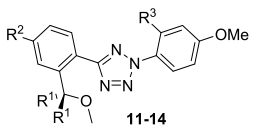 **11-14**	**11:** R^1 = CH_3; R^2 = H; R^3 = H	0	0	100	0
	12: R^1 = CH_3; R^2 = H; R^3 = Cl	0	0	100	0
	13: R^1 = CH_3; R^2 = OCH_3; R^3 = H	0	0	100	0
	14: R^1 = CH_3; R^2 = OCH_3; R^3 = OCH_3	0	0	100	0
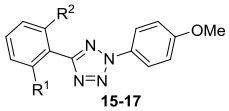 **15-17**	**15:** R^1 = R^2 = CH_3	10	10	80	0
	16: R^1 = R^2 = OCH_3	58	12	30	0
	17: R^1 = R^2 = CH_2OCH_3	32	46	22	0
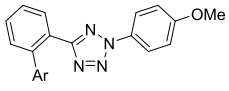 **18-23**	**18:** Ar = 2'-furan	37	58	5	0
	19: Ar = 2'-thiophene	36	56	8	0
	20: Ar = 2'-*N*-Boc-pyrrole	58	39	3	0
	21: Ar = 2'-methoxybenzene	56	41	3	0
	22: Ar = 2'-pyridine	1	1	0	98
	23: Ar = 2'-pyrrole	3	5	92	0
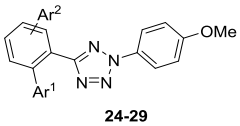 **24-29**	**24:** Ar^1 = Ar^2 = *o*-2'-furan	30	59	11	0
	25: Ar^1 = Ar^2 = *o*-2'-thiophene	27	63	10	0
	26: Ar^1 = Ar^2 = *o*-2'-*N*-Boc-pyrrole	92	2	6	0
	27: Ar^1 = Ar^2 = *o*-2'-pyrrole	1	1	98	0
	28: Ar^1 = Ar_2 = *o*-2'-*N*-Moc-pyrrole	78	20	2	0
	29: Ar^1 = *o*-2'-*N*-Boc-pyrrole; Ar^2 = *p*-2'-*N*-Boc-pyrrole	74	24	2	0

[a] A solution of 25 μM tetrazole and 500 μM each of acrylamide and glutathione (reduced form; GSH) in 500 μL phosphate buffer/acetonitrile (1:1), pH 7.4, was photoirradiated with a handheld 302-nm UV lamp at room temperature for 1 min. [b] The product distribution was analyzed by reverse-phase HPLC with absorbance set at 254 nm. The product peaks were assigned by comparing the trace of the product mixture to those of control reactions using either acrylamide or glutathione.

a)

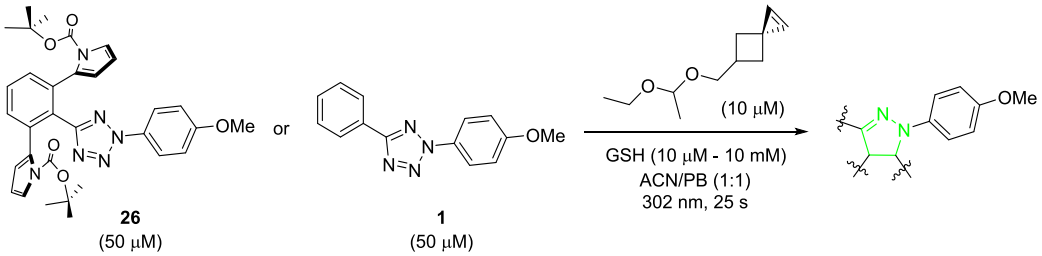

b)

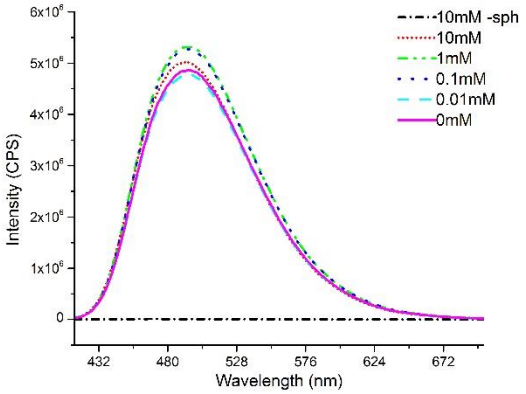

c)

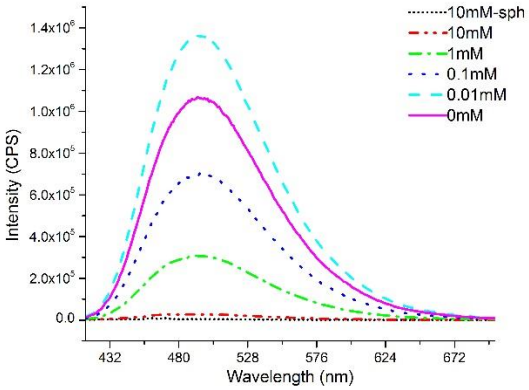

d)

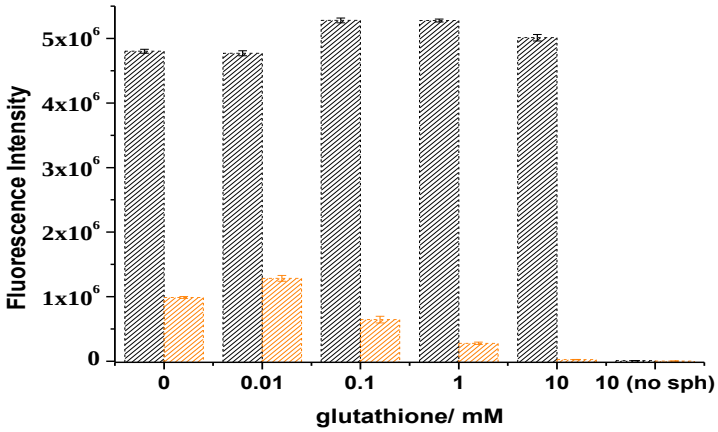

Figure S1. Fluorescence-based interference study of the cycloaddition reaction by glutathione in acetonitrile/phosphate buffer (1:1). (**a**) Reaction scheme. (**b**) Fluorescence spectra of the reaction involving tetrazole **26** and Sph in the presence of 0.01–10 mM glutathione; λ_{ex} = 405 nm. (**c**) Fluorescence spectra of the reaction involving tetrazole **1** and Sph in the presence of 0.01–10 mM glutathione; λ_{ex} = 405 nm. (**d**) Quantification of the inhibitory effect of glutathione on the formation of fluorescent pyrazoline adduct. The fluorescence measurements were repeated three times for each condition. Grey bar = **26**, orange bar = **1**.

a)

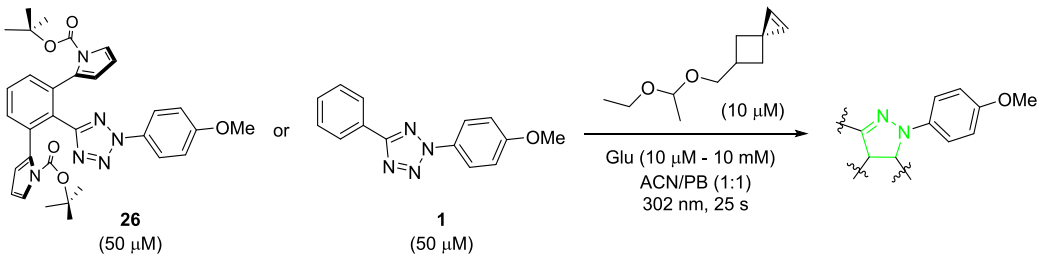

b)

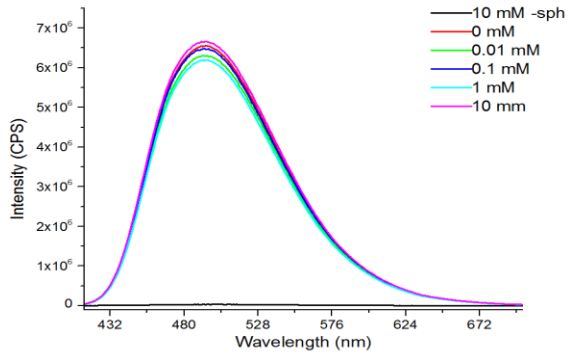

c)

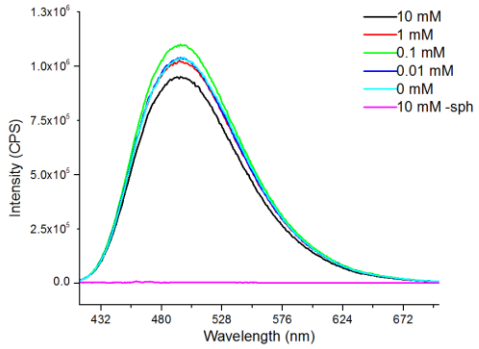

d)

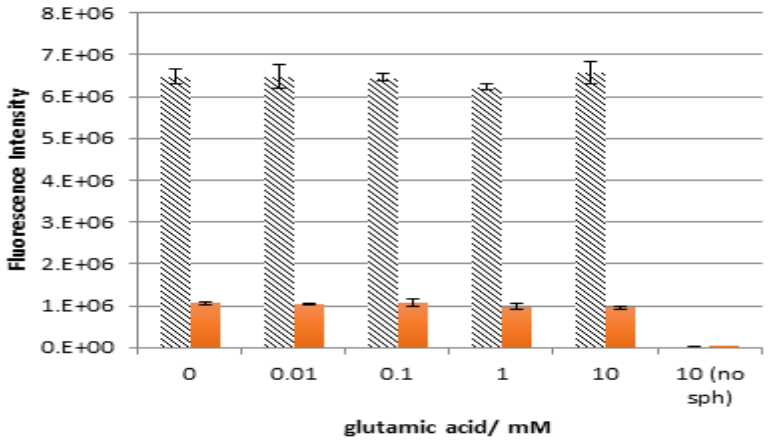

Figure S2. Fluorescence-based interference study of the cycloaddition reaction by glutamic acid in acetonitrile/phosphate buffer (1:1). (**a**) Reaction scheme. (**b**) Fluorescence spectra of the reaction involving tetrazole **26** and Sph in the presence of 0.01–10 mM glutamic acid; λ_{ex} = 405 nm. (**c**) Fluorescence spectra of the reaction involving tetrazole **1** and Sph in the presence of 0.01–10 mM glutamic acid; λ_{ex} = 405 nm. (**d**) Quantification of the inhibitory effect of glutamic acid on the formation of the fluorescent pyrazoline adduct. The fluorescence measurements were repeated three times for each condition. Grey bar = **26**, orange bar = **1**.

a)

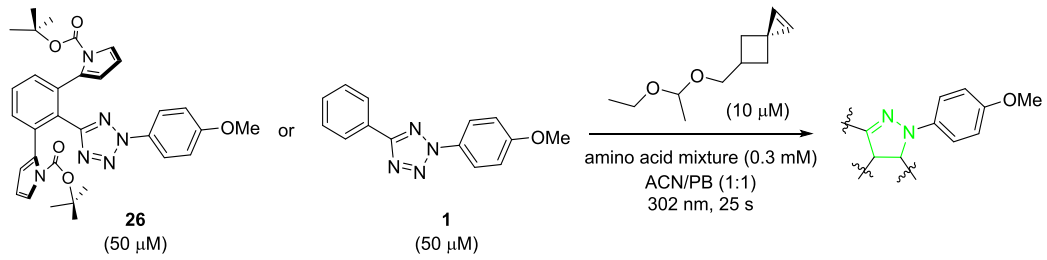

b) **c)**

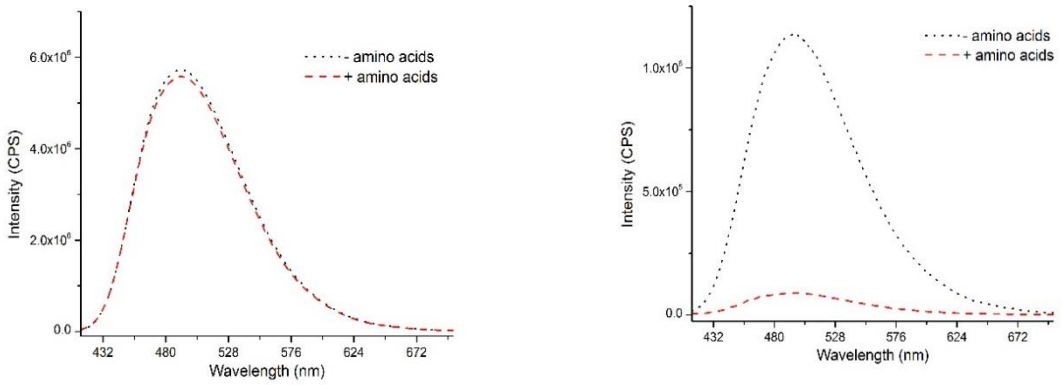

Figure S3. Fluorescence-based interference study of the cycloaddition reaction by a mixture of nucleophilic amino acids (methionine, cysteine, lysine, tryptophan, arginine, and tyrosine; 0.3 mM each) in acetonitrile/phosphate buffer (1:1). (**a**) Reaction scheme. (**b**) Fluorescence spectra of the reaction involving tetrazole **26** and Sph in the presence (red dashed line) and absence (black dashed line) of the amino acid mixture; λ_{ex} = 405 nm. (**c**) Fluorescence spectra of the reaction involving tetrazole **1** and Sph in the presence (red dashed line) and absence (black dashed line) of the amino acid mixture; λ_{ex} = 405 nm.

Table S2. Kinetic characterization of the cycloaddition reactions of tetrazole **1** or **26** with various dipolarophiles based on fluorescence of the pyrazoline adducts, and photophysical properties of the pyrazolines [a]

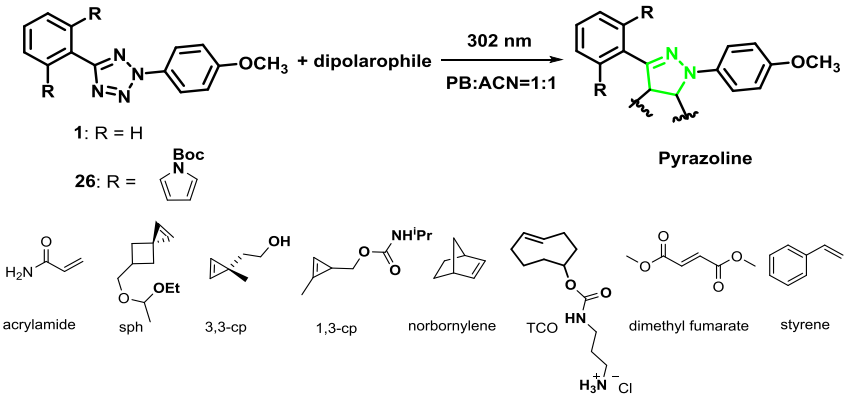

Tetrazole (μM)	Dipolarophile (μM)	Pyrazoline		k_2 (M^{-1} s^{-1})
		λ_{abs}(nm)	λ_{em} (nm)[b]	
1 (10)	acrylamide (100)	360	508	2000 ± 300
1 (10)	dimethyl fumarate (50)	366	516	4700 ± 500
1 (10)	styrene (100)	ND[c]	ND[c]	/
1 (10)	norbornene (100)	381	504	2200 ± 700
1 (10)	1,3-Cp (100)	ND[c]	ND[c]	/
1 (10)	3,3-Cp (100)	375	495	2800 ± 300
1 (10)	Sph (50)	376	494	3100 ± 600
1 (10)	TCO (50)	343	508	3800 ± 700
26 (10)	acrylamide (100)	340	503	860 ± 110
26 (10)	dimethyl fumarate (50)	351	502	2400 ± 300
26 (10)	styrene (100)	346	508	1000 ± 100
26 (10)	norbornene (100)	353	518	1000 ± 250
26 (10)	1,3-Cp (100)	360	488	520 ± 140
26 (10)	3,3-Cp (100)	360	496	1400 ± 130
26 (10)	Sph (50)	375	495	2800 ± 200
26 (10)	TCO (50)	323	490	2300 ± 300

[a]Performed in a quartz cuvette for direct fluorescence measurement.
[b]Emission maximum was recorded in phosphate buffer/acetonitrile (1:1).
[c]pyrazoline was not detected.

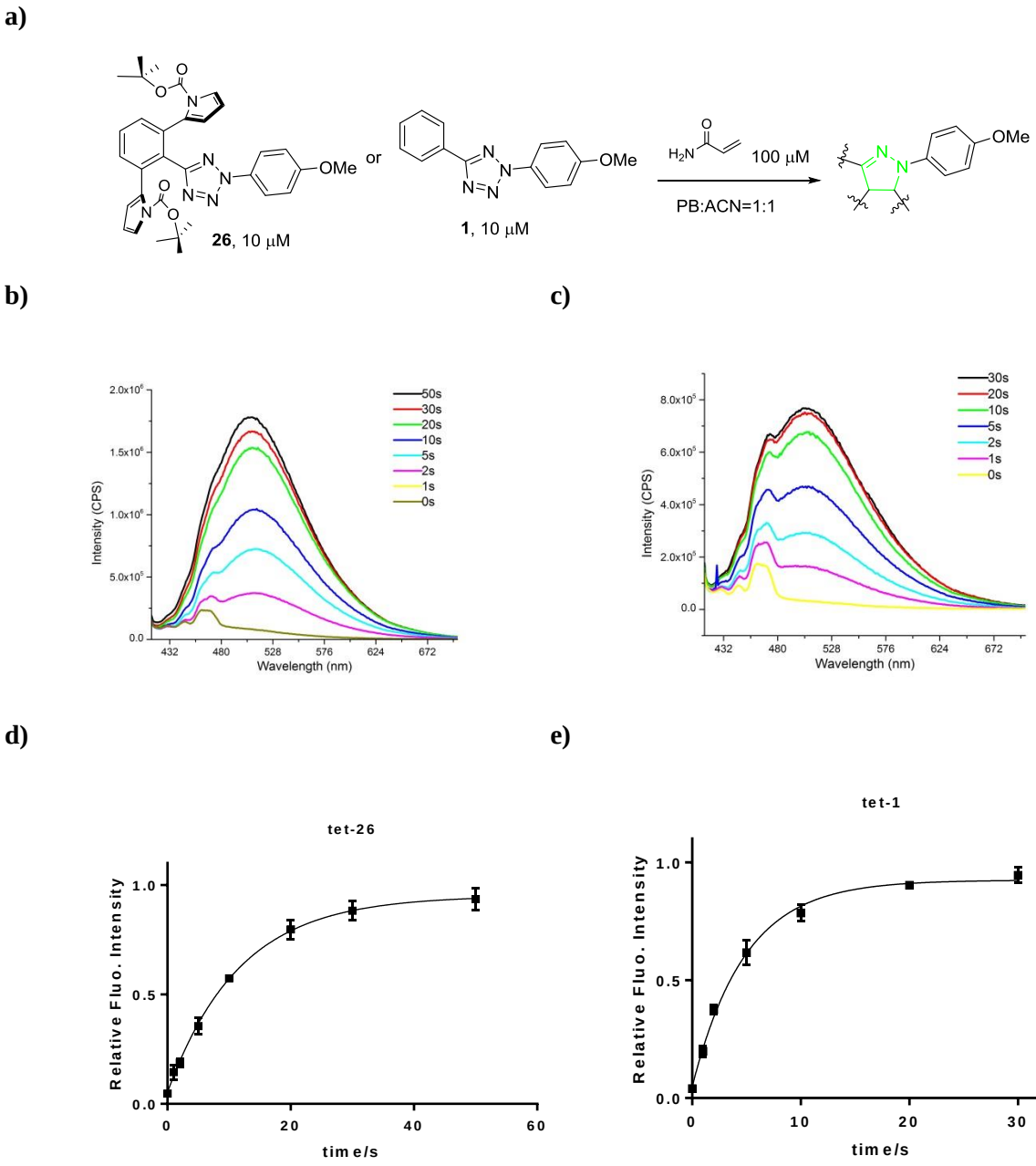

Figure S4. Fluorescence-based kinetics measurement of the cycloaddition between tetrazole **26** (10 μM) or **1** (10 μM) and acrylamide (100 μM) in phosphate buffer/acetonitrile (1:1) under 302 nm photoirradiation. (**a**) Reaction scheme. (**b**) Time course of the cycloaddition reaction between tetrazole **26** and acrylamide monitored by a spectrofluorometer (λ_{ex} = 405 nm). (**c**) Time course of the cycloaddition reaction between tetrazole **1** and acrylamide monitored by a spectrofluorometer (λ_{ex} = 405 nm). (**d**, **e**) Plots of relative fluorescence intensity vs. reaction time. The amounts of pyrazoline adduct were fitted to an exponential rise to maximum equation, $y = (y_0\text{-}a)\, e^{kt} + a$, to give k. The second-order rate constants, k_2, were calculated using the following equation: k_2 = k/[dipolarophile]. Measurements were repeated three times at each time point to derive the mean and standard deviation.

a)

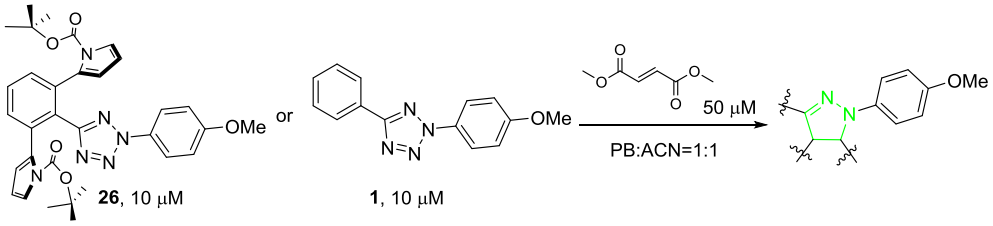

b)

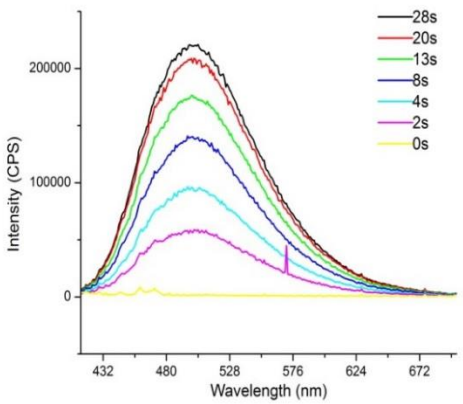

c)

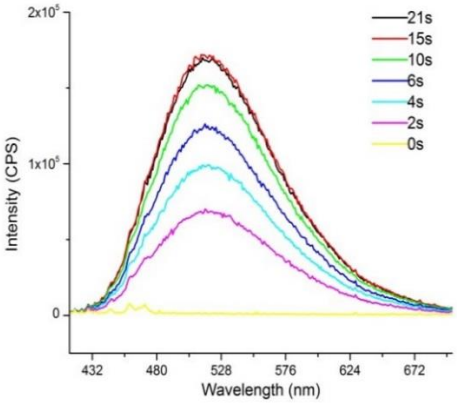

d)

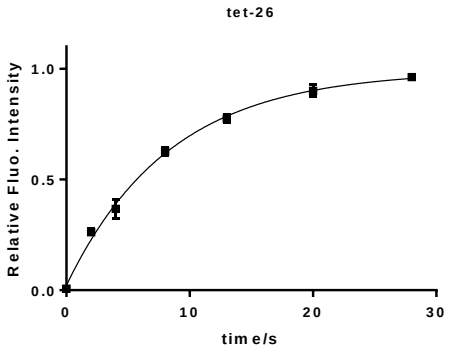

e)

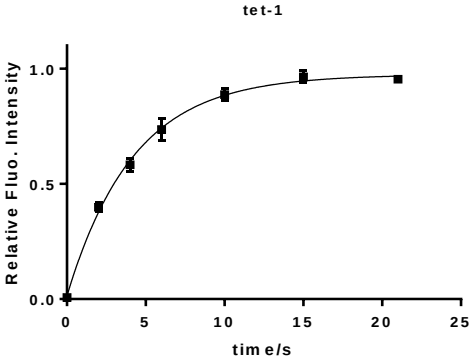

Figure S5. Fluorescence-based kinetics measurement of the cycloaddition between tetrazole **26** (10 μM) or **1** (10 μM) and dimethyl fumarate (50 μM) in phosphate buffer/acetonitrile (1:1) under 302 nm photoirradiation. (**a**) Reaction scheme. (**b**) Time course of the cycloaddition reaction between tetrazole **26** and dimethyl fumarate monitored by a spectrofluorometer (λ_{ex} = 405 nm). (**c**) Time course of the cycloaddition reaction between tetrazole **1** and dimethyl fumarate monitored by a spectrofluorometer (λ_{ex} = 405 nm). (**d**, **e**) Plots of relative fluorescence intensity vs. reaction time. The amounts of pyrazoline adduct were fitted to an exponential rise to maximum equation, $y = (y_0\text{-}a)\, e^{kt} + a$, to give k. The second-order rate constants, k_2, were calculated using the following equation: k_2 = k/[dipolarophile]. Measurements were repeated three times at each time point to derive the mean and standard deviation.

a)

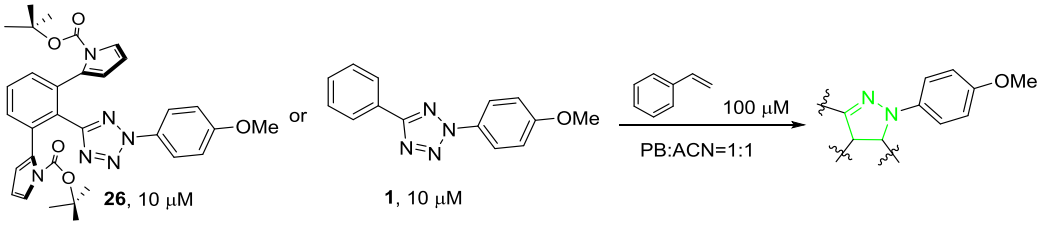

b) **c)**

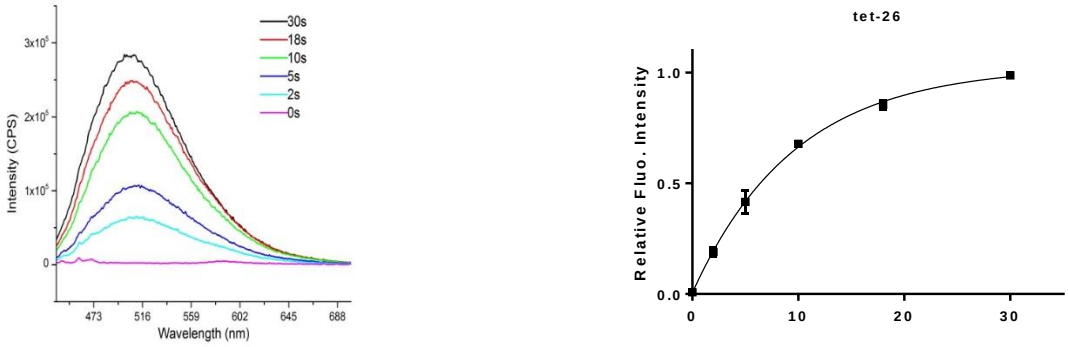

Figure S6. Fluorescence-based kinetics measurement of the cycloaddition between tetrazole **26** (10 μM) or **1** (10 μM) and styrene (100 μM) in phosphate buffer/acetonitrile (1:1) under 302 nm photoirradiation. (**a**) Reaction scheme. (**b**) Time course of the cycloaddition reaction between tetrazole **26** and styrene monitored by a spectrofluorometer (λ_{ex} = 405 nm). (**c**) Plot of relative fluorescence intensity vs. reaction time. The amounts of pyrazoline adduct were fitted to an exponential rise to maximum equation, $y = (y_0\text{-}a)\, e^{kt} + a$, to give k. The second-order rate constant, k_2, was calculated using the following equation: k_2 = k/[dipolarophile]. Measurements were repeated three times at each time point to derive the mean and standard deviation. The fluorescence was not detected for tetrazole **1** under the same reaction condition.

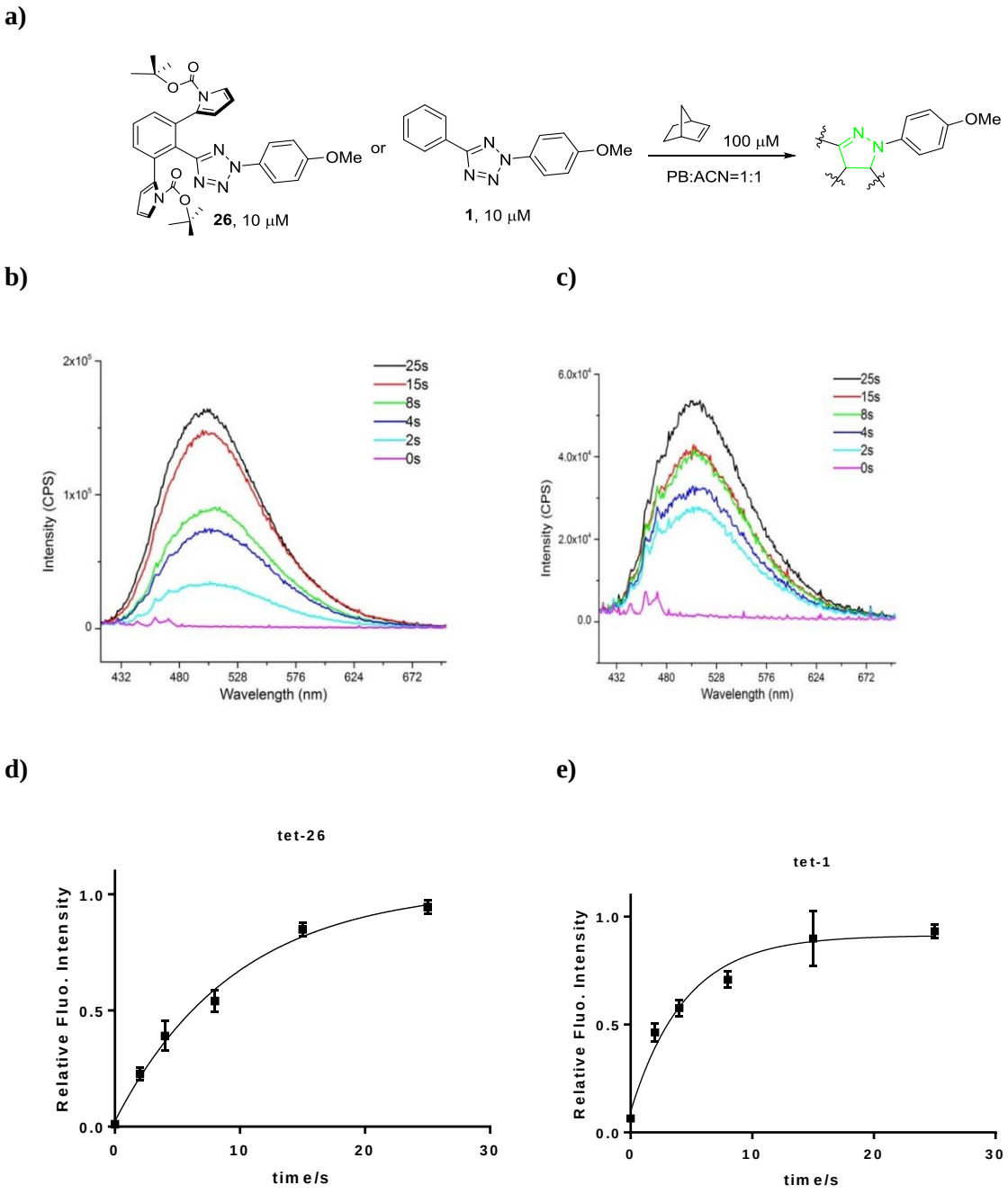

Figure S7. Fluorescence-based kinetics measurement of the cycloaddition between tetrazole **26** (10 μM) or **1** (10 μM) and norbornylene (100 μM) in phosphate buffer/acetonitrile (1:1) under 302 nm photoirradiation. (**a**) Reaction scheme. (**b**) Time course of the cycloaddition reaction between tetrazole **26** and norbornene monitored by a spectrofluorometer (λ_{ex} = 405 nm). (**c**) Time course of the cycloaddition reaction between tetrazole **1** and norbornene monitored by a spectrofluorometer (λ_{ex} = 405 nm). (**d**, **e**) Plots of relative fluorescence intensity vs. reaction time. The amounts of pyrazoline adduct were fitted to an exponential rise to maximum equation, $y = (y_0\text{-}a)\, e^{kt} + a$, to give k. The second-order rate constants, k_2, were calculated using the following equation: k_2 = k/[dipolarophile]. Measurements were repeated three times at each time point to derive the mean and standard deviation.

a)

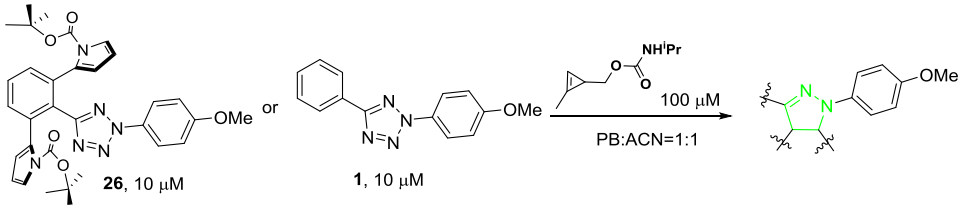

b) **c)**

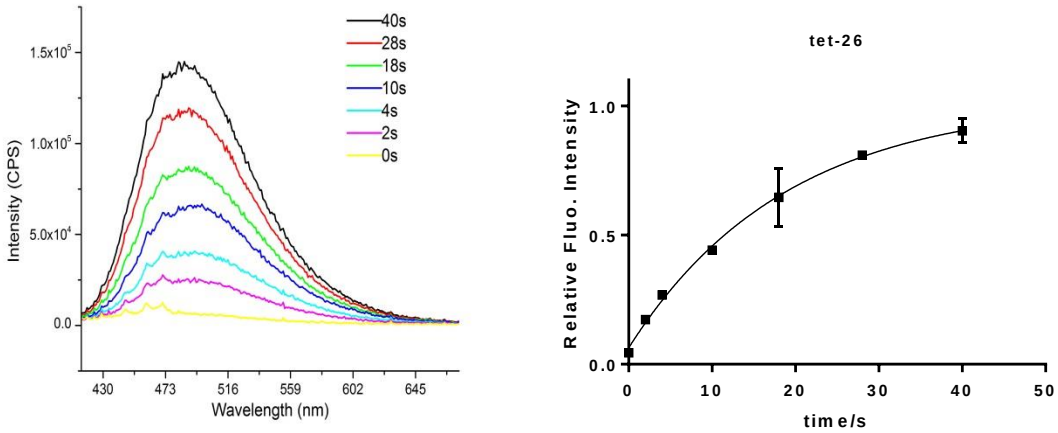

Figure S8. Fluorescence-based kinetics measurement of the cycloaddition between tetrazole **26** (10 μM) or **1** (10 μM) and 1,3-cyclopropene (100 μM) in phosphate buffer/acetonitrile (1:1) under 302 nm photoirradiation. (**a**) Reaction scheme. (**b**) Time course of the cycloaddition reaction between tetrazole **26** and 1,3-cyclopropene monitored by a spectrofluorometer (λ_{ex} = 405 nm). (**c**) Plot of relative fluorescence intensity vs. reaction time. The amounts of pyrazoline adduct were fitted to an exponential rise to maximum equation, $y = (y_0\text{-}a)\, e^{kt} + a$, to give k. The second-order rate constant, k_2, was calculated using the following equation: k_2 = k/[dipolarophile]. Measurements were repeated three times at each time point to derive the mean and standard deviation. The fluorescence was not detected for tetrazole **1** under the same reaction condition.

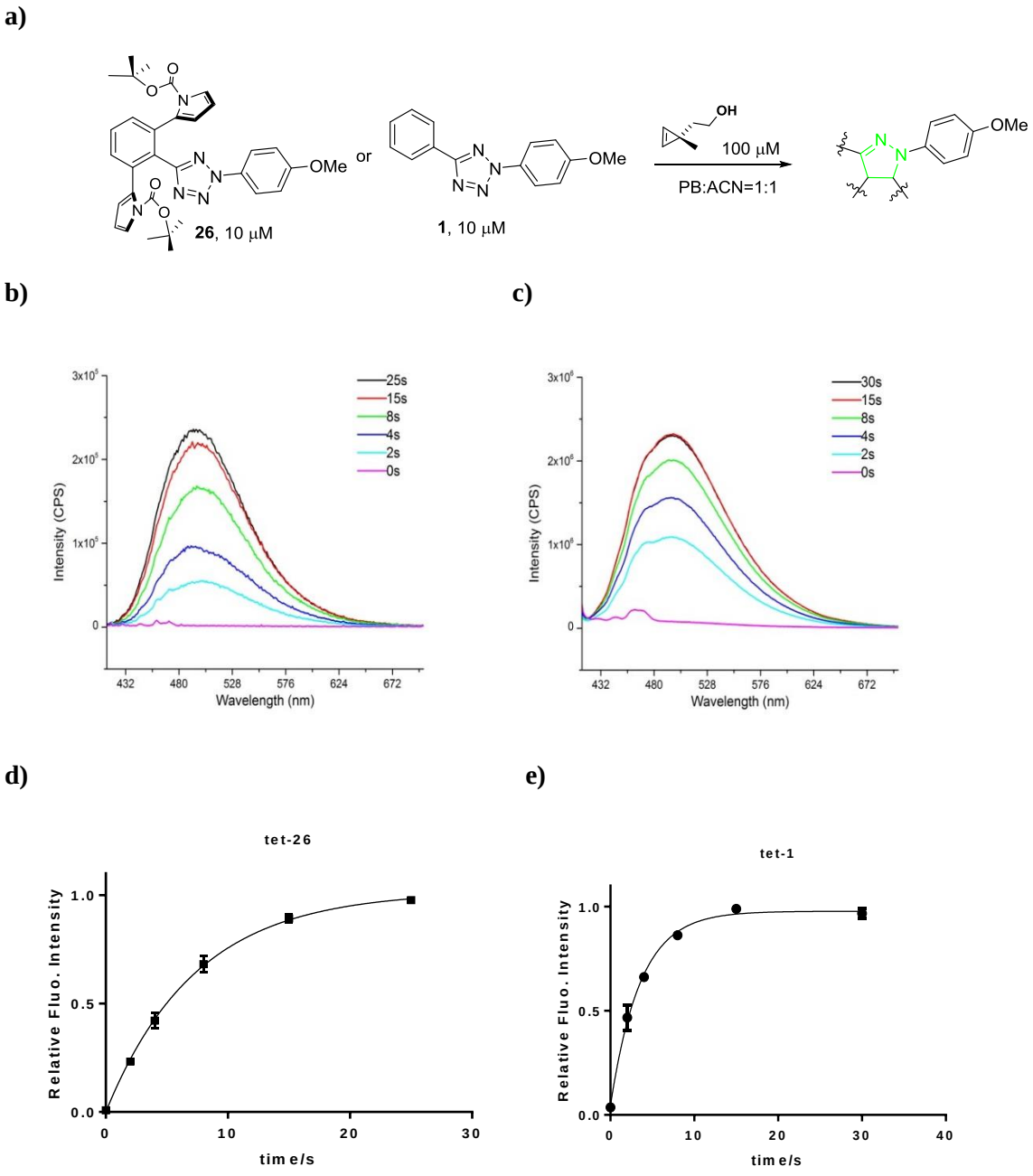

Figure S9. Fluorescence-based kinetics measurement of the cycloaddition between tetrazole **26** (10 μM) or **1** (10 μM) and 3,3-cyclopropene (100 μM) in phosphate buffer/acetonitrile (1:1) under 302 nm photoirradiation. (**a**) Reaction scheme. (**b**) Time course of the cycloaddition reaction between tetrazole **26** and 3,3-cyclopropene monitored by a spectrofluorometer (λ_{ex} = 405 nm). (**c**) Time course of the cycloaddition reaction between tetrazole **1** and 3,3-cyclopropene monitored by a spectrofluorometer (λ_{ex} = 405 nm). (**d**, **e**) Plots of relative fluorescence intensity vs. reaction time. The amounts of pyrazoline adduct were fitted to an exponential rise to maximum equation, $y = (y_0\text{-}a)\, e^{kt} + a$, to give k. The second-order rate constants, k_2, were calculated using the following equation: k_2 = k/[dipolarophile]. Measurements were repeated three times at each time point to derive the mean and standard deviation.

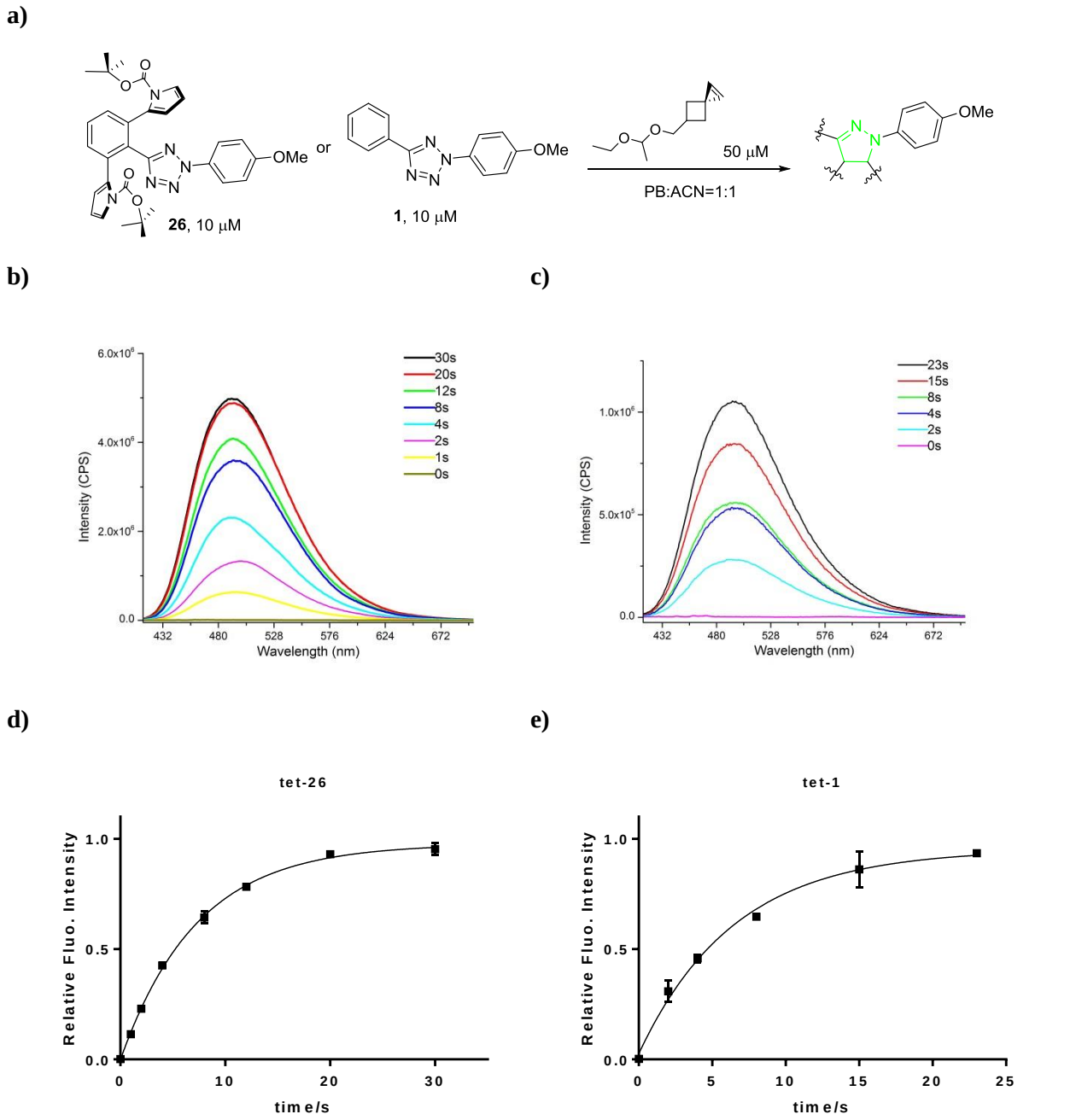

Figure S10. Fluorescence-based kinetics measurement of the cycloaddition between tetrazole **26** (10 μM) or **1** (10 μM) and spirohexene (Sph, 50 μM) in phosphate buffer/acetonitrile (1:1) under 302 nm photoirradiation. (**a**) Reaction scheme. (**b**) Time course of the cycloaddition reaction between tetrazole **26** and Sph monitored by a spectrofluorometer (λ_{ex} = 405 nm). (**c**) Time course of the cycloaddition reaction between tetrazole **1** and Sph monitored by a spectrofluorometer (λ_{ex} = 405 nm). (**d**, **e**) Plots of relative fluorescence intensity vs. reaction time. The amounts of pyrazoline adduct were fitted to an exponential rise to maximum equation, $y = (y_0\text{-}a)\, e^{kt} + a$, to give k. The second-order rate constants, k_2, were calculated using the following equation: k_2 = k/[dipolarophile]. Measurements were repeated three times at each time point to derive the mean and standard deviation.

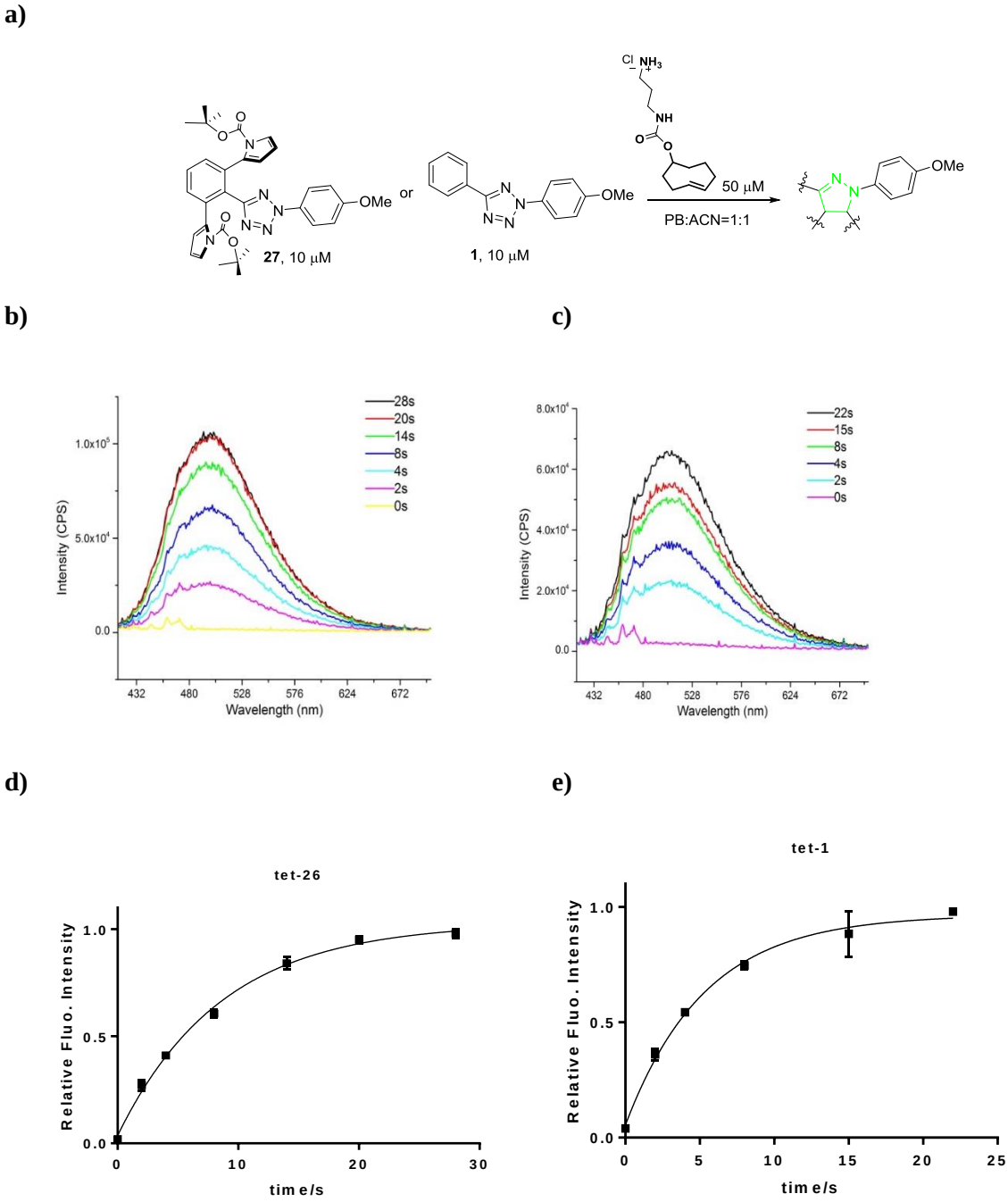

Figure S11. Fluorescence-based kinetics measurement of the cycloaddition between tetrazole **26** (10 μM) or **1** (10 μM) and TCO-amine (50 μM) in phosphate buffer/acetonitrile (1:1) under 302 nm photoirradiation. (**a**) Reaction scheme. (**b**) Time course of the cycloaddition reaction between tetrazole **26** and TCO-amine monitored by a spectrofluorometer (λ_{ex} = 405 nm). (**c**) Time course of the cycloaddition reaction between tetrazole **1** and TCO-amine monitored by a spectrofluorometer (λ_{ex} = 405 nm). (**d**, **e**) Plots of relative fluorescence intensity vs. reaction time. The amounts of pyrazoline adduct were fitted to an exponential rise to maximum equation, $y = (y_0\text{-}a)\, e^{kt} + a$, to give k. The second-order rate constants, k_2, were calculated

using the following equation: k_2 = k/[dipolarophile]. Measurements were repeated three times at each time point to derive the mean and standard deviation.

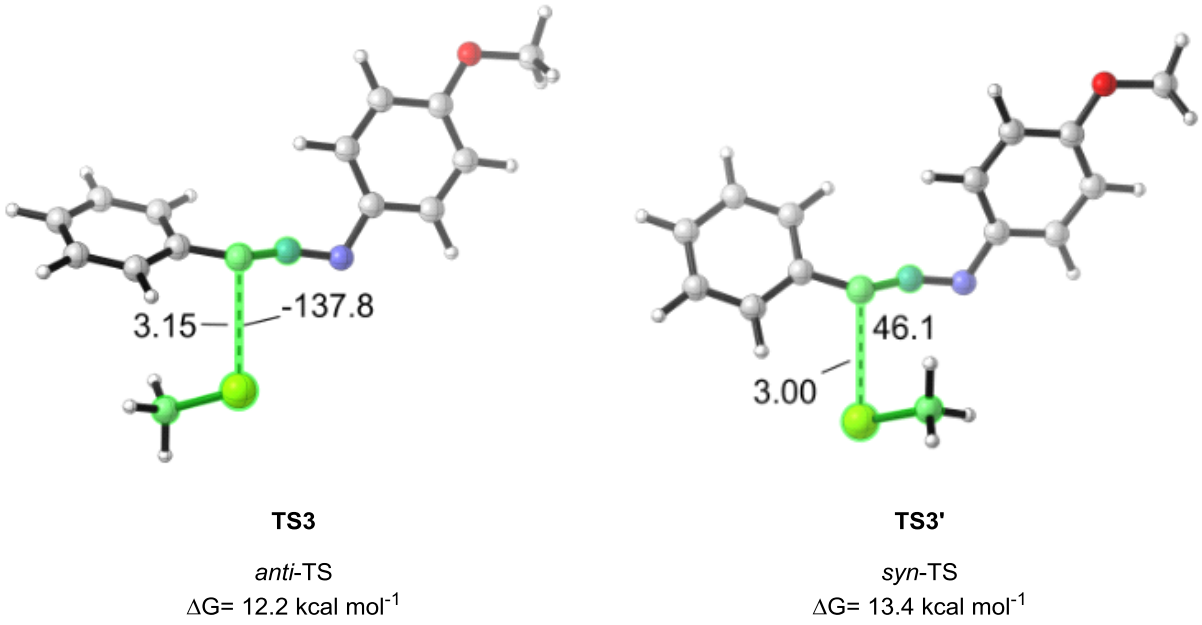

Figure S12. Transition state isomers and activation energies for the methyl thiolate addition reaction to nitrile imine-**1**. The distances shown are in Å, and dihedral angles are in degree. Two possible TS for the addition of methyl thiolate to nitrile imine-**1** are presented. The *anti*- and *syn*- transition states of nucleophilic addition of thiols are defined by the dihedral angle around the forming C—S bond (∠(C-S-C-N) = −137.8° and 46.1° for **TS3** and **TS3'**, respectively). *syn*-TS (**TS3'**) has a higher $\Delta G^{\ddagger}$ compared to the *anti*-TS (**TS3**) ($\Delta\Delta G^{\ddagger}_{\omega\text{-B97X-D}}$ = 1.2 kcal mol^{-1}).

Table S3. Crystal data and structure refinement for **26**.

	Single crystal of **26**
Empirical formula	$C_{32}H_{34}N_6O_5$
Formula weight	582.65
Temperature/K	90
Crystal system	monoclinic
Space group	$P2_1/n$
a/Å	11.8321(5)
b/Å	13.4953(6)
c/Å	19.2839(9)
α/°	90
β/°	105.5800(10)
γ/°	90
Volume/Å^3	2966.1(2)
Z	4
ρ_{calc}g/cm^3	1.305
μ/mm^{-1}	0.090
F(000)	1232.0
Crystal size/mm^3	0.1 × 0.08 × 0.07
Radiation	MoKα (λ = 0.71073)
2Θ range for data collection/°	3.656 to 56.654
Index ranges	$-15 \leq h \leq 15$, $-18 \leq k \leq 17$, $-25 \leq l \leq 25$
Reflections collected	59012
Independent reflections	7373 [R_{int} = 0.0256, R_{sigma} = 0.0132]
Data/restraints/parameters	7373/0/395
Goodness-of-fit on F^2	1.025
Final R indexes [I>=2σ (I)]	R_1 = 0.0374, wR_2 = 0.0963
Final R indexes [all data]	R_1 = 0.0412, wR_2 = 0.0997
Largest diff. peak/hole / e Å^{-3}	0.39/-0.24

Table S4. Crystal data and structure refinement for **27**.

	Single crystal of **27**
Empirical formula	$C_{22}H_{18}N_6O$
Formula weight	382.42
Temperature/K	90
Crystal system	monoclinic
Space group	$P2_1/n$
a/Å	18.7948(8)
b/Å	5.1334(2)
c/Å	21.0251(9)
α/°	90
β/°	116.3170(10)
γ/°	90
Volume/Å^3	1818.28(13)
Z	4
ρ_{calc}g/cm^3	1.397
μ/mm^{-1}	0.091
F(000)	800.0
Crystal size/mm^3	0.1 × 0.08 × 0.01
Radiation	MoKα (λ = 0.71073)
2Θ range for data collection/°	3.892 to 56.708
Index ranges	$-25 \leq h \leq 25$, $-6 \leq k \leq 6$, $-28 \leq l \leq 28$
Reflections collected	36043
Independent reflections	4528 [R_{int} = 0.0219, R_{sigma} = 0.0126]
Data/restraints/parameters	4528/0/263
Goodness-of-fit on F^2	1.045
Final R indexes [I>=2σ (I)]	R_1 = 0.0376, wR_2 = 0.0976
Final R indexes [all data]	R_1 = 0.0432, wR_2 = 0.1023
Largest diff. peak/hole / e Å^{-3}	0.35/-0.23

a)

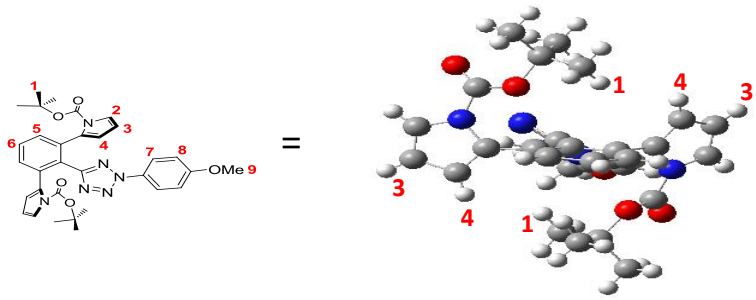

b)

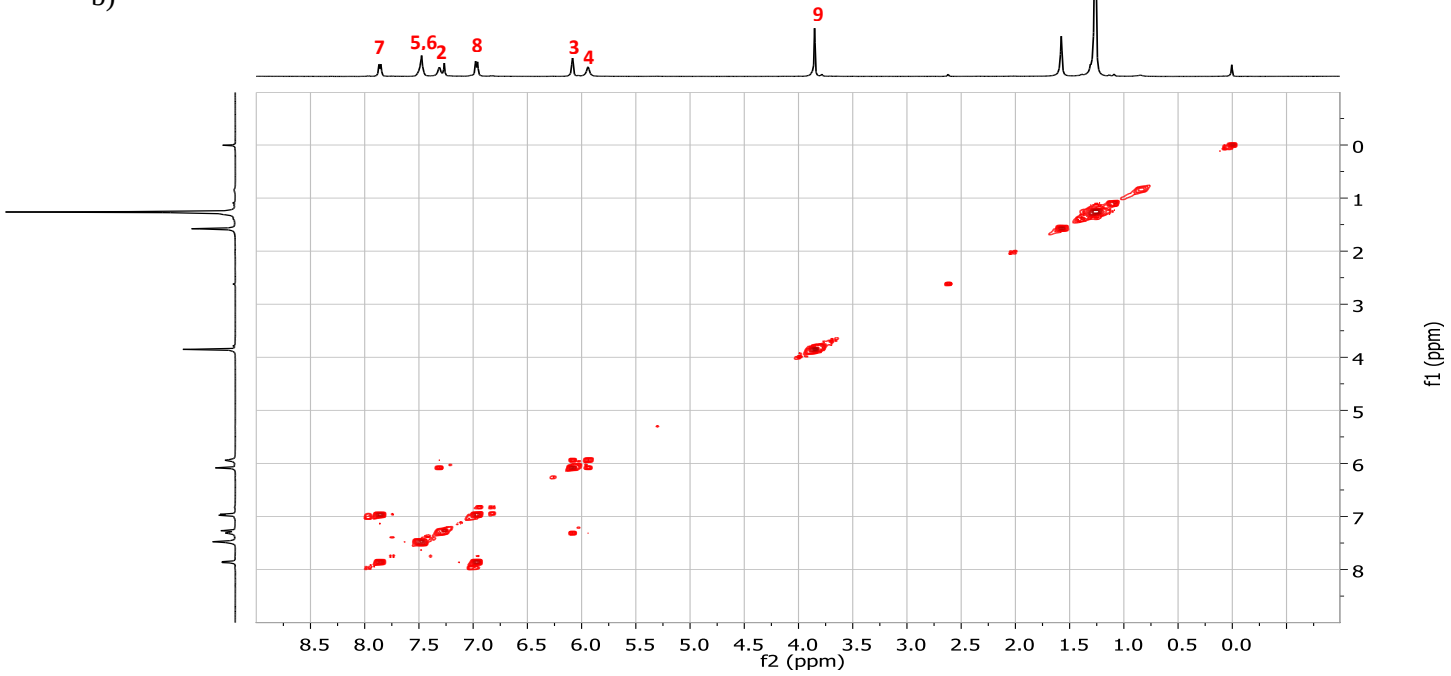

c)

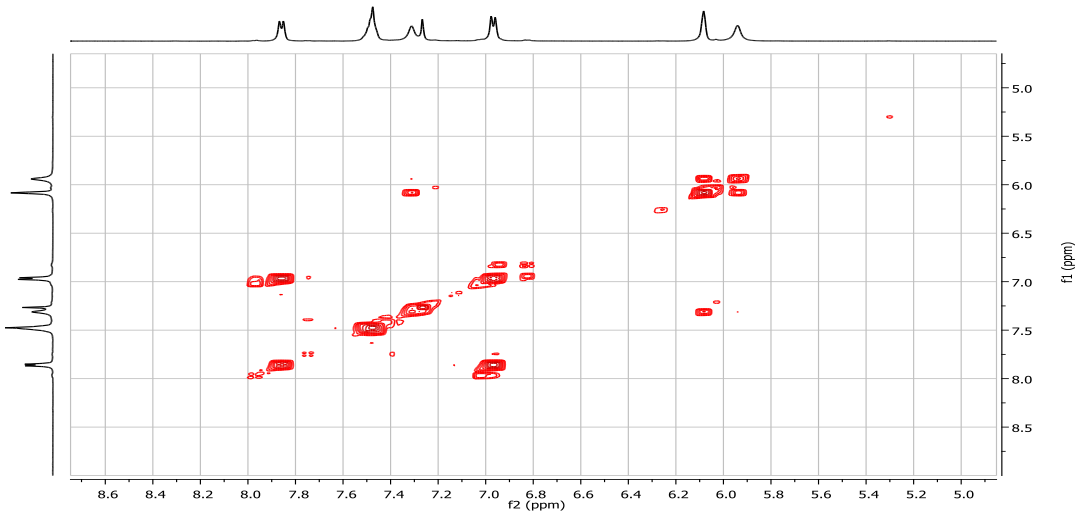

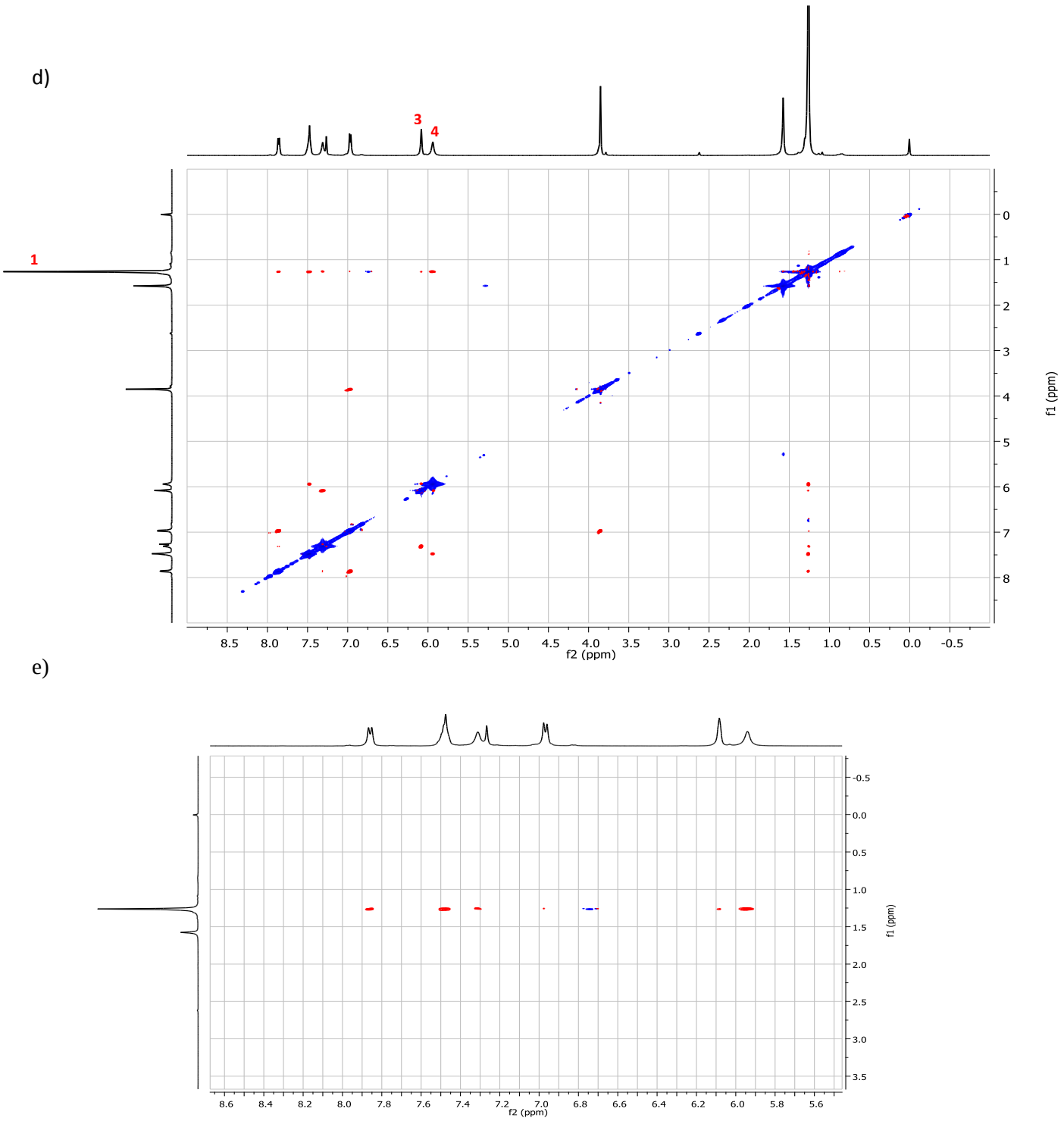

Figure S13. 2D NMR spectra of tetrazole **26**. (**a**) Structure of tetrazole **26** with number assigned for all protons. (**b**) 2D COSY spectrum (500 MHz, 10 mM, $CDCl_3$) of tetrazole **26**. (**c**) Partial zoomed-in 2D COSY spectrum of tetrazole **26**. (**d**) 2D ROESY spectrum (500 MHz, 10 mM, $CDCl_3$, 25 ^oC) of tetrazole **26**. (**e**) Partial zoomed-in 2D ROESY spectrum of tetrazole **26**.

a)

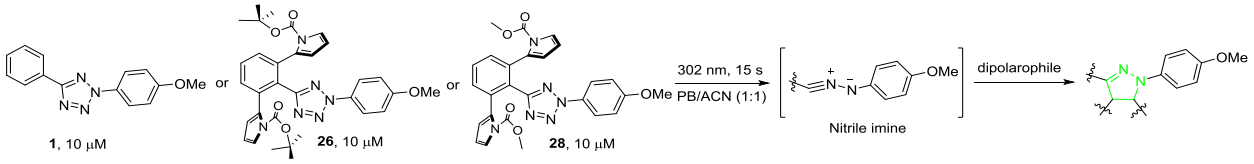
OMe
or
OMe
or
OMe
1, 10 μM
26, 10 μM
28, 10 μM
302 nm, 15 s
PB/ACN (1:1)
OMe
Nitrile imine
dipolarophile
OMe

b)

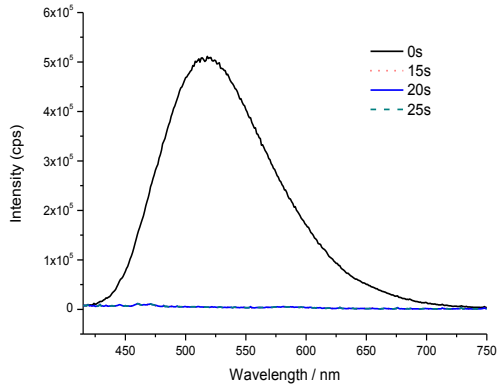
Intensity (cps)
Wavelength / nm
0s
15s
20s
25s

c)

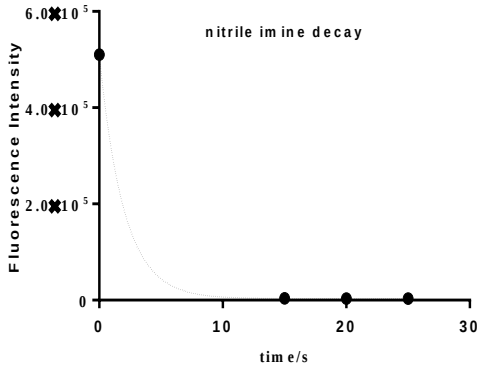
nitrile imine decay
Fluorescence Intensity
time/s

d)

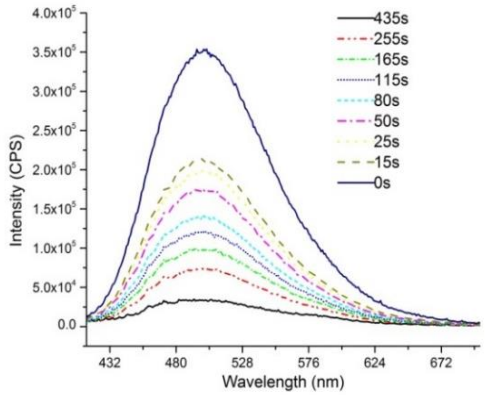
Intensity (CPS)
Wavelength (nm)
435s
255s
165s
115s
80s
50s
25s
15s
0s

e)

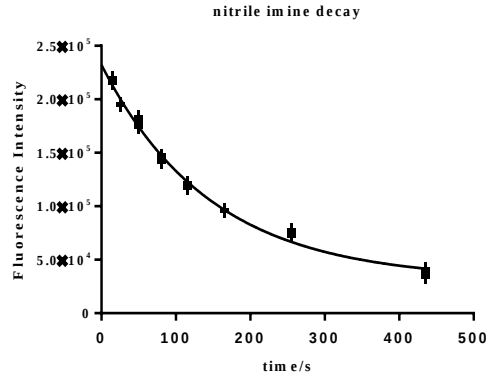
nitrile imine decay
Fluorescence Intensity
time/s

f)

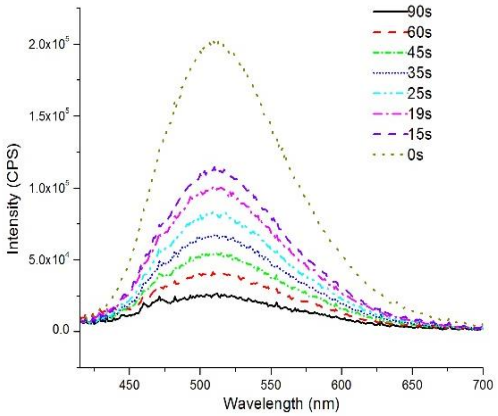
Intensity (CPS)
Wavelength (nm)
90s
60s
45s
35s
25s
19s
15s
0s

g)

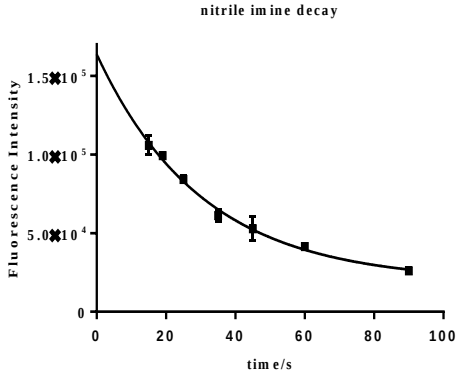
nitrile imine decay
Fluorescence Intensity
time/s

Figure S14. Fluorescence-based determination of the half-lives of nitrile imine-**1**, **-26**, and **-28** in phosphate buffer/acetonitrile (1:1). (**a**) Scheme showing measurement procedure: 10 μM tetrazole **1**, **26** or **28** was photoirradiated with a handheld 302 nm UV lamp for 15 sec. The resulting solution was left unperturbed for the in situ generated nitrile imine to decay for a period of time before dimethyl fumarate was added with a final concentration of 500 μM to capture the residual nitrile imine to produce the fluorescent pyrazoline product. (**b**) Fluorescence spectra of the pyrazoline products derived from the reaction of dimethyl fumarate with the residual nitrile imine-**1** after left unperturbed for various times; λ_{ex} = 405 nm. The zero-point sample was obtained by incubating dimethyl fumarate with tetrazole **1** prior to photoirradiation. (**c**) Plot of fluorescence intensity vs. delay time for nitrile imine-**1**. No fluorescence was detected after adding dimethyl fumarate, indicating that the half-life of nitrile imine-**1** must be shorter than 7.5 sec. (**d**) Fluorescence spectra of the pyrazoline products derived from the reaction of dimethyl fumarate with the residual nitrile imine-**26** after left unperturbed for various times; λ_{ex} = 405 nm. (**e**) Plot of fluorescent intensity vs. delay time for nitrile imine-**26**. Based on the curve-fitting, the half-life of nitrile imine-**26** was determined to be 102 sec. (**f**) Fluorescence spectra of the pyrazoline products derived from the reaction of dimethyl fumarate with the residual nitrile imine-**28** after left unperturbed for various times; λ_{ex} = 405 nm. (**g**) Plot of the fluorescence intensity vs. the delay time for nitrile imine-**28**. Based on the curve-fitting, the half-life of nitrile imine-**28** was determined to be 21 sec. Each fluorescence measurement was repeated three times to obtain the mean values and standard deviations.

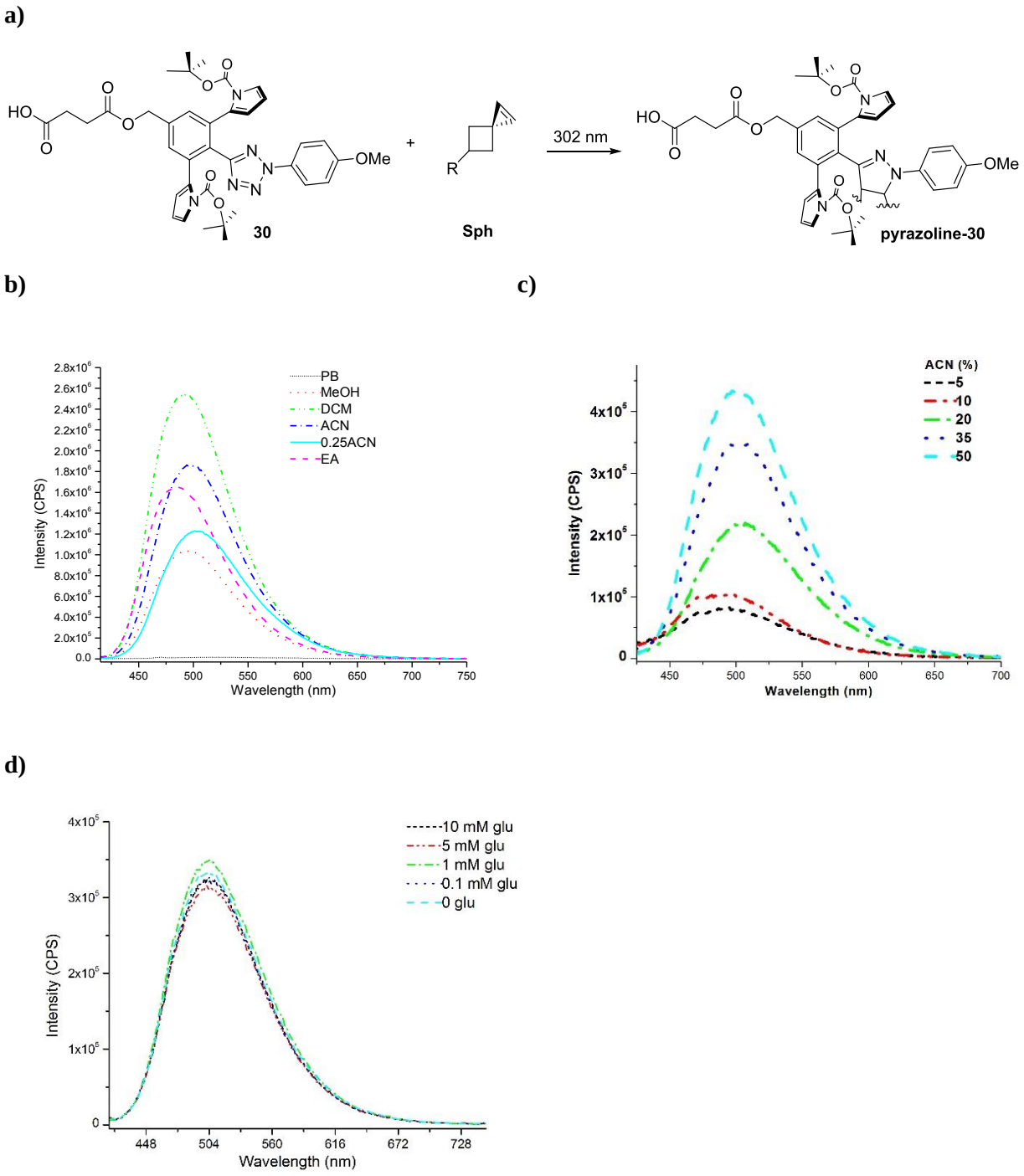

Figure S15. Fluorescent properties of pyrazoline-**30** under different conditions. (**a**) Scheme for pyrazoline-**30** synthesis. (**b**) Fluorescence spectra of pyrazoline-**30** (5 μM) in different solvents: PB = phosphate buffer, DCM = dichloromethane, 0.25ACN = 25% acetonitrile in PB, EA = ethyl acetate. (**c**) Fluorescence spectra of pyrazoline-**30** in PB containing varying amounts of acetonitrile (v/v). (**d**) Response of pyrazoline-**30** fluorescence after adding varying amounts of glutamine. Pyrazoline-**30** was dissolved in 20% ACN in phosphate buffer.

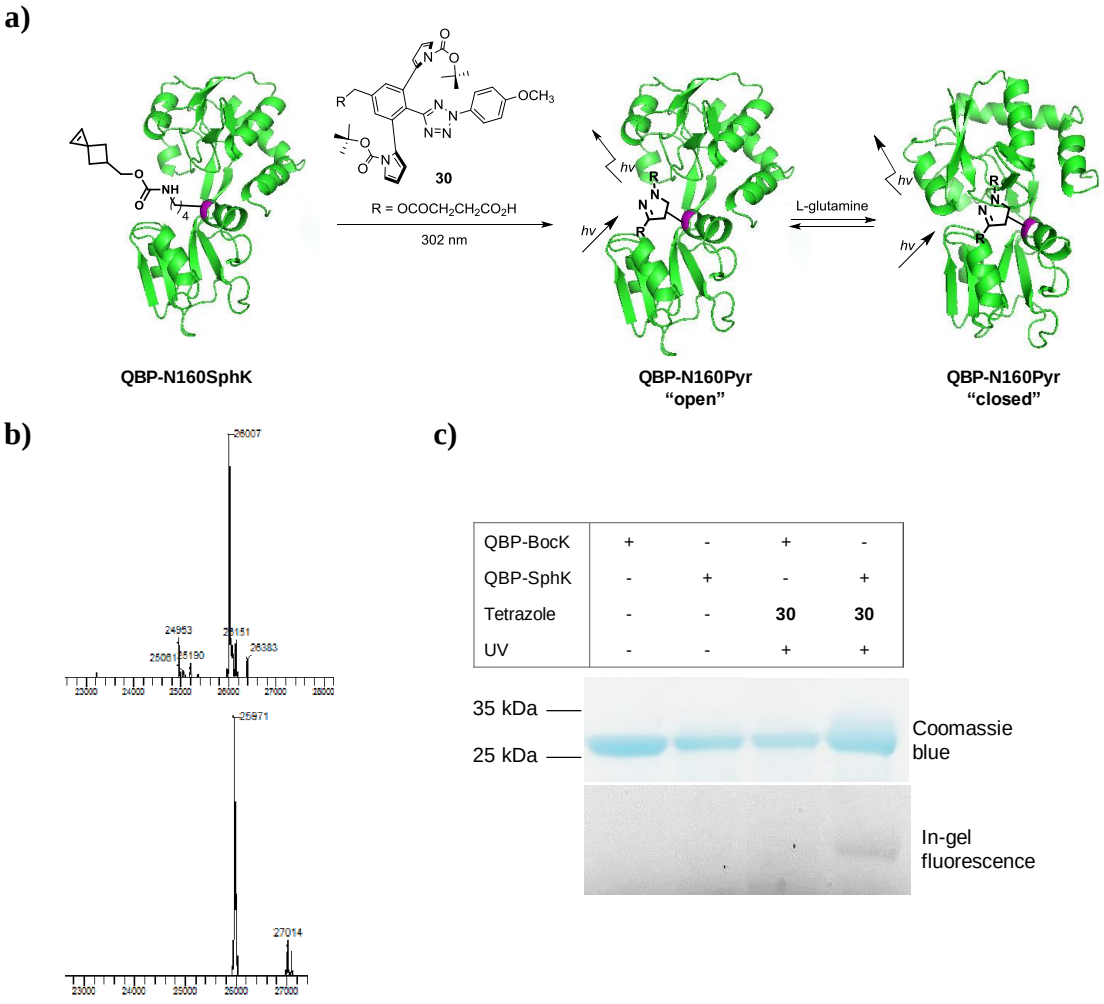

Figure S16. *In situ* synthesis of a pyrazoline-based QBP fluorescence sensor. (**a**) Scheme for reaction of a QBP mutant encoding SphK at position-160 (purple color) with a water-soluble tetrazole **30**. (**b**) ESI-MS analyses of QBP mutants. For QBP-N160SphK, calcd mass 26006 Da, found 26007 Da; for QBP-N160BocK, calcd mass 25970 Da, found 25971 Da. (**c**) SDS-PAGE analyses of the reaction products showing alkene-dependent fluorescent labeling of QBP protein. Top panel, Coomassie staining; bottom panel, in-gel fluorescence analysis.

a)

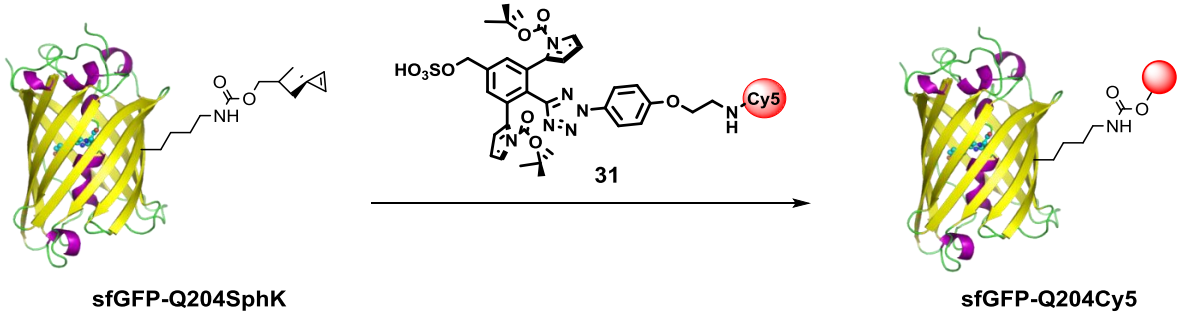

sfGFP-Q204SphK

sfGFP-Q204Cy5

b)

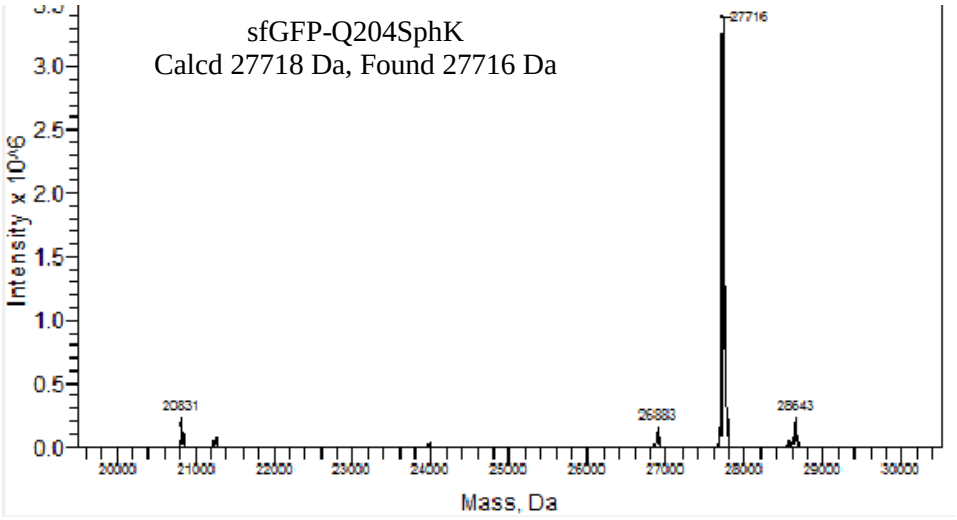

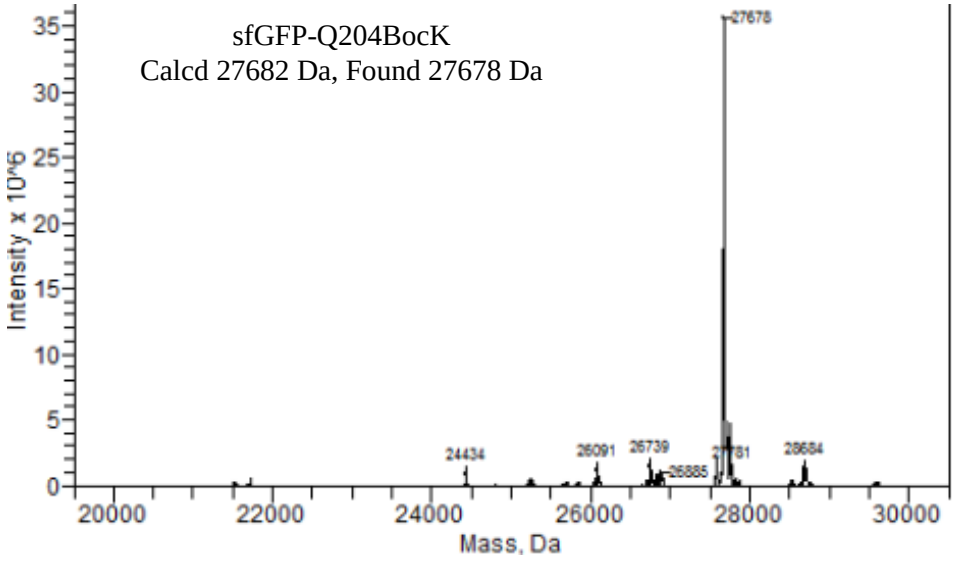

c)

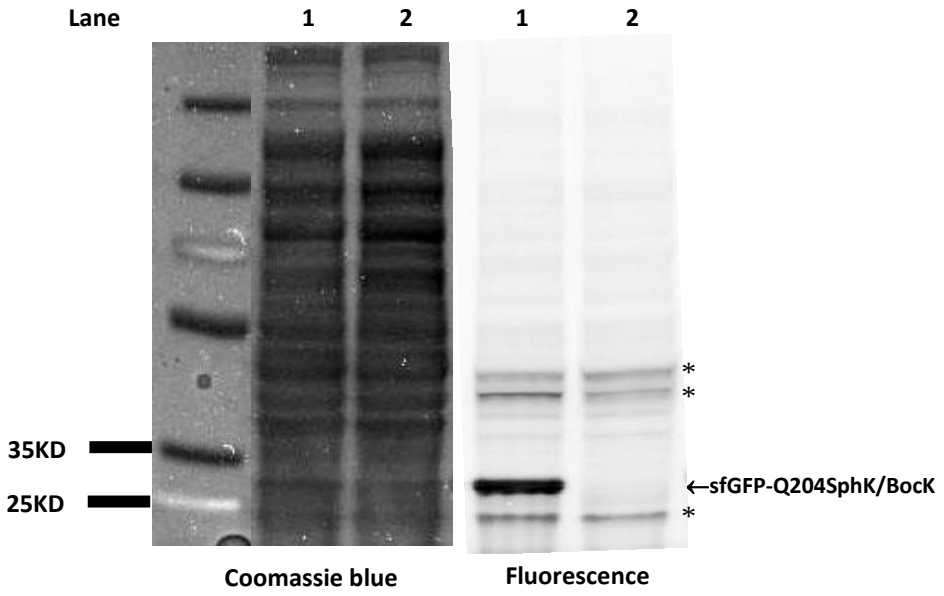

Figure S17. SDS-PAGE analysis of fluorescent labeling the SphK-encoded sfGFP in *E. coli* cell lysates. (**a**) Reaction scheme. (**b**) De-convoluted masses of sfGFP-Q204SphK and sfGFP-Q204BocK. The sfGFP construct we used here contains the T65G and Y66G mutations, which effectively knocks out the intrinsic GFP fluorescence. (**c**) SDS-PAGE analysis of the lysates of *E. coli* cells expressing either sfGFP-Q204SphK (lane 1) or sfGFP-Q204BocK (lane 2) after treating the lysates with the Cy5-conjugated tetrazole **31**: left panel, Coomassie blue staining; right panel, in-gel fluorescence imaging. Asterisks indicate weak background labeling, likely due to non-specific association of tetrazole **31** with these proteins in the cell lysates.

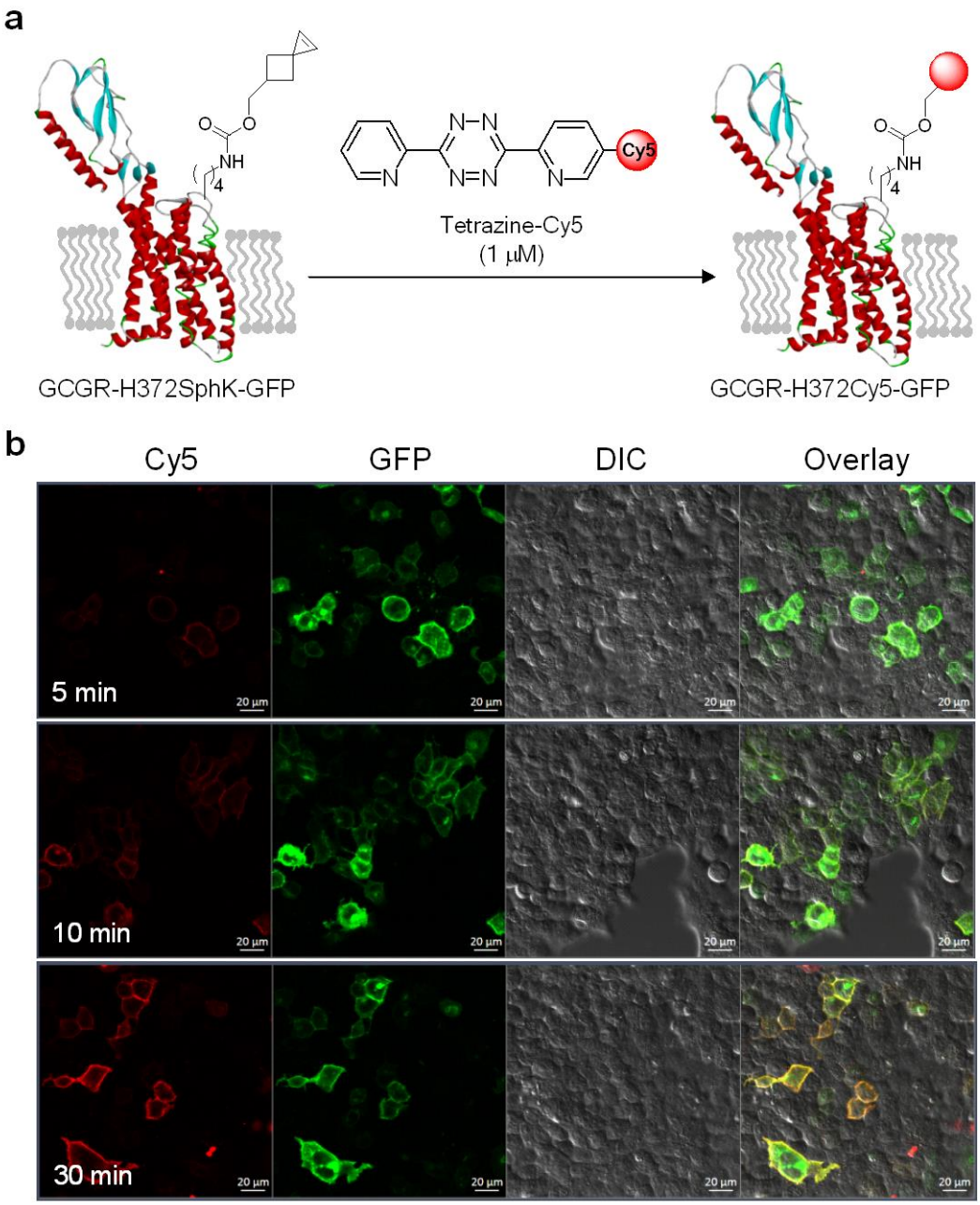

Figure S18. Bioorthogonal labeling of GCGR in live HEK 293T cells via tetrazine ligation. (**a**) Scheme for bioorthogonal labeling of a GCGR-GFP mutant encoding SphK at position-372 with a Cy5-funtionalized tetrazine. (**b**) Confocal micrographs of HEK 293T cells expressing GCGR-GFP-H372SphK after treated with 1 μM tetrazine-Cy5[S1] for 5, 10, or 30 min in DMEM medium. Scale bar = 20 μm.

a)

	Events	% of Vis	X Mean	Y Mean
All events	10,000	100.00	137.81	4.85
Left Bottom	9,961	99.61	134.85	4.55
Right Bottom	23	0.23	837.70	32.31
Left Top	7	0.07	473.40	112.14
Right Top	9	0.09	1,373.34	186.50

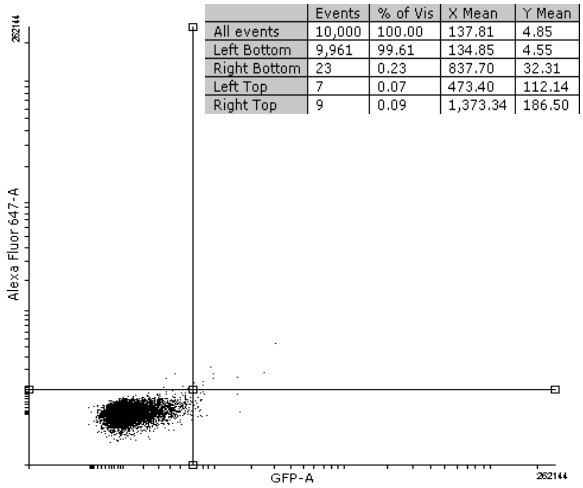

b)

	Events	% of Vis	X Mean	Y Mean
All events	10,000	100.00	3,292.24	6.53
Left Bottom	6,726	67.26	233.20	3.87
Right Bottom	3,231	32.31	9,693.65	5.61
Left Top	30	0.30	229.30	517.21
Right Top	13	0.13	2,063.84	435.48

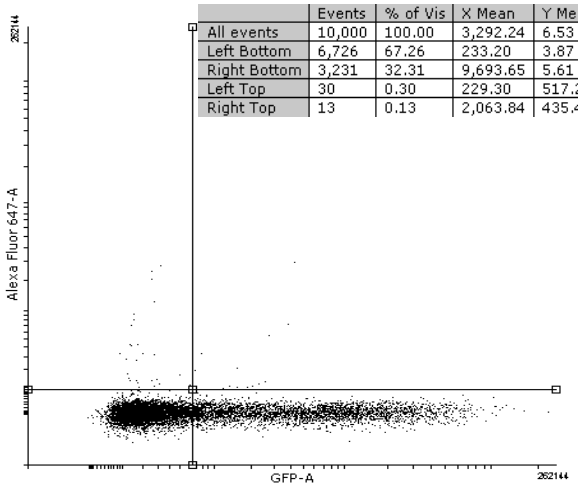

c)

	Events	% of Vis	X Mean	Y Mean
All events	10,000	100.00	3,190.76	298.32
Left Bottom	5,547	55.47	207.62	46.78
Right Bottom	378	3.78	1,321.70	62.94
Left Top	1,038	10.38	351.27	568.14
Right Top	3,037	30.37	9,842.50	694.83

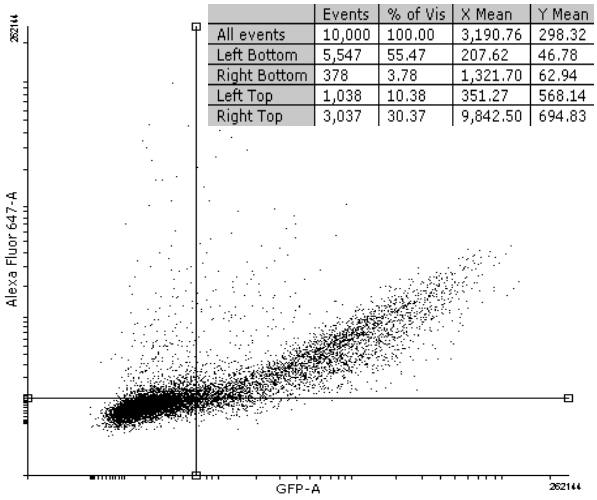

Figure S19. Flow cytometry analysis of the GCGR-expressing HEK 293T cells after treated with the Cy5-conjugated tetrazole **31**. (**a**) GCGR-H372SphK-expressing HEK 293T cells. (**b**) GCGR-GFP-H372SphK-expressing HEK 293T cells prior to treatment. (**c**) GCGR-GFP-H372SphK-expressing HEK 293T cells after treated with 500 nM tetrazole-Cy5 for 1 min. The cell number and mean Cy5 fluorescence (Y mean) in each quadrant are shown in the tables. The cell labeling efficiency is calculated as follows: % labeling = #cells in right top / (# cells in right bottom + # cells in right top). For GCGR-GFP-H372SphK, % labeling = 3037 / (3037 + 378) = 3037/3415= 89%.

Supplemental Methods

Expression and purification of unnatural amino acid-containing sfGFP mutants. BL21(DE3) cells were transformed with the pEVOL-PylT-mmPylKRS and pET-sfGFP-GGG-Q204TAG plasmids. The cells were recovered in 1 mL SOC medium following transformation and incubated at 37 ºC for 1 hour before plating on LB agar plate containing chloramphenicol (Cam) (34 μg/mL) and ampicillin (Amp) (100 μg/mL). A 5-mL overnight culture from a single colony was used to inoculate 25 mL LB medium supplemented with Cam and Amp. Cells were grown at 37 ºC in a shaker-incubator (250 rpm), and the protein expression was induced by adding 1 mM IPTG, 0.2% arabinose, and 1 mM SphK for sfGFP-Q204SphK or 1 mM BocK for sfGFP-Q204BocK when OD_{600} reached 0.6. After 6-hour induction, cells were harvested, resuspended in a lysis buffer (50 mM NaH_2PO_4, 300 mM NaCl, 10 mM imidazole, pH 8.0), and sonicated in an ice/water bath ten times (10 sec each with 20 sec interval). The lysate was centrifuged (30 min, 4 ºC). The supernatant was incubated with 0.1 mL Ni-NTA resin (Thermo HisPur™) (2 hours, 25 ºC). The slurry was then loaded to a column and the protein-bound resin was washed twice with 3 mL washing buffer (50 mM Na_2HPO_4, 300 mM NaCl, 50 mM imidazole, pH 8.0). The protein was eluted off the resin using the elution buffer (50 mM Na_2HPO_4, 300 mM NaCl, 250 mM imidazole, pH 8.0). The eluted fractions were collected, concentrated, and subjected to buffer-exchange to DPBS containing 100 μM TCEP using 10 kD MWCO spin column column (Thermo Scientific). The protein identity was verified by LC/ESI-MS. For SDS-PAGE analysis, protein in cell lysates was added 25 μM tetrazole-Cy5 and the mixture was irradiated with a handheld 302-nm UV lamp for 1 min. The sample was then added with the loading buffer and heated to 100 ºC for 10 min before loaded to the gel. Sodium dodecyl sulfate-polyacrylamide gel electrophoresis of proteins was performed on an XCell SureLock Mini-Cell apparatus using the precast NuPAGE 4-12% Bis-Tris gels (Invitrogen). BenchMark Prestained Protein Ladder was applied to one lane of each gel for estimation of apparent molecular weight.

Cloning and mutagenesis. The cloning of GCGR-GFP and site-specific amber mutagenesis of glucagon receptor (GCGR) were carried out as reported previously.[S1] The bacterial expression construct QBP-N160TAG was derived from pETtrio-1-AcKRS-pylT(TAA)-QBP141TAA in which position-141 was mutated back to Asn using the following primer pair: 5'–CTGCGTCAGTTCCCGAACATCGATAATGC CTATATGG–3' and 5'–GTTGGTGCCCAGTTCCATATAGGCATTATCGATGTTC–3'. Afterwards, Asn160 was mutated to TAG using the following primer pair: 5'–CGATACGCCATAGATTCTGTACTT CATCAAAACCG–3' and 5'–TGCAGAACGGCGTCTGCG–3'.

HEK 293T cell culture and transfection. HEK 293T cells were maintained in a growth medium containing Dulbecco's modified eagle medium (DMEM, Life Technologies) supplemented with 10% (v/v) fetal bovine serum (FBS, Life Technologies) and 10 μg/mL gentamicin (Life Technologies). Transfection was performed at 70-80% confluency using 3:1 reagent/DNA ratio of Lipofectamine 2000 (Life Technologies) with 2.5 μg total DNA or polyethylenimine (PEI, Polysciences Inc.) with 3 μg total DNA per 35-mm dish. For imaging experiments, cells were maintained in 35-mm glass bottom culture dishes using FluoroBrite DMEM medium (Life Technologies) supplemented with 10% FBS, 4 mM L-glutamine, and 25 mM HEPES.

General Information

Solvents and chemicals were purchased from commercial sources and used directly without further purification. N^{ε}-Boc-lysine (BocK) was purchased from Chem-Impex (Cat. No. 00363). TCO-amine was purchased from Click Chemistry Tools. Sph and 3,3-cyclopropene were synthesized by following our previous report[S2]. 1,3-Cylopropene was synthesized by following the reported procedure[S3]. Flash chromatography was performed either manually with SiliCycle P60 silica gel (40-63 μm, 60 Å) or an automatic Yamazen AKROS flash system equipped with SiliaSep HP pre-packed columns. ^{1}H NMR spectra were recorded with Inova-300, -400 or -500 MHz spectrometers. Chemical shifts were reported in ppm using TMS or deuterated solvents as internal standards (TMS, 0.00; $CDCl_3$, 7.26; CD_3OD, 3.31; DMSO-d_6, 2.50; acetone-d_6, 2.05). Multiplicity was reported as follows: s = singlet, d = doublet, t = triplet, q = quartet, m = multiplet, brs = broad. ^{13}C NMR spectra were recorded at 75.4 MHz, and chemical shifts were reported in ppm using deuterated solvents as internal standards ($CDCl_3$, 77.0; DMSO-d_6, 39.5; CD_3OD, 49.05; acetone-d_6, 30.0). UV-Vis absorption spectra were recorded using 1-cm quartz cuvette on a HP-8452 Diode Array Spectrophotometer. Fluorescence spectra were recorded using 1-cm quartz cuvette on a Horiba FluoroMax-4 spectrofluorometer at 25 ºC. High resolution mass spectrometry was performed on a Thermo LTQ-Orbitrap XL mass spectrometer equipped with collision cells for collision induced dissociation. Low resolution mass spectrometry was performed on a Thermo LCQ mass spectrometer.

Scheme S1

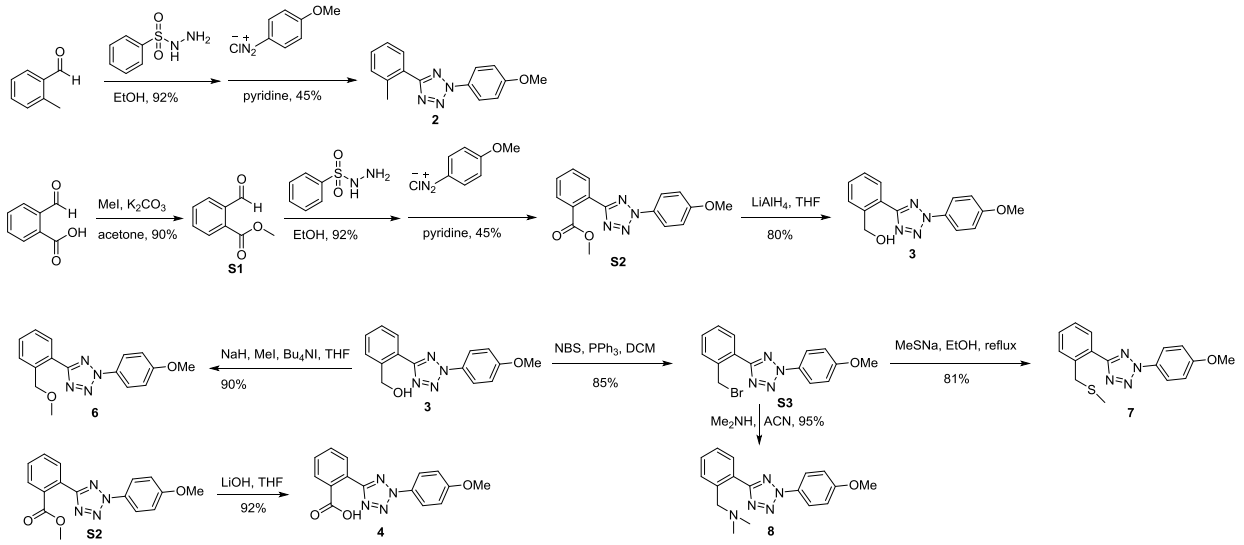

2-(4-Methoxyphenyl)-5-(o-tolyl)-2*H*-tetrazole (2): To a solution of benzenesulfonohydrazide (1.43 g, 8.3 mmol) in ethanol was added 2-methylbenzaldehyde (962 μL, 8.3 mmol), and the mixture was stirred at room temperature for 3 hours. The solvent was removed and small amount of water was added to precipitate the solid, which was then collected by filtration and dried to give the sulfohydrazone intermediate as a white solid (2.1 g, 45%). Preparation of diazonium salt: to a mixed solution of 4-methoxyaniline (1.1 g, 9.0 mmol) in ethanol/water (2:1;10 mL,) cooled with an ice-water bath was added sequentially 2.0 mL concentrated HCl and 1.0 mL sodium nitrite (0.69 g, 10.0 mmol) solution in water, and the mixture was stirred for about 10 min before the color turned purple. To a solution of sulfohydrazone (1.0 g, 3.7 mmol) in pyridine (50 mL) cooled with an ice-salt bath was added the freshly prepared diazonium salt, and the mixture was stirred while temperature was allowed to gradually increase to room temperature. After about 6 hours, the solvent

was removed and DCM (50 mL) was added. The mixture was washed with 1 N HCl before the solvent was evaporated under reduced pressure. The residue was purified by silica gel flash chromatography using ethyl acetate/hexanes as eluent to give the title product as a colorless solid (435 mg, 45%): ^{1}H NMR (400 MHz, $CDCl_3$) δ 8.12 (d, J = 9.1 Hz, 3H), 7.49–7.30 (m, 3H), 7.07 (d, J = 9.1 Hz, 2H), 3.90 (s, 3H), 2.71 (s, 3H); ^{13}C NMR (100 MHz, $CDCl_3$) δ 165.28, 160.34, 137.48, 131.34, 129.90, 129.44, 126.28, 125.96, 124.24, 121.21, 114.57, 114.06, 55.55, 21.73; HRMS calcd for $C_{15}H_{14}N_4O$ 267.1240 [M+H$^+$], found 267.1235.

Methyl 2-formylbenzoate (S1): Compound **S1** was synthesized as a colorless solid with 90% yield: ^{1}H NMR (400 MHz, $CDCl_3$) δ 10.61 (s, 1H), 7.88 (m, 2H), 7.62 (m, 2H), 3.99 (s, 3H).

Methyl 2-(2-(4-methoxyphenyl)-2*H*-tetrazol-5-yl)benzoate (S2): Compound **S2** was synthesized using the same procedure as compound **2** with 45% yield: ^{1}H NMR (400 MHz, $CDCl_3$) δ 8.07 (d, J = 9.2 Hz, 2H), 7.97–7.89 (m, 1H), 7.83–7.76 (m, 1H), 7.58 (m, 2H), 7.03 (d, J = 9.2 Hz, 2H), 3.86 (s, 3H), 3.80 (s, 3H).

(2-(2-(4-Methoxyphenyl)-2*H*-tetrazol-5-yl)phenyl)methanol (3): To a solution of tetrazole **S2** (158 mg, 0.51 mmol) in 10 mL anhydrous THF at 0 ºC was add $LiAlH_4$ (58 mg, 1.53 mmol). After TLC showed complete disappearance of the starting materials, the reaction was quenched by adding 1 mL methanol. The solvent was evaporated in vacuum, and the residue was purified by flash chromatography using ethyl acetate/hexanes as eluent to give the title product as a white solid (115 mg, 80%): ^{1}H NMR (400 MHz, $CDCl_3$) δ 8.17 (dd, J = 7.3, 1.6 Hz, 1H), 8.04 (d, J = 9.1 Hz, 2H), 7.55–7.47 (m, 1H), 7.47–7.39 (m, 2H), 7.01 (d, J = 9.1 Hz, 2H), 4.81 (d, J = 7.5 Hz, 2H), 4.60 (t, J = 7.5 Hz, 1H), 3.84 (s, 3H); ^{13}C NMR (100 MHz, $CDCl_3$) δ 164.43, 160.62, 139.87, 130.63, 130.43, 129.90, 129.43, 128.12, 125.50, 121.26, 114.63, 64.25, 55.53; HRMS calcd for $C_{15}H_{14}N_4O_2$ 283.1190 [M+H$^+$], found 283.1188.

5-(2-(Methoxymethyl)phenyl)-2-(4-methoxyphenyl)-2*H*-tetrazole (6): To a solution of alcohol **3** (53 mg, 0.19 mmol) in anhydrous THF at 0 ºC was added NaH (60%, 23 mg, 0.56 mmol), and the mixture was stirred at room temperature for 10 min. Then tetrabutylammonium iodide (14 mg, 0.038 mmol) and methyl iodide (35 μL, 0.56 mmol) were added. The mixture was stirred at room temperature until the starting material was completely consumed. Afterwards, several drops of saturated NH_4Cl solution were added followed by addition of water. The solution was extracted with ethyl acetate, and the organic layer was collected and evaporated. The residue was purified by flash chromatography using ethyl acetate/hexanes as eluent to give the title product as a white solid (50 mg, 90%): ^{1}H NMR (500 MHz, $CDCl_3$) δ 8.18 (d, J = 7.7 Hz, 1H), 8.11 (d, J = 9.0 Hz, 2H), 7.70 (d, J = 7.7 Hz, 1H), 7.52 (t, J = 7.5 Hz, 1H), 7.44 (t, J = 7.5 Hz, 1H), 7.07 (d, J = 9.0 Hz, 2H), 4.97 (s, 2H), 3.90 (s, 3H), 3.48 (s, 3H); ^{13}C NMR (75 MHz, $CDCl_3$) δ 164.56, 160.43, 137.67, 130.17, 129.39, 128.08, 127.46, 124.91, 121.24, 114.62, 72.59, 58.54, 55.57; HRMS calcd for $C_{16}H_{16}N_4O_2$ 297.1346 [M+H$^+$], found 297.1344.

5-(2-(Bromomethyl)phenyl)-2-(4-methoxyphenyl)-2*H*-tetrazole (S3): To a solution of alcohol **3** (55 mg, 0.20 mmol) in DCM cooled to 0 °C was added PPh_3 (102 mg, 0.39 mmol) and NBS (69 mg, 0.39 mmol), and the reaction mixture was stirred overnight. The mixture was filtered through a thin pad of neutral alumina, and the filtrate was concentrated to give a yellow solid. The residue was purified by silica gel flash chromatography to give the desired product as a white solid (57 mg, 85%): ^{1}H NMR (400 MHz, $CDCl_3$) δ 8.23 (dd, J = 5.5, 3.6 Hz, 1H), 8.10 (d, J = 9.1 Hz, 2H), 7.54 (dd, J = 5.4, 3.6 Hz, 1H), 7.44 (dd, J = 5.8, 3.4 Hz, 2H), 7.04 (d, J = 9.1 Hz, 2H), 5.14 (s, 2H), 3.85 (s, 3H); ^{13}C NMR (100 MHz, $CDCl_3$) δ 163.84, 160.43, 136.53, 131.60, 130.43, 130.16, 129.88, 128.83, 125.81, 121.21, 114.59, 55.54, 32.48; HRMS calcd for $C_{15}H_{13}BrN_4O$ 345.0346 [M+H$^+$], found 345.0344.

2-(4-Methoxyphenyl)-5-(2-((methylthio)methyl)phenyl)-2*H*-tetrazole (7): To a solution of Me_2S_2 (4 g, 43.6 mmol) in 50 mL anhydrous THF was added sodium (0.5 g, 21.7 mmol), and the mixture was stirred

at room temperature under argon overnight. The precipitated white solid was filtered, washed with diethyl ether, and dried to give sodium thiomethylate. To a solution of tetrazole **S3** (20 mg, 0.058 mmol) in ethanol (5 mL) was added sodium thiomethylate (8.3 mg, 0.116 mmol) solution in 2 mL ethanol. The suspension was stirred while refluxing for 1 hour. The reaction mixture was cooled to room temperature, and the mixture was diluted with water and extracted with diethyl ether. The organic layer was collected, concentrated, and purified by silica gel flash chromatography to give the desired product as a white solid (15 mg, 81%): ^{1}H NMR (400 MHz, $CDCl_3$) δ 8.20 (d, J = 6.6 Hz, 1H), 8.11 (d, J = 9.1 Hz, 2H), 7.47–7.34 (m, 3H), 7.06 (d, J = 9.1 Hz, 2H), 4.26 (s, 2H), 3.89 (s, 3H), 2.01 (s, 3H); ^{13}C NMR (100 MHz, $CDCl_3$) δ 164.66, 160.48, 137.69, 130.91, 130.41, 130.21, 129.92, 127.38, 126.02, 121.33, 114.68, 55.64, 36.73, 15.10; HRMS calcd for $C_{16}H_{16}N_4OS$ 313.1118 [M+H$^+$], found 313.1112.

1-(2-(2-(4-Methoxyphenyl)-2*H*-tetrazol-5-yl)phenyl)-*N*,*N*-dimethylmethanamine (8): To a solution of tetrazole **S3** (24 mg, 0.07 mmol) in acetonitrile was added dimethyl amine (40%; 88 μL, 0.7 mmol), and the reaction mixture was stirred at room temperature for 1 hour. The reaction mixture was diluted with water and extracted with DCM, and the organic layer was washed with brine, dried over Na_2SO_4, and concentrated to give the title compound as a white solid (20 mg, 95%): ^{1}H NMR (400 MHz, $CDCl_3$) δ 8.11–8.07 (m, 3H), 7.59 (d, J = 7.4 Hz, 1H), 7.50–7.36 (m, 2H), 7.06 (d, J = 9.1 Hz, 2H), 3.90 (d, J = 9.6 Hz, 5H), 2.25 (s, 6H); ^{13}C NMR (100 MHz, $CDCl_3$) δ 165.06, 160.40, 138.27, 130.75, 130.02, 129.91, 127.25, 126.65, 121.30, 114.65, 77.30, 76.99, 76.67, 61.53, 55.62, 45.51; HRMS calcd for $C_{17}H_{19}N_5O$ 310.1662 [M+H$^+$], found 310.1664.

2-(2-(4-Methoxyphenyl)-2*H*-tetrazol-5-yl)benzoic acid (4): Compound **4** was synthesized as a colorless solid with 92% yield from **S2**: ^{1}H NMR (500 MHz, acetone-d_6) δ 8.04 (d, J = 8.5 Hz, 2H), 7.91 (d, J = 7.3 Hz, 1H), 7.84 (d, J = 7.3 Hz, 1H), 7.70–7.56 (m, 2H), 7.11 (d, J = 7.3 Hz, 2H), 3.87 (s, 3H).

Scheme S2

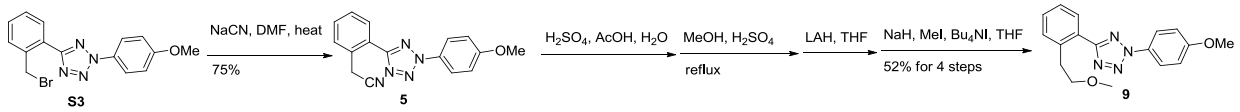

2-(2-(2-(4-Methoxyphenyl)-2*H*-tetrazol-5-yl)phenyl)acetonitrile (5): To a solution of tetrazole **S3** (100 mg, 0.29 mmol) in DMF (10 mL) was added NaCN (43 mg, 0.87 mmol), and the suspension was stirred at 80 °C overnight. After cooling to room temperature, the reaction mixture was added water and extracted with diethyl ether. The ether layer was concentrated, and the resulting residue was purified by silica gel flash chromatography to give the desired product as a white solid (63 mg, 75%): ^{1}H NMR (500 MHz, $CDCl_3$) δ 8.32 (dd, J = 7.2, 1.7 Hz, 1H), 8.10 (d, J = 9.0 Hz, 2H), 7.66 (d, J = 6.9 Hz, 1H), 7.61–7.44 (m, 2H), 7.07 (d, J = 9.0 Hz, 2H), 4.36 (s, 2H), 3.90 (s, 3H); ^{13}C NMR (126 MHz, $CDCl_3$) δ 163.91, 160.69, 130.83, 130.04, 129.92, 128.95, 128.62, 125.73, 121.40, 117.85, 114.75, 55.65, 23.52; HRMS calcd for $C_{16}H_{13}N_5O$ 292.1193 [M+H$^+$], found 292.1189.

5-(2-(2-Methoxyethyl)phenyl)-2-(4-methoxyphenyl)-2*H*-tetrazole (9): To a round bottom flask was added tetrazole **5** (60 mg, 0.21 mmol), water (5.3 mL), acetic acid (6 mL), concentrated sulfuric acid (5 mL), and the mixture was stirred at 110 °C overnight. After cooling to room temperature, water was added and the mixture was extracted with ethyl acetate. The organic layer was collected, dried over Na_2SO_4, and concentrated to give the carboxylic acid intermediate. The acid was then dissolved in methanol and heated to reflux in the presence of catalytic amount of sulfuric acid until TLC showed complete conversion of the

carboxylic acid to the ester. Water was then added and the mixture was extracted by ethyl acetate. The organic layer was washed sequentially with water and saturated $NaHCO_3$ solution, dried over Na_2SO_4, and concentrated to give the ester intermediate. To the solution of ester in hydrous THF was added $LiAlH_4$ (20 mg, 0.5 mmol), the mixture was stirred at room temperature until TLC showed complete consumption of the starting material. The reaction was quenched by adding 1 mL methanol, and the mixture was filtered through Celite, washed with ethyl acetate, and concentrated to give the alcohol intermediate. Finally, to a solution of alcohol in anhydrous THF at 0 °C was added NaH (60%; 21 mg, 0.51 mmol), and the mixture was stirred at room temperature for 10 min. Then tetrabutylammonium iodide (13 mg, 0.036 mmol) and methyl iodide (105 μL, 1.70 mmol) were added. The mixture was stirred at room temperature for 8 hours. Several drops of saturated NH_4Cl solution were added followed by water. The mixture was extracted with ethyl acetate. After evaporating the solvent under reduced pressure, the residue was purified by silica gel flash chromatography using ethyl acetate/hexanes as eluent to give the title compound as a white solid (33 mg, 52%): ^{1}H NMR (500 MHz, $CDCl_3$) δ 8.22–8.01 (m, 3H), 7.49–7.31 (m, 3H), 7.06 (d, J = 9.0 Hz, 2H), 3.89 (s, 3H), 3.69 (t, J = 7.1 Hz, 2H), 3.44–3.25 (m, 5H); ^{13}C NMR (126 MHz, $CDCl_3$) δ 165.00, 160.44, 138.10, 131.43, 130.07, 129.92, 126.68, 126.32, 121.24, 114.67, 73.14, 58.56, 55.62, 34.49; HRMS calcd for $C_{17}H_{18}N_4O_2$ 311.1503 [M+H$^+$], found 311.1538.

Scheme S3

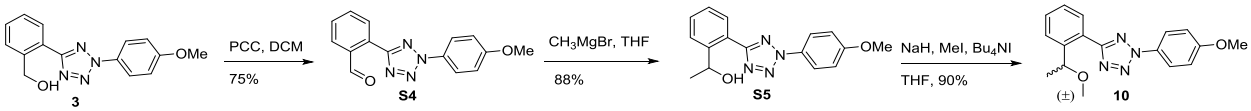

2-(2-(4-Methoxyphenyl)-2*H*-tetrazol-5-yl)benzaldehyde (S4): To a solution of tetrazole **3** (110 mg, 0.39 mmol) in DCM was added PCC (126 mg, 0.59 mmol), and the mixture was stirred at room temperature overnight. The solution was concentrated under reduced pressure, and the residue was purified by silica gel flash chromatography to give the desired product as a white solid (82 mg, 75%): ^{1}H NMR (500 MHz, $CDCl_3$) δ 10.81 (s, 1H), 8.24 (d, J = 7.8 Hz, 1H), 8.15–8.06 (m, 3H), 7.76 (t, J = 7.6 Hz, 1H), 7.65 (t, J = 7.6 Hz, 1H), 7.09 (d, J = 8.9 Hz, 2H), 3.91 (s, 3H); ^{13}C NMR (100 MHz, $CDCl_3$) δ 192.07, 163.04, 160.77, 134.67, 133.71, 130.47, 130.08, 128.97, 128.11, 121.40, 114.76, 55.66; HRMS calcd for $C_{15}H_{12}N_4O_2$ 281.1033 [M+H$^+$], found 281.1030.

(±)1-(2-(2-(4-Methoxyphenyl)-2*H*-tetrazol-5-yl)phenyl)ethanol (S5): To a solution of tetrazole **S4** (50 mg, 0.18 mmol) was in anhydrous THF was added methylmagnesium bromide (3 M in ether; 0.30 mL, 0.89 mmol), and the mixture was stirred at 50 °C under argon. After TLC showed complete disappearance of the starting materials, drops of saturated NH_4Cl solution was added followed by water. The mixture was then extracted with ethyl acetate, and the organic layer was separated and concentrated. The residue was purified by silica gel flash chromatography to give the desired product as a white solid (47 mg, 88%): ^{1}H NMR (400 MHz, $CDCl_3$) δ 8.17–7.97 (m, 3H), 7.74 (dd, J = 7.7, 0.6 Hz, 1H), 7.53 (td, J = 7.6, 1.3 Hz, 1H), 7.43 (td, J = 7.6, 1.3 Hz, 1H), 7.07 (d, J = 9.2 Hz, 2H), 5.37 (dd, J = 6.4, 4.7 Hz, 1H), 3.92 (d, J = 6.5 Hz, 1H), 3.89 (s, 3H), 1.62 (d, J = 6.5 Hz, 3H); ^{13}C NMR (100 MHz, $CDCl_3$) δ 164.72, 160.68, 144.34, 130.74, 130.15, 129.97, 127.63, 126.35, 124.90, 121.37, 114.75, 66.64, 55.66, 22.45; HRMS calcd for $C_{16}H_{16}N_4O_2$ 297.1346 [M+H$^+$], found 297.1343.

(±)5-(2-(1-Methoxyethyl)phenyl)-2-(4-methoxyphenyl)-2*H*-tetrazole (10): Tetrazole **10** was synthesized using the same etherification procedure as **6** with 90% yield: ^{1}H NMR (400 MHz, $CDCl_3$) δ 8.19–7.99 (m, 3H), 7.74 (d, J = 7.8 Hz, 1H), 7.55 (t, J = 7.5 Hz, 1H), 7.42 (t, J = 7.5 Hz, 1H), 7.07 (d, J =

9.1 Hz, 2H), 5.20 (d, *J* = 6.2 Hz, 1H), 3.89 (s, 3H), 3.21 (s, 3H), 1.55 (d, *J* = 6.3 Hz, 3H); ^{13}C NMR (100 MHz, $CDCl_3$) δ 164.60, 160.52, 143.55, 130.68, 130.34, 129.62, 127.26, 126.08, 125.13, 121.25, 114.71, 75.82, 56.60, 55.64, 23.86; HRMS calcd for $C_{17}H_{18}N_4O_2$ 311.1503 [M+H$^+$], found 311.1538.

Scheme S4

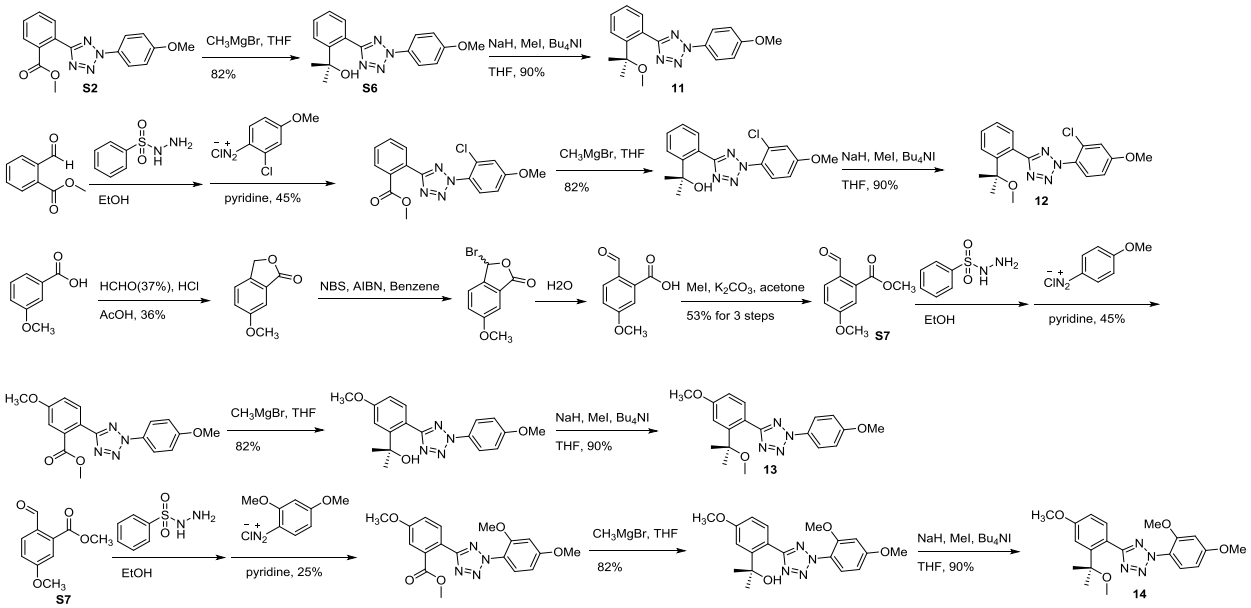

2-(2-(2-(4-Methoxyphenyl)-2*H*-tetrazol-5-yl)phenyl)propan-2-ol (S6): To a solution of tetrazole **S2** (60 mg, 0.19 mmol) in anhydrous THF was added methylmagnesium bromide (3 M in ether; 0.33 mL, 1.0 mmol), and the mixture was stirred at 70 °C under argon until TLC showed complete disappearance of the starting materials. Drops of saturated NH_4Cl solution were then added followed by water. The mixture was extracted with ethyl acetate and the organic layer was collected and concentrated to dryness. The residue was purified by silica gel flash chromatography to give the desired product as a white solid (49 mg, 82%): ^{1}H NMR (400 MHz, $CDCl_3$) *δ* 8.18–8.02 (m, 2H), 7.92 (dd, *J* = 7.7, 1.4 Hz, 1H), 7.67 (dd, *J* = 8.0, 1.0 Hz, 1H), 7.50 (td, *J* = 7.7, 1.6 Hz, 1H), 7.41 (td, *J* = 7.5, 1.2 Hz, 1H), 7.15–6.97 (m, 2H), 5.52 (s, 1H), 3.89 (s, 3H), 1.61 (s, 6H); ^{13}C NMR (100 MHz, $CDCl_3$) *δ* 166.75, 160.71, 147.51, 132.42, 130.41, 129.99, 127.08, 126.49, 124.73, 121.36, 114.72, 72.26, 55.62, 30.77; HRMS calcd for $C_{17}H_{16}N_4O_2$ 311.1502 [M+H$^+$], found 311.1496.

2-(4-Methoxyphenyl)-5-(2-(2-methoxypropan-2-yl)phenyl)-2*H*-tetrazole (11): Tetrazole **11** was synthesized using the same etherification procedure as **6** with 90% yield: ^{1}H NMR (400 MHz, $CDCl_3$) *δ* 8.09 (d, *J* = 9.2 Hz, 2H), 7.62–7.41 (m, 2H), 7.41–7.29 (m, 2H), 7.05 (d, *J* = 9.2 Hz, 2H), 3.88 (s, 3H), 2.89 (s, 3H), 1.63 (s, 6H); ^{13}C NMR (100 MHz, $CDCl_3$) *δ* 166.90, 160.31, 146.06, 132.55, 130.54, 130.01, 127.17, 126.75, 126.27, 121.24, 114.61, 77.96, 55.61, 50.55, 28.97; HRMS calcd for $C_{18}H_{20}N_4O_2$ 325.1659 [M+H$^+$], found 325.1654.

2-(2-Chloro-4-methoxyphenyl)-5-(2-(2-methoxypropan-2-yl)phenyl)-2*H*-tetrazole (12): Tetrazole **12** was synthesized using the same procedure as **11** except 2-chloro-4-methoxyaniline was used a starting material: ^{1}H NMR (500 MHz, $CDCl_3$) *δ* 7.58 (d, *J* = 8.9 Hz, 1H), 7.54–7.46 (m, 2H), 7.43–7.31 (m, 2H), 7.13 (d, *J* = 2.3 Hz, 1H), 6.97 (dd, *J* = 8.8, 2.3 Hz, 1H), 3.89 (s, 3H), 2.91 (s, 3H), 1.63 (s, 6H); ^{13}C NMR (126 MHz, $CDCl_3$) *δ* 167.01, 161.33, 146.21, 132.64, 130.87, 130.04, 128.54, 127.16, 126.68, 125.96,

115.88, 113.31, 77.96, 55.93, 50.53, 28.91; HRMS calcd for $C_{18}H_{19}ClN_4O_2$ 359.1269 [M+H$^+$], found 359.1265.

Methyl 2-formyl-5-methoxybenzoate (S7) Aldehyde **S7** was synthesized using a reported procedure[S4]: ^{1}H NMR (300 MHz, $CDCl_3$) δ 10.48 (s, 1H), 7.95 (d, J = 6.0 Hz, 1H), 7.40 (s, 1H), 7.11 (d, J = 6.0 Hz, 1H), 3.98 (s, 3H), 3.90 (s, 3H).

5-(4-Methoxy-2-(2-methoxypropan-2-yl)phenyl)-2-(4-methoxyphenyl)-2*H*-tetrazole (13): Tetrazole **13** was synthesized using the same procedure as **11** from aldehyde **S5**: ^{1}H NMR (500 MHz, $CDCl_3$) δ 8.08 (d, J = 9.1 Hz, 2H), 7.34 (d, J = 8.4 Hz, 1H), 7.05 (dd, J = 15.8, 5.7 Hz, 3H), 6.88 (dd, J = 8.4, 2.5 Hz, 1H), 3.88 (s, 6H), 2.90 (s, 3H), 1.61 (s, 6H); ^{13}C NMR (126 MHz, $CDCl_3$) δ 166.75, 160.75, 160.26, 147.86, 133.89, 121.21, 118.49, 114.59, 113.98, 110.95, 77.92, 55.61, 55.33, 50.61, 28.79; HRMS calcd for $C_{19}H_{22}N_4O_3$ 355.1765 [M+H$^+$], found 355.1759.

2-(2,4-Dimethoxyphenyl)-5-(4-methoxy-2-(2-methoxypropan-2-yl)phenyl)-2*H*-tetrazole (14): Tetrazole **14** was synthesized using the same procedure as **11** with **S7** and 2,4-dimethoxyaniline as the starting materials: ^{1}H NMR (400 MHz, $CDCl_3$) δ 7.52 (d, J = 8.6 Hz, 1H), 7.36 (d, J = 8.4 Hz, 1H), 7.10 (d, J = 2.2 Hz, 1H), 6.87 (dd, J = 8.4, 2.2 Hz, 1H), 6.61 (dd, J = 11.8, 2.9 Hz, 2H), 3.89 (s, 3H), 3.88 (s, 3H), 3.85 (s, 3H), 2.95 (s, 3H), 1.59 (s, 6H); ^{13}C NMR (100 MHz, $CDCl_3$) δ 166.36, 162.30, 160.67, 154.65, 147.93, 133.94, 127.77, 118.61, 113.75, 110.98, 104.45, 99.77, 77.99, 56.09, 55.71, 55.32, 50.60, 28.71; HRMS calcd for $C_{10}H_{24}N_4O_4$ 385.1870 [M+H$^+$], found 385.1863.

Scheme S5

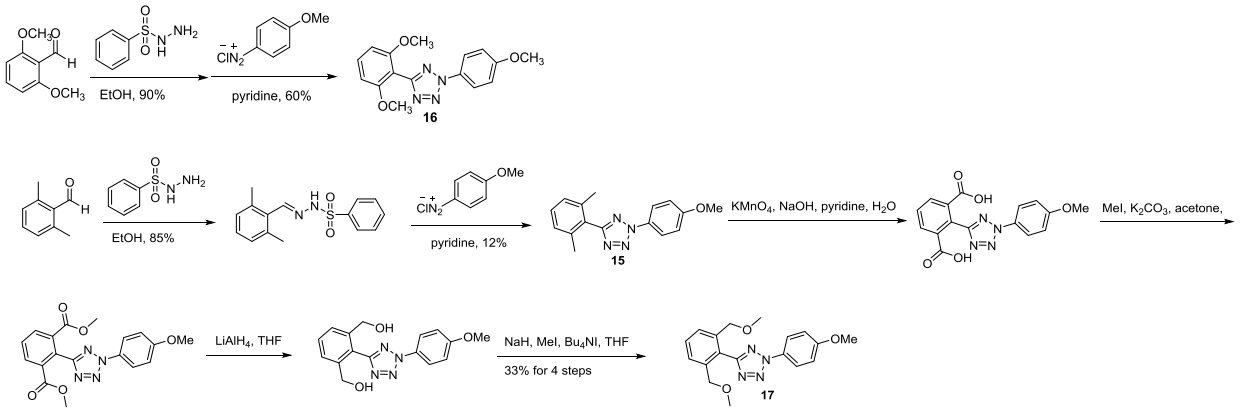

5-(2,6-Dimethoxyphenyl)-2-(4-methoxyphenyl)-2*H*-tetrazole (16): Tetrazole **16** was synthesized using the same procedure as tetrazole **2** with 60% yield: ^{1}H NMR (500 MHz, $CDCl_3$) δ 8.11 (d, J = 9.0 Hz, 2H), 7.41 (t, J = 8.4 Hz, 1H), 7.03 (d, J = 9.0 Hz, 2H), 6.66 (d, J = 8.5 Hz, 2H), 3.87 (s, 3H), 3.76 (s, 6H); ^{13}C NMR (126 MHz, $CDCl_3$) δ 160.31, 159.69, 159.51, 131.93, 130.68, 121.49, 114.53, 105.84, 103.96, 56.03, 55.62; HRMS calcd for $C_{16}H_{16}N_4O_3$ 313.1295 [M+H$^+$], found 313.1298.

5-(2,6-Dimethylphenyl)-2-(4-methoxyphenyl)-2*H*-tetrazole (15): Tetrazole **15** was synthesized using the same procedure as tetrazole **2** with 12% yield: ^{1}H NMR (400 MHz, $CDCl_3$) δ 8.12 (d, J = 9.1 Hz, 2H), 7.28 (dd, J = 14.0, 6.4 Hz, 1H), 7.16 (d, J = 7.6 Hz, 2H), 7.06 (d, J = 9.1 Hz, 2H), 3.89 (s, 3H), 2.22 (s, 6H); ^{13}C NMR (100 MHz, $CDCl_3$) δ 164.04, 160.46, 138.26, 129.67, 127.74, 127.10, 121.27, 114.68, 55.65, 20.49; HRMS calcd for $C_{16}H_{16}N_4O$ 281.1397 [M+H$^+$], found 281.1394.

5-(2,6-Bis(methoxymethyl)phenyl)-2-(4-methoxyphenyl)-2*H*-tetrazole (17): To a mixture of tetrazole **15** (127 mg, 0.45 mmol) in pyridine (2 mL), a solution of NaOH (182 mg, 4.54 mmol) in 6 mL water and solid KMnO4 (358 mg, 2.27 mmol) were added. The reaction mixture was refluxed with stirring overnight. Ethanol (20 mL) was then slowly added to the mixture over 10 min before the reaction was cooled down to room temperature. The mixture was filtered, washed with hot water, acidified with 1 N HCl, and extracted with ethyl acetate. The organic layer was separated and concentrated to give the crude dicarboxylic acid. To a solution of dicarboxylic acid in acetone was added methyl iodide (183 μL, 2.94 mmol) and K_2CO_3 (406 mg, 2.94 mmol), and the mixture was refluxed for 8 hours. After cooled down, the solution was filtered through Celite and washed with ethyl acetate. The filtrate was concentrated to give the crude diester. To a solution of diester in hydrous THF was added $LiAlH_4$ (35 mg, 0.93 mmol), and the mixture was stirred at room temperature until all starting materials were consumed. The reaction was then quenched by adding 1 mL methanol. The mixture was filtered through Celite and washed with ethyl acetate. The filtrate was concentrated to give the crude diol. To a solution of diol in anhydrous THF at 0 °C was added NaH (60%; 44 mg, 1.08 mmol), and the mixture was stirred a room temperature for 10 min. Then tetrabutylammonium iodide (13 mg, 0.036 mmol) and methyl iodide (112 μL, 1.80 mmol) were added. The mixture was stirred at room for 8 hours. Several drops of saturated NH_4Cl solution were then added followed by water. The mixture was extracted with ethyl acetate, and the organic layers were combined. After evaporating the solvent under reduced pressure, the residue was purified by silica gel flash chromatography using ethyl acetate/hexanes as eluent to give the title product as white solid (50 mg, 33%): ^{1}H NMR (400 MHz, $CDCl_3$) δ 8.12 (d, J = 9.1 Hz, 2H), 7.54 (m, 3H), 7.07 (d, J = 9.1 Hz, 2H), 4.46 (s, 4H), 3.89 (s, 3H), 3.26 (s, 6H); ^{13}C NMR (100 MHz, $CDCl_3$) δ 162.59, 160.56, 138.67, 130.13, 127.40, 124.77, 121.27, 114.72, 72.15, 58.20, 55.66; HRMS calcd for $C_{18}H_{20}N_4O_3$ 341.1608 [M+H$^+$], found 341.1605.

Scheme S6

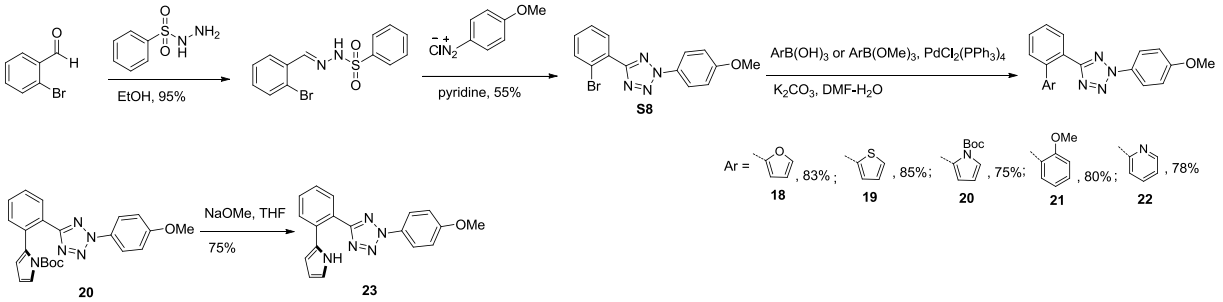

5-(2-Bromophenyl)-2-(4-methoxyphenyl)-2*H*-tetrazole (S8): Tetrazole **S8** was synthesized using the same procedure as tetrazole **2** with 55% yield: ^{1}H NMR (400 MHz, $CDCl_3$) δ 8.10 (d, J = 9.0 Hz, 2H), 7.95 (d, J = 6.7 Hz, 1H), 7.75 (d, J = 7.9 Hz, 1H), 7.45 (t, J = 7.4 Hz, 1H), 7.33 (t, J = 7.1 Hz, 1H), 7.04 (d, J = 9.0 Hz, 2H), 3.87 (s, 3H); ^{13}C NMR (100 MHz, $CDCl_3$) δ 163.92, 160.53, 134.13, 131.64, 131.25, 128.37, 127.42, 122.06, 121.40, 114.64, 55.60; HRMS calcd for $C_{14}H_{11}BrN_4O$ 331.0189 [M+H$^+$], found 331.0189.

5-(2-(Furan-2-yl)phenyl)-2-(4-methoxyphenyl)-2*H*-tetrazole (18): To a mixture of tetrazole **S8** (100 mg, 0.30 mmol), furan-2-ylboronic acid (51 mg, 0.45 mmol), K_2CO_3 (125 mg, 0.91 mmol) and bis(triphenylphosphine)palladium(II) dichloride (11 mg, 0.015 mmol) was added DMF (3 mL) and H_2O (500 μL) under argon. The reaction was stirred at 100 °C overnight under argon. The reaction mixture was then concentrated under reduced pressure, and the residue was purified by silica gel flash chromatography to give the desired product as a white solid (80 mg, 83%): ^{1}H NMR (400 MHz, $CDCl_3$) δ 8.04 (d, J = 9.0

Hz, 2H), 7.88–7.73 (m, 2H), 7.54 (dd, *J* = 7.7, 1.1 Hz, 1H), 7.46 (td, *J* = 7.5, 1.0 Hz, 1H), 7.36 (s, 1H), 7.03 (d, *J* = 9.0 Hz, 2H), 6.40 (d, *J* = 1.5 Hz, 1H), 6.32 (s, 1H), 3.88 (s, 3H); ^{13}C NMR (100 MHz, $CDCl_3$) δ 164.90, 160.34, 152.31, 142.16, 130.89, 130.76, 130.30, 130.11, 128.63, 127.83, 124.91, 121.17, 114.55, 111.28, 108.68, 55.51; HRMS calcd for $C_{18}H_{14}N_4O_2$ 319.1190 [M+H$^+$], found 319.1186.

2-(4-Methoxyphenyl)-5-(2-(thiophen-2-yl)phenyl)-2*H*-tetrazole (19): Tetrazole **19** was synthesized using the same procedure as tetrazole **18** with 85% yield: ^{1}H NMR (500 MHz, $CDCl_3$) δ 7.95 (d, *J* = 9.0 Hz, 2H), 7.89 (d, *J* = 6.7 Hz, 1H), 7.61 (d, *J* = 7.0 Hz, 1H), 7.56–7.41 (m, 2H), 7.32–7.20 (m, 1H), 7.05–6.86 (m, 4H), 3.87 (s, 3H); ^{13}C NMR (100 MHz, $CDCl_3$) δ 164.69, 160.37, 141.80, 134.67, 131.36, 130.61, 130.33, 130.04, 128.00, 127.07, 126.96, 126.66, 125.83, 121.21, 114.57, 55.58; HRMS calcd for $C_{18}H_{14}N_4OS$ 335.0961 [M+H$^+$], found 335.0958.

***tert*-Butyl 2-(2-(2-(4-methoxyphenyl)-2*H*-tetrazol-5-yl)phenyl)-1*H*-pyrrole-1-carboxylate (20):** Tetrazole **20** was synthesized using the same procedure as tetrazole **18** with 75% yield: ^{1}H NMR (500 MHz, $CDCl_3$) δ 8.36–8.25 (m, 1H), 7.95 (d, *J* = 9.0 Hz, 2H), 7.48 (dd, *J* = 9.9, 6.5 Hz, 4H), 7.01 (d, *J* = 9.0 Hz, 2H), 6.27 (s, 1H), 6.11 (s, 1H), 3.86 (s, 3H), 1.08 (s, 9H); ^{13}C NMR (126 MHz, $CDCl_3$) δ 164.47, 160.29, 149.32, 134.21, 132.68, 131.52, 129.62, 128.49, 128.07, 127.47, 121.11, 121.00, 114.58, 113.93, 110.69, 82.98, 55.58, 27.23; HRMS calcd for $C_{23}H_{23}N_5O_3$ 418.1874 [M+H$^+$], found 418.1871.

5-(2'-Methoxy-[1,1'-biphenyl]-2-yl)-2-(4-methoxyphenyl)-2*H*-tetrazole (21): Tetrazole **21** was synthesized using the same procedure as tetrazole **18** with 80% yield: ^{1}H NMR (400 MHz, $CDCl_3$) δ 8.14 (dd, *J* = 7.5, 1.3 Hz, 1H), 7.77 (d, *J* = 9.2 Hz, 2H), 7.60–7.40 (m, 3H), 7.40–7.22 (m, 2H), 6.97–7.06 (m, 1H), 6.95 (d, *J* = 9.2 Hz, 2H), 6.83 (d, *J* = 8.2 Hz, 1H), 3.83 (s, 3H), 3.44 (s, 3H); ^{13}C NMR (100 MHz, $cdcl_3$) δ 165.20, 160.17, 156.47, 138.29, 131.30, 130.77, 130.44, 129.93, 129.14, 128.82, 127.51, 126.92, 120.95, 120.62, 114.50, 110.41, 55.54, 55.10; HRMS calcd for $C_{21}H_{18}N_4O_2$ 359.1503 [M+H$^+$], found 359.1501.

2-(2-(2-(4-Methoxyphenyl)-2*H*-tetrazol-5-yl)phenyl)pyridine (22): Tetrazole **22** was synthesized using the same procedure as tetrazole **18** with 78% yield: ^{1}H NMR (500 MHz, $CDCl_3$) δ 8.58 (d, *J* = 4.1 Hz, 1H), 8.08 (d, *J* = 7.3 Hz, 1H), 7.86 (d, *J* = 8.9 Hz, 2H), 7.71–7.61 (m, 2H), 7.61–7.53 (m, 2H), 7.34 (d, *J* = 7.8 Hz, 1H), 7.23 (d, *J* = 6.7 Hz, 1H), 6.98 (d, *J* = 8.9 Hz, 2H), 3.86 (s, 3H); ^{13}C NMR (75 MHz, $CDCl_3$) δ 164.86, 160.30, 159.06, 149.15, 140.83, 135.97, 130.48, 130.36, 130.20, 130.14, 128.59, 125.97, 124.14, 121.98, 121.10, 114.53, 55.60; HRMS calcd for $C_{19}H_{15}N_5O$ 330.1349 [M+H$^+$], found 330.1344.

5-(2-(1*H*-Pyrrol-2-yl)phenyl)-2-(4-methoxyphenyl)-2*H*-tetrazole (23): To a solution of tetrazole **20** (35 mg, 0.084 mmol) in anhydrous THF was added NaOMe (25% in methanol; 100 μL, 0.42 mmol) at 0 °C slowly via syringe under argon. The solution was stirred at 0 °C for 10 min and then room temperature for 30 min. Water was then added, and the mixture was extracted with diethyl ether. The organic layer was collected and concentrated under reduced pressure. The resulting residue was purified by silica gel flash chromatography using ethyl acetate/hexanes as eluent to give the title compound as a white solid (20 mg, 75%): ^{1}H NMR (400 MHz, $CDCl_3$) δ 10.39 (s, 1H), 8.05 (d, *J* = 9.1 Hz, 2H), 7.82 (dd, *J* = 7.8, 1.1 Hz, 1H), 7.74 (dd, *J* = 7.9, 0.9 Hz, 1H), 7.59–7.47 (m, 1H), 7.44–7.33 (m, 1H), 7.05 (d, *J* = 9.1 Hz, 2H), 6.87 (dd, *J* = 4.1, 2.6 Hz, 1H), 6.43 (dd, *J* = 4.3, 3.1 Hz, 1H), 6.32–6.18 (m, 1H), 3.89 (s, 3H); ^{13}C NMR (100 MHz, $CDCl_3$) δ 165.70, 160.65, 133.12, 131.65, 130.47, 130.20, 130.11, 126.46, 123.55, 121.44, 118.88, 114.70, 109.50, 109.22, 55.61; HRMS calcd for $C_{18}H_{15}N_5O$ 318.1349 [M+H$^+$], found 318.1348.

Scheme S7

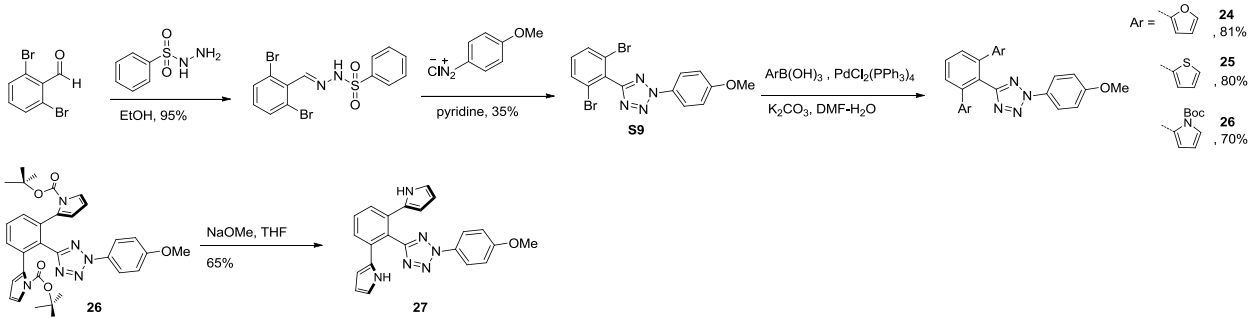

5-(2,6-Dibromophenyl)-2-(4-methoxyphenyl)-2*H*-tetrazole (S9): Tetrazole **S9** was synthesized using the same procedure as tetrazole **2** with 35% yield: ^{1}H NMR (400 MHz, $CDCl_3$) δ 8.13 (d, J = 8.4 Hz, 2H), 7.69 (dd, J = 8.1, 0.7 Hz, 2H), 7.32–7.18 (m, 1H), 7.07 (d, J = 8.4 Hz, 2H), 3.90 (d, J = 0.5 Hz, 3H); ^{13}C NMR (100 MHz, $CDCl_3$) δ 163.28, 160.68, 132.39, 131.87, 130.74, 130.30, 125.36, 121.50, 114.71, 55.67; HRMS calcd for $C_{14}H_{10}Br_2N_4O$ 408.9294 [M+H$^+$], found 408.9287.

5-(2,6-Di(furan-2-yl)phenyl)-2-(4-methoxyphenyl)-2*H*-tetrazole (24): To a mixture of tetrazole **S9** (25 mg, 0.06 mmol), furan-2-ylboronic acid (34 mg, 0.31 mmol), K_2CO_3 (42 mg, 0.31 mmol) and bis(triphenylphosphine)palladium(II) dichloride (4.3 mg, 0.006 mmol) were added DMF (2 mL) and H_2O (300 μL) under argon. The reaction was stirred at 90 °C overnight under argon. The reaction mixture was then cooled down and concentrated under reduced pressure. The residue was purified by silica gel flash chromatography to give the desired product as a white solid (19 mg, 81%): ^{1}H NMR (400 MHz, $CDCl_3$) δ 8.08 (d, J = 9.1 Hz, 2H), 7.80 (d, J = 7.9 Hz, 2H), 7.61 (dd, J = 8.3, 7.6 Hz, 1H), 7.30 (dd, J = 1.7, 0.6 Hz, 2H), 7.05 (d, J = 9.2 Hz, 2H), 6.24 (dd, J = 3.4, 1.8 Hz, 2H), 5.75 (dd, J = 3.4, 0.6 Hz, 2H), 3.88 (s, 3H); ^{13}C NMR (100 MHz, $CDCl_3$) δ 163.31, 160.57, 151.68, 142.35, 132.77, 130.42, 126.35, 121.37, 120.73, 114.70, 111.45, 109.02, 55.68; HRMS calcd for $C_{22}H_{16}N_4O_3$ 385.1295 [M+H$^+$], found 385.1294.

5-(2,6-Di(thiophen-2-yl)phenyl)-2-(4-methoxyphenyl)-2*H*-tetrazole (25): Tetrazole **25** was synthesized using a similar procedure as tetrazole **24** with 80% yield: ^{1}H NMR (500 MHz, $CDCl_3$) δ 7.93 (d, J = 9.0 Hz, 2H), 7.65–7.55 (m, 3H), 7.20–7.13 (m, 2H), 7.00 (d, J = 9.0 Hz, 2H), 6.92–6.82 (m, 4H), 3.86 (s, 3H); ^{13}C NMR (75 MHz, $CDCl_3$) δ 163.14, 160.49, 141.36, 136.80, 130.22, 129.89, 127.40, 127.04, 126.31, 121.43, 119.52, 114.62, 55.66; HRMS calcd for $C_{22}H_{16}N_4OS_2$ 417.0838 [M+H$^+$], found 417.0835.

Di-*tert*-butyl 2,2'-(2-(2-(4-methoxyphenyl)-2*H*-tetrazol-5-yl)-1,3-phenylene)-bis(1*H*-pyrrole-1-carboxylate) (26): Tetrazole **26** was synthesized using a similar procedure as tetrazole **24** with 70% yield: ^{1}H NMR (400 MHz, $CDCl_3$) δ 7.85 (d, J = 9.0 Hz, 2H), 7.51–7.44 (m, 3H), 7.30 (s, 2H), 6.96 (d, J = 9.1 Hz, 2H), 6.08 (t, J = 3.1 Hz, 2H), 5.93 (s, 2H), 3.84 (s, 3H), 1.26 (s, 18H); ^{13}C NMR (100 MHz, $CDCl_3$) δ 163.31, 160.08, 149.18, 135.78, 131.89, 130.66, 130.35, 128.19, 121.11, 120.91, 119.51, 114.68, 114.47, 110.14, 83.12, 55.54, 27.42; Orbitrap LC-MS calcd for $C_{32}H_{34}N_6O_5$ 583.2663 [M+H$^+$], found 583.2651.

5-(2,6-Di(1*H*-pyrrol-2-yl)phenyl)-2-(4-methoxyphenyl)-2*H*-tetrazole (27): Tetrazole **27** was synthesized using a similar procedure as tetrazole **23** with 65% yield: ^{1}H NMR (400 MHz, $CDCl_3$) δ 8.60 (s, 2H), 7.91 (d, J = 8.8 Hz, 2H), 7.47 (s, 3H), 6.99 (d, J = 8.8 Hz, 2H), 6.64 (s, 2H), 6.08 (d, J = 11.6 Hz, 4H), 3.85 (s, 3H); ^{13}C NMR (100 MHz, $CDCl_3$) δ 164.64, 160.69, 135.57, 130.66, 130.38, 130.10, 127.27, 121.90, 121.59, 119.04, 114.67, 109.25, 109.23, 55.65; HRMS calcd for $C_{22}H_{18}N_6O$ 383.1615 [M+H$^+$], found 383.1614.

Scheme S8

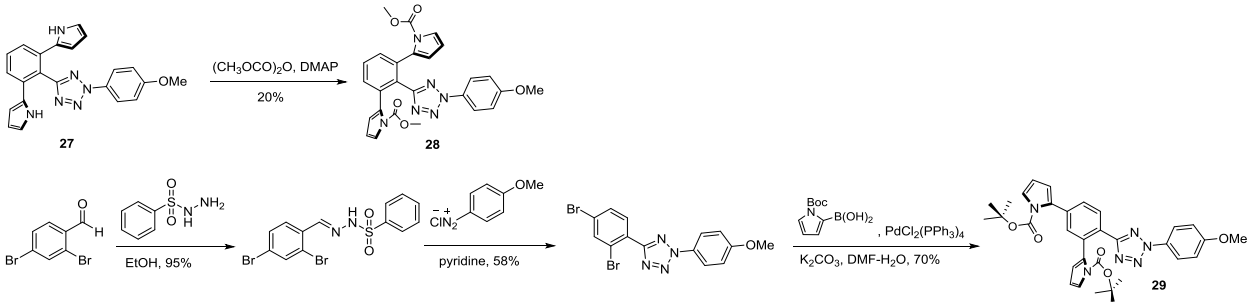

Dimethyl 2,2'-(2-(2-(4-methoxyphenyl)-2*H*-tetrazol-5-yl)-1,3-phenylene)bis(1*H*-pyrrole-1-carboxylate) (28): To a solution of tetrazole **27** (25 mg, 0.065 mmol) in acetonitrile (5 mL) was added dimethyl dicarbonate (21 μL, 0.196 mmol) and DMAP (1.6 mg, 0.013 mmol), and the mixture was stirred at room temperature under argon for 24 hours. The solution was then concentrated, and the residue was purified by silica gel flash chromatography to give the desired product as a white solid (6.5 mg, 20%): ^{1}H NMR (400 MHz, $CDCl_3$) δ 7.79 (d, J = 9.0 Hz, 2H), 7.56–7.44 (m, 3H), 7.25 (d, J = 6.4 Hz, 2H), 6.96 (d, J = 9.1 Hz, 2H), 6.11–5.99 (br, 4H), 3.84 (s, 3H), 3.73 (s, 6H); ^{13}C NMR (100 MHz, $CDCl_3$) δ 163.49, 160.22, 151.06, 134.97, 132.33, 130.46, 130.28, 128.58, 128.25, 121.24, 121.17, 115.12, 114.48, 111.00, 55.57, 53.73; HRMS calcd for $C_{26}H_{22}N_6O_5$ 499.1724 [M+H$^+$], found 499.1708.

Di-*tert*-butyl 2,2'-(4-(2-(4-methoxyphenyl)-2H-tetrazol-5-yl)-1,3-phenylene)bis(1H-pyrrole-1-carboxylate) (29): Tetrazole **29** was synthesized using a similar procedure as tetrazole **26** except 2,4-dibromobenzaldehyde was used as the starting material: ^{1}H NMR (400 MHz, $CDCl_3$) δ 8.31 (d, J = 7.9 Hz, 1H), 7.95 (d, J = 9.1 Hz, 2H), 7.55–7.44 (m, 3H), 7.37 (dd, J = 3.3, 1.8 Hz, 1H), 7.01 (d, J = 9.1 Hz, 2H), 6.33–6.22 (m, 3H), 6.14 (dd, J = 3.2, 1.8 Hz, 1H), 3.87 (s, 3H), 1.44 (s, 9H), 1.11 (s, 9H); ^{13}C NMR (100 MHz, $CDCl_3$) δ 164.37, 160.27, 149.26, 149.11, 135.61, 134.01, 133.42, 132.62, 131.99, 130.38, 128.55, 127.69, 126.00, 123.17, 121.11, 120.99, 115.14, 114.57, 113.88, 110.70, 110.67, 83.87, 83.01, 55.57, 27.71, 27.25; HRMS calcd for $C_{32}H_{34}N_6O_5$ 583.2663 [M+H$^+$], found 583.2651.

Scheme S9

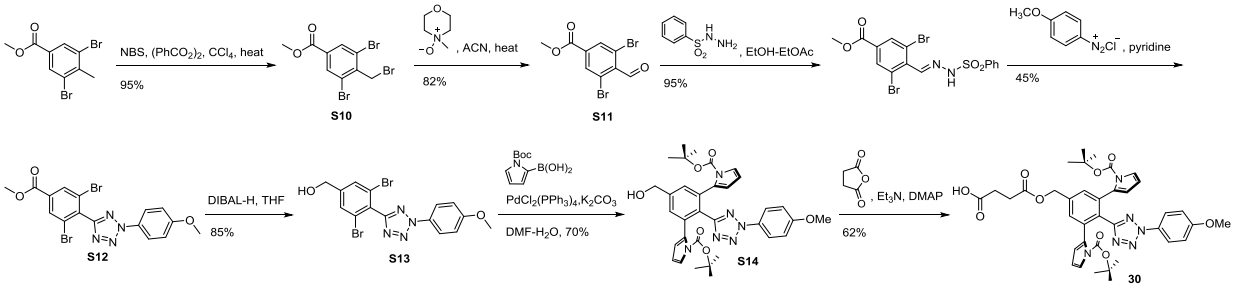

Methyl 3,5-dibromo-4-(bromomethyl)benzoate (S10): Compound **S10** was synthesized by following a literature procedure[S5]. To a solution of methyl 3,5-dibromo-4-methylbenzoate (154 mg, 0.5 mmol) in carbon tetrachloride was added NBS (107 mg, 0.6 mmol) followed by benzoyl peroxide (70%; 17 mg, 0.05 mmol). The mixture was refluxed until TLC showed complete disappearance of the starting materials. The reaction was then cooled down to room temperature, and the solvent was removed under reduced pressure. The residue was redissolved in ethyl acetate, washed with water, and concentrated. The residue was purified

by silica gel flash chromatography to give the desired product as a white solid (182 mg, 95%): ^{1}H NMR (400 MHz, $CDCl_3$) δ 8.20 (s, 2H), 4.83 (s, 2H), 3.93 (s, 3H).

Methyl 3,5-dibromo-4-formylbenzoate (S11): To a solution of **S10** (180 mg, 0.47 mmol) in acetonitrile was added 4 Å molecular sieves and *N*-methylmorpholine-*N*-oxide (82 mg, 1.70 mmol), and the mixture was stirred at 50 °C overnight. The reaction mixture was washed with brine and extracted with ethyl acetate, and the organic phase was concentrated. After evaporating the solvents, the residue was purified by silica gel flash chromatography to give the desired product as a white solid (123 mg, 82%): ^{1}H NMR (400 MHz, $CDCl_3$) δ 10.22 (s, 2H), 8.26 (s, 2H), 3.97 (s, 3H).

Methyl 3,5-dibromo-4-(2-(4-methoxyphenyl)-2*H*-tetrazol-5-yl)benzoate (S12): Tetrazole **S12** was synthesized using a similar procedure as tetrazole **2** with 45% yield: ^{1}H NMR (400 MHz, $CDCl_3$) δ 8.33 (s, 2H), 8.12 (d, J = 9.0 Hz, 2H), 7.07 (d, J = 9.0 Hz, 2H), 3.98 (s, 3H), 3.90 (s, 3H); ^{13}C NMR (100 MHz, $CDCl_3$) δ 164.02, 162.73, 160.81, 134.78, 133.98, 132.72, 130.22, 125.49, 121.56, 114.77, 55.70, 52.96; HRMS calcd for $C_{16}H_{12}Br_2N_4O_3$ 466.9349 [M+H$^+$], found 466.9344.

(3,5-Dibromo-4-(2-(4-methoxyphenyl)-2*H*-tetrazol-5-yl)phenyl)methanol (**S13**) Tetrazole **S13** was synthesized using the same procedure as tetrazole **17** and used directly without further purification.

Di-*tert*-butyl 2,2'-(5-(hydroxymethyl)-2-(2-(4-methoxyphenyl)-2*H*-tetrazol-5-yl)-1,3-phenylene) bis(1*H*-pyrrole-1-carboxylate) (S14): To a round bottom flask containing a solution of tetrazole **S14** (30 mg, 0.068 mmol) in DMF (1.5 mL) and H_2O (100 μL) was added (1-(*tert*-butoxycarbonyl)-1*H*-pyrrol-2-yl)boronic acid (58 mg, 0.273 mmol), K_2CO_3 (38 mg, 0.273 mmol), and bis(triphenylphosphine)palladium (II) dichloride (5 mg, 0.007 mmol) under argon. The reaction was stirred at 80 °C under argon overnight. The reaction mixture was then concentrated under reduced pressure, and the residue was purified by silica gel flash chromatography to give the title compound as a white solid (29 mg, 70%): ^{1}H NMR (400 MHz, $CDCl_3$) δ 7.84 (d, J = 9.1 Hz, 2H), 7.48 (s, 2H), 7.29 (s, 2H), 6.96 (d, J = 9.1 Hz, 2H), 6.08 (d, J = 3.2 Hz, 2H), 5.95 (s, 2H), 4.81 (s, 2H), 3.84 (s, 3H), 1.26 (s, 18H); ^{13}C NMR (100 MHz, $CDCl_3$) δ 160.08, 149.30, 141.13, 135.92, 131.90, 130.31, 128.86, 127.63, 121.11, 120.90, 114.46, 110.21, 83.11, 64.49, 55.53, 27.44; HRMS calcd for $C_{33}H_{36}N_6O_6$ 613.2769 [M+H$^+$], found 613.2764.

4-((3,5-Bis(1-(*tert*-butoxycarbonyl)-1*H*-pyrrol-2-yl)-4-(2-(4-methoxyphenyl)-2*H*-tetrazol-5-yl)benzyl) oxy)-4-oxobutanoic acid (30): To a solution of tetrazole **S14** (20 mg, 0.033 mmol) in dioxane was added succinic anhydride (16.3 mg, 0.163 mmol), triethylamine (46 μL, 0.327 mmol), and DMAP (2.0 mg, 0.016 mmol). The mixture was stirred at 70 °C under argon for 5 hours until TLC showed complete disappearance of the starting materials. The reaction mixture was cooled down and concentrated, and the residue was purified by silica gel flash chromatography to give the desired product as a white solid (20 mg, 86%): ^{1}H NMR (500 MHz, CD_3OD) δ 7.82 (d, J = 10.0 Hz, 2H), 7.49 (s, 2H), 7.26 (s, 2H), 7.06 (d, J = 10.0 Hz, 2H), 6.10 (d, J = 5.0 Hz, 2H), 5.95 (s, 2H), 3.86 (s, 2H), 2.69 (d, J = 5.0 Hz, 2H), 2.64 (d, J = 5.0 Hz, 2H), 1.27 (s, 18H); ^{13}C NMR (126 MHz, CD_3OD) δ 172.54, 160.73, 148.95, 137.25, 131.40, 129.86, 120.80, 120.72, 114.35, 109.96, 83.20, 65.18, 54.76, 28.75, 28.51, 26.41; HRMS calcd for $C_{37}H_{40}N_6O_9$ 713.2930 [M+H$^+$], found 713.2918.

Scheme S10

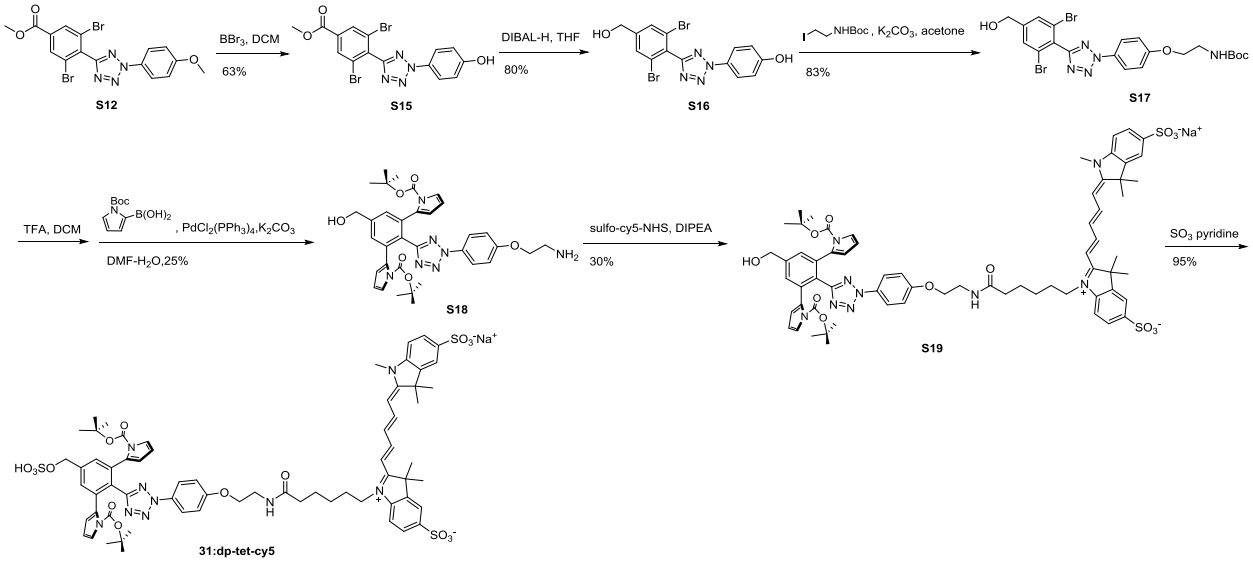

Methyl 3,5-dibromo-4-(2-(4-hydroxyphenyl)-2*H*-tetrazol-5-yl)benzoate (S15): To a solution of **S12** (210 mg, 0.45 mmol) in DCM (30 mL) cooled with an ice-water bath was slowly added boron tribromide (430 μL, 4.5 mmol), and the mixture was stirred at room temperature overnight. After cooling the reaction mixture with an ice-water bath, 1 mL methanol was slowly added and the solution was concentrated. The residue was purified by silica gel flash chromatography to give the desired product as a white solid (128 mg, 63%): ^{1}H NMR (400 MHz, acetone-d_6) δ 8.34 (s, 2H), 8.06 (d, J = 9.0 Hz, 2H), 7.13 (d, J = 9.0 Hz, 2H), 3.98 (s, 3H), 2.95 (s, 1H); ^{13}C NMR (100 MHz, acetone-d_6) δ 163.42, 159.26, 134.69, 132.50, 125.08, 121.70, 116.38, 52.50; HRMS calcd for $C_{15}H_{10}Br_2N_4O_3$ 452.9192 [M+H$^+$], found 452.9184.

4-(5-(2,6-Dibromo-4-(hydroxymethyl)phenyl)-2*H*-tetrazol-2-yl)phenol (S16): To a solution of **S15** (130 mg, 0.29 mmol) in anhydrous THF in a round-bottom flask cooled in a water-ice bath was added diisobutylaluminium hydride (1 M in hexane; 1.43 mL, 1.43 mmol). The reaction mixture was stirred at room temperature with TLC monitoring. The Rochelle salt solution was added after TLC showed complete disappearance of the starting materials. The mixture was stirred while ethyl acetate was added. The organic layer was collected and concentrated. The residue was purified by silica gel flash chromatography to give the desired product as a white solid (98 mg, 80%): ^{1}H NMR (400 MHz, CD_3OD) δ 8.00 (d, J = 9.0 Hz, 2H), 7.78 (s, 2H), 7.01 (d, J = 9.0 Hz, 2H), 4.69 (s, 2H); ^{13}C NMR (100 MHz, CD_3OD) δ 163.08, 159.37, 148.12, 129.49, 128.96, 128.62, 124.51, 121.31, 115.86, 61.79; HRMS calcd for $C_{14}H_{10}Br_2N_4O_2$ 424.9243 [M+H$^+$], found 452.9241.

***tert*-Butyl (2-(4-(5-(2,6-dibromo-4-(hydroxymethyl)phenyl)-2*H*-tetrazol-2-yl)phenoxy)ethyl) carbamate (S17):** To a solution of **S16** (90 mg, 0.21 mmol) in acetone was added K_2CO_3 (146 mg, 1.06 mmol) and *tert*-butyl (2-iodoethyl) carbamate (92 mg, 0.34 mmol), and the mixture was refluxed under argon overnight. Then the mixture was filtered through Celite after cooling down and washed with ethyl acetate. The filtrate was concentrated under reduced pressure, and the residue was purified by silica gel flash chromatography to give the desired product as a white solid (100 mg, 83%): ^{1}H NMR (500 MHz, $CDCl_3$) δ 8.12 (d, J = 9.1 Hz, 2H), 7.65 (s, 2H), 7.06 (d, J = 9.1 Hz, 2H), 5.07 (s, 1H), 4.76 (s, 2H), 4.10 (t, J = 5.1 Hz, 2H), 3.70–3.44 (m, 3H), 1.46 (s, 9H); ^{13}C NMR (126 MHz, $CDCl_3$) δ 163.18, 159.72, 147.08,

130.44, 129.29, 128.62, 125.01, 121.59, 115.24, 67.59, 62.75, 28.35; HRMS calcd for $C_{21}H_{23}Br_2N_5O_4$ 568.0190 [M+H$^+$], found 568.0178.

Di-*tert*-butyl 2,2'-(2-(2-(4-(2-aminoethoxy)phenyl)-2*H*-tetrazol-5-yl)-5-(hydroxymethyl)-1,3-phenylene)bis(1*H*-pyrrole-1-carboxylate) (S18): To a solution of **S17** (95 mg, 0.167 mmol) in DCM (6 mL) was added 2,2,2-trifluoroacetic acid (4 mL), and the mixture was stirred at 0 °C until all starting materials were consumed. The solvent was removed to obtain the crude tetrazole-amine intermediate. To a solution of tetrazole-amine in 2 mL DMF and 300 μL H_2O was added 1-(*tert*-butoxycarbonyl)-1*H*-pyrrol-2-yl)boronic acid (187 mg, 0.887 mmol), K_2CO_3 (162 mg, 1.17 mmol) and bis(triphenylphosphine)palladium(II) dichloride (16 mg, 0.022 mmol), and the mixture was stirred at 80 °C overnight under argon. The reaction mixture was cooled down and concentrated. The residue was purified by silica gel flash chromatography to give the desired product as a white solid (27 mg, 25%): ^{1}H NMR (400 MHz, CD_3OD) δ 7.84 (d, J = 9.0 Hz, 2H), 7.45 (s, 2H), 7.23 (s, 2H), 7.15 (d, J = 9.1 Hz, 2H), 6.08 (s, 2H), 5.94 (s, 2H), 4.75 (s, 2H), 4.37–4.26 (m, 2H), 3.43–3.35 (m, 2H), 3.08 (s, 1H), 1.25 (s, 18H); ^{13}C NMR (100 MHz, CD_3OD) δ 159.20, 158.89, 157.20, 142.55, 135.79, 131.98, 130.66, 128.40, 120.79, 120.68, 115.16, 109.96, 83.13, 64.49, 62.88, 38.82, 26.41; HRMS calcd for $C_{34}H_{39}N_7O_6$ 642.3035 [M+H$^+$], found 642.3024.

Sodium 1-(6-((2-(4-(5-(2,6-bis(1-(*tert*-butoxycarbonyl)-1*H*-pyrrol-2-yl)-4-(hydroxymethyl)phenyl)-2*H*-tetrazol-2-yl)phenoxy)ethyl)amino)-6-oxohexyl)-3,3-dimethyl-2-((1*E*,3*E*,5*E*)-5-(1,3,3-trimethyl-5-sulfonatoindolin-2-ylidene)penta-1,3-dien-1-yl)-3*H*-indol-1-ium-5-sulfonate (S19): To a solution of **S18** (2.28 mg, 0.0038 mmol) in 500 μL DMF was added *N*,*N*-diisopropylethylamine (2 μL, 0.0078 mmol) and sulfo-Cy5-NHS ester (2.0 mg, 0.0026 mmol), and the mixture was stirred at room temperature overnight. The product mixture was concentrated and the residue purified by reverse-phase HPLC using acetonitrile/H_2O as eluent to give the title compound as a green solid (1.35 mg, 30%): HRMS calcd for $C_{66}H_{74}N_9NaO_{13}S_2$ 1264.4853 [M-Na$^-$], found 1264.4860.

Sodium 1-(6-((2-(4-(5-(2,6-bis(1-(*tert*-butoxycarbonyl)-1*H*-pyrrol-2-yl)-4-((sulfooxy)methyl)phenyl)-2*H*-tetrazol-2-yl)phenoxy)ethyl)amino)-6-oxohexyl)-3,3-dimethyl-2-((1*E*,3*E*,5*E*)-5-(1,3,3-trimethyl-5-sulfonatoindolin-2-ylidene)penta-1,3-dien-1-yl)-3*H*-indol-1-ium-5-sulfonate (Tetrazole-Cy5; 31): To a solution of **S19** (1.00 mg, 0.0008 mmol) in 200 μL DMF was added SO_3-pyridine complex (1.64 mg, 0.0103 mmol), and the mixture was stirred until MS (LCQ) showed disappearance of the starting materials. The solvent was removed and dried thoroughly under vacuum to give the title compound as a green solid with 95% yield: HRMS calcd for $C_{66}H_{74}N_9NaO_{16}S_3$ 1344.4421 [M-Na$^-$], found 1344.4456.

Computational Details:

All calculations were carried out with the Gaussian 09 program package.[S6] Geometry optimizations were performed with the B3LYP[S7] functional with Grimme's DFT-D3 dispersion correction,[S8] the 6-31+G(d) basis set, and the SMD[S9] solvation model with water as the solvent. Frequency analysis was conducted at the same level of theory to verify the stationary points to be minima or saddle points and to obtain zero-point energy (ZPE) and thermal energy corrections at 298.15 K. Single-point energy calculations on the B3LYP-D3-optimized geometries were performed with the ωB97X-D[S10] functional, using 6-311++G(d,p) basis set and the SMD solvation model with water as the solvent. Computed structures are illustrated using CYLView.[S11]

References:

[S1] Ramil, C. P.; Dong, M.; An, P.; Lewandowski, T. M.; Yu, Z.; Miller, L. J.; Lin, Q. Spirohexene-tetrazine ligation enables bioorthogonal labeling of class B G protein-coupled receptors in live cells. *J. Am. Chem. Soc.* **2017**, *139*, 13376-13386.

[S2] Yu, Z. & Lin, Q. Design of Spiro[2.3]hex-1-ene, a Genetically Encodable Double-Strained Alkene for Superfast Photoclick Chemistry. *J. Am. Chem. Soc.* **2014**, *136*, 4153-4156.

[S3] Kamber, D. N.; Nazarova, L. A.; Liang, Y.; Lopez, S. A.; Patterson, D. M.; Shih, H.-W.; Houk, K. N.; Prescher, J. A. Isomeric Cyclopropenes Exhibit Unique Bioorthogonal Reactivities. *J. Am. Chem. Soc.* **2013**, *135*, 13680-13683.

[S4] He, Y.; Cheng, C.; Chen, B.; Duan, K.; Zhuang, Y.; Yuan, B.; Zhang, M.; Zhou, Y.; Zhou, Z.; Su, Y. J.; Cao, R.; Qiu, L. Highly enantioselective synthesis of 2,3-dihydro-1*H*-imidazo[2,1-a]isoindol-5(9bH)-ones via catalytic asymmetric intramolecular cascade imidization-nucleophilic addition-lactamization. *Org. Lett.* **2014**, *16*, 6366-6369.

[S5] Kelly, M. J.; Pietranico-Cole, S.; Larigan, J. D.; Haynes, N. E.; Reynolds, C. H.; Scott, N.; Vermeulen, J.; Dvorozniak, M.; Conde-Knape, K.; Huang, K. S.; So, S. S.; Thakkar, K.; Qian, Y.; Banner, B.; Mennona, F.; Danzi, S.; Klein, I.; Taub, R.; Tilley, J. Discovery of 2-[3,5-dichloro-4-(5-isopropyl-6-oxo-1,6-dihydropyridazin-3 yloxy)phenyl]-3,5-dio xo-2,3,4,5-tetrahydro[1,2,4]triazine-6-carbonitrile (MGL-3196), a Highly Selective Thyroid Hormone Receptor beta agonist in clinical trials for the treatment of dyslipidemia. *J. Med. Chem.* **2014**, *57*, 3912-3923.

[S6] Frisch, M. J.; Trucks, G. W.; Schlegel, H. B.; Scuseria, G. E.; Robb, M. A.; Cheeseman, J. R.; Scalmani, G.; Barone, V.; Mennucci, B.; Petersson, G. A.; Nakatsuji, H.; Caricato, M.; Li, X.; Hratchian, H. P.; Izmaylov, A. F.; Bloino, J.; Zheng, G.; Sonnenberg, J. L.; Hada, M.; Ehara, M.; Toyota, K.; Fukuda, R.; Hasegawa, J.; Ishida, M.; Nakajima, T.; Honda, Y.; Kitao, O.; Nakai, H.; Vreven, T.; Montgomery, J. A.; Peralta, J. E.; Ogliaro, F.; Bearpark, M.; Heyd, J. J.; Brothers, E.; Kudin, K. N.; Staroverov, V. N.; Kobayashi, R.; Normand, J.; Raghavachari, K.; Rendell, A.; Burant, J. C.; Iyengar, S. S.; Tomasi, J.; Cossi, M.; Rega, N.; Millam, J. M.; Klene, M.; Knox, J. E.; Cross, J. B.; Bakken, V.; Adamo, C.; Jaramillo, J.; Gomperts, R.; Stratmann, R. E.; Yazyev, O.; Austin, A. J.; Cammi, R.; Pomelli, C.; Ochterski, J. W.; Martin, R. L.; Morokuma, K.; Zakrzewski, V. G.; Voth, G. A.; Salvador, P.; Dannenberg, J. J.; Dapprich, S.; Daniels, A. D.; Farkas; Foresman, J. B.; Ortiz, J. V.; Cioslowski, J.; Fox, D. J., Gaussian 09, Revision D.01. Wallingford CT, 2009.

[S7] (a) Becke, A. D., Density-functional thermochemistry. III. The role of exact exchange. *J. Chem. Phys.* 98, 5648-5652 (1993); (b) Lee, C.; Yang, W.; Parr, R. G., Development of the Colle-Salvetti correlation-energy formula into a functional of the electron density. *Phys. Rev. B.* **1988**, *37*, 785-789.

[S8] Grimme, S.; Antony, J.; Ehrlich, S.; Krieg, H., A consistent and accurate ab initio parametrization of density functional dispersion correction (DFT-D) for the 94 elements H-Pu. *J. Chem. Phys.* **2010**, *132*, 154104.

[S9] Marenich, A. V.; Cramer, C. J.; Truhlar, D. G., Universal Solvation Model Based on Solute Electron Density and on a Continuum Model of the Solvent Defined by the Bulk Dielectric Constant and Atomic Surface Tensions. *J. Phys. Chem. B.* **2009**, *113*, 6378-6396.

[S10] Chai, J.-D.; Head-Gordon, M., Long-range corrected hybrid density functionals with damped atom-atom dispersion corrections. *Phys. Chem. Chem. Phys.* **2008**, *10*, 6615-6620.

[S11] Legault, C. Y., CYLview, 1.0b. Université de Sherbrooke.

NMR spectra:

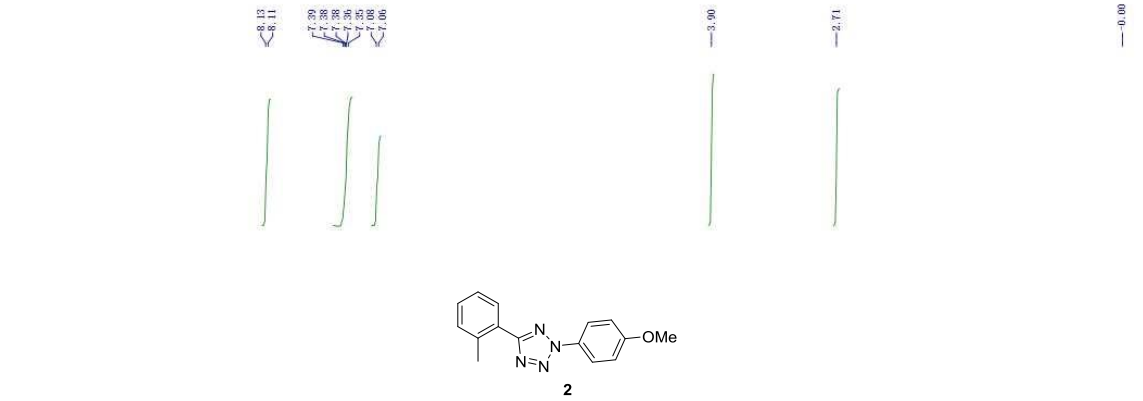
8.13
8.11
7.39
7.38
7.38
7.36
7.35
7.08
7.06
3.90
2.71
0.00
OMe
2

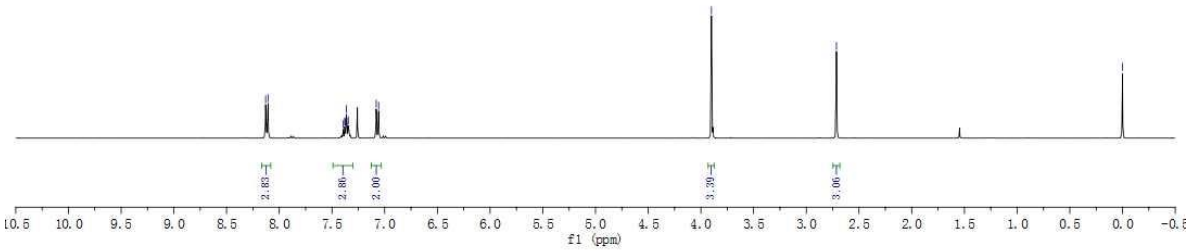
2.83
2.86
2.00
3.39
3.06
f1 (ppm)


165.28
160.34
137.48
131.34
129.90
129.44
126.28
125.96
124.24
121.21
114.57
114.06
77.31
77.00
76.68
55.55
21.73


OMe
2

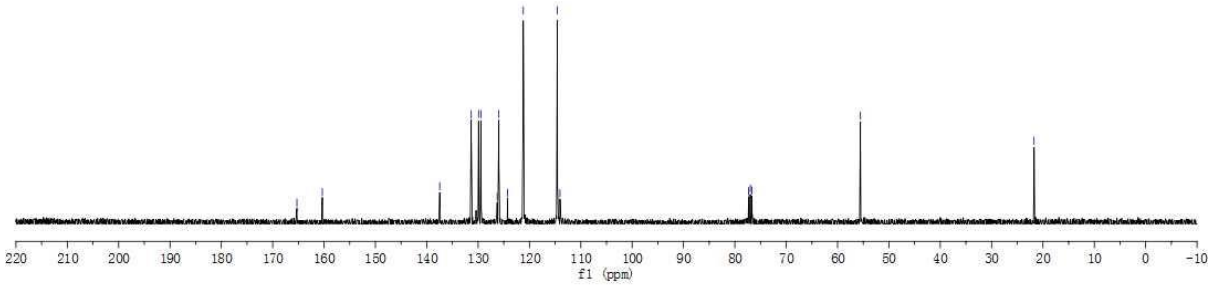
f1 (ppm)


8.18
8.18
8.16
8.16
8.05
8.05
7.51
7.46
7.46
7.44
7.00
4.82
4.80
4.62
4.60
4.58
3.84

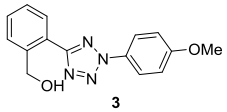
OMe
OH
N
N
N

3

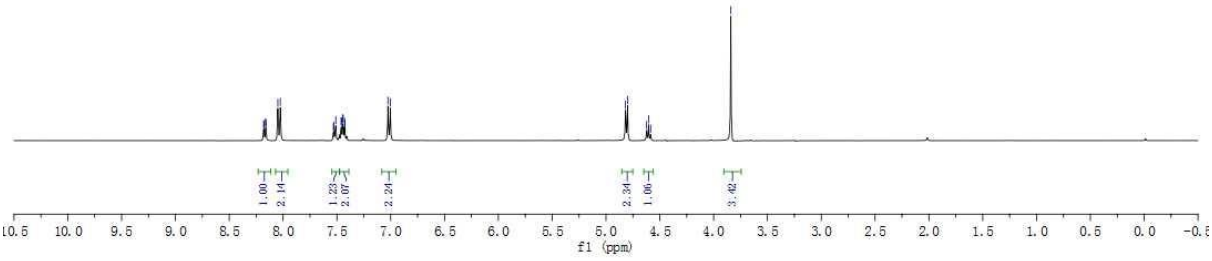
1.00
2.14
1.23
2.07
2.24
2.34
1.06
3.42
10.5
10.0
9.5
9.0
8.5
8.0
7.5
7.0
6.5
6.0
5.5
5.0
4.5
4.0
3.5
3.0
2.5
2.0
1.5
1.0
0.5
0.0
f1 (ppm)


164.43
160.62
139.87
130.63
130.43
129.90
129.43
128.12
125.59
121.26
114.63
77.31
76.99
76.67
64.25
55.53

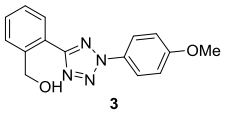
OMe
OH
N
N
N

3

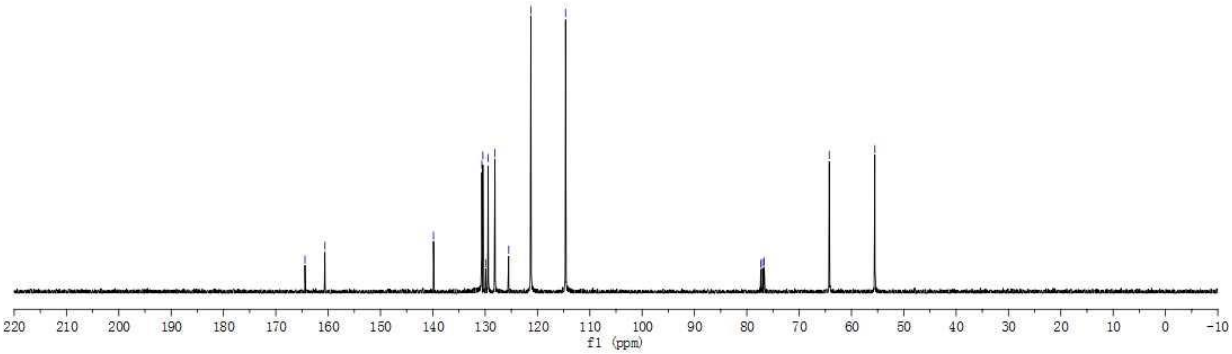
220
210
200
190
180
170
160
150
140
130
120
110
100
90
80
70
60
50
40
30
20
10
0
-10
f1 (ppm)


8.24
8.23
8.23
8.22
8.11
8.09
7.46
7.45
7.44
7.03
7.03
5.14
3.85

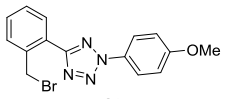
N
N
N
N
OMe
Br

S3

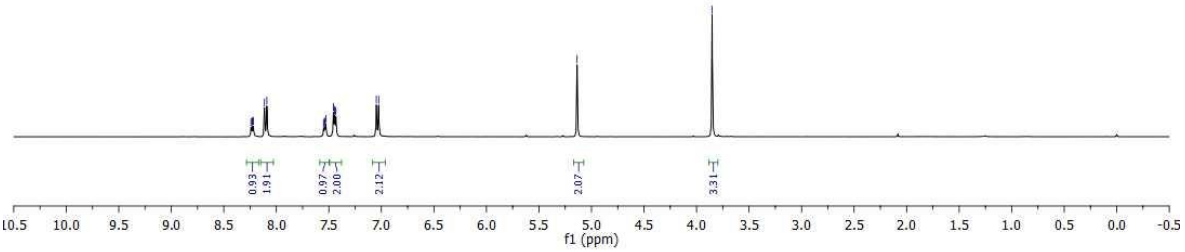
0.93
1.91
0.97
2.00
2.12
2.07
3.31
10.5 10.0 9.5 9.0 8.5 8.0 7.5 7.0 6.5 6.0 5.5 5.0 4.5 4.0 3.5 3.0 2.5 2.0 1.5 1.0 0.5 0.0 -0.5
f1 (ppm)


163.84
160.43
136.53
131.60
130.43
130.16
129.88
128.83
125.81
121.21
114.59
77.31
76.99
76.67
55.54
32.48

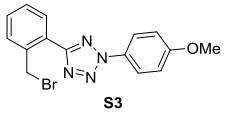
N
N
N
N
OMe
Br

S3

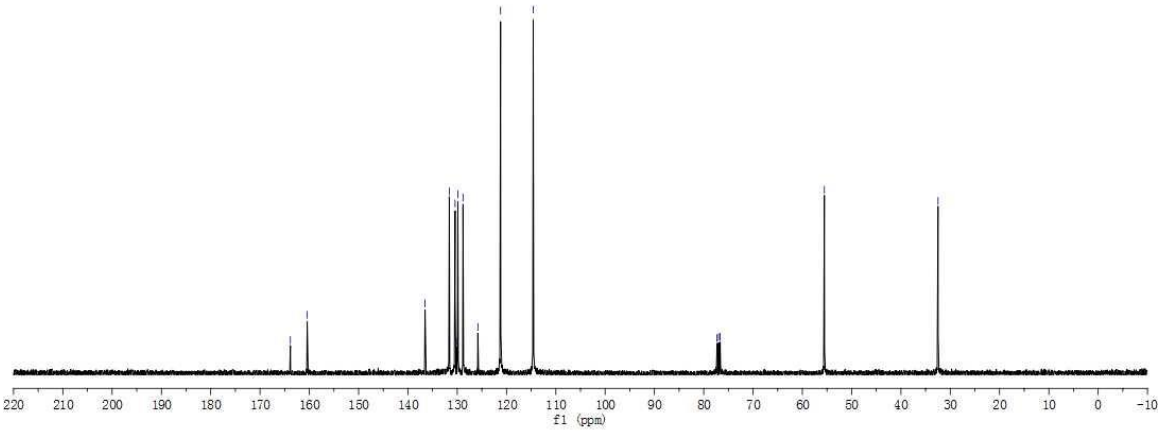
220 210 200 190 180 170 160 150 140 130 120 110 100 90 80 70 60 50 40 30 20 10 0 -10
f1 (ppm)


8.19
8.17
8.12
8.10
7.71
7.69
7.52
7.50
7.46
7.44
7.06
4.97
3.90
3.48

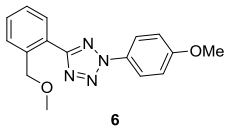
OMe

6

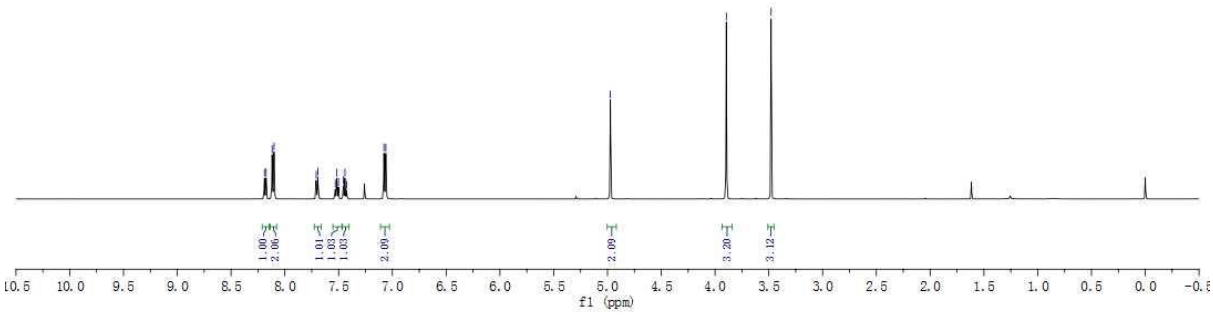
1.00
2.06
1.01
1.03
1.03
2.09
2.09
3.20
3.12
10.5 10.0 9.5 9.0 8.5 8.0 7.5 7.0 6.5 6.0 5.5 5.0 4.5 4.0 3.5 3.0 2.5 2.0 1.5 1.0 0.5 0.0
f1 (ppm)


164.56
160.43
137.67
130.17
129.39
128.08
127.46
124.91
121.24
114.62
77.41
76.98
76.56
72.59
68.54
55.57

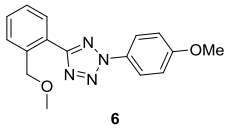
OMe

6

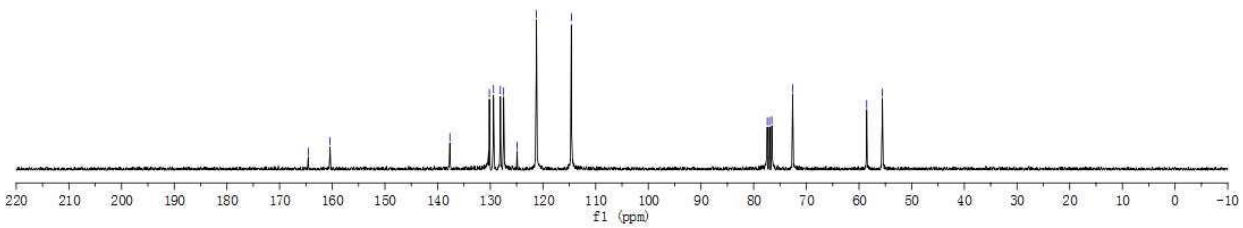
220 210 200 190 180 170 160 150 140 130 120 110 100 90 80 70 60 50 40 30 20 10 0 -10
f1 (ppm)


8.21
8.19
8.12
8.10
7.44
7.43
7.41
7.40
7.07
7.05
4.26
3.89
2.01

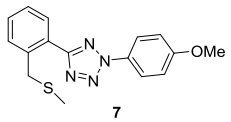
N
N
N
S
OMe

7

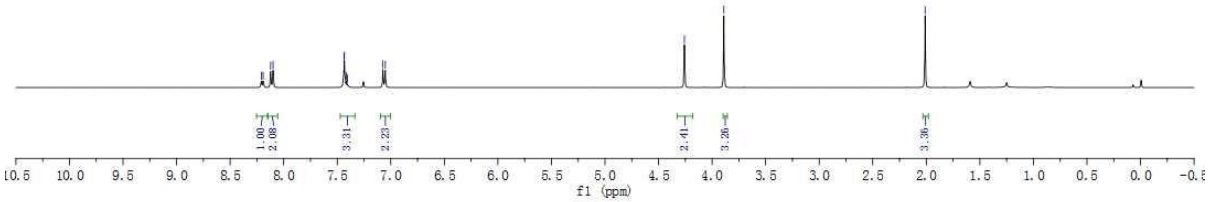
1.00
2.08
3.31
2.23
2.41
3.26
3.36
f1 (ppm)


164.66
160.48
137.69
130.91
130.21
129.92
127.38
121.68
121.33
114.68
77.31
76.99
76.67
55.64
36.73
15.10

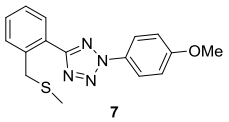
N
N
N
S
OMe

7

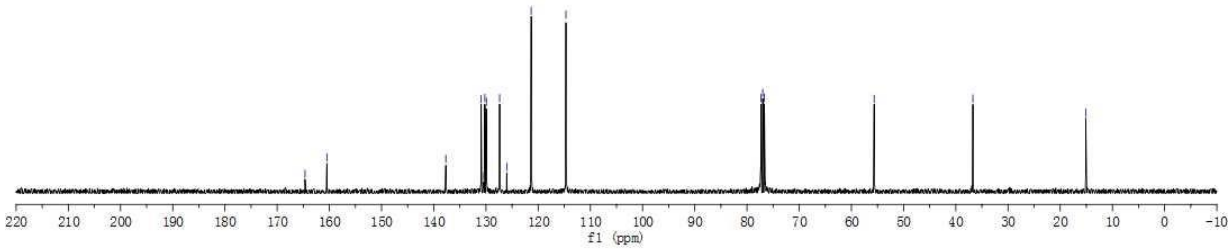
f1 (ppm)

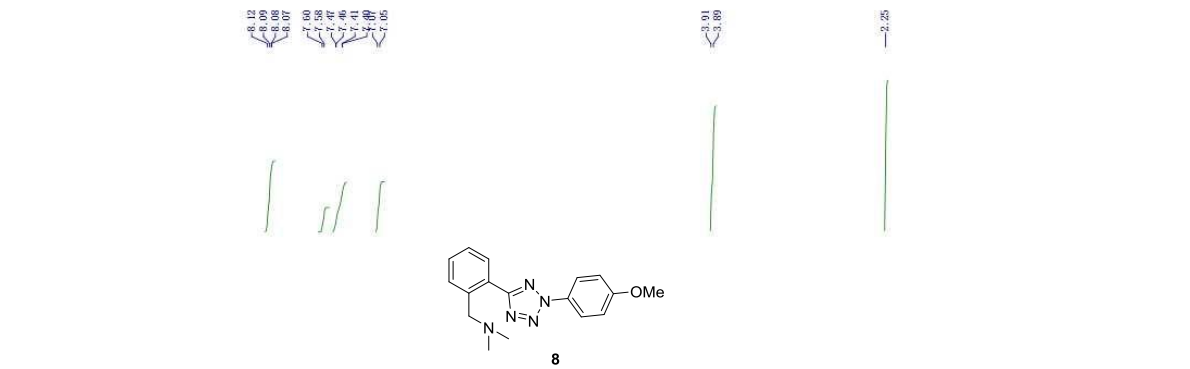
8.12
8.09
8.08
8.07
7.60
7.58
7.47
7.46
7.41
7.05
3.91
3.89
2.25
OMe
N
N
N
N
8

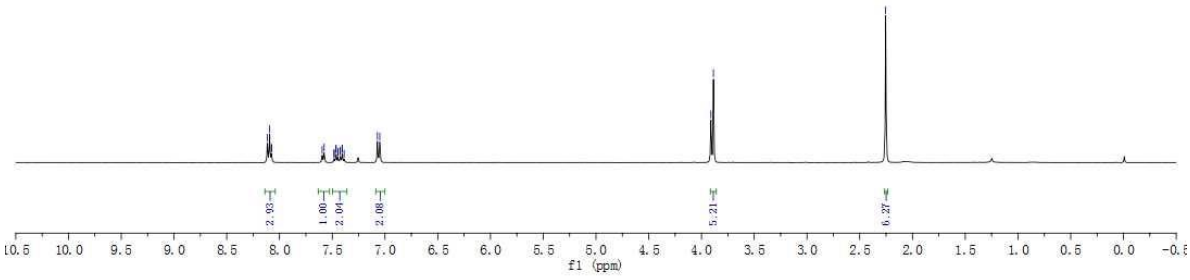
2.93
1.06
2.04
2.08
5.21
6.27
10.5 10.0 9.5 9.0 8.5 8.0 7.5 7.0 6.5 6.0 5.5 5.0 4.5 4.0 3.5 3.0 2.5 2.0 1.5 1.0 0.5 0.0
f1 (ppm)


165.06
160.40
138.27
130.75
130.02
129.91
127.35
126.65
121.39
114.65
77.30
76.99
76.67
61.53
55.62
45.51

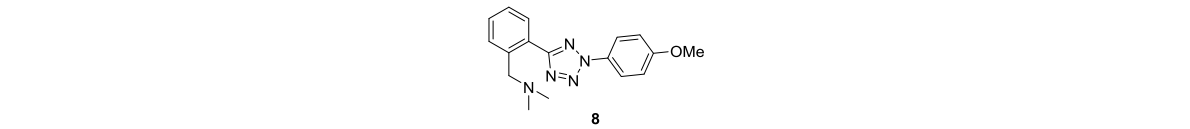
OMe
N
N
N
N
8

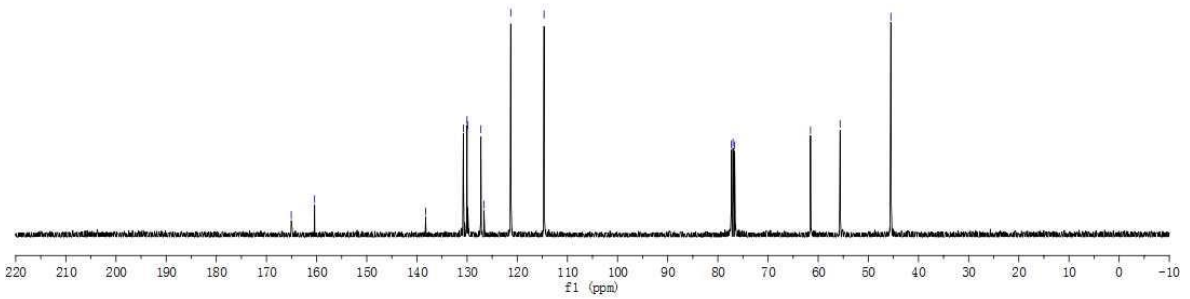
220 210 200 190 180 170 160 150 140 130 120 110 100 90 80 70 60 50 40 30 20 10 0 -10
f1 (ppm)

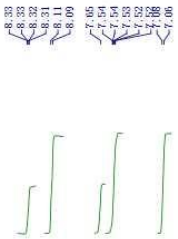

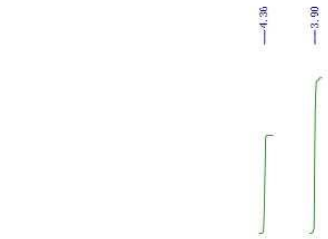

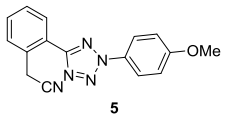

5

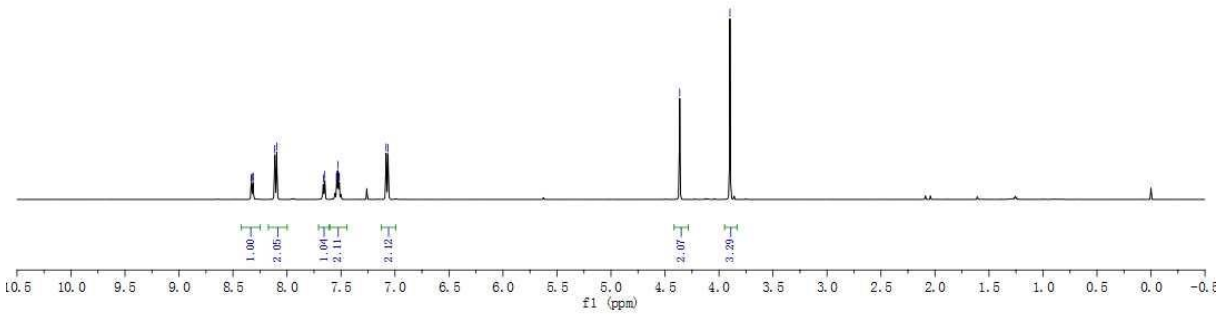

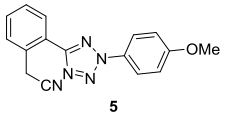

5

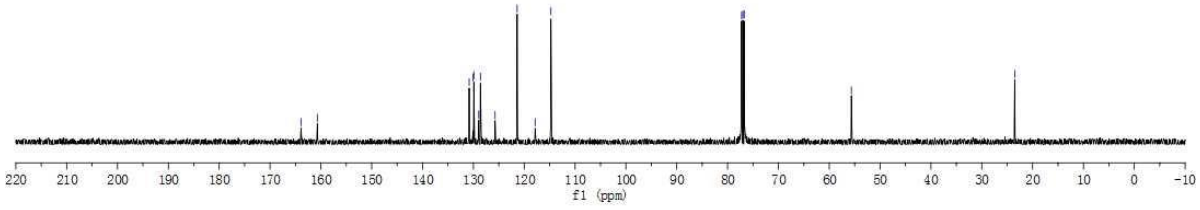


8.12
8.10
8.10
7.44
7.43
7.42
7.39
7.39
7.38
7.05
3.89
3.71
3.69
3.68
3.39
3.37
3.36

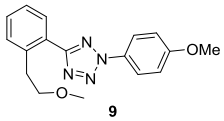
OMe
N
N
N
O

9

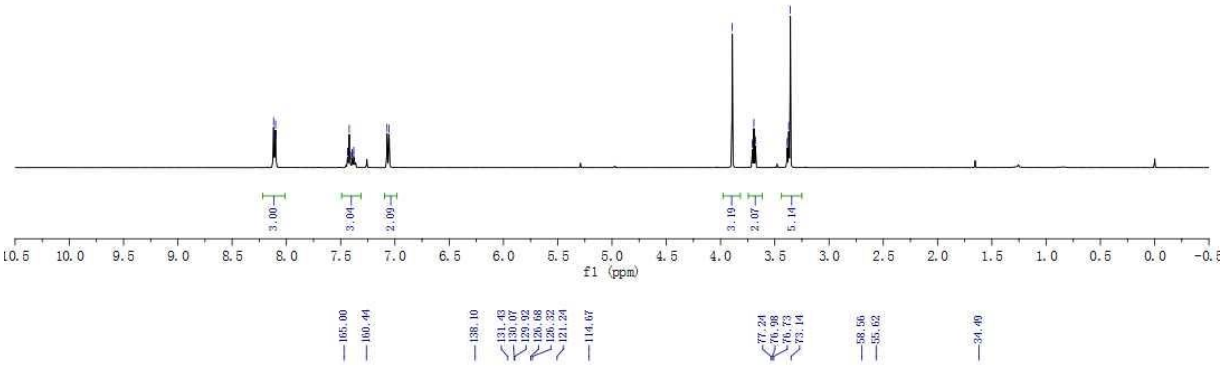
3.00
3.04
2.09
3.19
2.07
5.14
f1 (ppm)

165.00
160.44
138.10
131.43
130.07
129.92
126.68
126.32
121.24
114.67
77.24
76.98
76.73
73.14
58.56
55.62
34.49

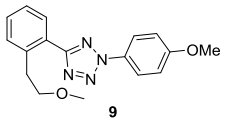
OMe
N
N
N
O

9

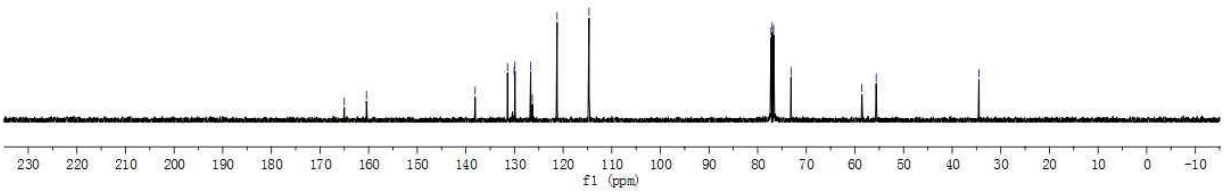
f1 (ppm)

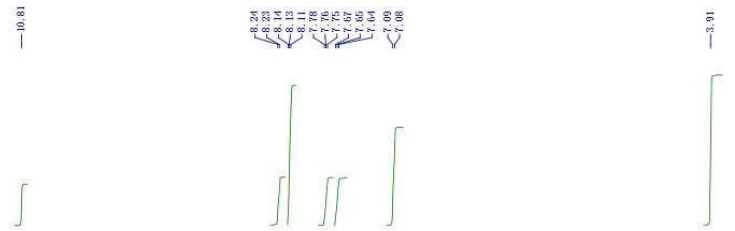
10.81
8.24
8.23
8.14
8.13
8.11
7.78
7.76
7.75
7.67
7.65
7.64
7.09
7.08
3.91

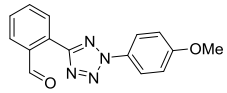
N
N
N
O
OMe

S4

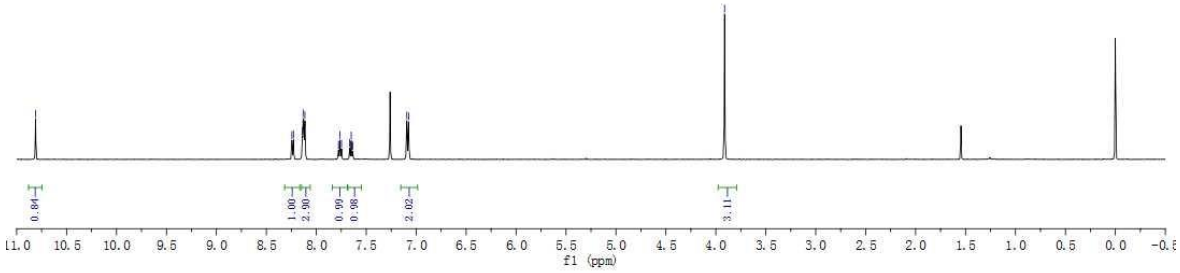
0.84
1.00
2.90
0.99
0.98
2.02
3.11
f1 (ppm)


192.07
163.04
160.77
134.67
133.71
130.47
130.08
128.97
128.11
121.40
114.76
77.30
76.98
76.67
55.66

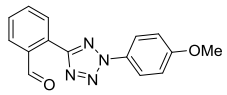
N
N
N
O
OMe

S4

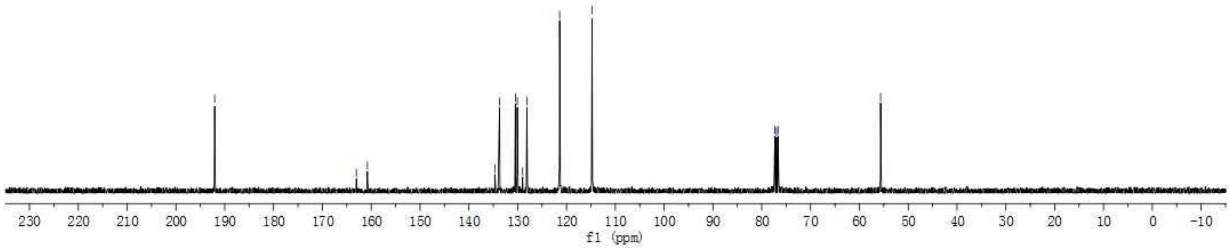
f1 (ppm)

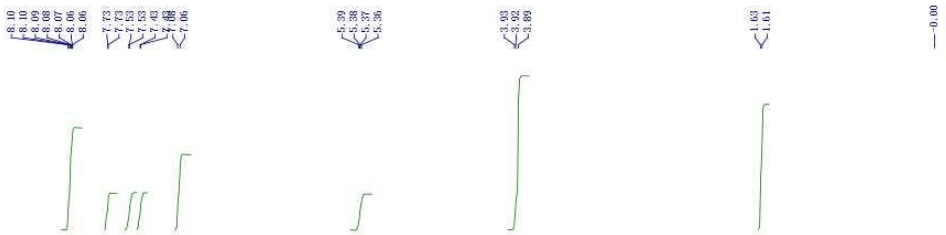

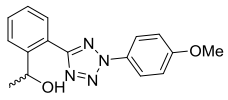
OMe
OH
N
N
N

S5

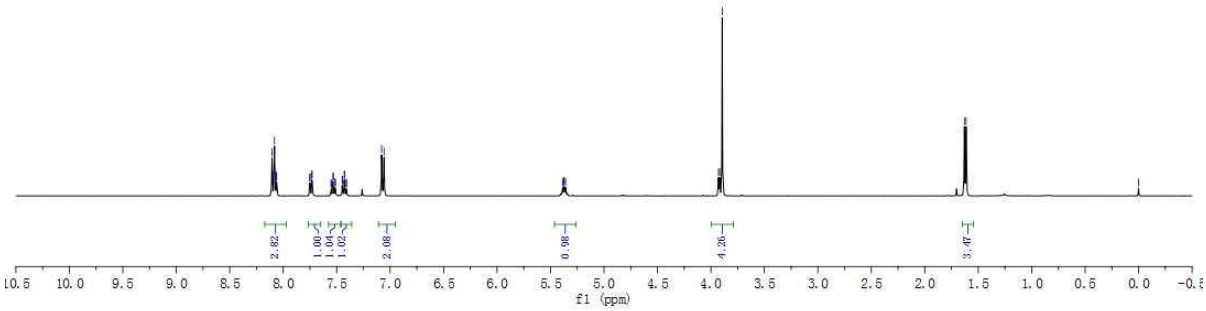
2.82
1.00
1.04
1.02
2.08
0.98
4.26
3.47
f1 (ppm)

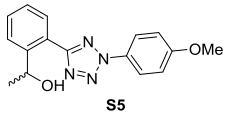
OMe
OH
N
N
N

S5

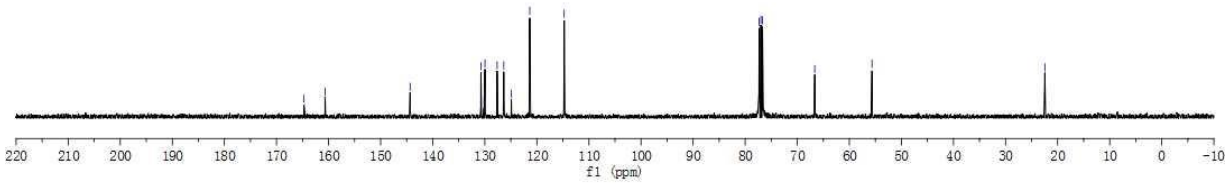
f1 (ppm)


8.11
8.09
8.07
8.05
7.75
7.73
7.55
7.53
7.43
7.06
5.21
5.19
3.89
3.21
1.56
1.55

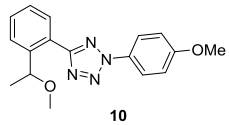
OMe
O

10

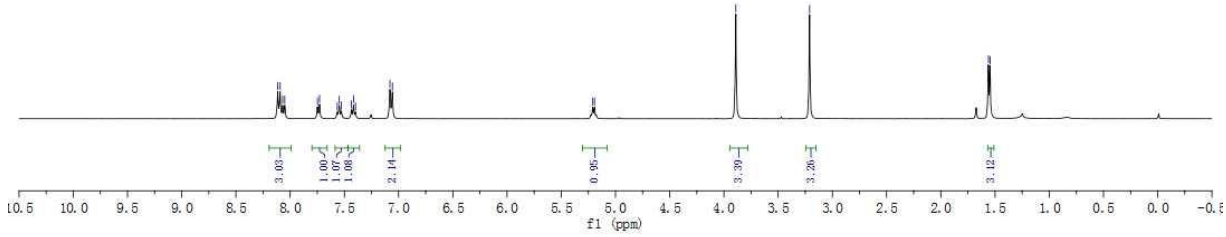
3.03
1.00
1.07
1.08
2.14
0.95
3.39
3.26
3.12
f1 (ppm)


164.60
160.52
143.55
130.68
130.34
129.62
127.26
126.08
125.13
121.25
114.71
77.31
76.99
76.67
75.82
56.60
55.64
23.86

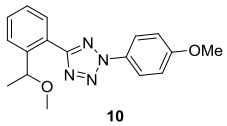
OMe
O

10

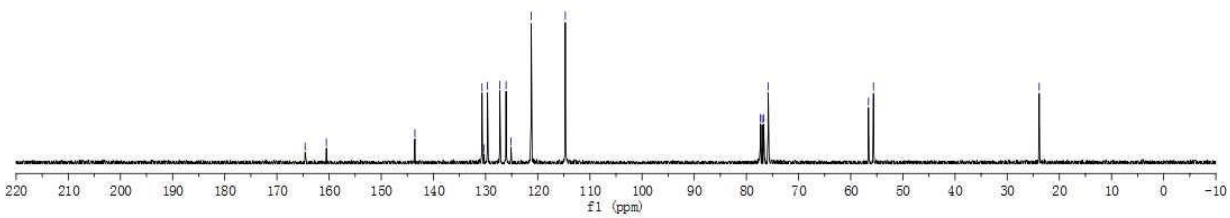
f1 (ppm)

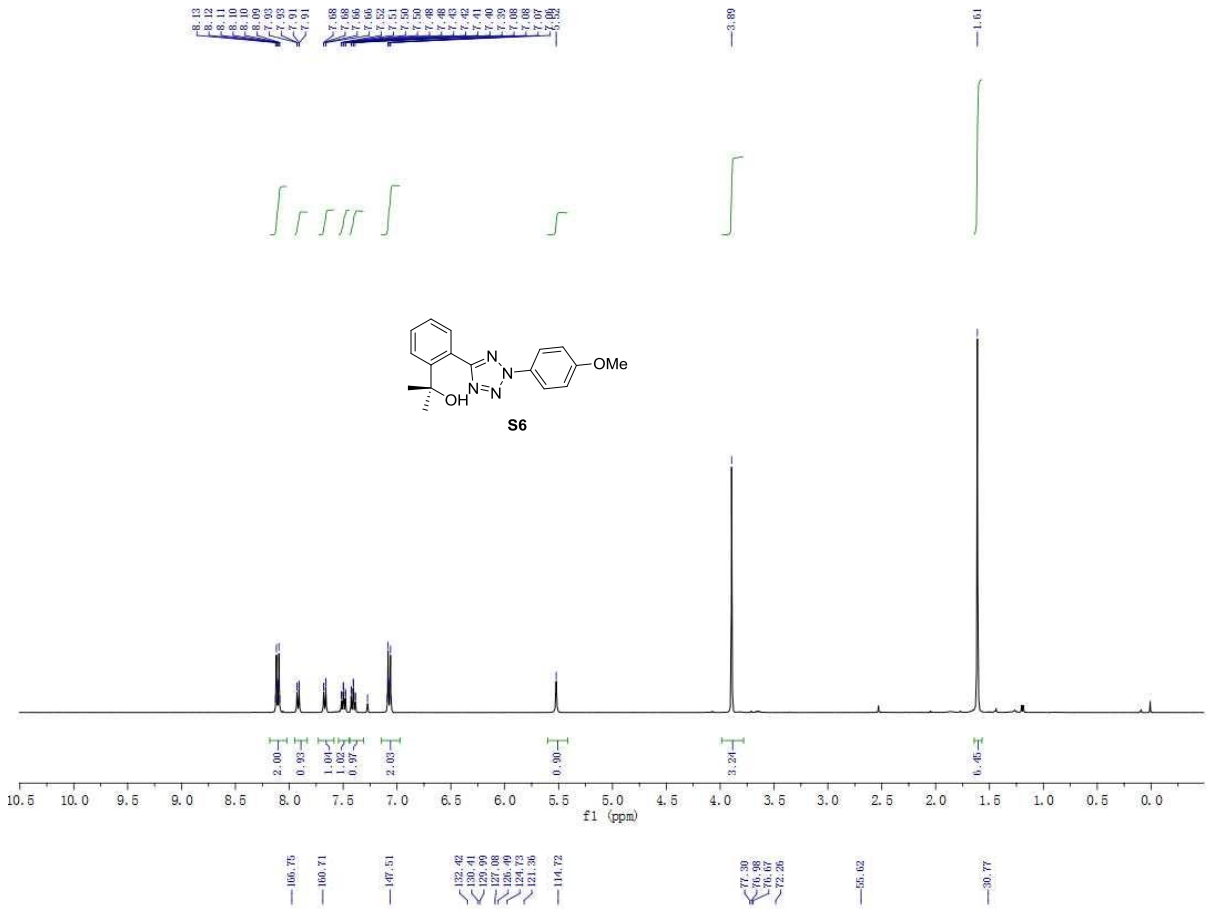
8.13
8.12
8.11
8.10
8.09
7.93
7.91
7.91
7.68
7.68
7.66
7.66
7.52
7.51
7.50
7.50
7.48
7.48
7.43
7.42
7.41
7.40
7.39
7.08
7.08
7.07
7.07
5.52
3.89
1.61
OMe
OH
S6
2.00
0.93
1.04
1.02
0.97
2.03
0.90
3.24
6.45
10.5 10.0 9.5 9.0 8.5 8.0 7.5 7.0 6.5 6.0 5.5 5.0 4.5 4.0 3.5 3.0 2.5 2.0 1.5 1.0 0.5 0.0
f1 (ppm)

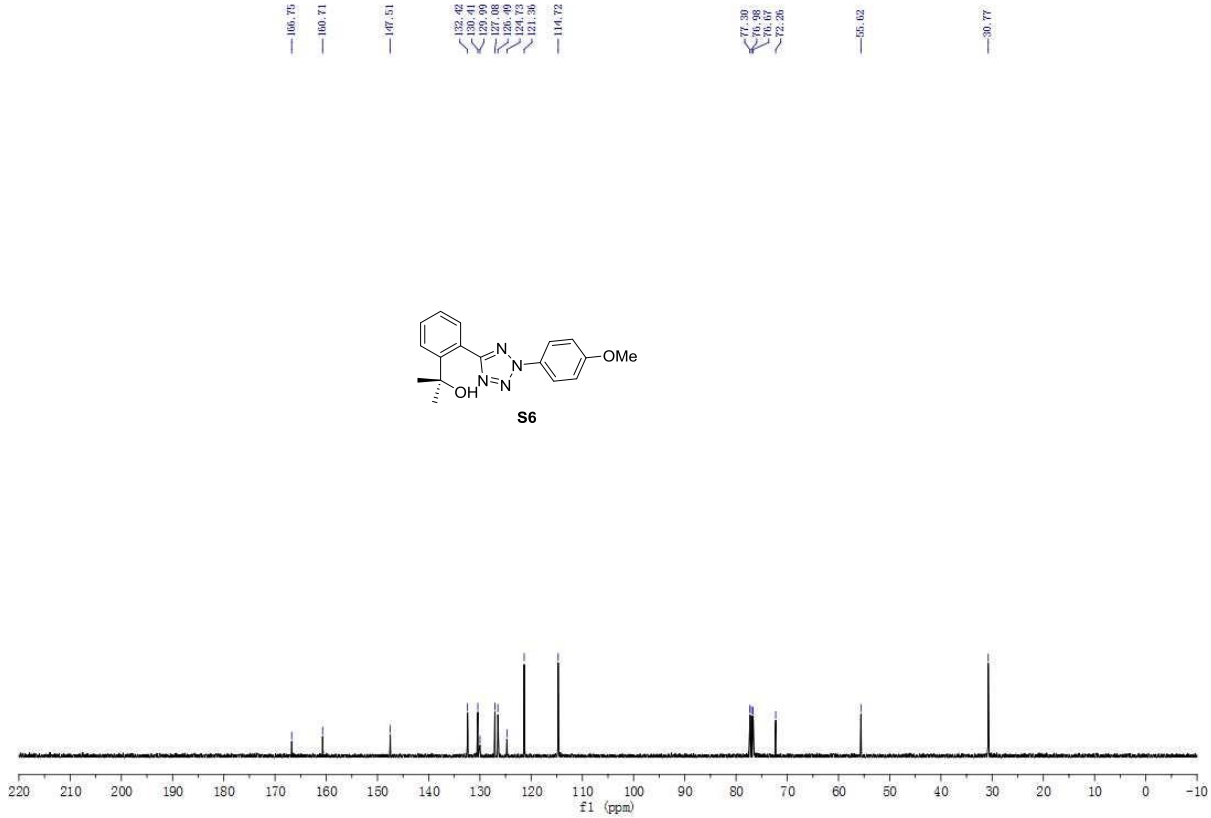
166.75
160.71
147.51
132.42
130.41
129.99
127.08
126.49
124.73
121.36
114.72
77.30
76.98
76.67
72.26
55.62
30.77
OMe
OH
S6
220 210 200 190 180 170 160 150 140 130 120 110 100 90 80 70 60 50 40 30 20 10 0 -10
f1 (ppm)

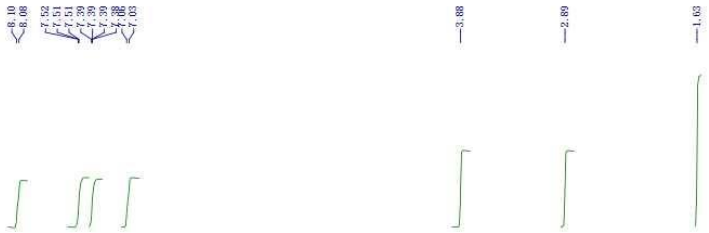

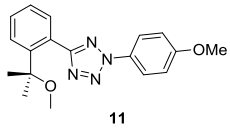

11

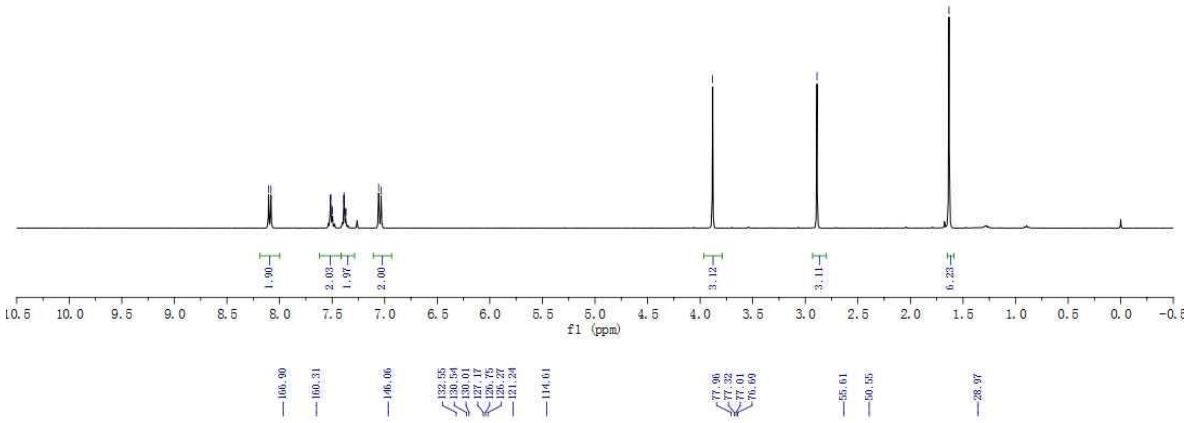

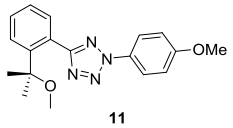

11

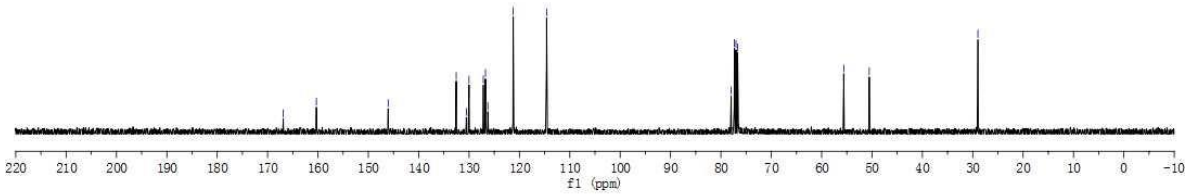

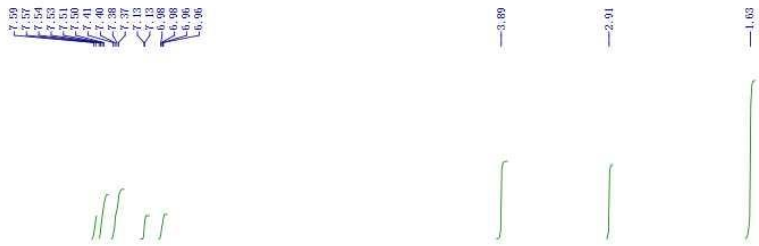
7.59
7.57
7.54
7.53
7.51
7.50
7.41
7.40
7.38
7.37
7.15
7.13
6.98
6.98
6.96
6.96
3.89
2.91
1.63

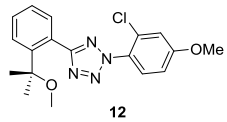
Cl
OMe
N
N
N
O

12

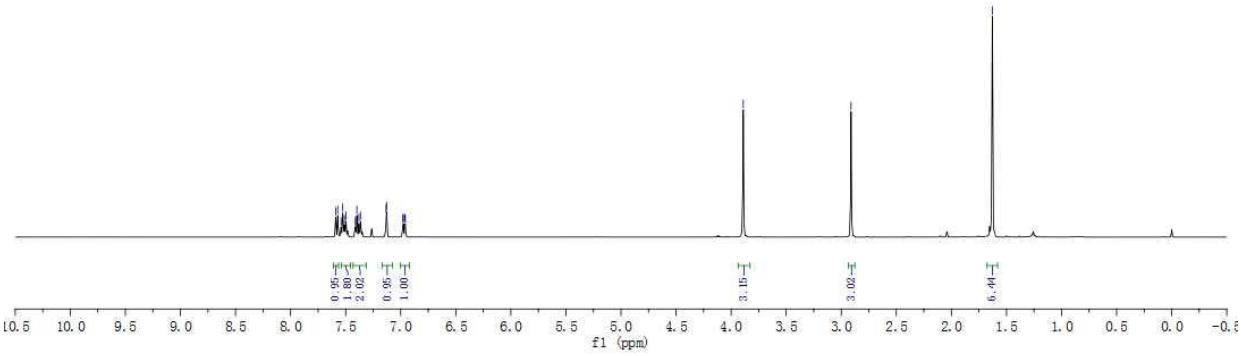
0.95
1.80
2.02
0.95
1.00
3.15
3.02
6.44
f1 (ppm)


167.01
161.33
146.21
132.64
130.87
130.04
128.54
127.16
126.68
125.96
115.88
113.31
77.96
77.25
76.89
76.74
55.93
50.53
28.91

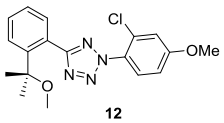
Cl
OMe
N
N
N
O

12

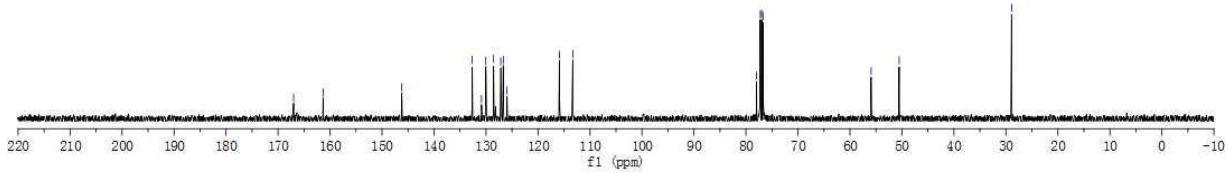
f1 (ppm)

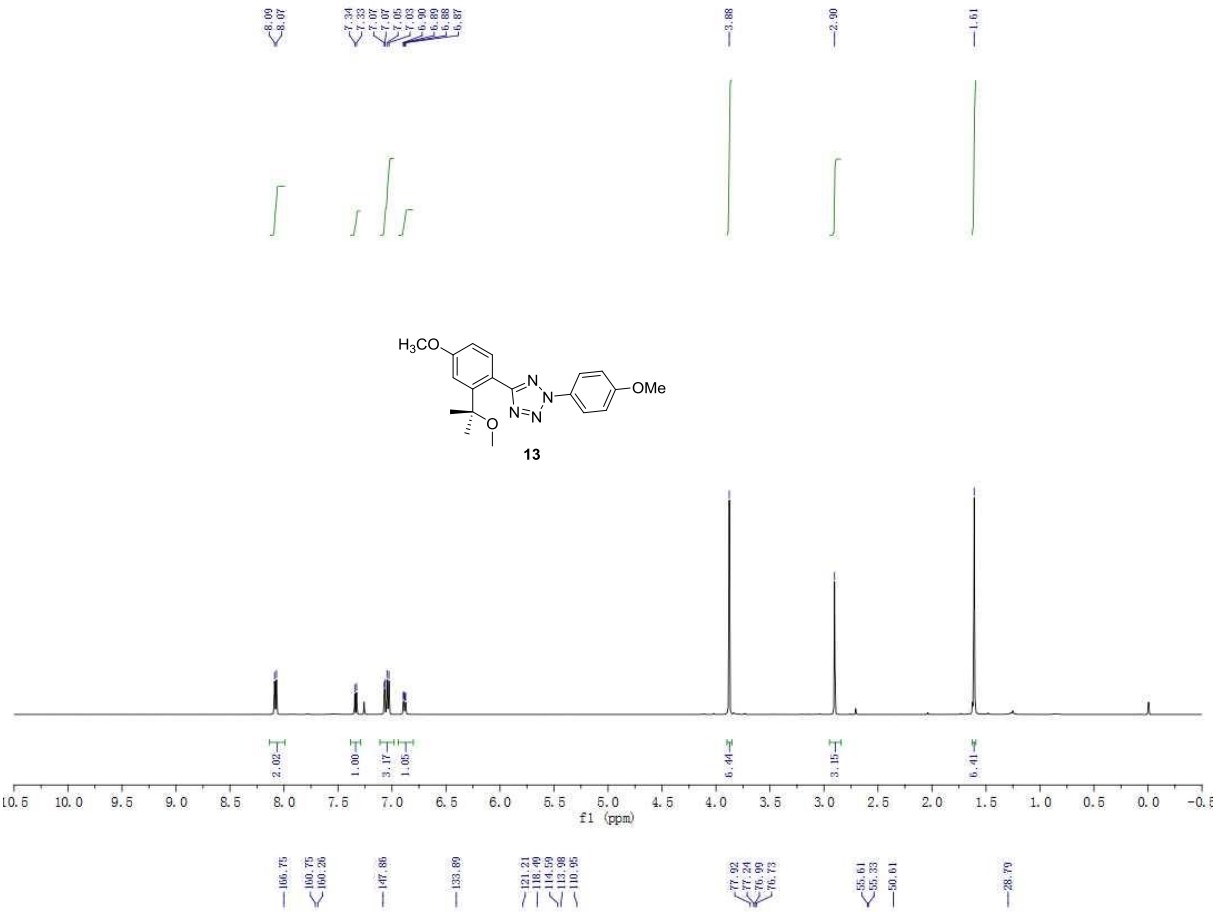
8.09
8.07
7.34
7.33
7.07
7.07
7.06
7.03
6.90
6.89
6.88
6.87
3.88
2.90
1.61
H3CO
OMe
13
2.02
1.00
3.17
1.05
6.44
3.15
6.41
f1 (ppm)

166.75
160.75
160.26
147.86
133.89
121.21
118.49
114.59
113.98
110.95
77.92
77.24
76.99
76.73
55.61
55.33
50.61
28.79

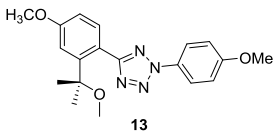
H3CO
OMe
13

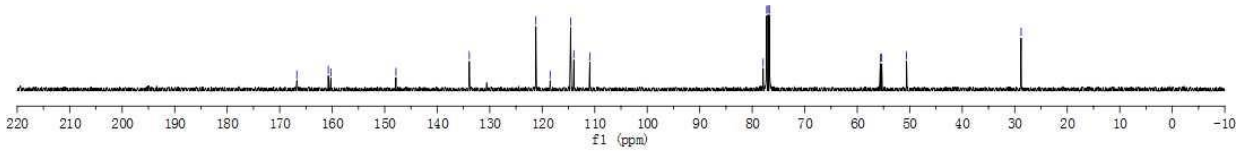
f1 (ppm)

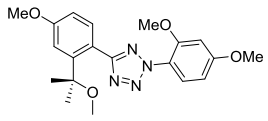
MeO
MeO
OMe
N
N
N
O

14

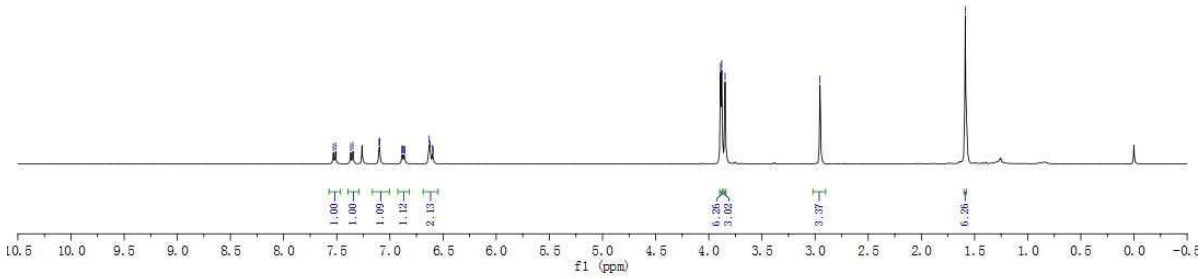
1.00
1.00
1.09
1.12
2.13
6.26
3.02
3.37
6.26
f1 (ppm)


166.36
162.30
160.67
154.65
147.93
133.94
127.77
118.61
113.75
110.98
104.45
99.77
77.99
77.31
76.99
76.67
56.09
55.71
55.32
50.60
28.71

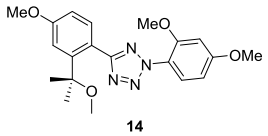
MeO
MeO
OMe
N
N
N
O

14

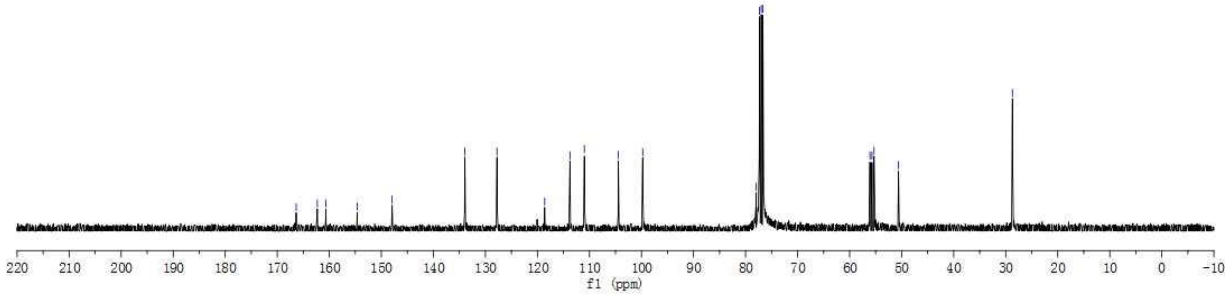
f1 (ppm)

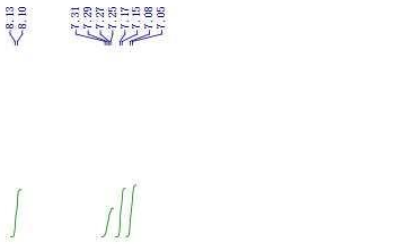
8.13
8.10
7.31
7.29
7.27
7.25
7.17
7.15
7.08
7.05
3.89
2.22

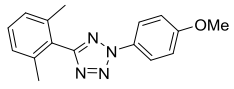
OMe
N
N
N=N

15

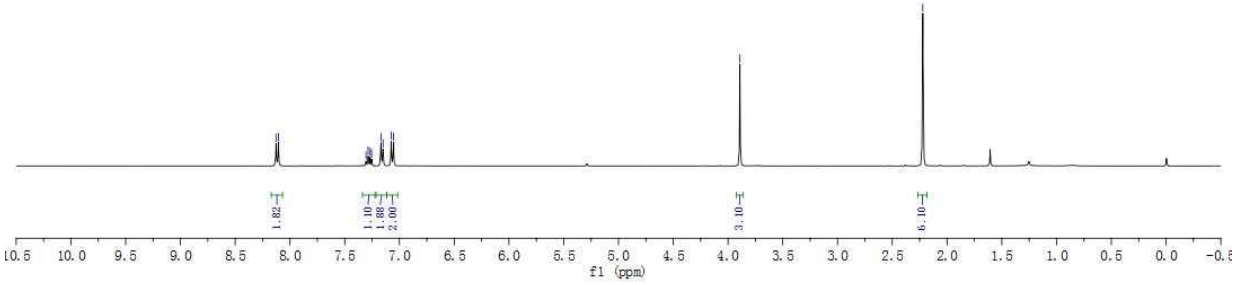
1.82
1.10
1.88
2.00
3.10
6.10
f1 (ppm)


164.04
160.46
138.26
129.67
127.74
127.10
121.27
114.68
77.31
77.00
76.67
55.65
20.40

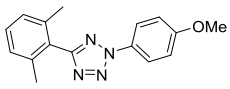
OMe
N
N
N=N

15

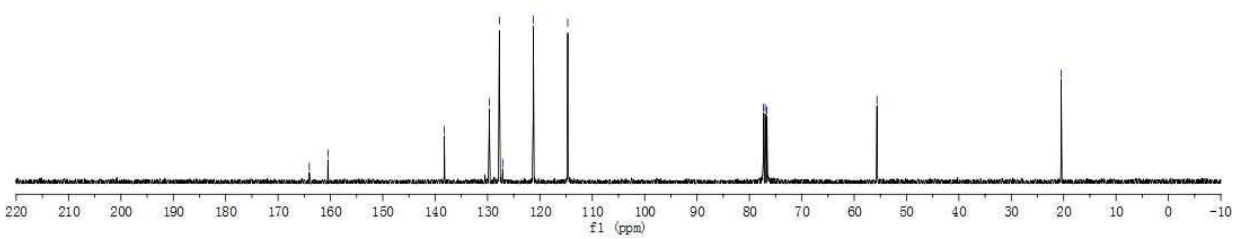
f1 (ppm)

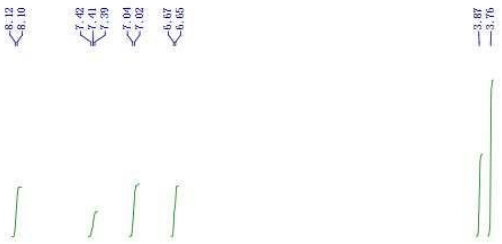
8.12
8.10
7.42
7.41
7.39
7.04
7.02
6.67
6.65
3.87
3.76

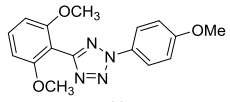
OCH3
OMe
N
N
N=N
OCH3

16

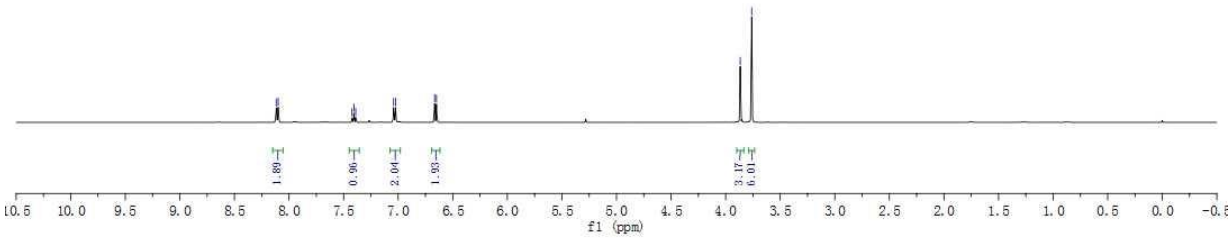
1.89
0.96
2.04
1.93
3.17
6.01
f1 (ppm)

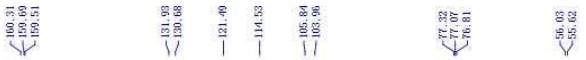
160.31
159.99
159.51
131.93
130.68
121.49
114.53
105.84
103.96
77.32
77.07
76.81
56.63
55.62

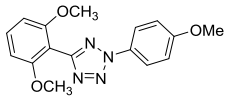
OCH3
OMe
N
N
N=N
OCH3

16

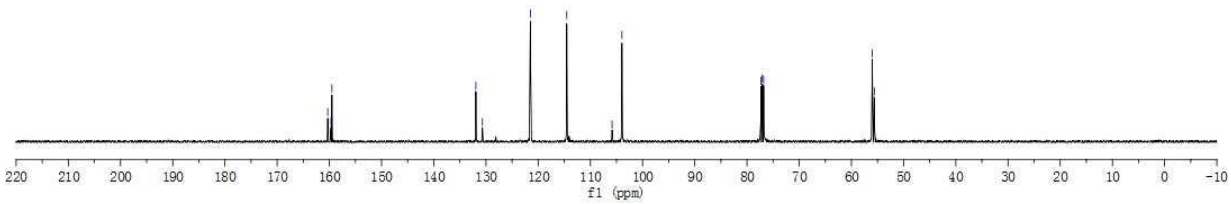
f1 (ppm)


8.13
8.11
7.56
7.55
7.54
7.53
7.08
7.06
4.46
3.89
3.26

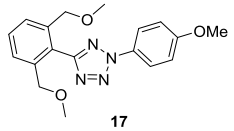
O
OMe
N
N
N=N
O

17

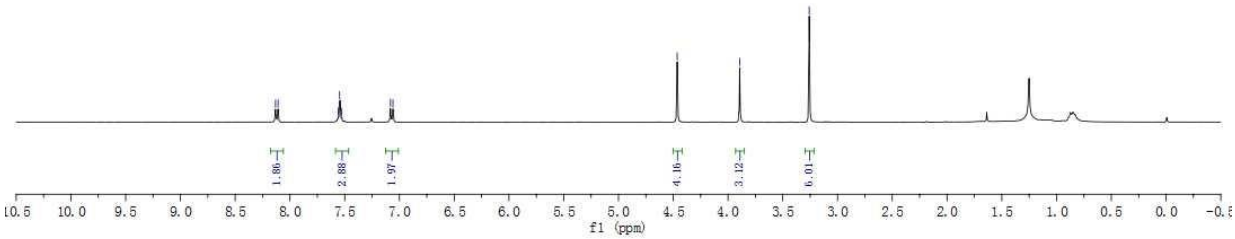
1.86
2.88
1.97
4.16
3.12
6.01
10.5 10.0 9.5 9.0 8.5 8.0 7.5 7.0 6.5 6.0 5.5 5.0 4.5 4.0 3.5 3.0 2.5 2.0 1.5 1.0 0.5 0.0
f1 (ppm)


162.59
160.56
138.67
130.43
127.40
124.77
121.27
114.72
77.31
76.99
76.67
72.15
58.20
55.66

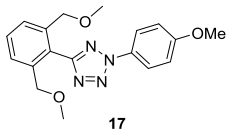
O
OMe
N
N
N=N
O

17

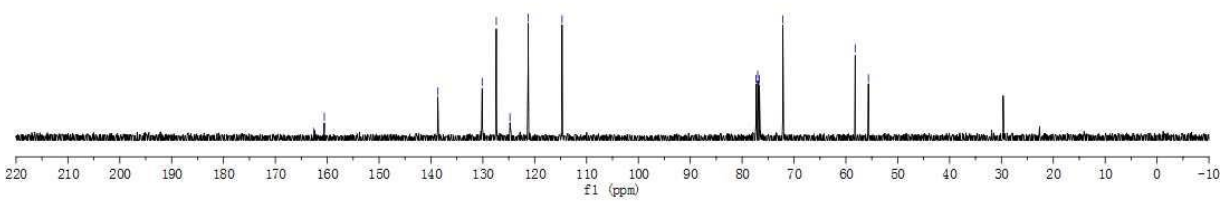
220 210 200 190 180 170 160 150 140 130 120 110 100 90 80 70 60 50 40 30 20 10 0 -10
f1 (ppm)

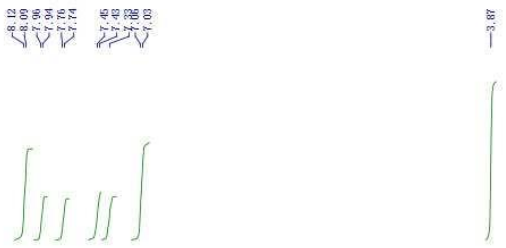
8.12
8.09
7.96
7.94
7.76
7.74
7.45
7.43
7.33
7.06
7.03
3.87

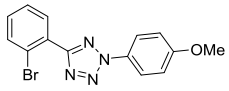
Br
N
N
N
OMe

S8

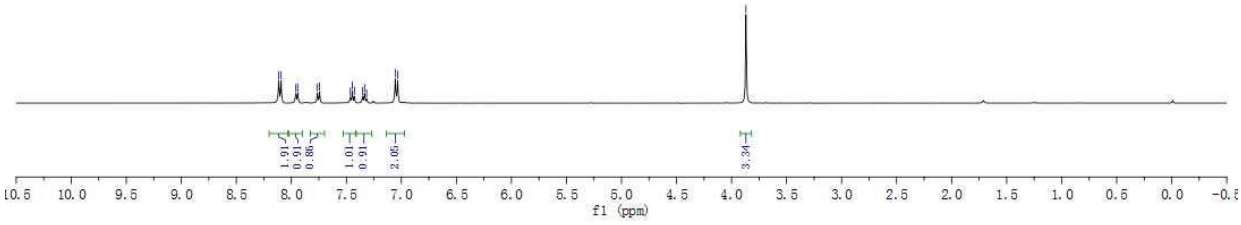
1.91
0.91
0.86
1.01
0.91
2.05
3.34
10.5 10.0 9.5 9.0 8.5 8.0 7.5 7.0 6.5 6.0 5.5 5.0 4.5 4.0 3.5 3.0 2.5 2.0 1.5 1.0 0.5 0.0
f1 (ppm)


163.92
160.53
134.13
131.64
131.25
128.37
127.42
122.06
121.40
114.64
77.31
76.99
76.68
55.60

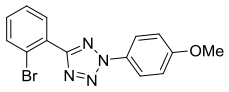
Br
N
N
N
OMe

S8

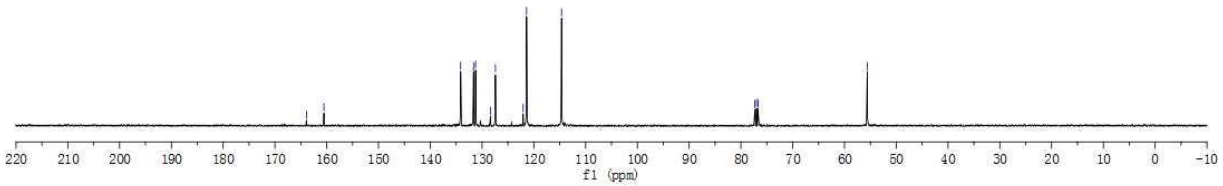
220 210 200 190 180 170 160 150 140 130 120 110 100 90 80 70 60 50 40 30 20 10 0 -10
f1 (ppm)

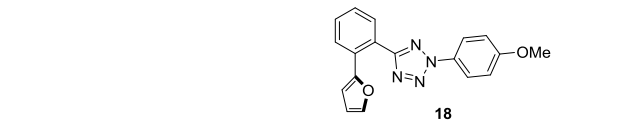

18

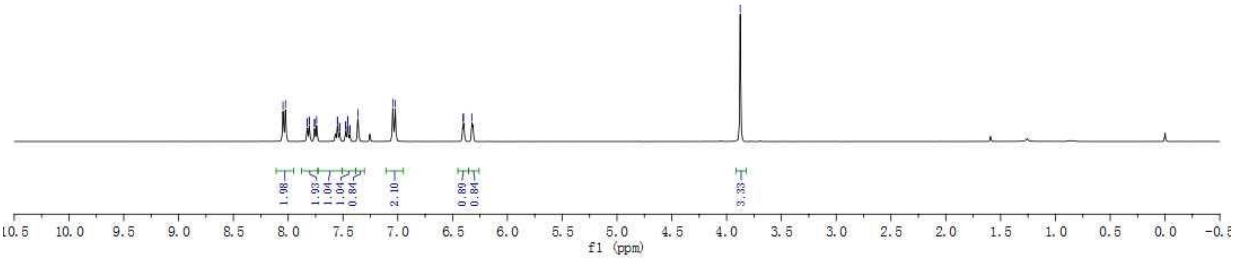

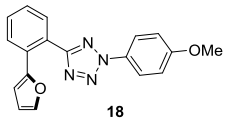

18

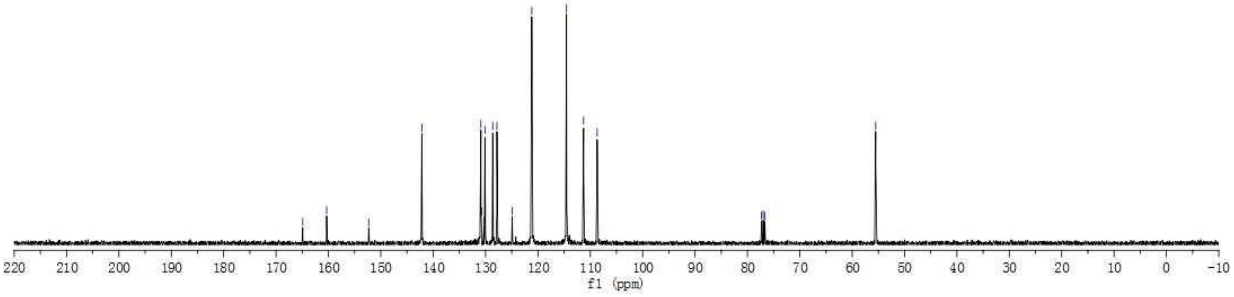

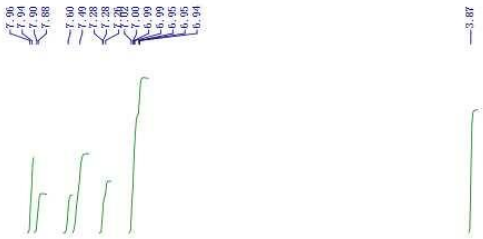

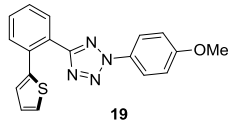

19

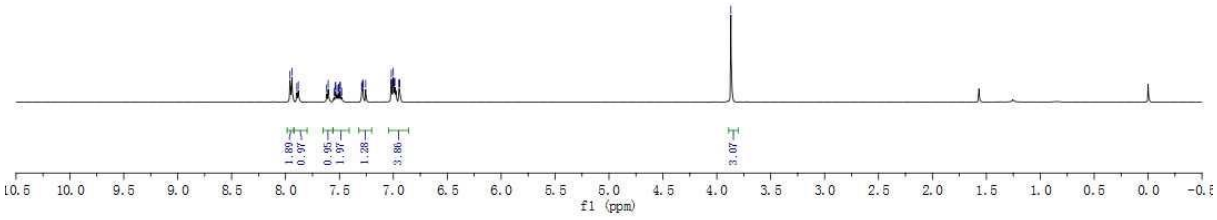

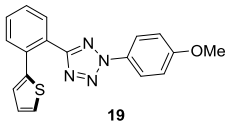

19

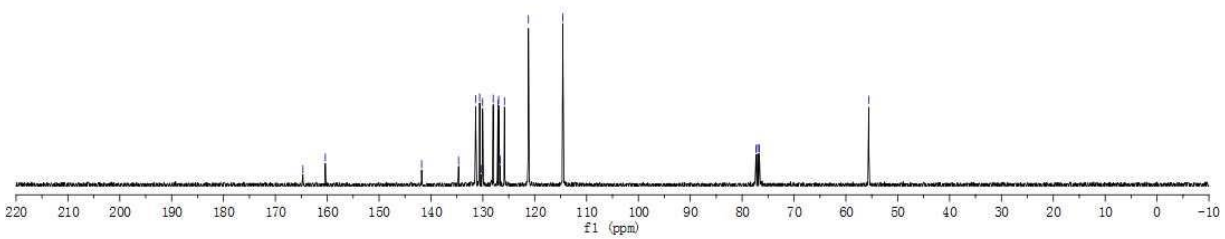


8.31
8.31
8.29
7.96
7.94
7.50
7.48
7.48
7.47
7.01
7.00
6.27
6.11
3.86
1.08

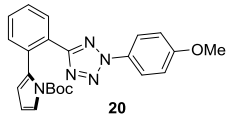
OMe
NBoc

20

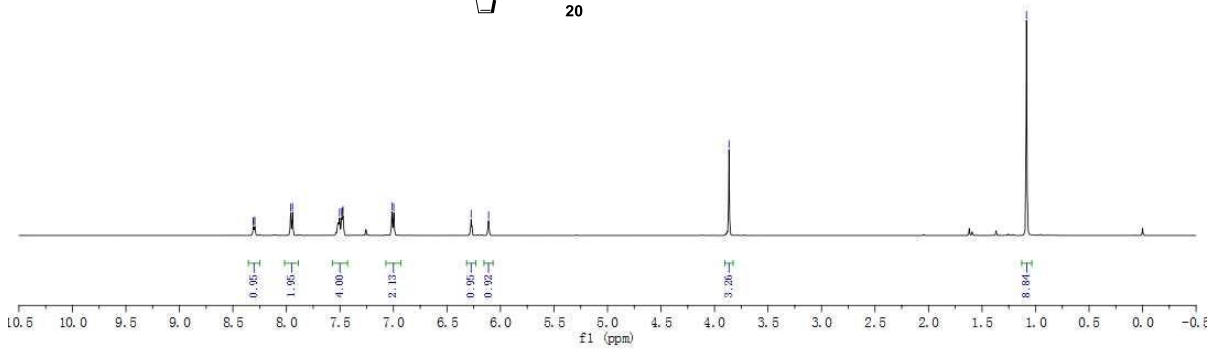
0.95
1.95
4.00
2.13
0.95
0.92
3.26
8.84
f1 (ppm)


164.47
160.29
149.32
134.21
132.68
131.52
129.02
128.49
128.07
127.47
121.11
121.00
114.58
113.03
110.69
82.98
77.25
76.99
76.74
55.58
27.23

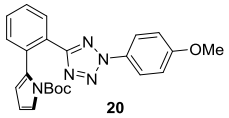
OMe
NBoc

20

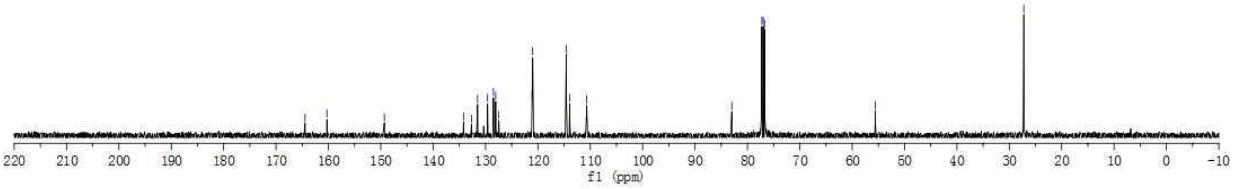
f1 (ppm)

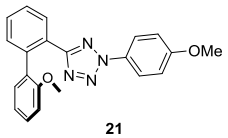

21

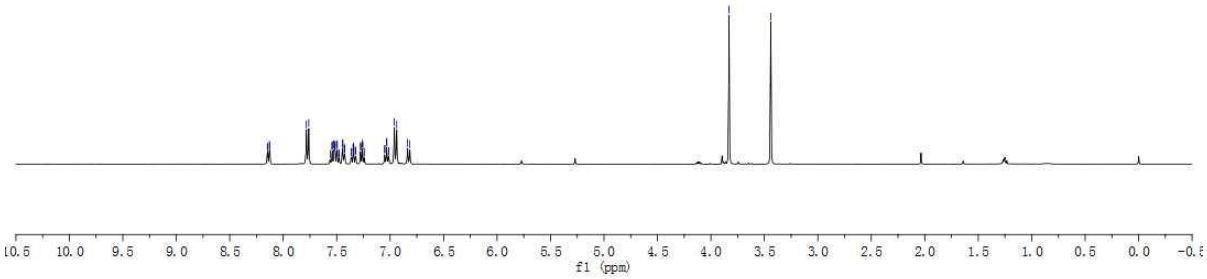

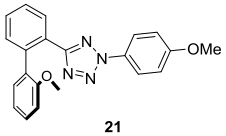

21

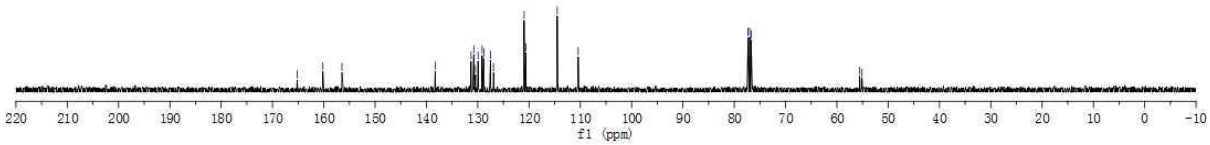

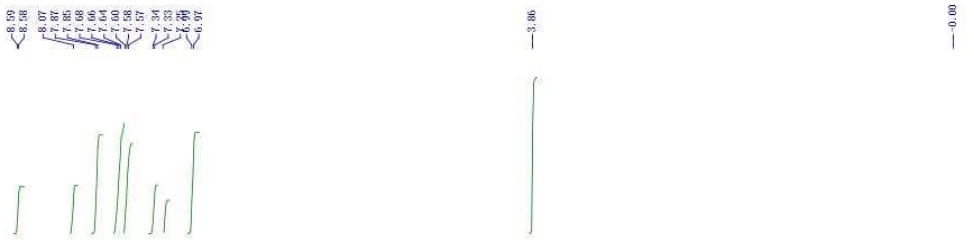

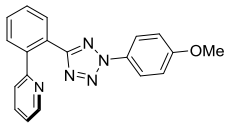

22

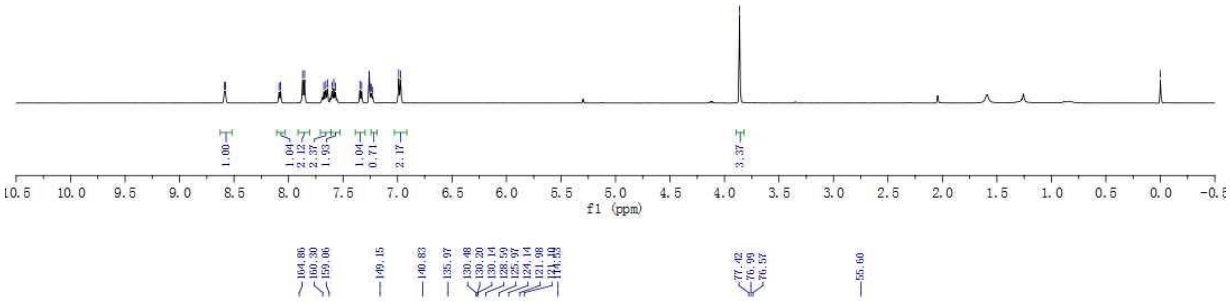

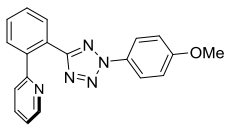

22

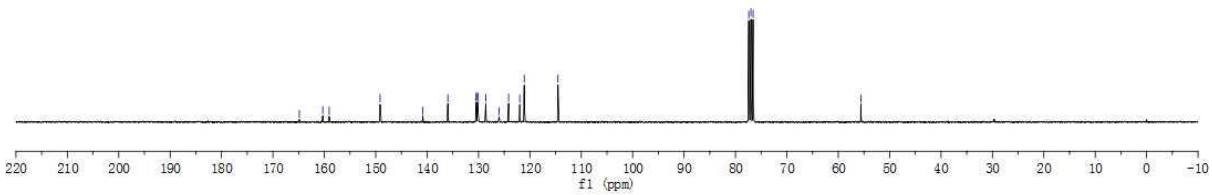

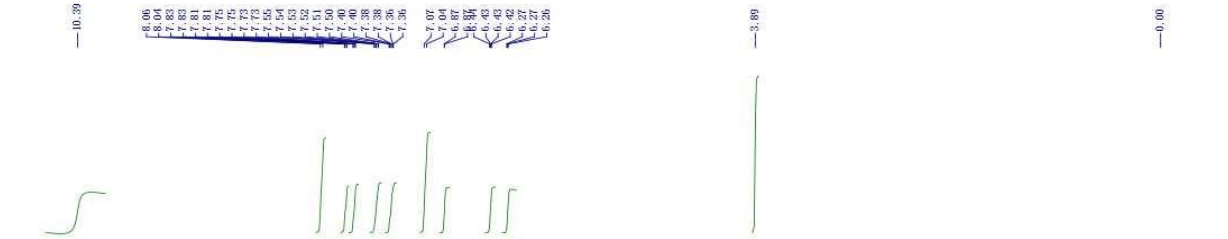

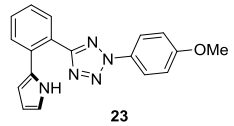

23

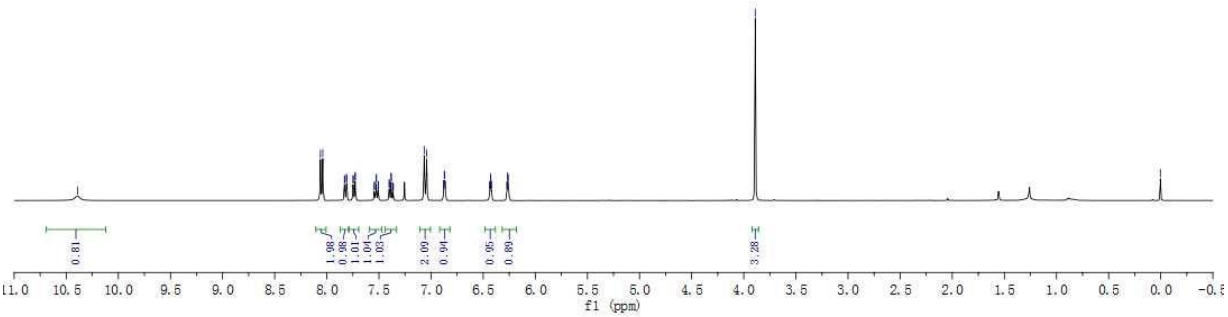

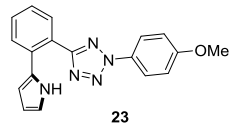

23

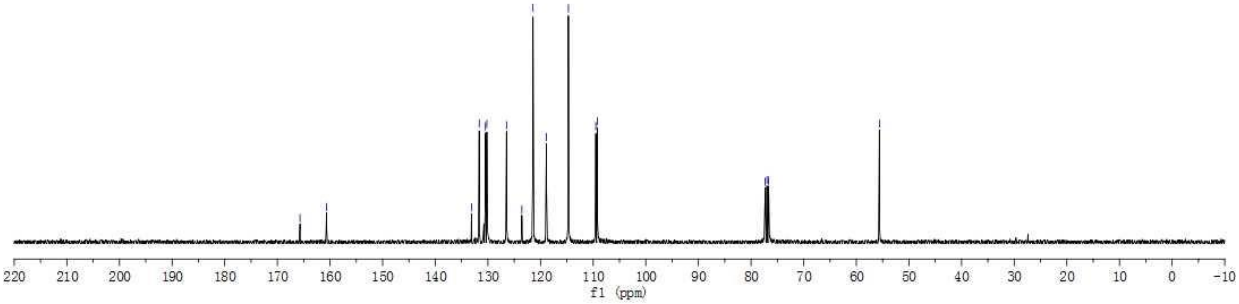

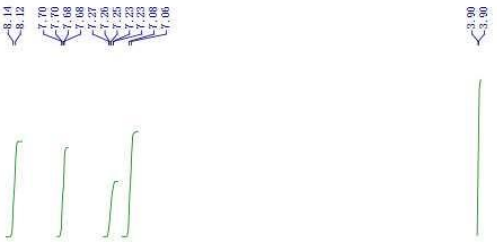
8.14
8.12
7.70
7.70
7.68
7.68
7.27
7.26
7.25
7.23
7.23
7.08
7.06
3.90
3.90

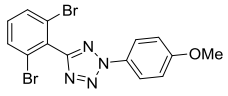
Br
Br
N
N
N
N
OMe

S9

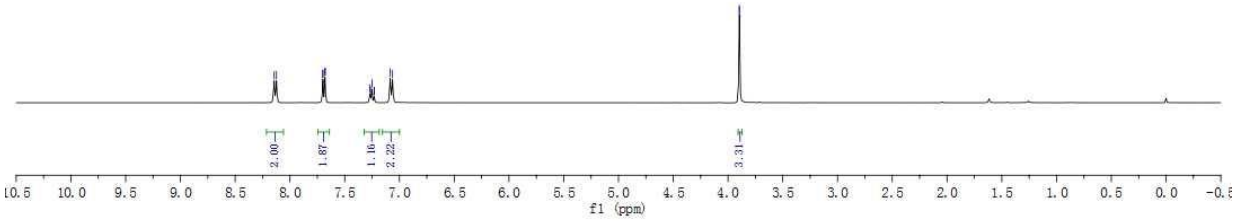
2.00
1.87
1.16
2.22
3.31
10.5
10.0
9.5
9.0
8.5
8.0
7.5
7.0
6.5
6.0
5.5
5.0
4.5
4.0
3.5
3.0
2.5
2.0
1.5
1.0
0.5
0.0
f1 (ppm)


163.28
160.68
132.39
131.87
130.74
130.39
125.36
121.50
114.71
77.30
76.99
76.67
55.67

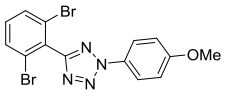
Br
Br
N
N
N
N
OMe

S9

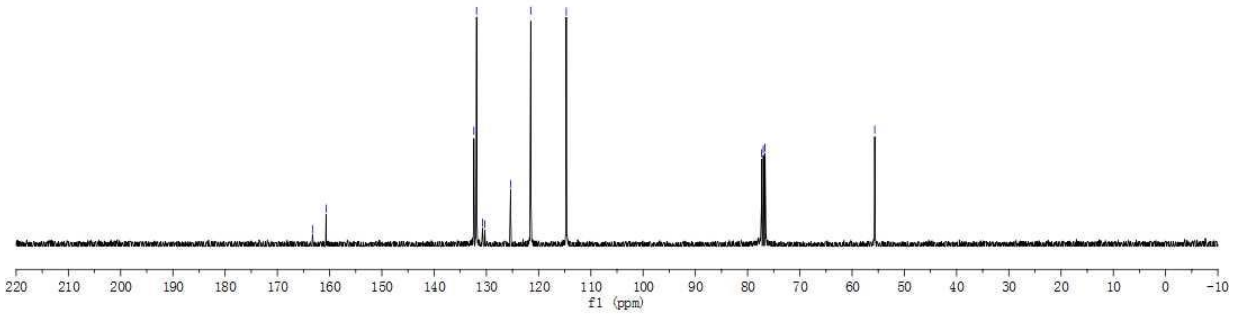
220
210
200
190
180
170
160
150
140
130
120
110
100
90
80
70
60
50
40
30
20
10
0
-10
f1 (ppm)

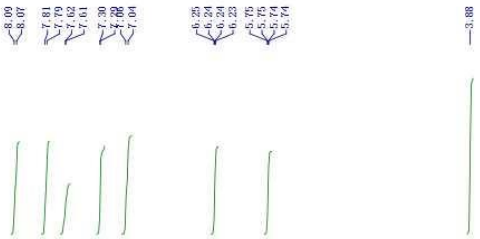
8.09
8.07
7.81
7.79
7.62
7.61
7.30
7.28
7.05
7.04
6.25
6.24
6.23
5.75
5.75
5.74
5.74
3.88

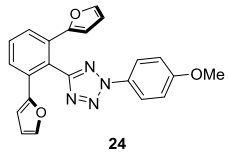
O
N
N
N
OMe
O

24

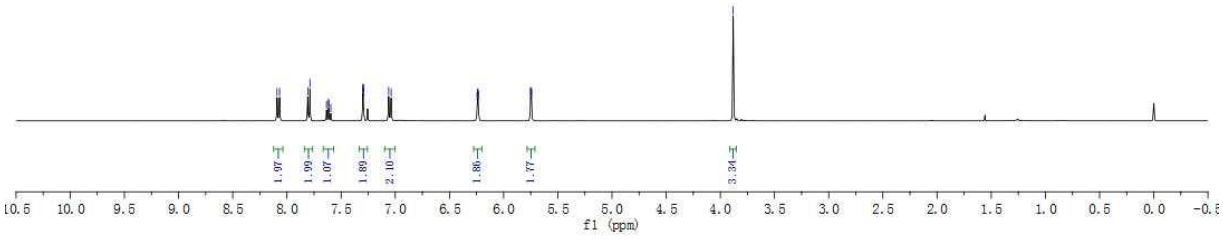
1.97
1.99
1.07
1.89
2.10
1.86
1.77
3.34
f1 (ppm)


163.31
160.57
151.68
142.35
132.77
130.42
126.35
121.37
120.73
114.70
111.45
109.02
77.31
76.99
76.67
55.68

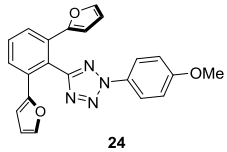
O
N
N
N
OMe
O

24

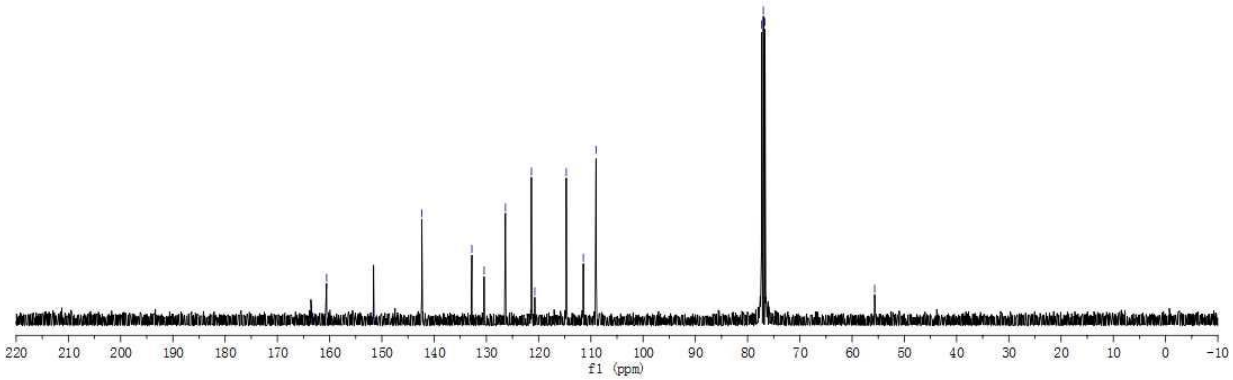
f1 (ppm)

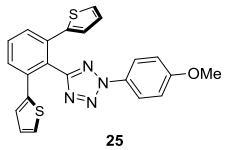

25

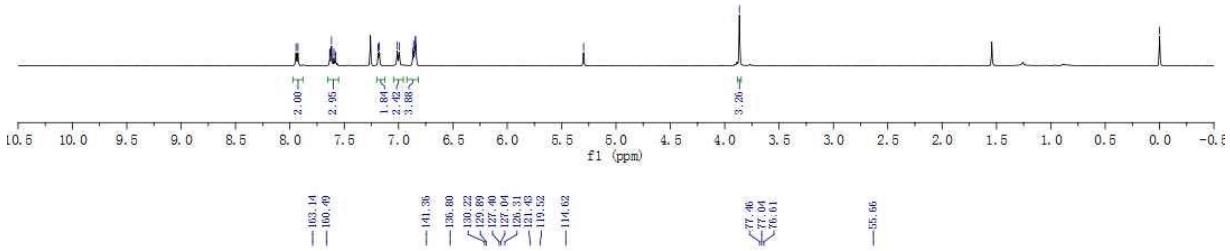

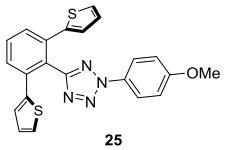

25

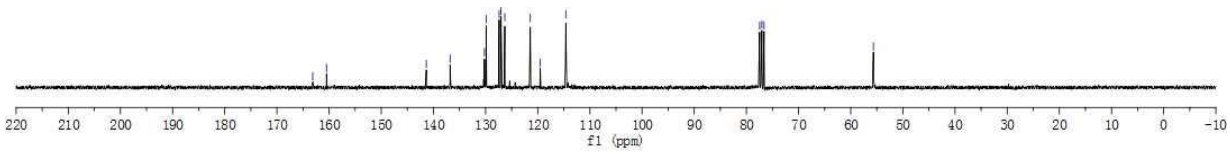

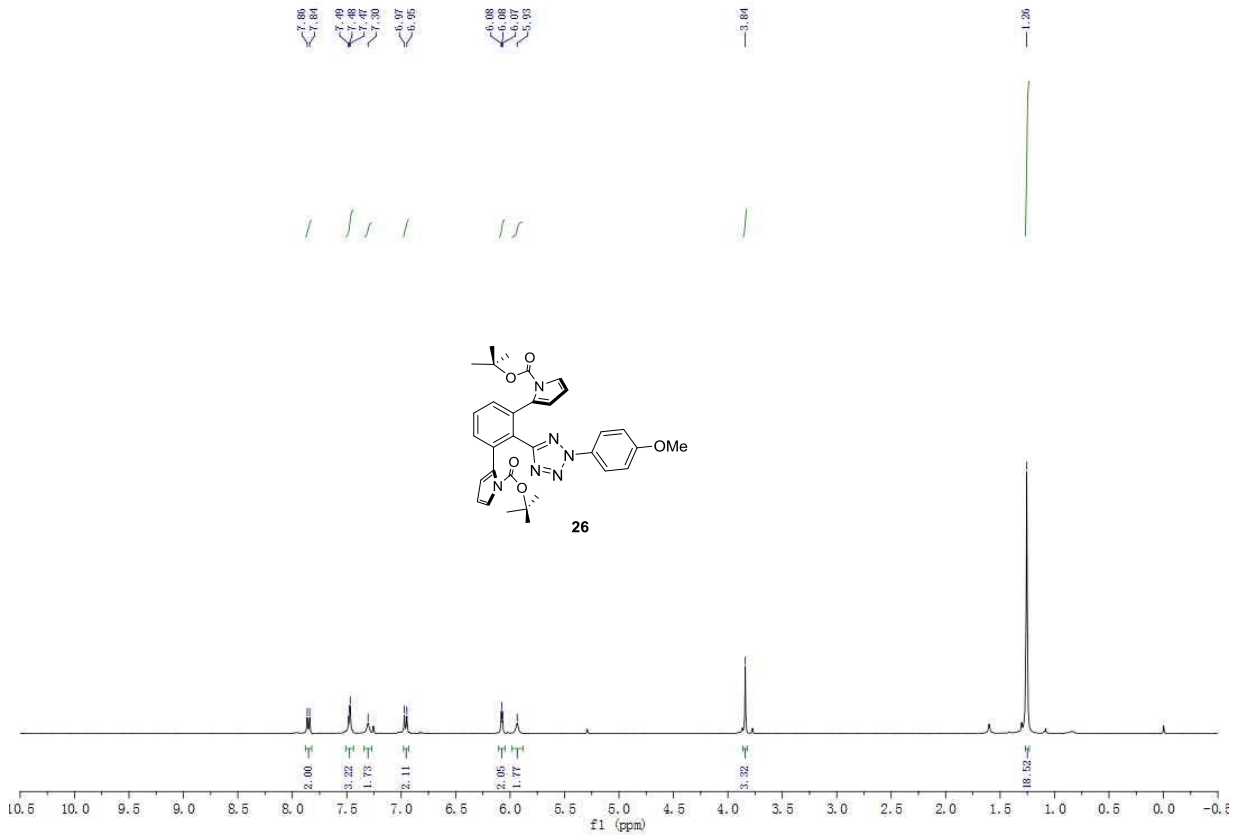
7.86
7.84
7.49
7.48
7.47
7.30
6.97
6.95
6.08
6.08
6.07
5.93
3.84
1.26
OMe
26
2.00
3.22
1.73
2.11
2.05
1.77
3.32
18.52
f1 (ppm)

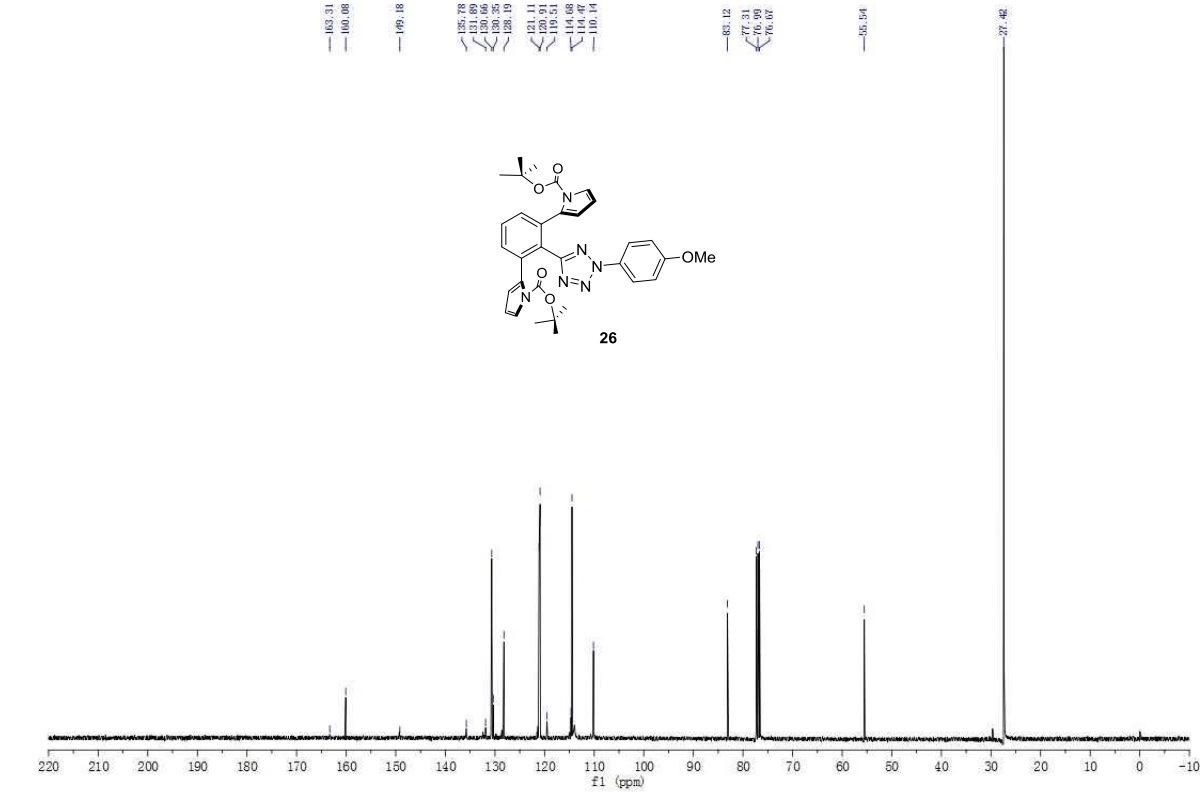
163.31
160.08
149.18
135.78
131.89
130.66
130.35
128.19
121.11
120.91
119.51
114.68
114.47
110.14
83.12
77.31
76.99
76.67
55.54
27.42
OMe
26
f1 (ppm)

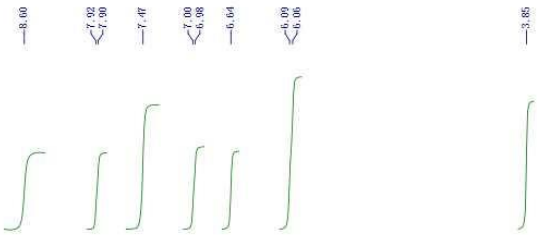
8.60
7.92
7.90
7.47
7.00
6.98
6.64
6.09
6.06
3.85

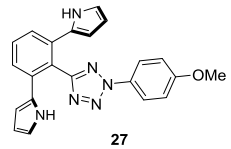
HN
N
N
N
OMe
NH

27

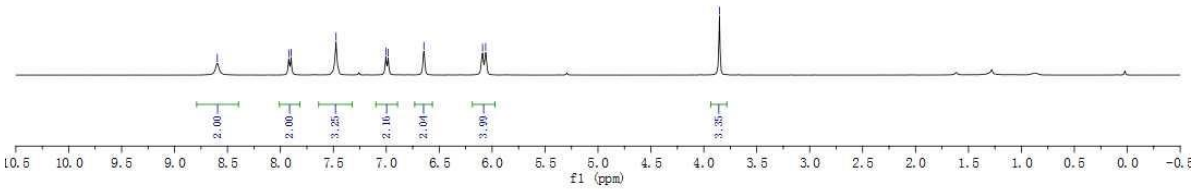
2.00
2.00
3.25
2.16
2.04
3.99
3.35
10.5 10.0 9.5 9.0 8.5 8.0 7.5 7.0 6.5 6.0 5.5 5.0 4.5 4.0 3.5 3.0 2.5 2.0 1.5 1.0 0.5 0.0
f1 (ppm)


164.64
160.60
135.57
130.66
130.38
130.10
127.27
121.90
121.59
119.94
114.67
109.25
109.23
77.36
77.04
76.72
55.65

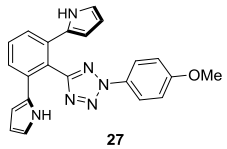
HN
N
N
N
OMe
NH

27

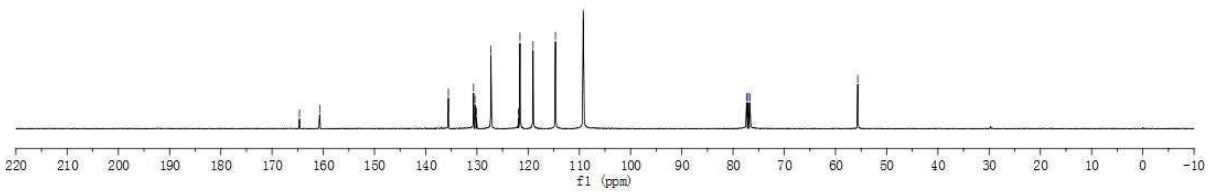
220 210 200 190 180 170 160 150 140 130 120 110 100 90 80 70 60 50 40 30 20 10 0 -10
f1 (ppm)

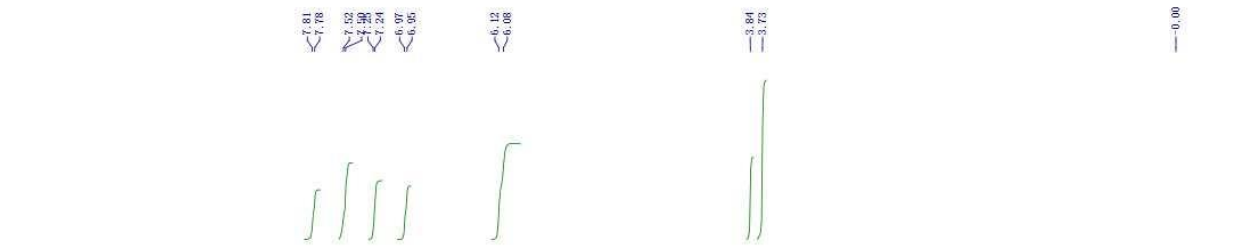

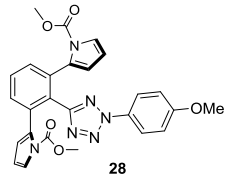

28

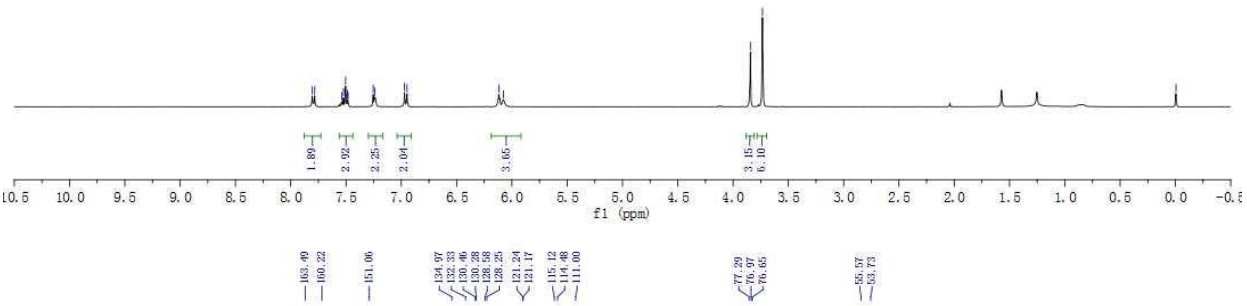

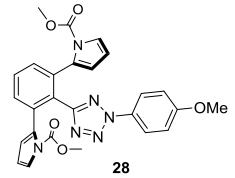

28

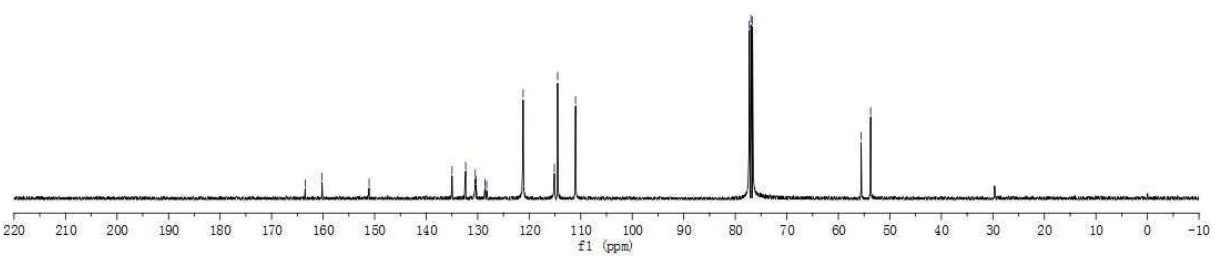

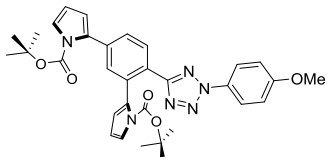

29

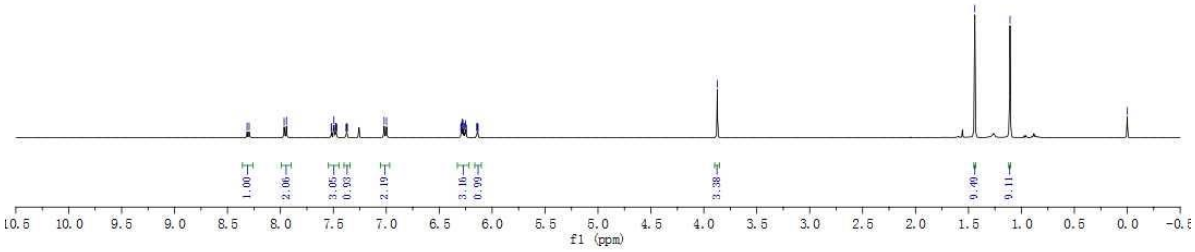

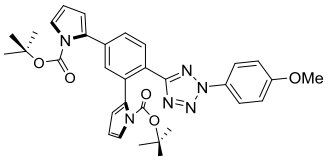

29

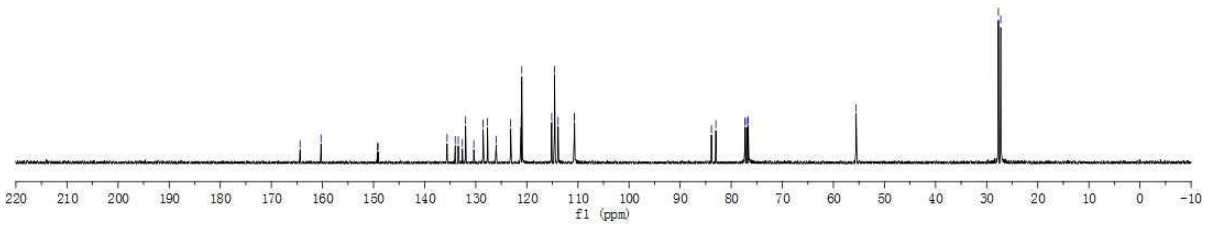


8.33
8.13
8.11
7.08
7.06
3.98
3.90
0.01

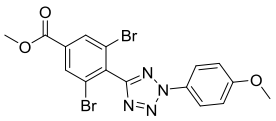

S12

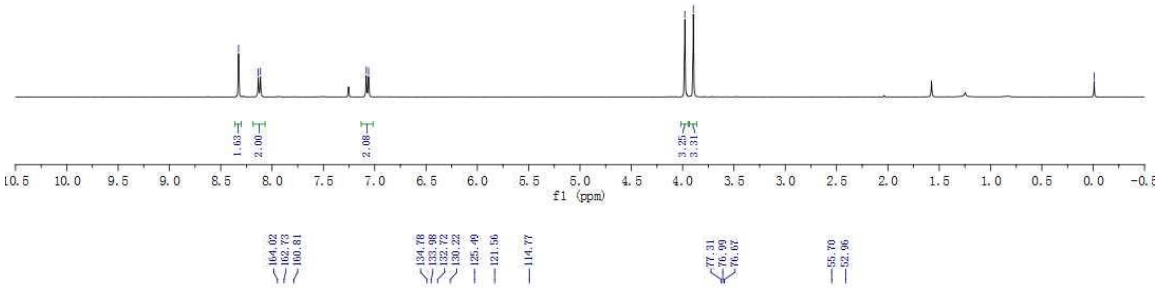
1.63
2.00
2.08
3.25
3.31
f1 (ppm)

164.62
162.73
160.81
134.78
133.98
132.72
130.22
125.49
121.56
114.77
77.31
76.99
76.67
55.70
52.96

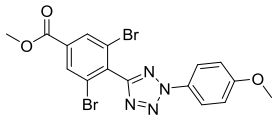

S12

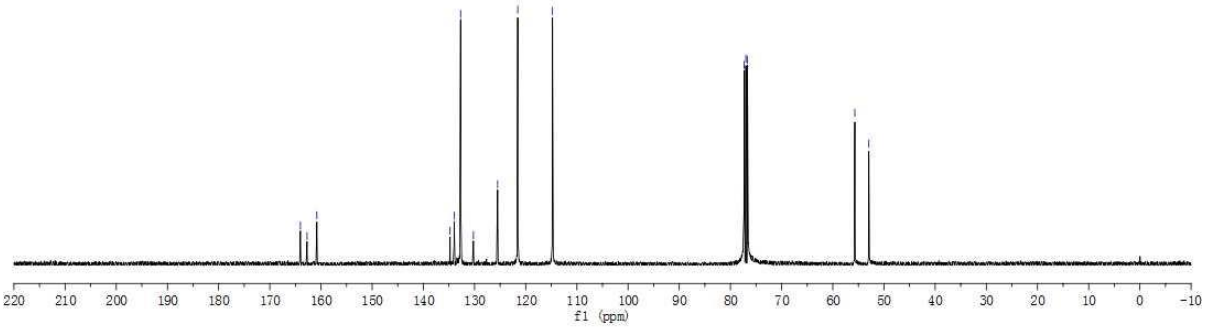
f1 (ppm)

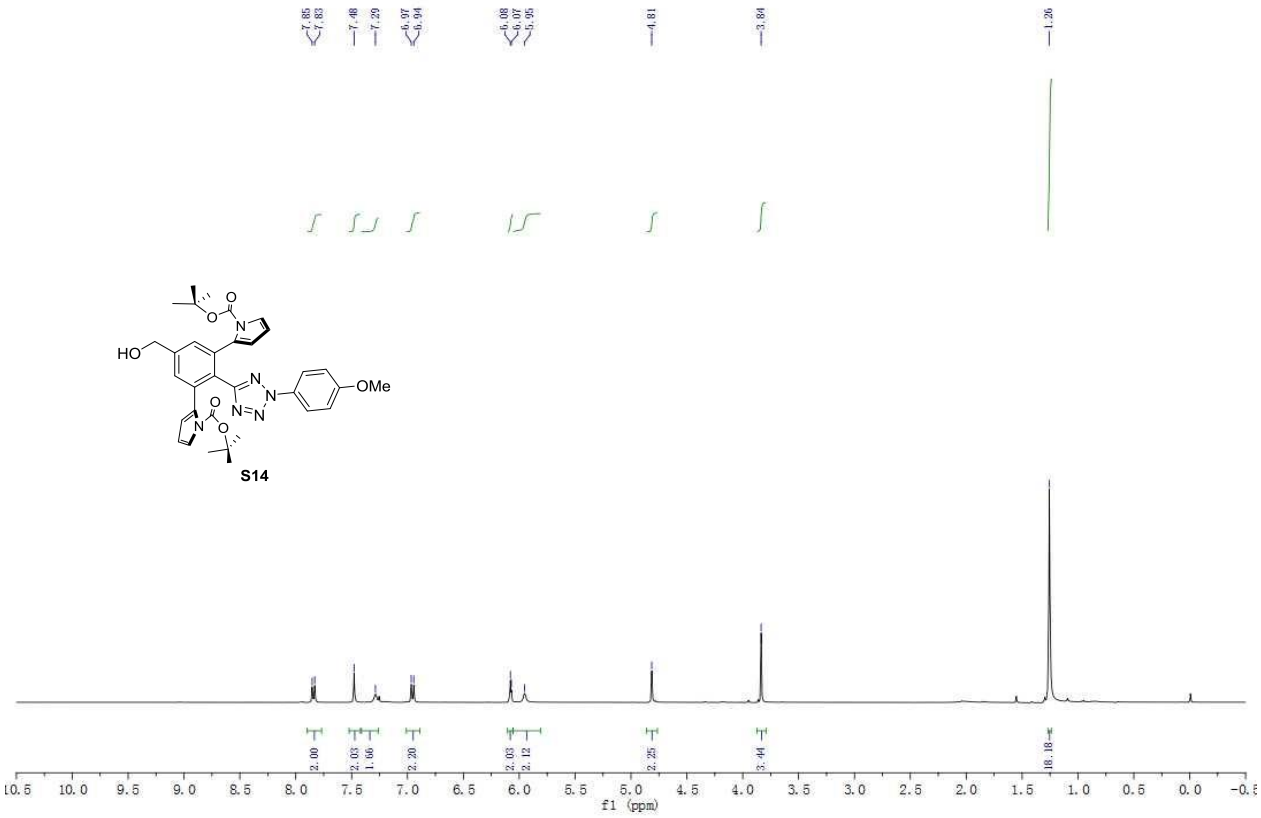
HO
OMe
S14
f1 (ppm)

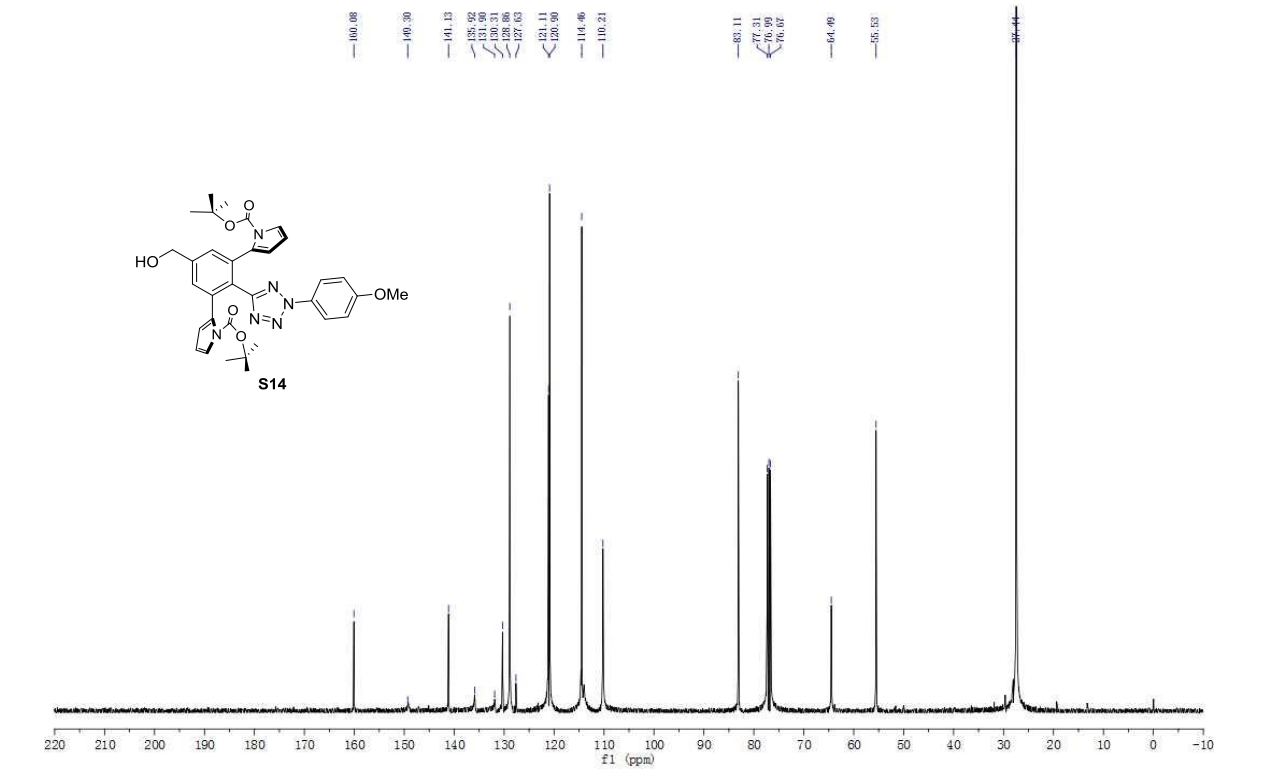
HO
OMe
S14
f1 (ppm)

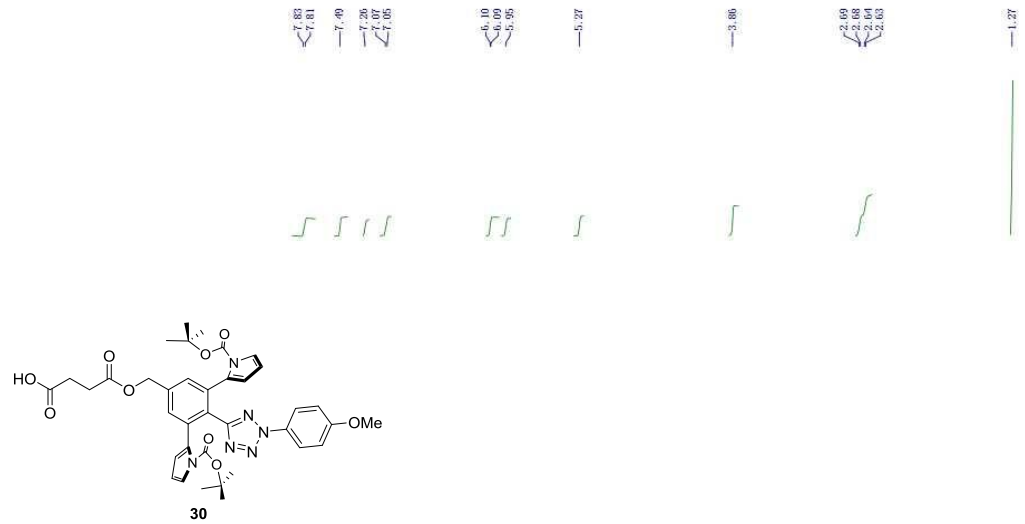
7.83
7.81
7.49
7.26
7.07
7.05
6.10
6.09
5.95
5.27
3.86
2.69
2.68
2.64
2.63
1.27
HO
O
O
O
N
N
N
N
N
O
O
OMe
30

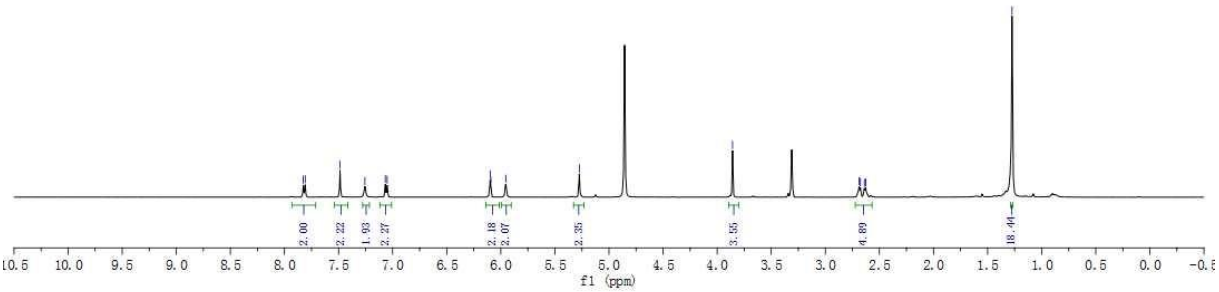
2.00
2.22
1.93
2.27
2.18
2.07
2.35
3.55
4.89
18.44
10.5
10.0
9.5
9.0
8.5
8.0
7.5
7.0
6.5
6.0
5.5
5.0
4.5
4.0
3.5
3.0
2.5
2.0
1.5
1.0
0.5
0.0
f1 (ppm)

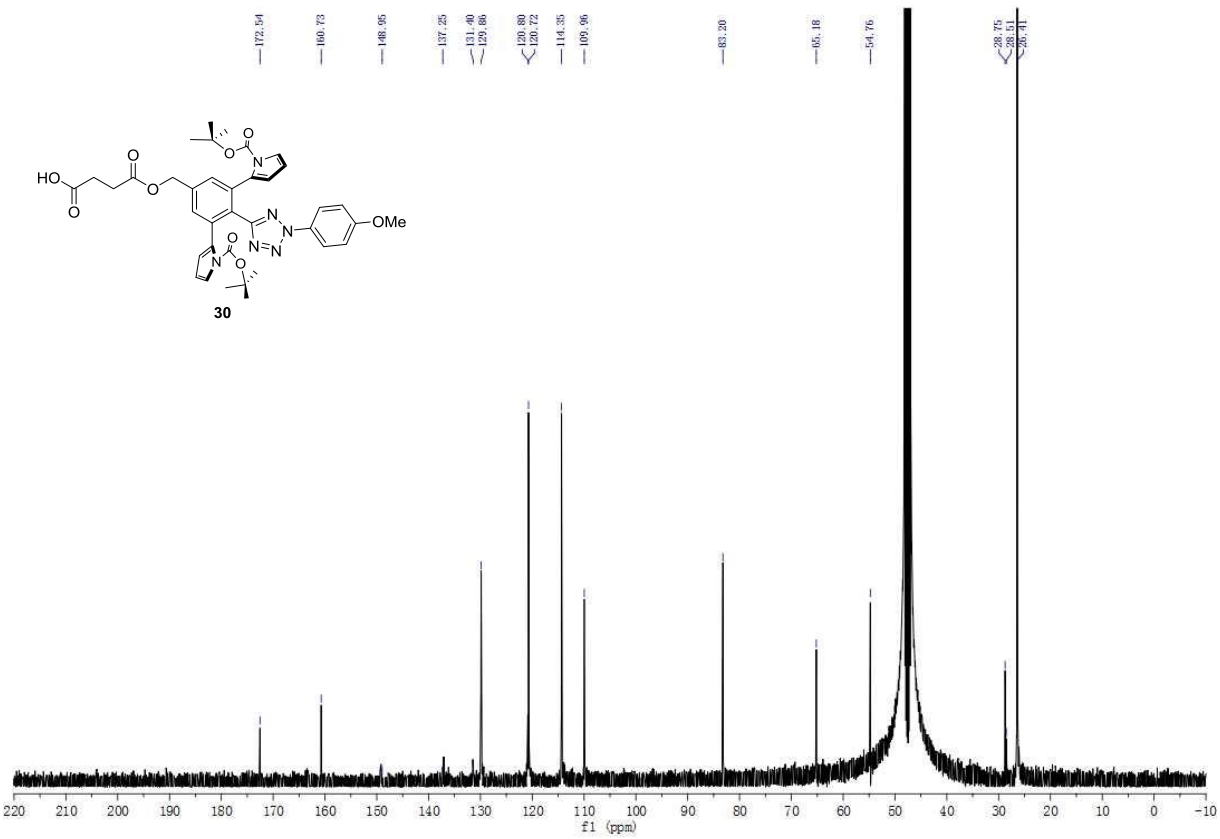
172.54
160.73
148.95
137.25
131.40
129.86
120.80
120.72
114.35
109.96
83.20
65.18
54.76
28.75
28.51
26.41
HO
O
O
O
N
N
N
N
N
O
O
OMe
30
220
210
200
190
180
170
160
150
140
130
120
110
100
90
80
70
60
50
40
30
20
10
0
-10
f1 (ppm)

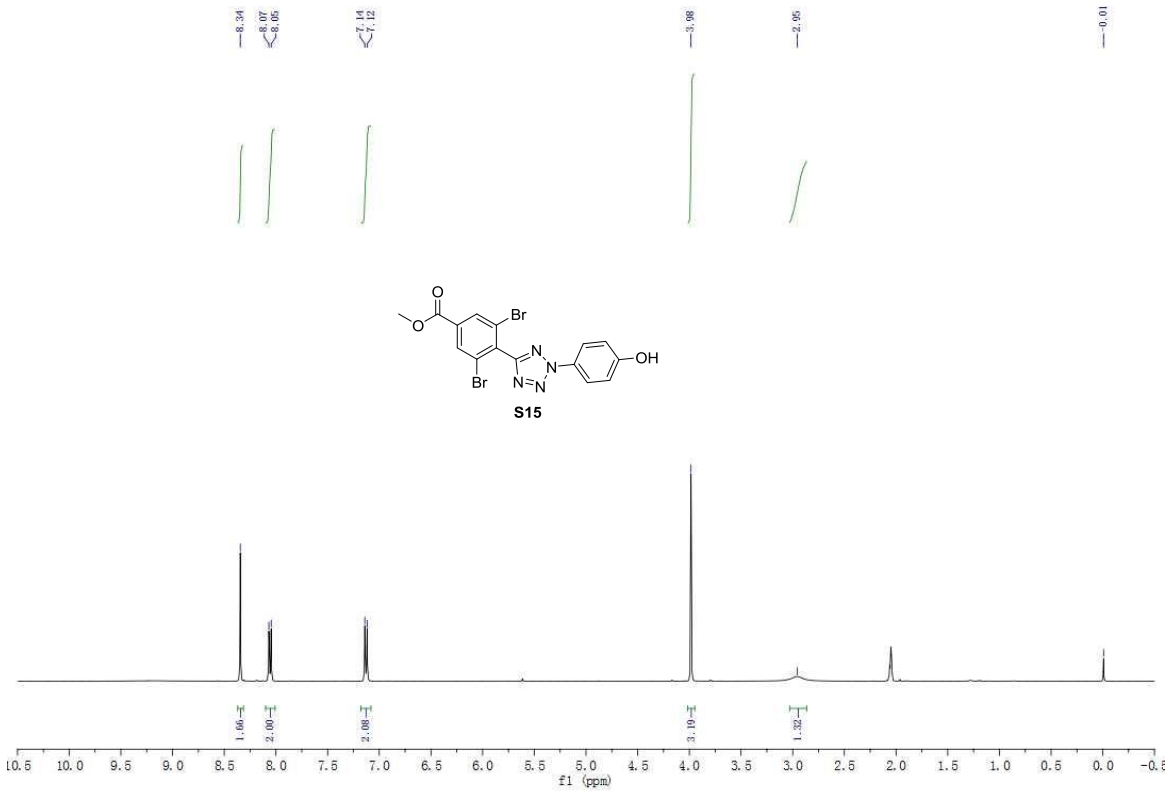
8.34
8.07
8.05
7.14
7.12
3.98
2.95
0.01
Br
Br
OH
S15
1.66
2.00
2.08
3.19
1.32
f1 (ppm)

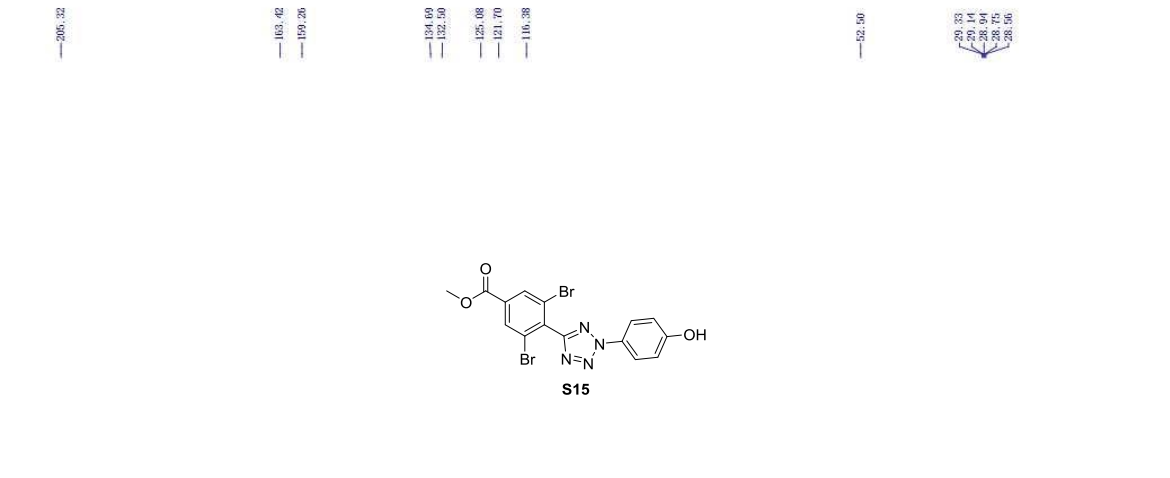
205.32
163.42
159.26
134.69
132.50
125.08
121.70
116.38
52.50
29.33
29.14
28.94
28.75
28.56
Br
Br
OH
S15
f1 (ppm)

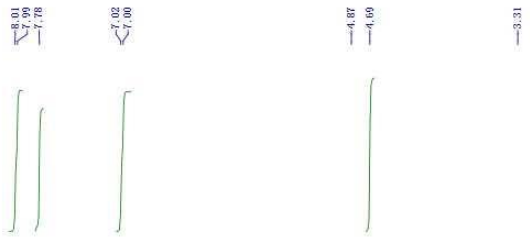
8.01
7.99
7.78
7.02
7.00
4.87
4.69
3.31

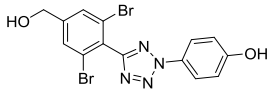
HO
Br
Br
N
N
N
OH

S16

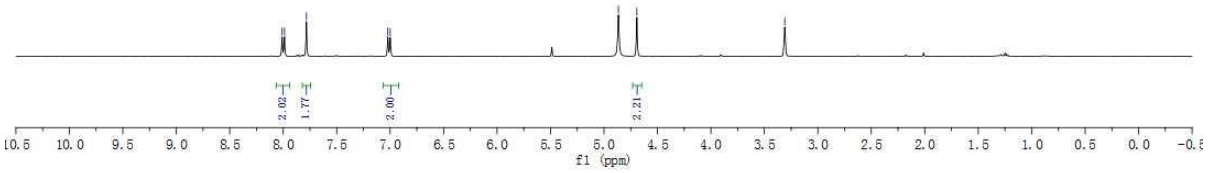
2.02
1.77
2.00
2.21
10.5 10.0 9.5 9.0 8.5 8.0 7.5 7.0 6.5 6.0 5.5 5.0 4.5 4.0 3.5 3.0 2.5 2.0 1.5 1.0 0.5 0.0
f1 (ppm)


163.08
159.37
148.12
129.49
128.96
128.62
124.51
121.31
115.86
61.79
48.02
47.80
47.59
47.38
47.16

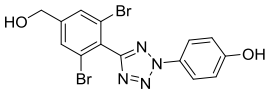
HO
Br
Br
N
N
N
OH

S16

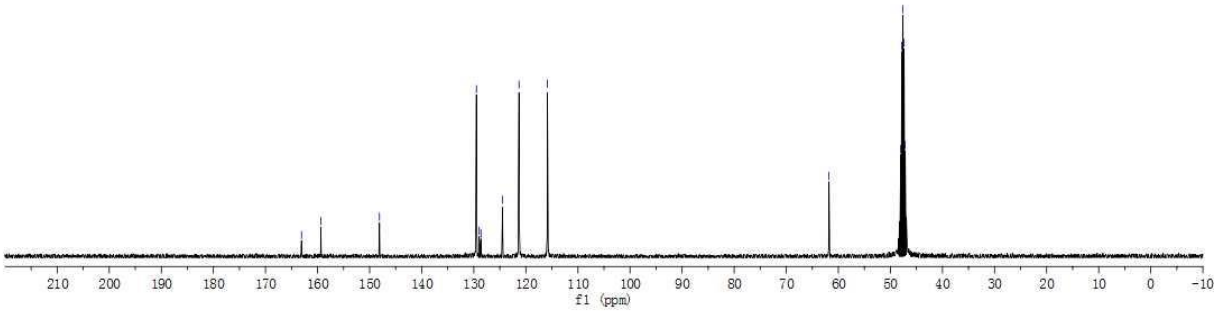
210 200 190 180 170 160 150 140 130 120 110 100 90 80 70 60 50 40 30 20 10 0 -10
f1 (ppm)

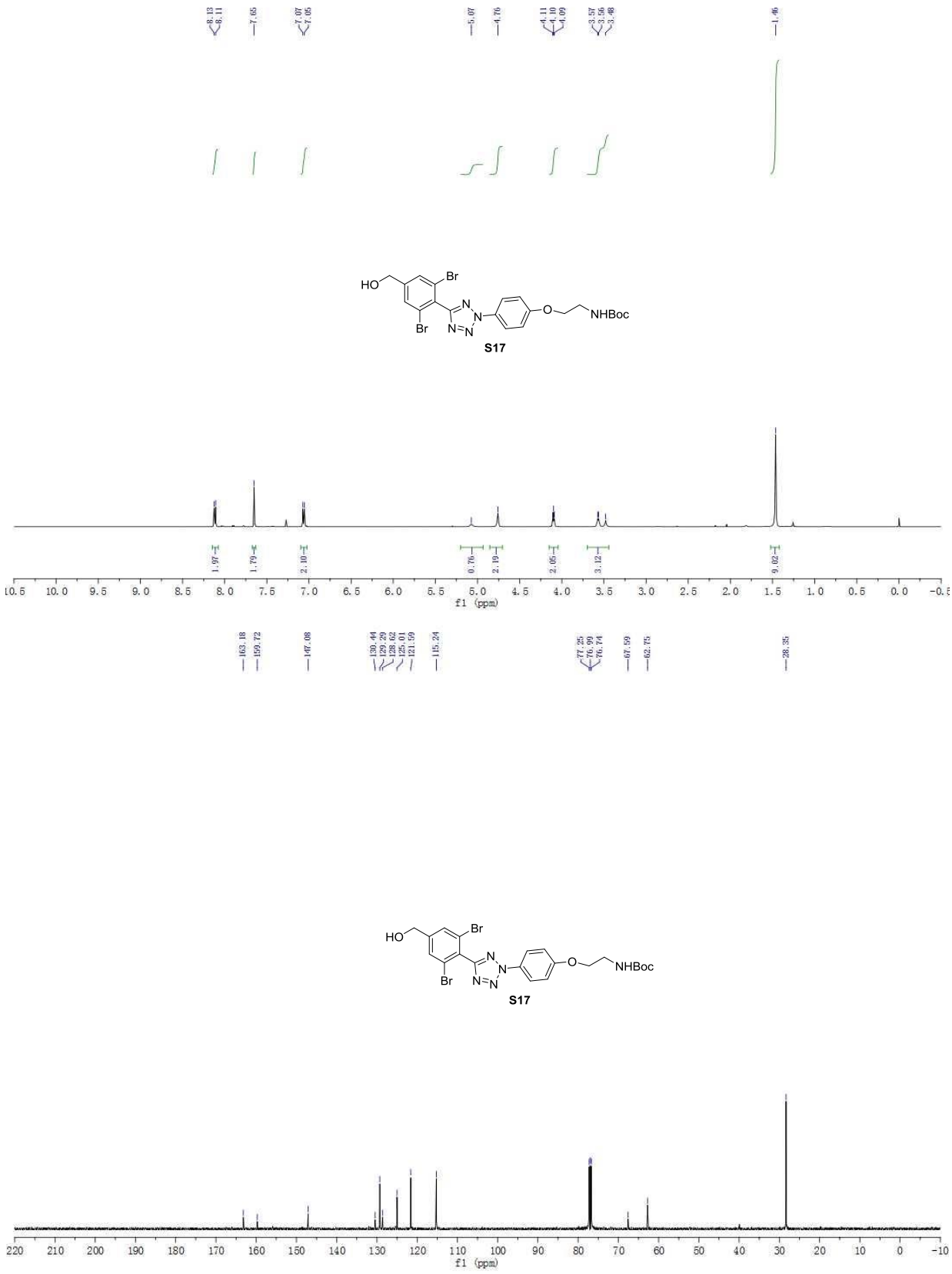
8.13
8.11
7.65
7.07
7.05
5.07
4.76
4.11
4.10
4.09
3.57
3.56
3.48
1.46
HO
Br
Br
N
N
N
O
NHBoc
S17
1.97
1.79
2.10
0.76
2.19
2.05
3.12
9.02
f1 (ppm)
163.18
159.72
147.08
130.44
129.29
128.62
125.01
121.99
115.24
77.25
76.99
76.74
67.59
62.75
28.35
HO
Br
Br
N
N
N
O
NHBoc
S17
f1 (ppm)

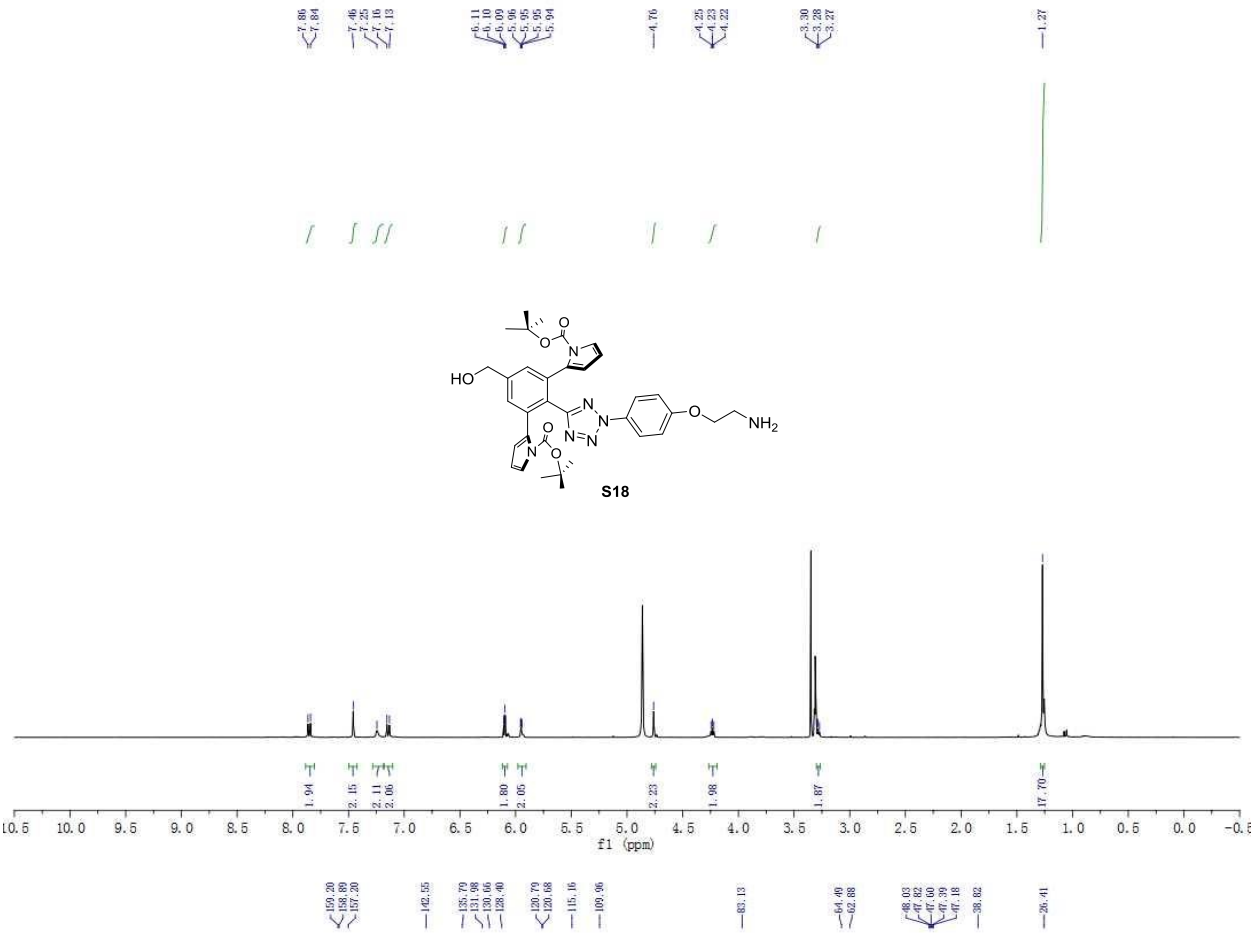
HO
O
N
O
O
N
N
N
N
O
NH2
S18
f1 (ppm)

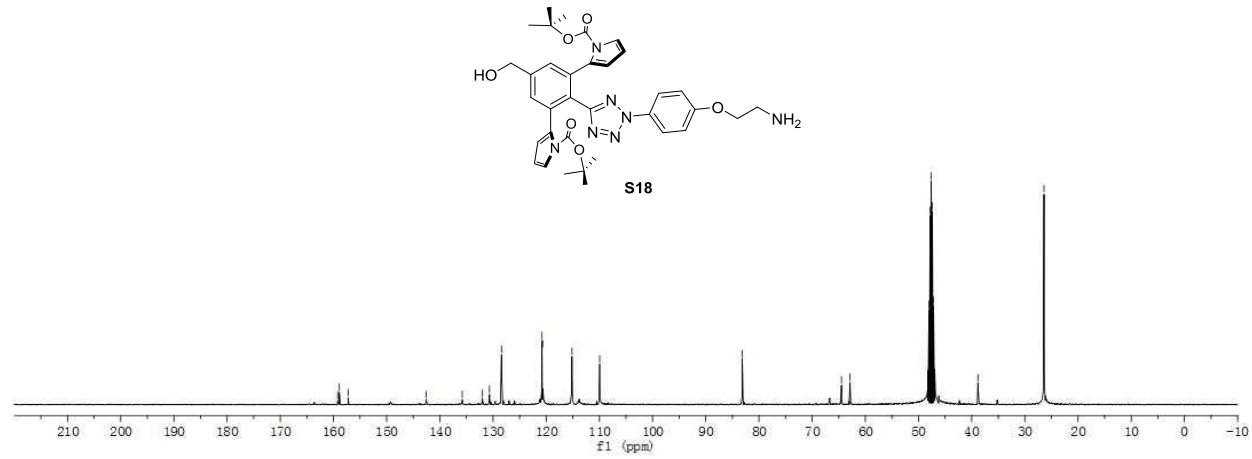
HO
O
N
O
O
N
N
N
N
O
NH2
S18
f1 (ppm)

Appendix

Table S1, entry 1:

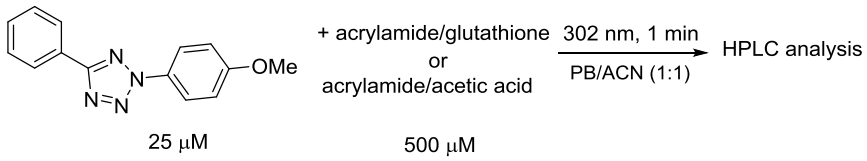

Tetrazole

500 μM acrylamide

500 μM glutathione

500 μM acrylamide+500 μM glutathione

500 μM acrylamide + 500 μM acetic acid

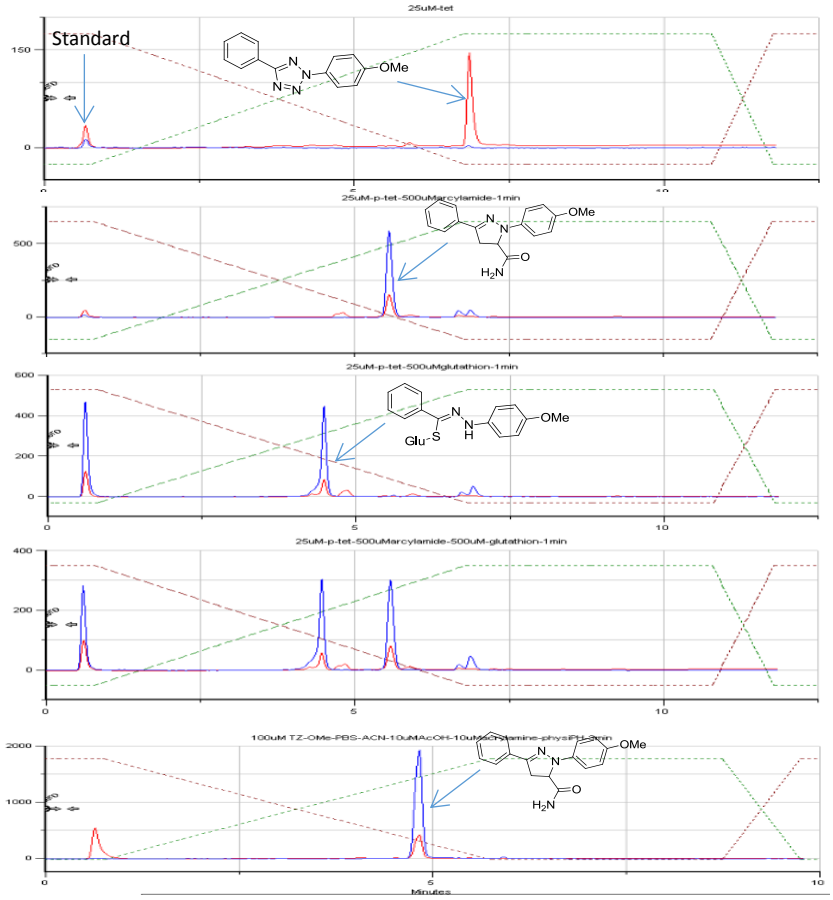

Based on the peak integration (red line, 254 nm), the ratio of glutathione addition product over the acrylamide cycloaddition product was 0.51:0.42. In the presence of acrylamide, the acetic acid addition product was not detected.

Table S1, entry 2:

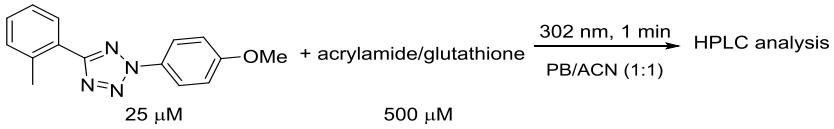

Tetrazole

500 μM acrylamide

500 μM glutathione

500 μM acrylamide + 500 μM glutathione

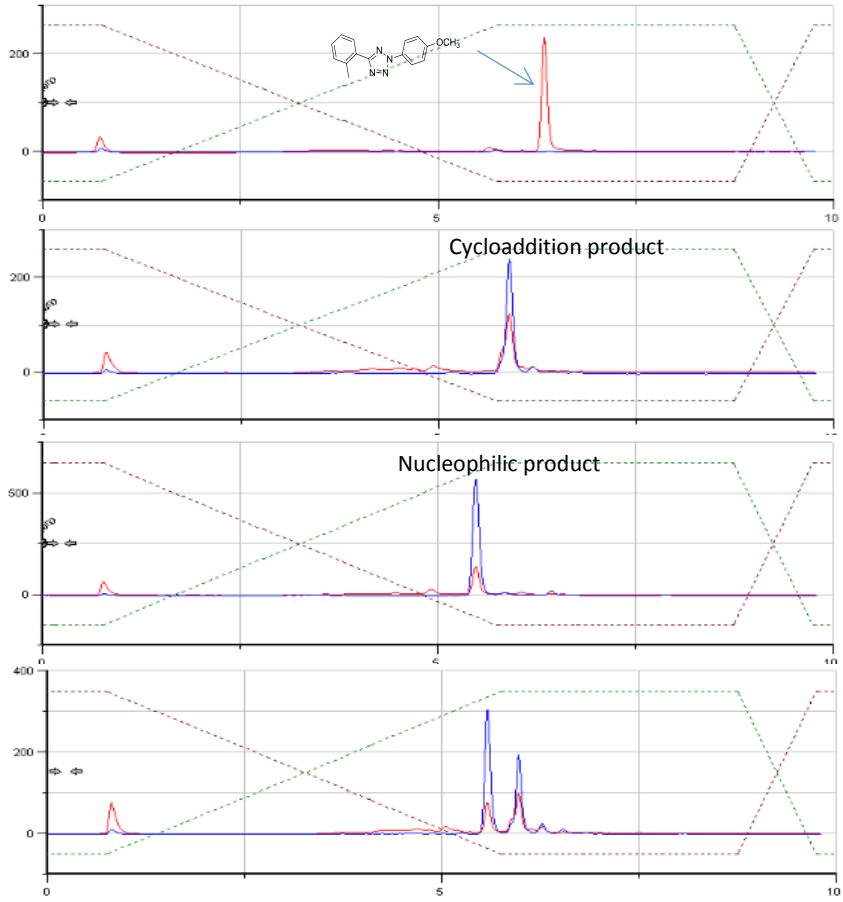

Based on the integration, the ratio of glutathione addition product over the acrylamide cycloaddition product was 1:1.

Table S1, entry 3:

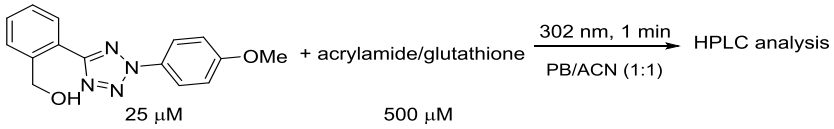

Tetrazole

500 μM acrylamide

500 μM glutathione

500 μM acrylamide+500 μM glutathione

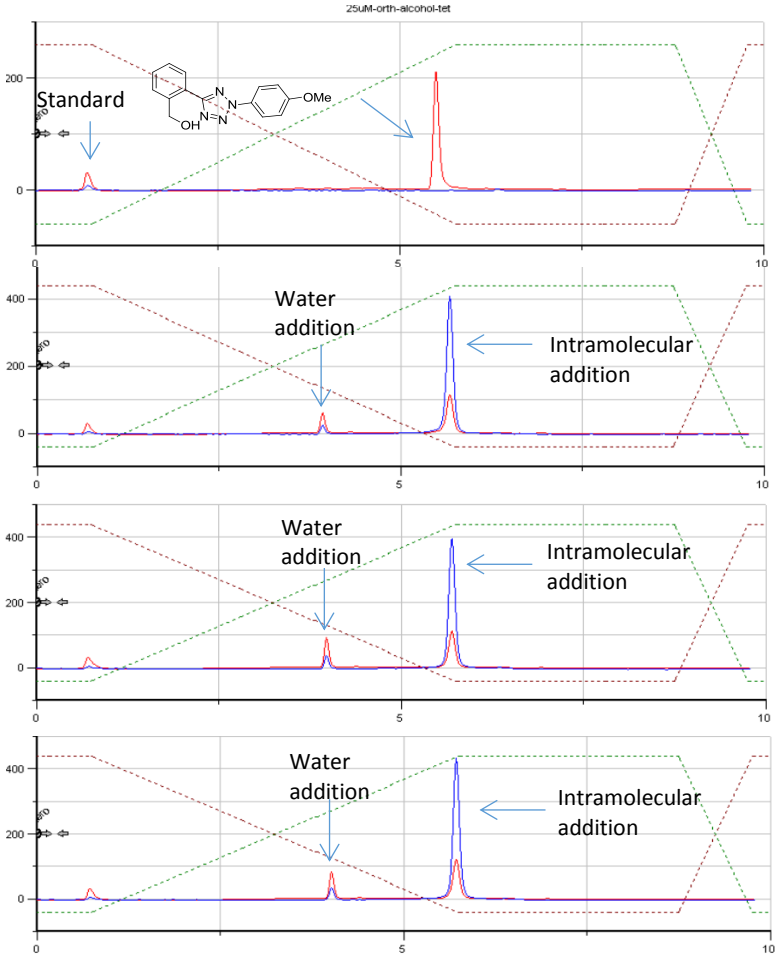

Based on the chromatogram, the intramolecular addition product was the major product. The acrylamide cycloaddition product and the glutathione addition product were not observed.

Table S1, entry 4:

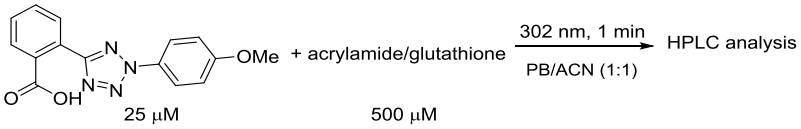

Tetrazole

500 μM acrylamide

500 μM glutathione

500 μM acrylamide+500 μM glutathione

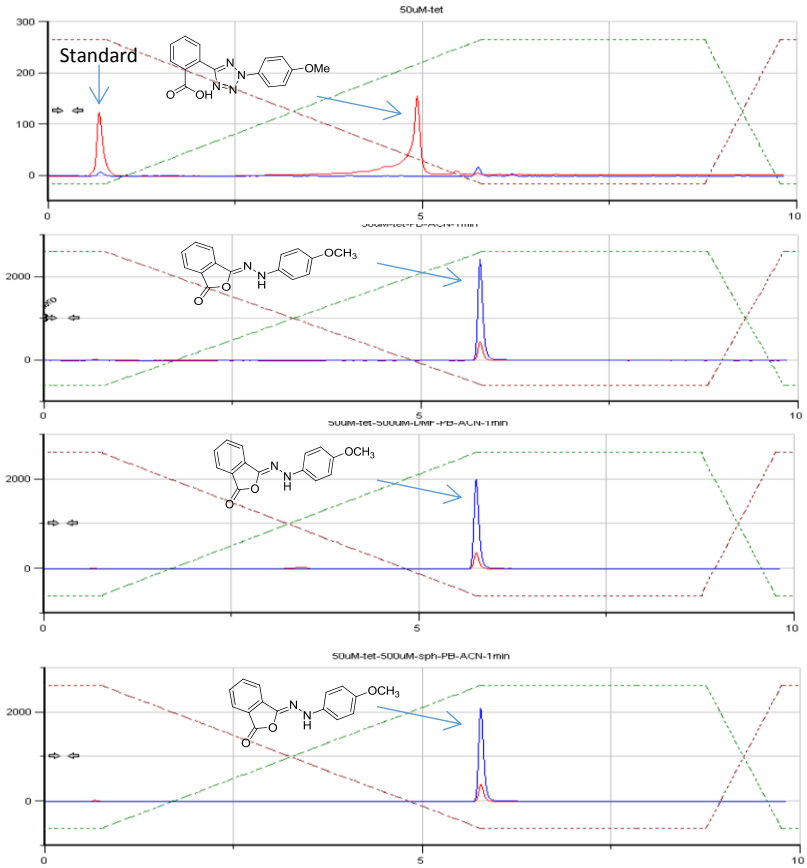

Based on the integration, only the intramolecular addition product was detected when acrylamide and glutathione were present.

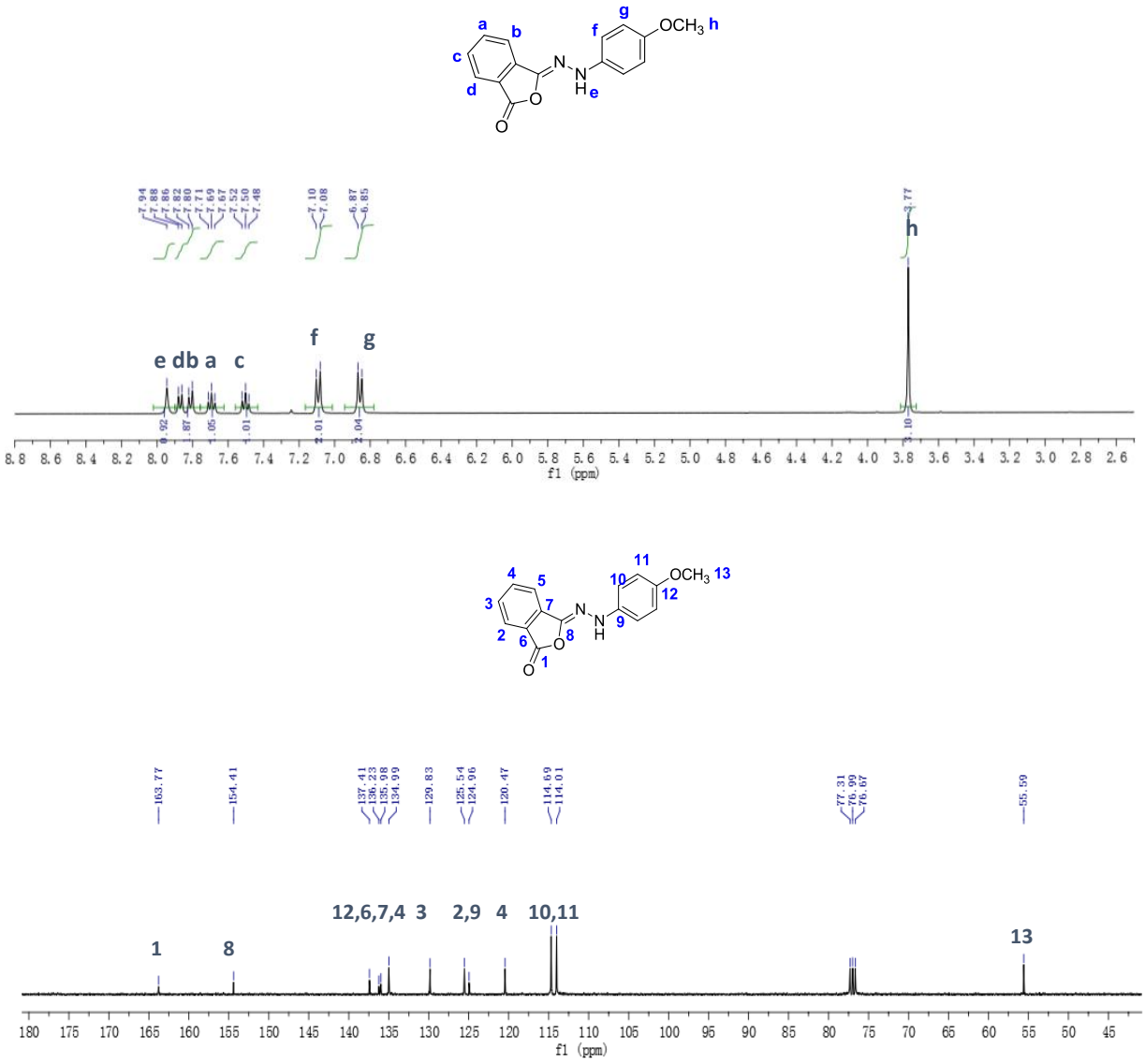

The intramolecular addition product was confirmed by ^{1}H and ^{13}C NMR spectra.

Table S1, entry 5:

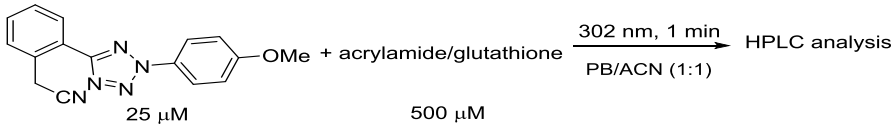

Tetrazole

PB/ACN only

500 μM acrylamide

500 μM glutathione

500 μM acrylamide+500 μM glutathione

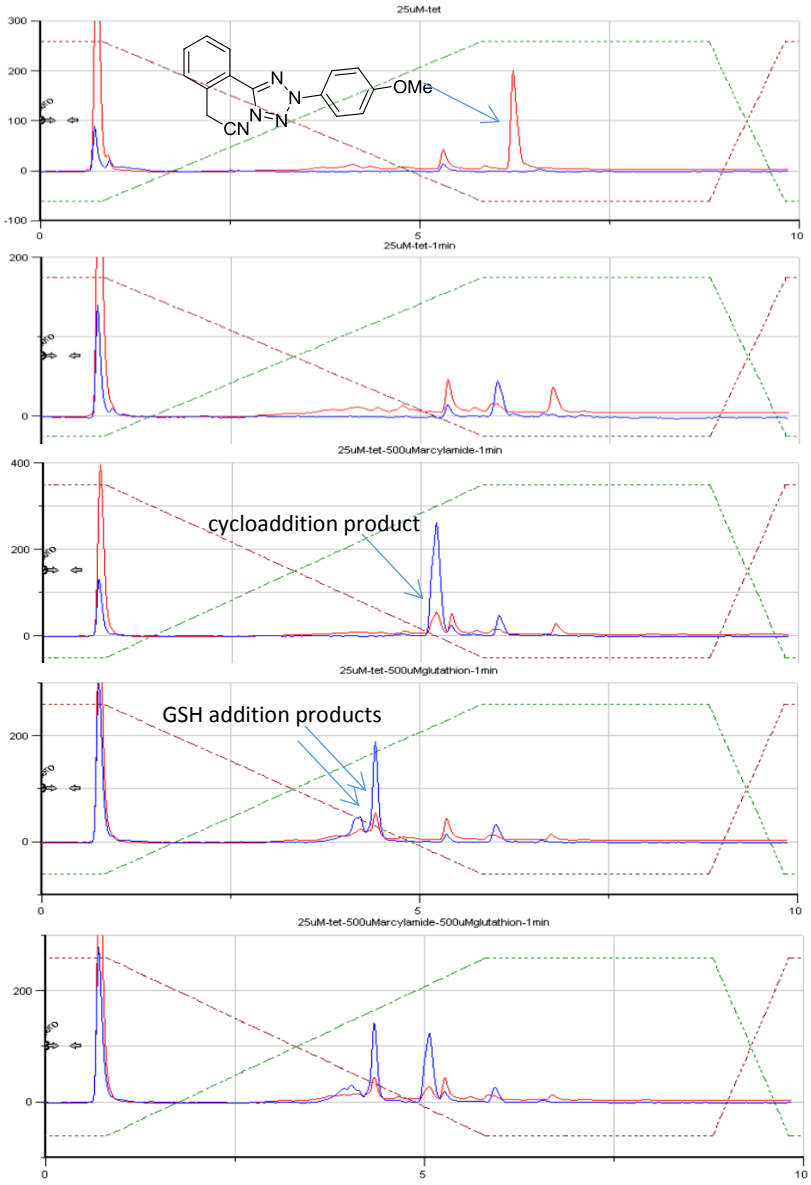

Based on the integration, the ratio of glutathione addition products over the acrylamide cycloaddition product was determined to be 1:1.

Table S1, entry 6:

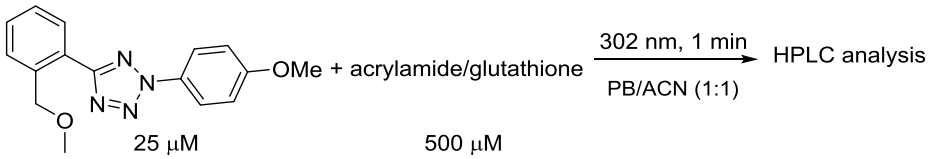

Tetrazole

500 μM acrylamide

500 μM glutathione

500 μM acrylamide+500 μM glutathione

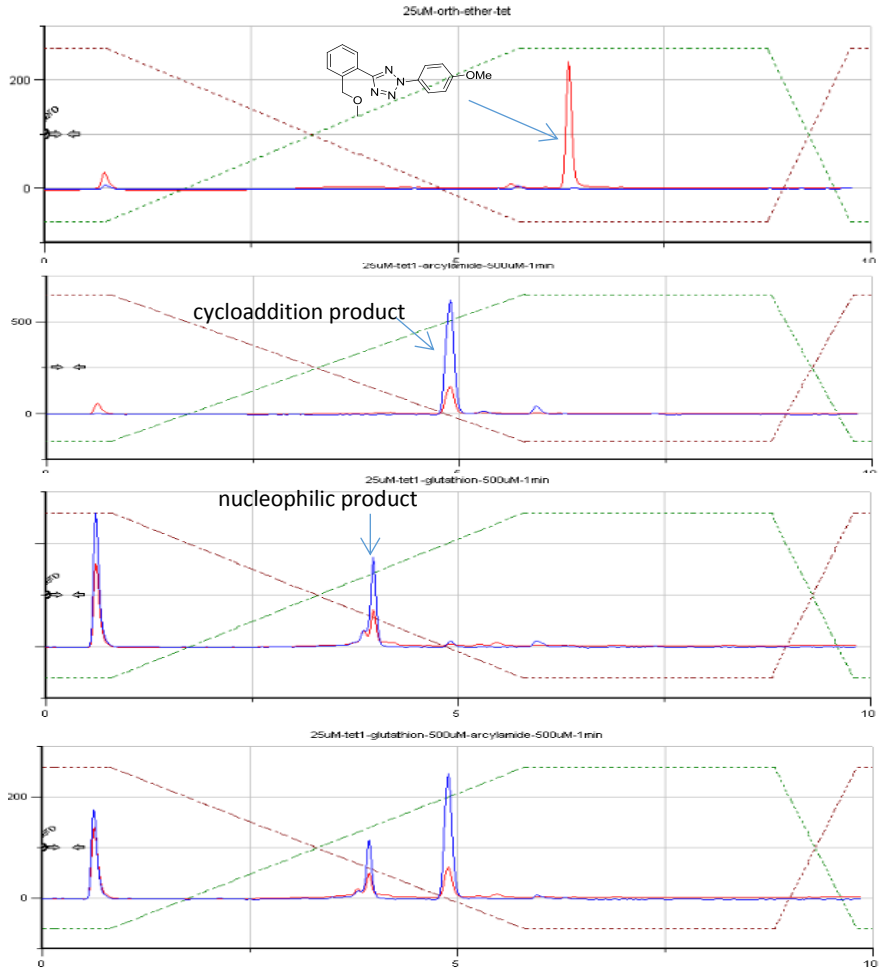

Based on the integration, the ratio of the glutathione addition product over the acrylamide cycloaddition product was determined to be 0.45:0.55.

Table S1, entry 7:

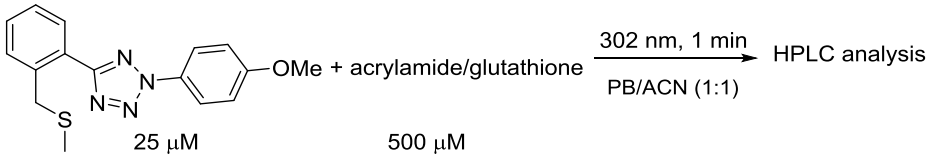

Tetrazole

PB/ACN only

500 μM acrylamide

500 μM acrylamide + 500 μM glutathione

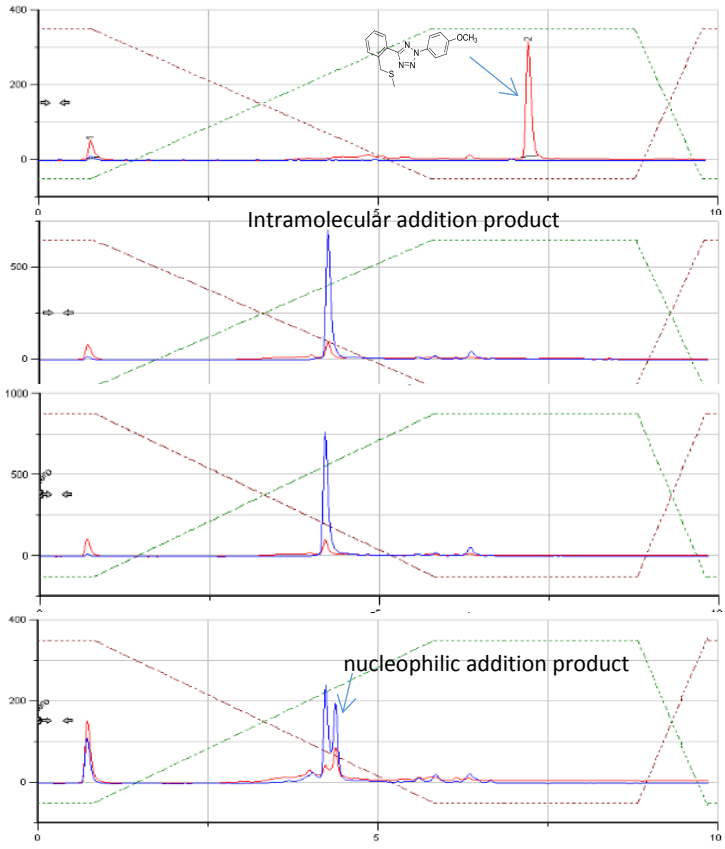

Based on chromatograms, only the intramolecular addition and nucleophilic addition products were observed.

Table S1, entry 8:

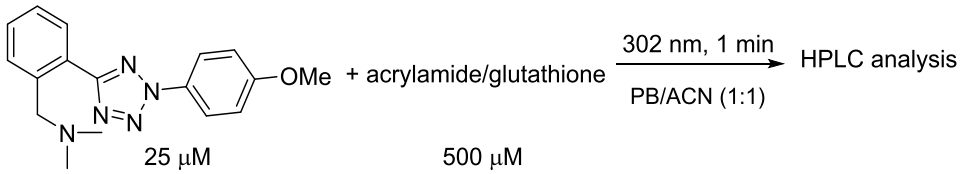

Tetrazole

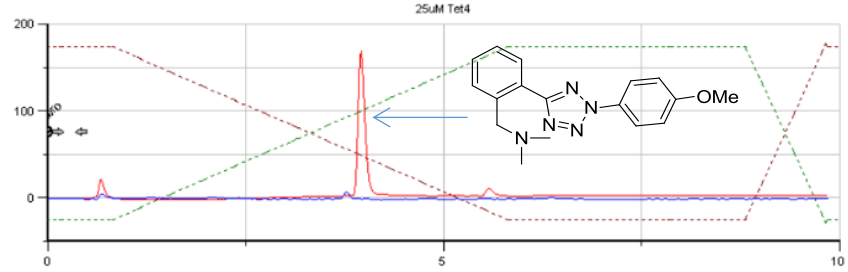

500 μM acrylamide

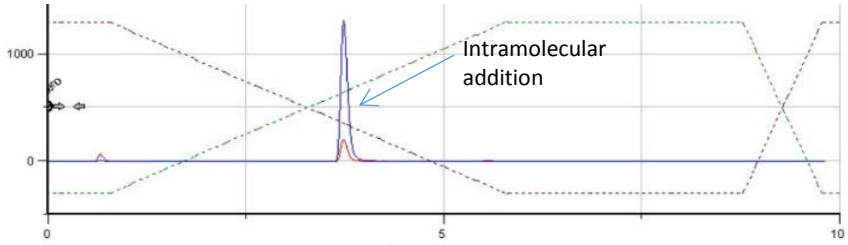

500 μM glutathione

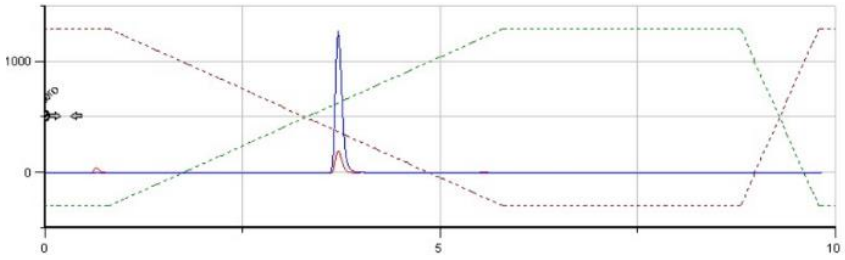

500 μM acrylamide + 500 μM glutathione

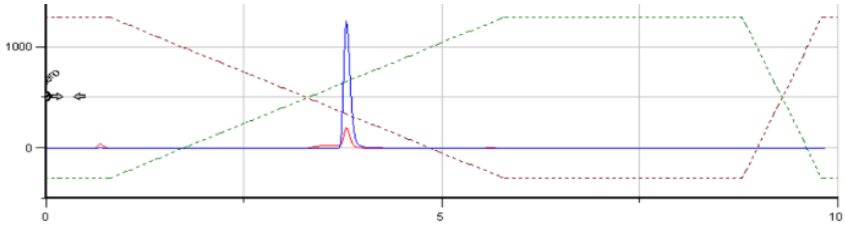

Based on HPLC chromatograms, only the intramolecular addition product was detected.

Table S1, entry 9:

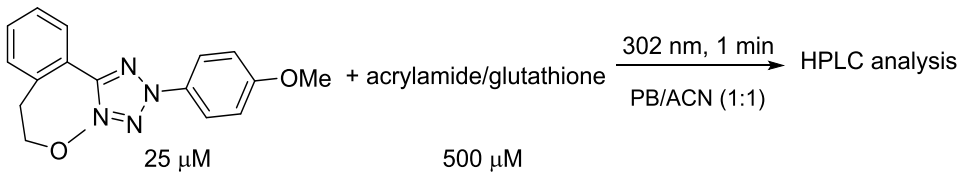

Tetrazole

500 μM acrylamide

500 μM glutathione

500 μM acrylamide + 500 μM glutathione

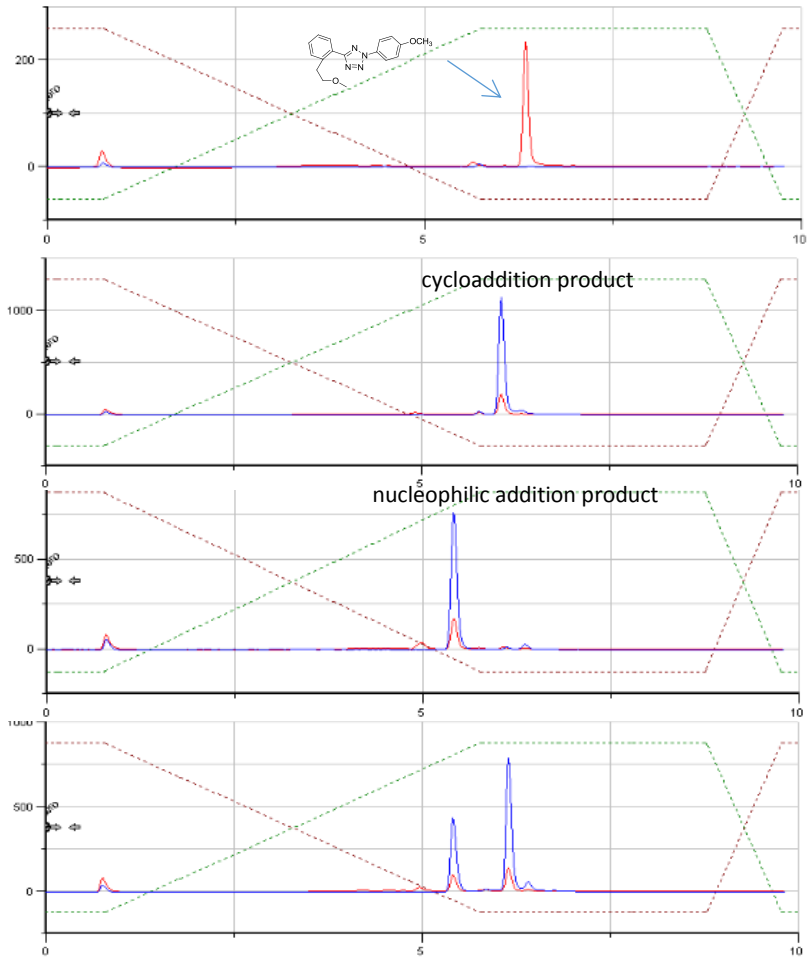

Based on the integration, the ratio of glutathione addition product over the acrylamide cycloaddition product was determined to be 1:1.

.

Table S1, entry 10:

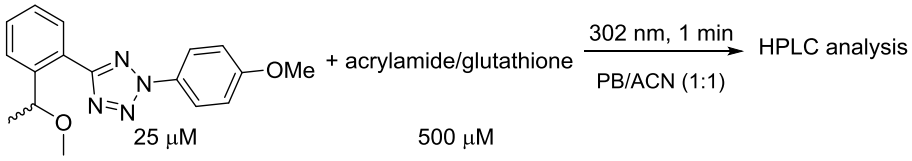

Tetrazole

PB/ACN only

500 μM glutathione

500 μM acrylamide

500 μM acrylamide + 500 μM glutathione

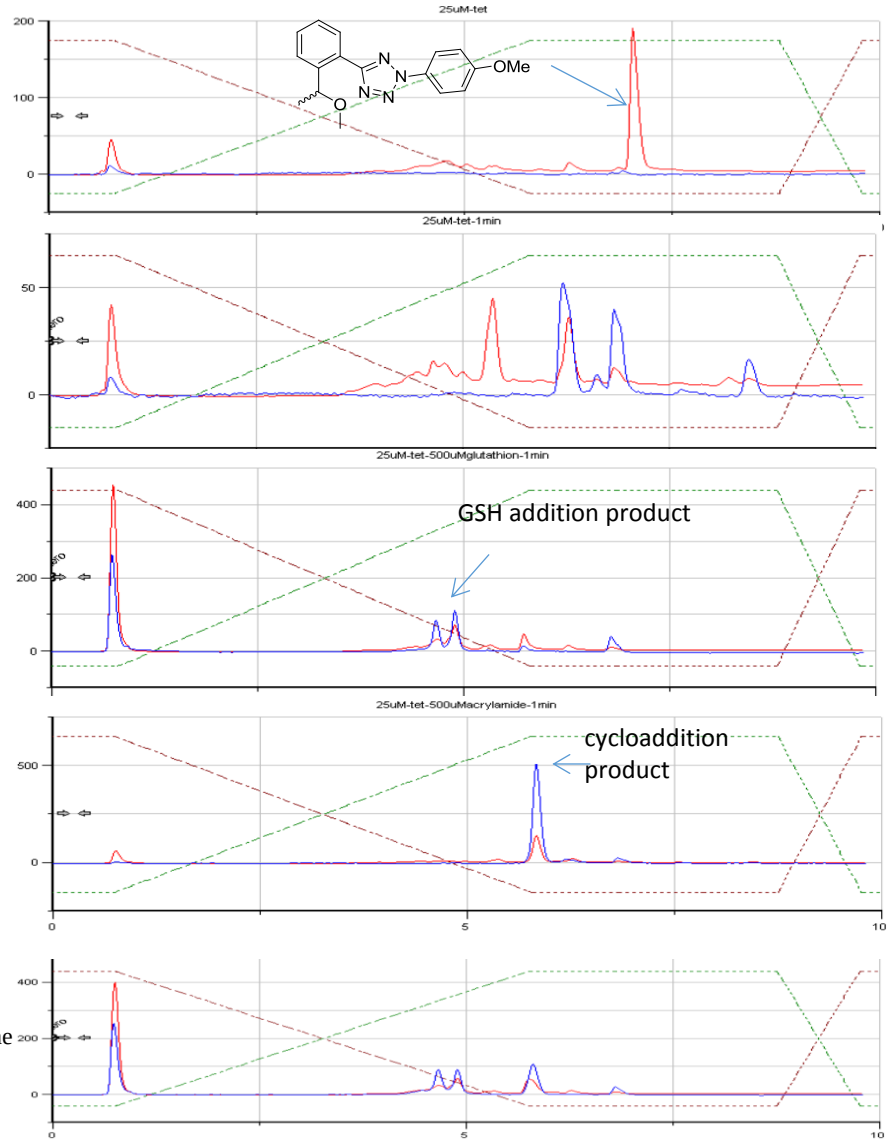

Based on HPLC chromatogram, the glutathione addition products were the major products.

Table S1, entry 11:

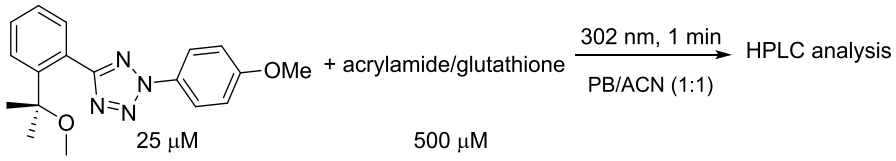

Tetrazole

500 μM acrylamide

500 μM glutathione

500 μM acrylamide + 500 μM glutathione

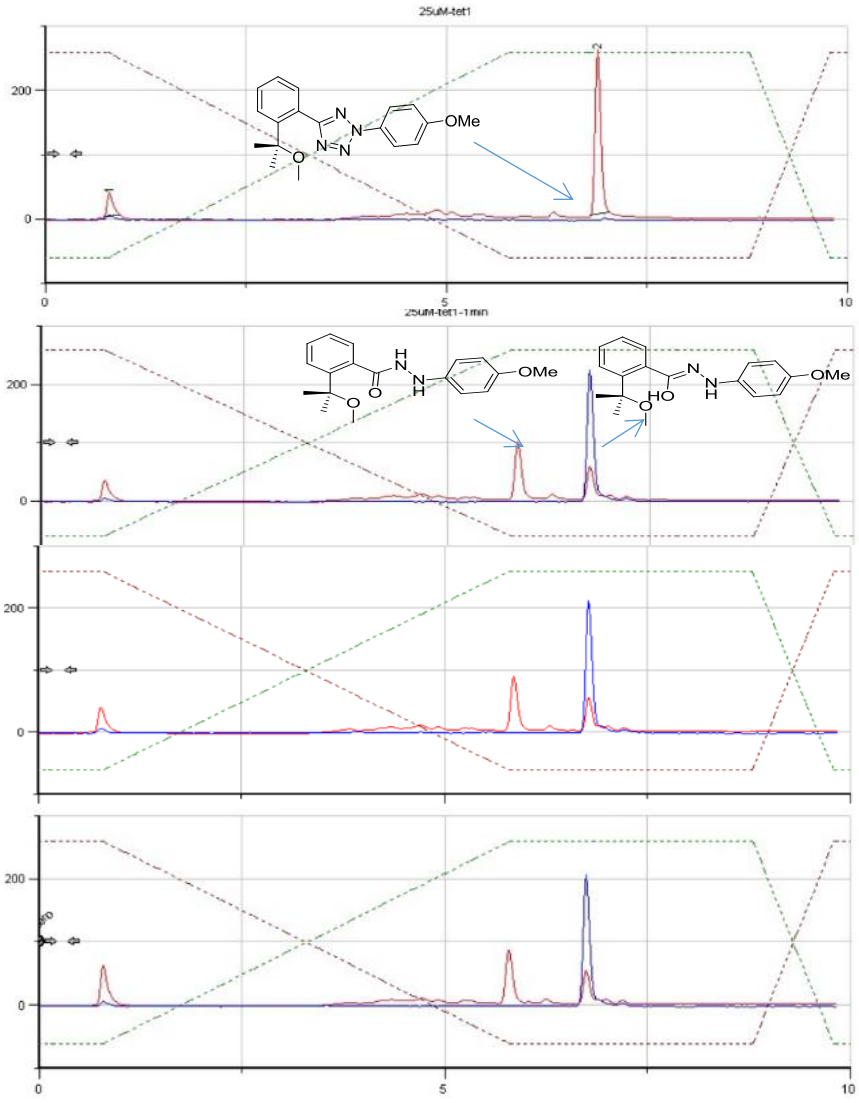

Based on HPLC chromatograms, both the glutathione addition and the acrylamide cycloaddition were blocked.

Table S1, entry 12:

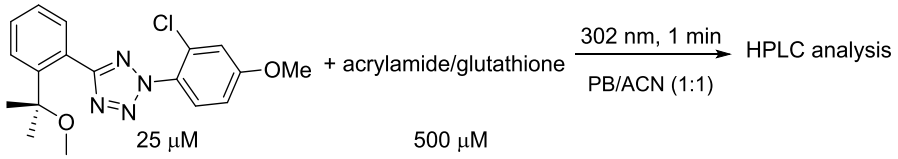

Tetrazole

500 μM acrylamide

500 μM glutathione

500 μM acrylamide + 500 μM glutathione

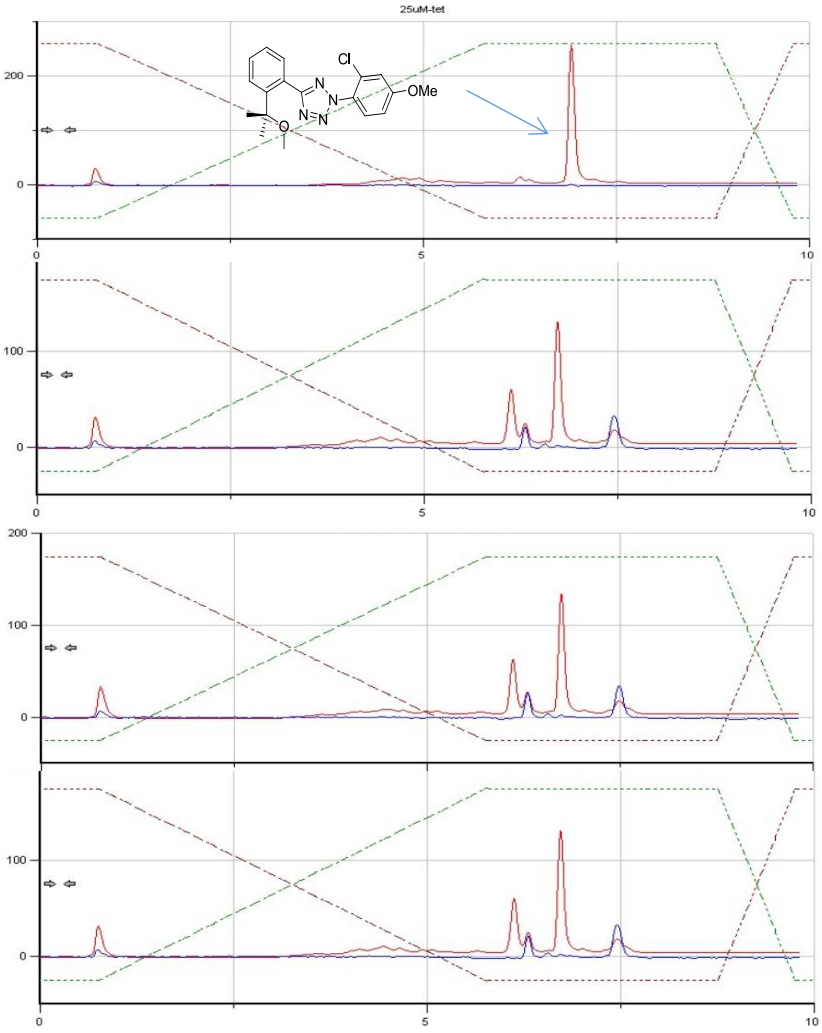

Based on HPLC chromatograms, both the glutathione addition and the acrylamide cycloaddition were blocked.

Table S1, entry 13:

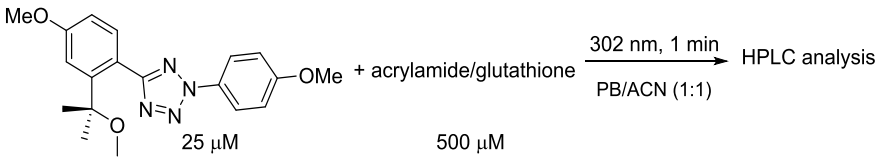

Tetrazole

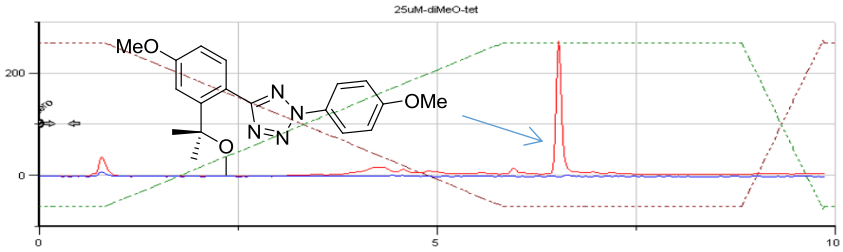

500 μM acrylamide

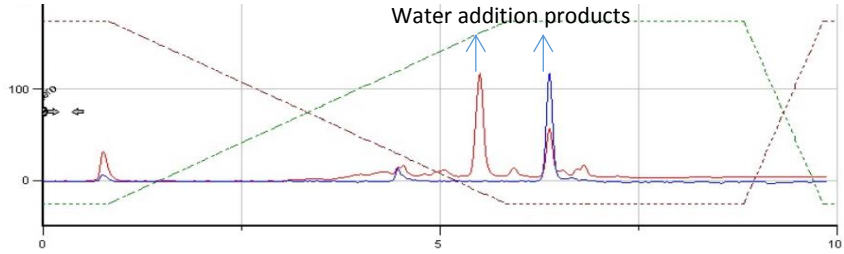

500 μM glutathione

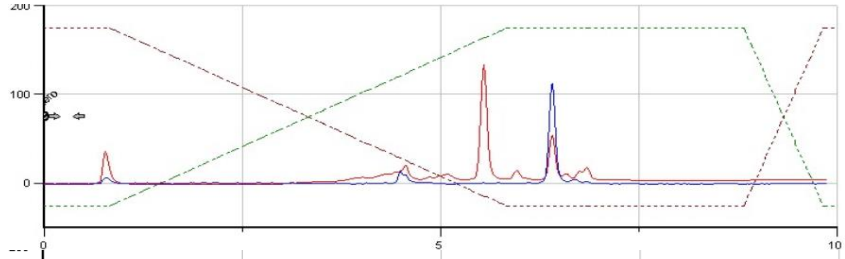

500 μM acrylamide + 500 μM glutathione

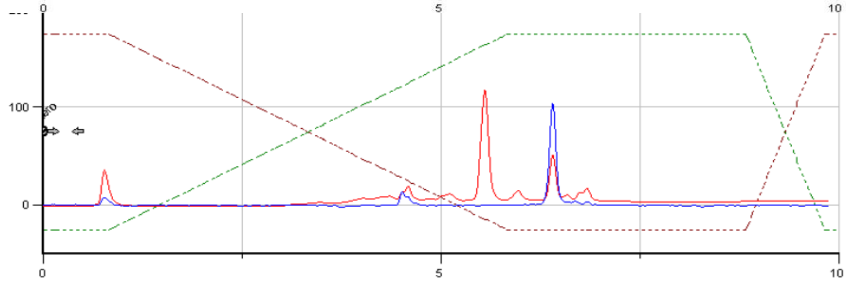

Based on HPLC chromatograms, both the glutathione addition and the acrylamide cycloaddition were blocked.

Table S1, entry 14:

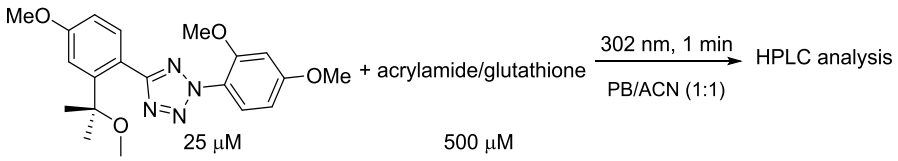

Tetrazole

500 μM acrylamide

500 μM glutathione

500 μM acrylamide +

500 μM glutathione

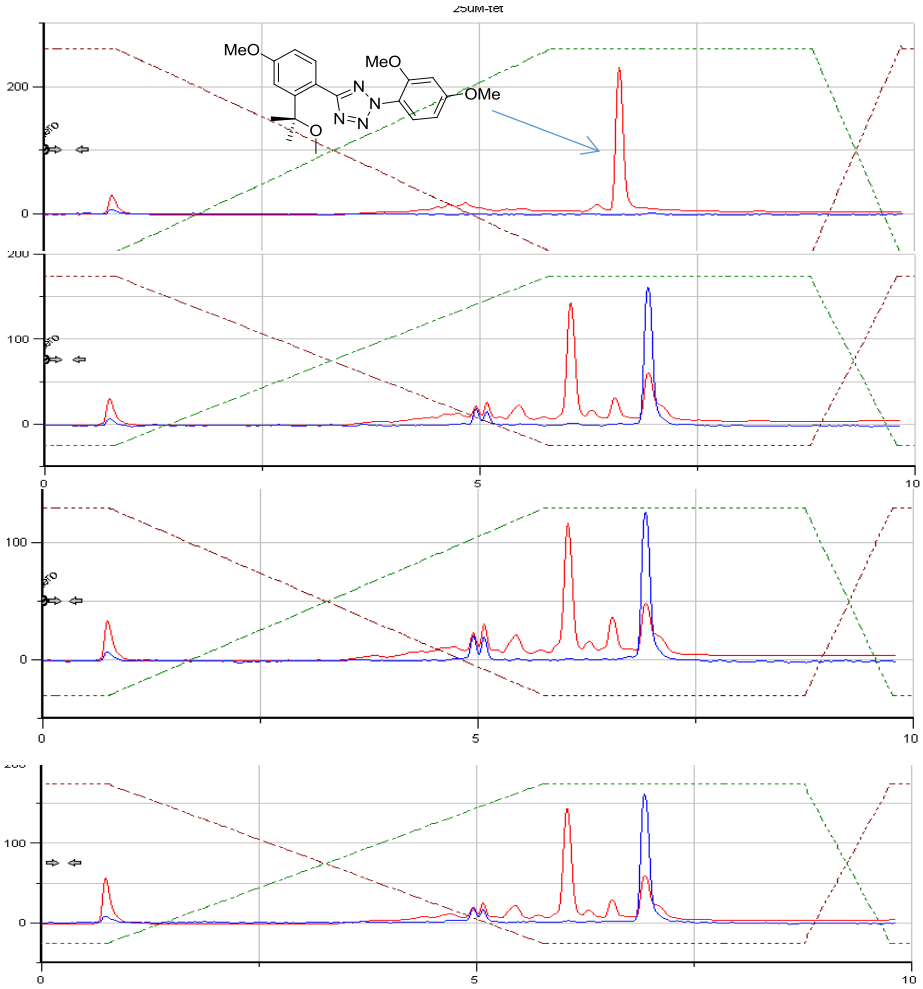

Based on HPLC chromatograms, both the glutathione addition and the acrylamide cycloaddition were blocked.

Table S1, entry 15:

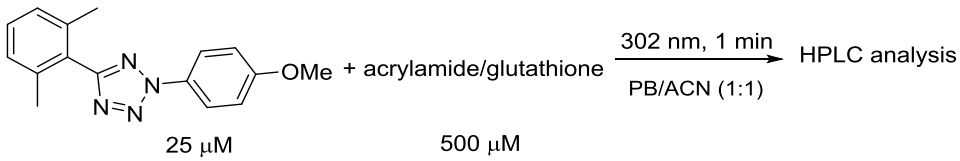

Tetrazole

PB/ACN only

500 μM acrylamide

500 μM glutathione

500 μM acrylamide +

500 μM glutathione

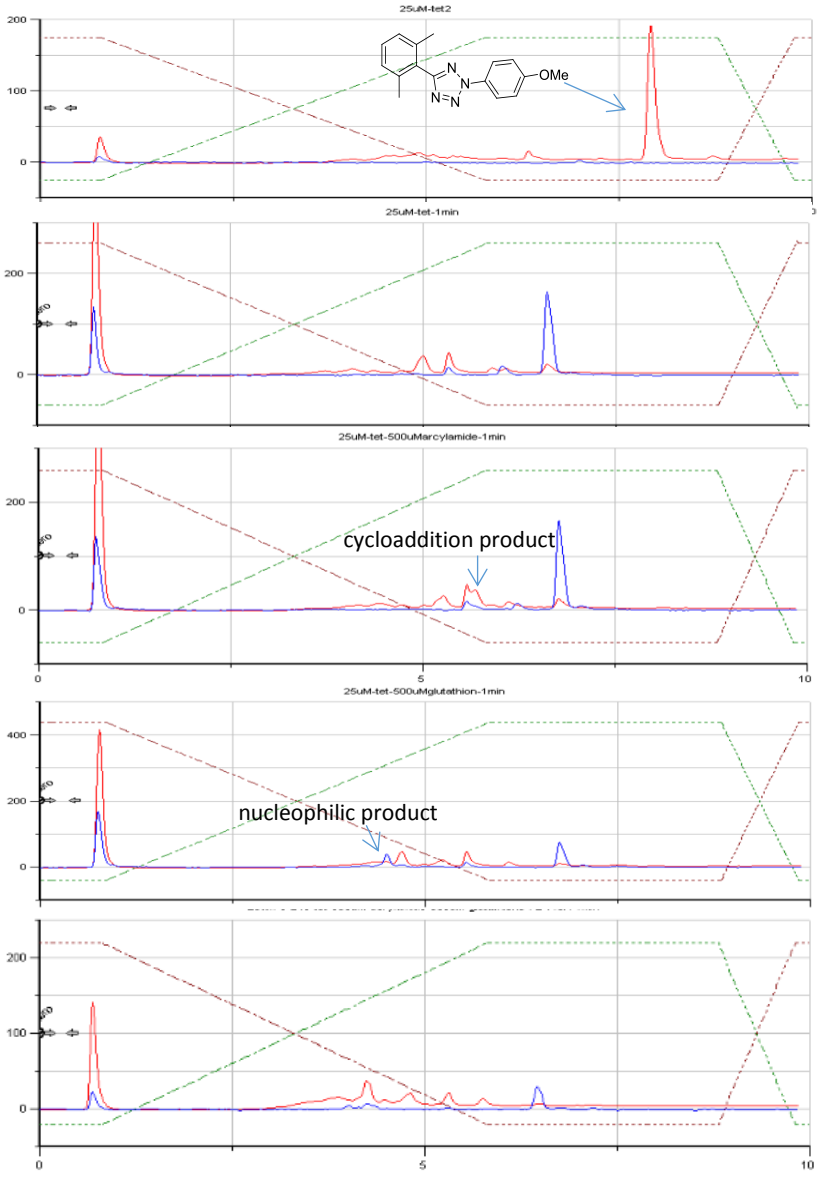

Based on HPLC chromatograms, both the glutathione addition and the acrylamide cycloaddition were blocked.

Table S1, entry 16:

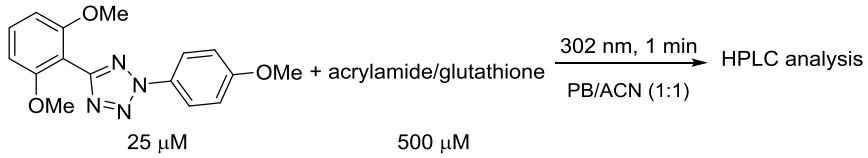

Tetrazole

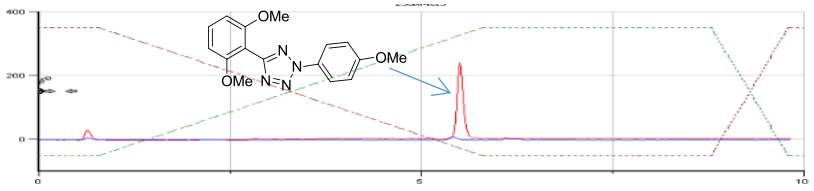

PB/ACN only

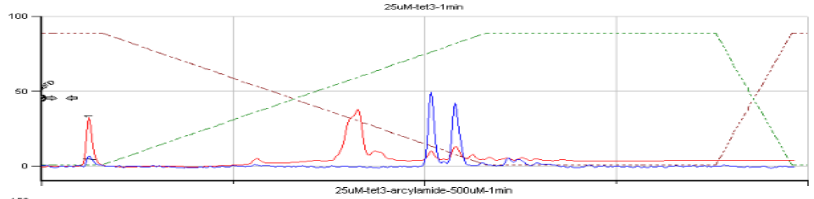

500 μM acrylamide

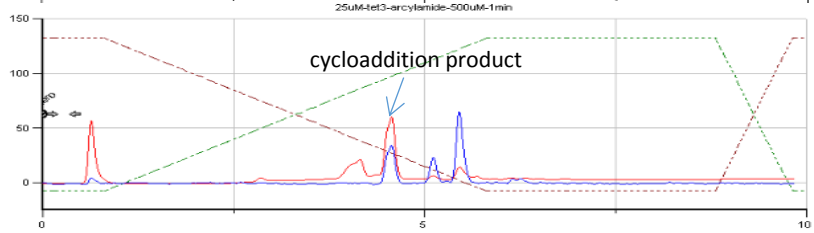

500 μM glutathione

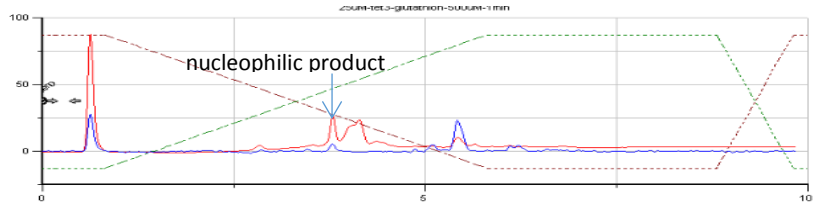

500 μM acrylamide + 500 μM glutathione

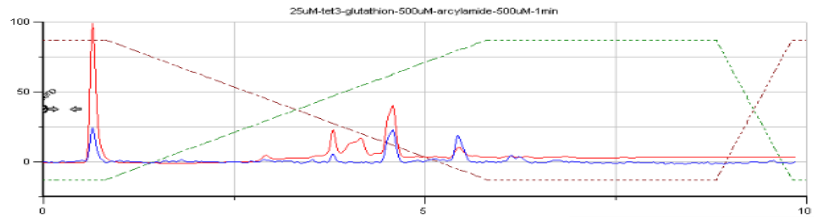

Based on HPLC chromatograms, the solvent quenching products were significant.

Table S1, entry 17:

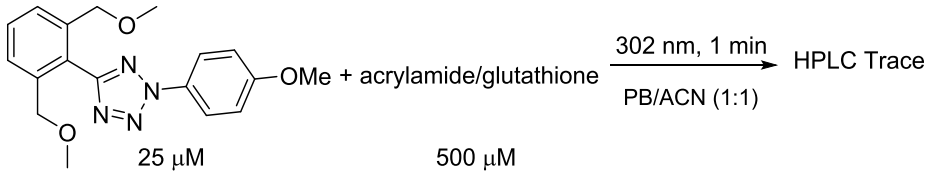

Tetrazole

PB/ACN only

500 μM acrylamide

500 μM glutathione

500 μM acrylamide + 500 μM glutathione

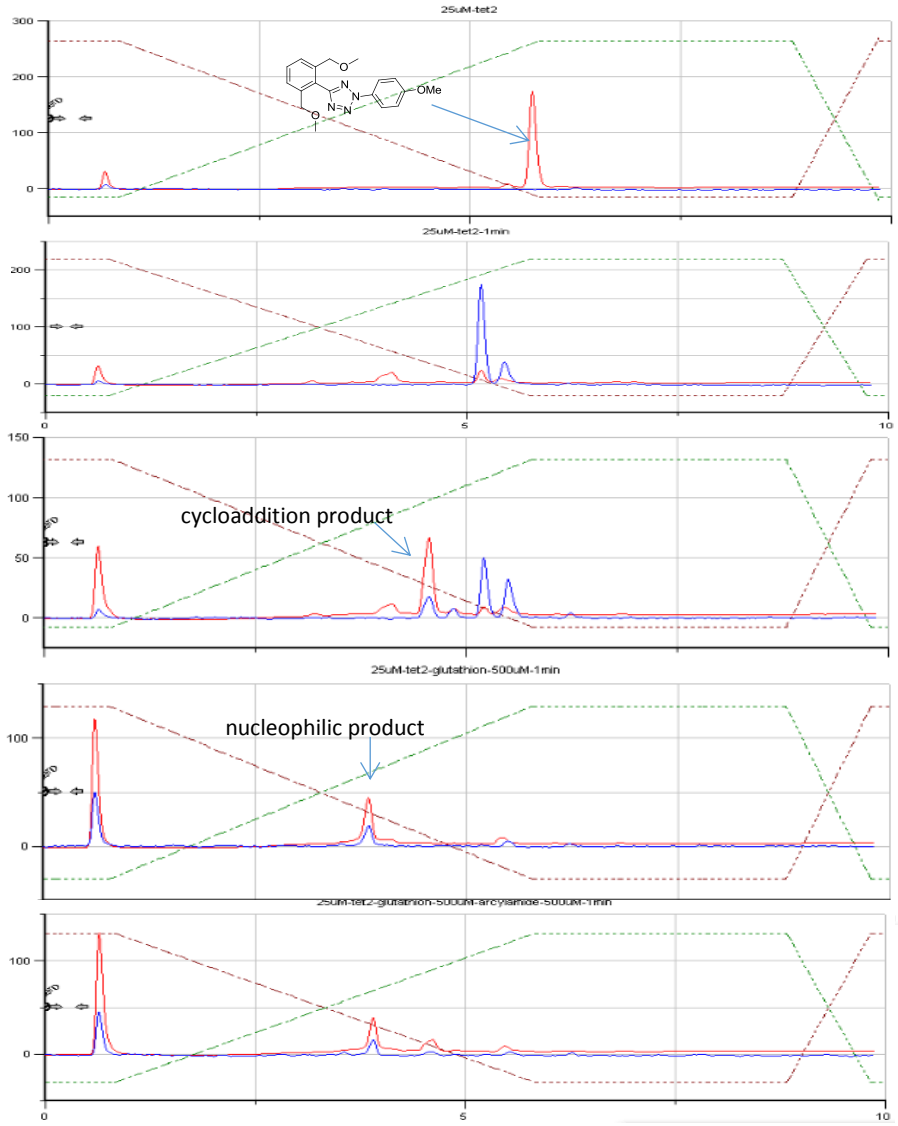

Based on HPLC chromatograms, the acrylamide cycloaddition were significantly blocked. The glutathione addition product was the major product.

Table S1, entry 18:

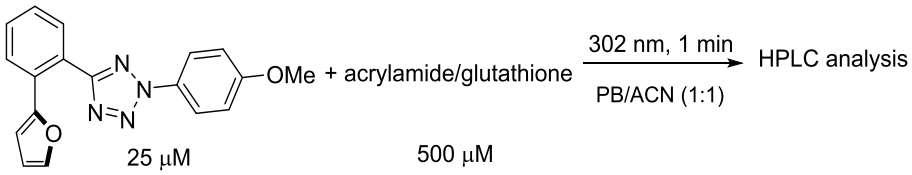

Tetrazole

PB/ACN only

500 μM acrylamide

500 μM glutathione

500 μM acrylamide+500 μM glutathione

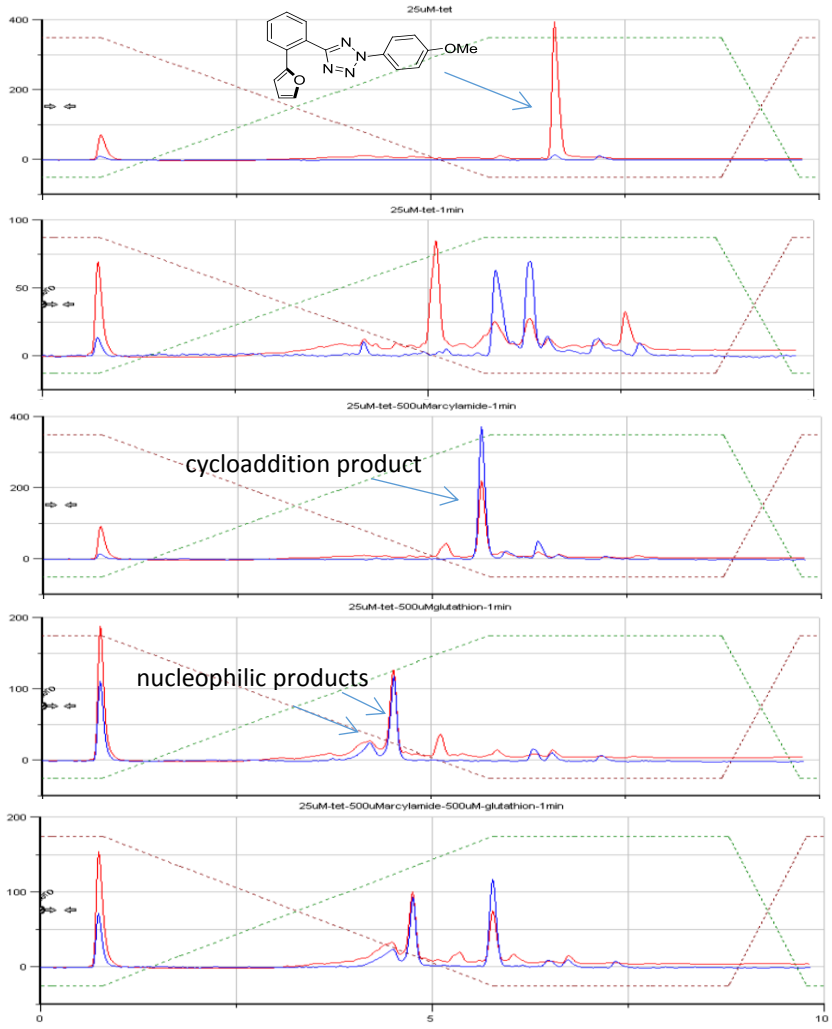

Based on the integration, the ratio of glutathione addition product over the acrylamide cycloaddition product was determined to be 0.58:0.37.

Table S1, entry 19:

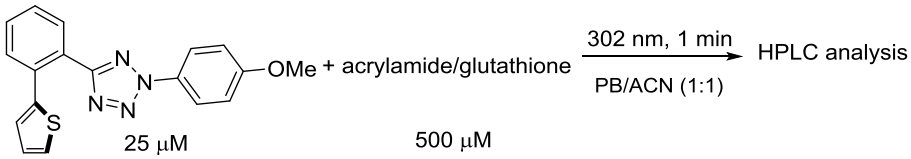

Tetrazole

PB/ACN only

500 μM acrylamide

500 μM glutathione

500 μM acrylamide+500 μM glutathione

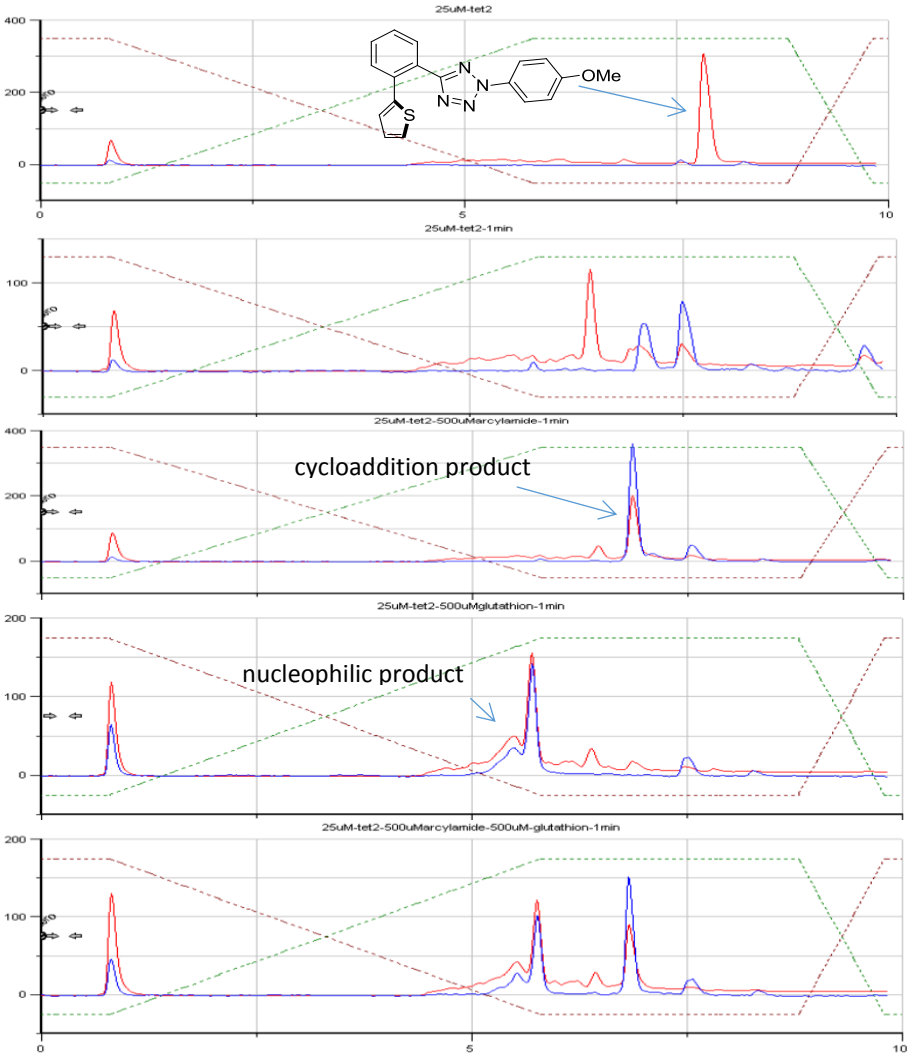

Based on the integration, the ratio of glutathione addition product over the acrylamide cycloaddition product was determined to be 0.56:0.36.

Table S1, entry 20:

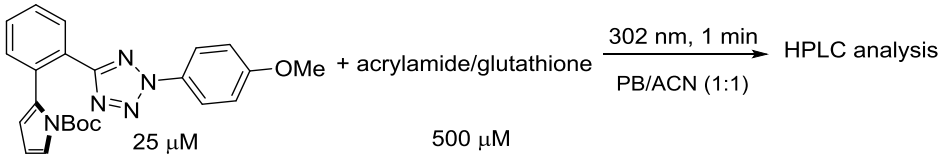

Tetrazole

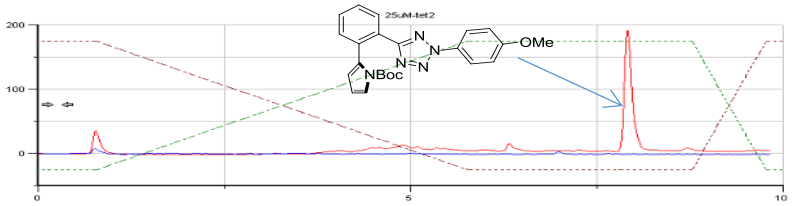

PB/ACN only

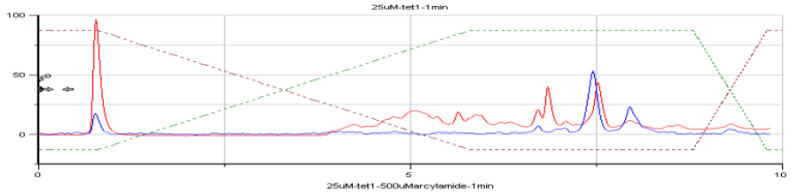

500 μM acrylamide

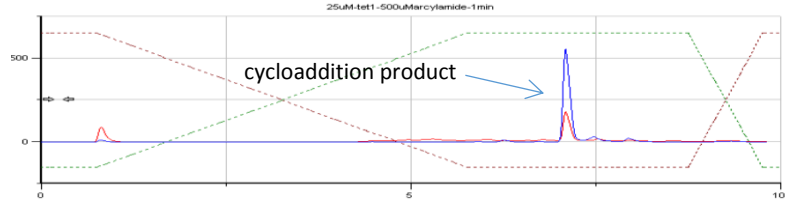

500 μM glutathione

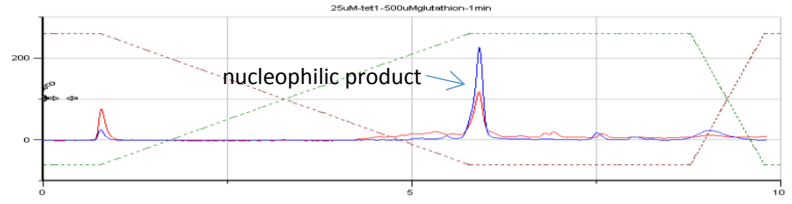

500 μM acrylamide + 500 μM glutathione

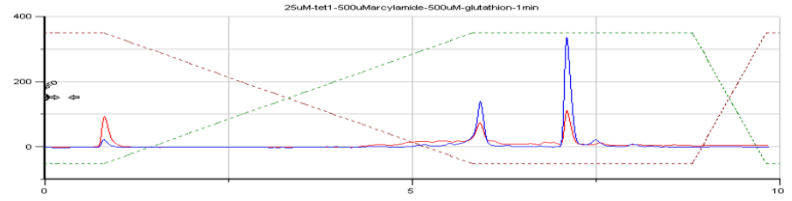

Based on the integration, the ratio of glutathione addition product over the acrylamide cycloaddition product was determined to be 0.39:0.58.

Table S1, entry 21:

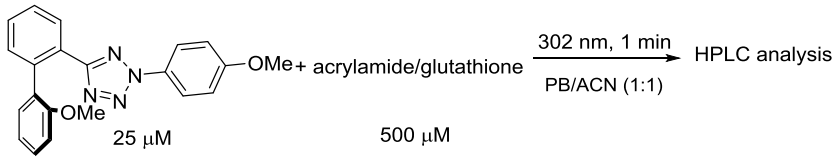

Tetrazole

PB/ACN only

500 μM acrylamide

500 μM glutathione

500 μM acrylamide + 500 μM glutathione

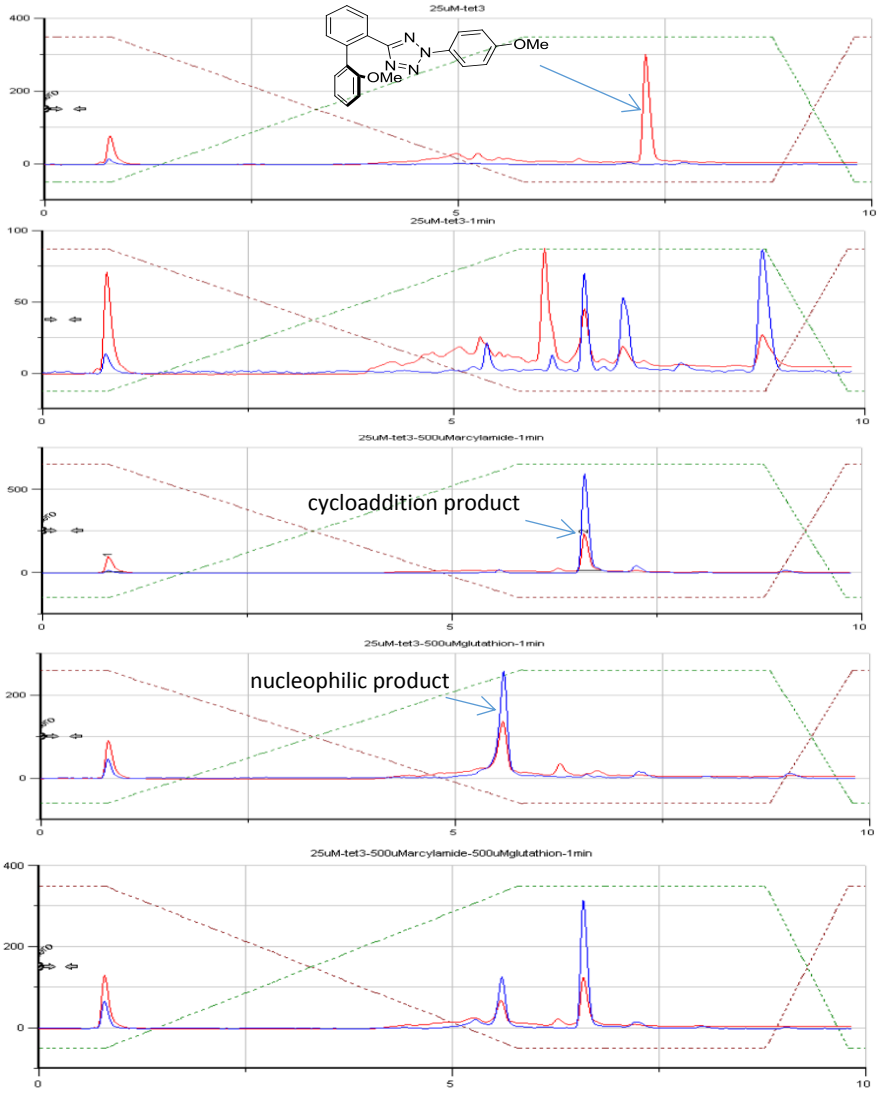

Based on the integration, the ratio of glutathione addition product over the acrylamide cycloaddition product was determined to be 0.41:0.56.

Table S1, entry 22:

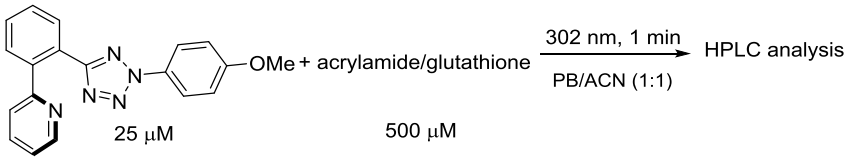

Tetrazole

PB/ACN only

500 μM acrylamide

500 μM glutathione

500 μM acrylamide + 500 μM glutathione

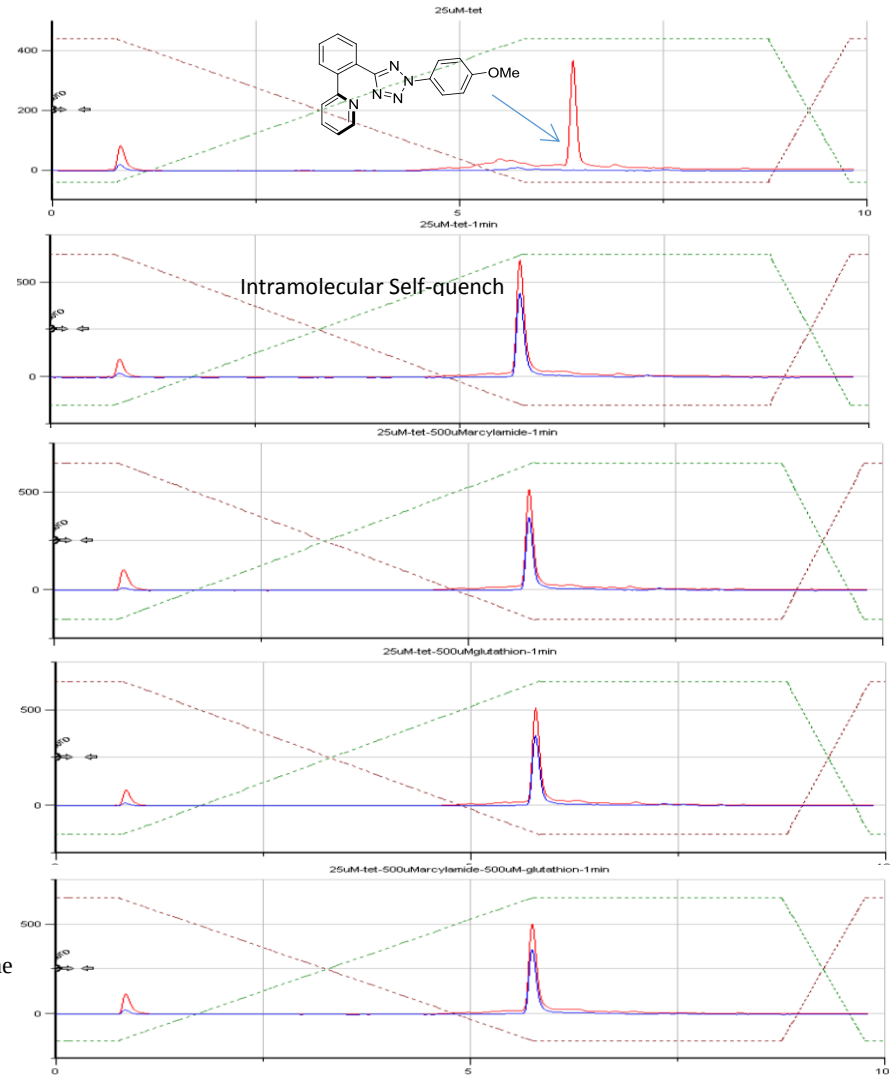

Based on HPLC chromatogram, only the intramolecular addition product was detected.

Table S1, entry 23:

Tetrazole

PB/ACN only

500 μM acrylamide

500 μM glutathione

500 μM acrylamide+500 μM glutathione

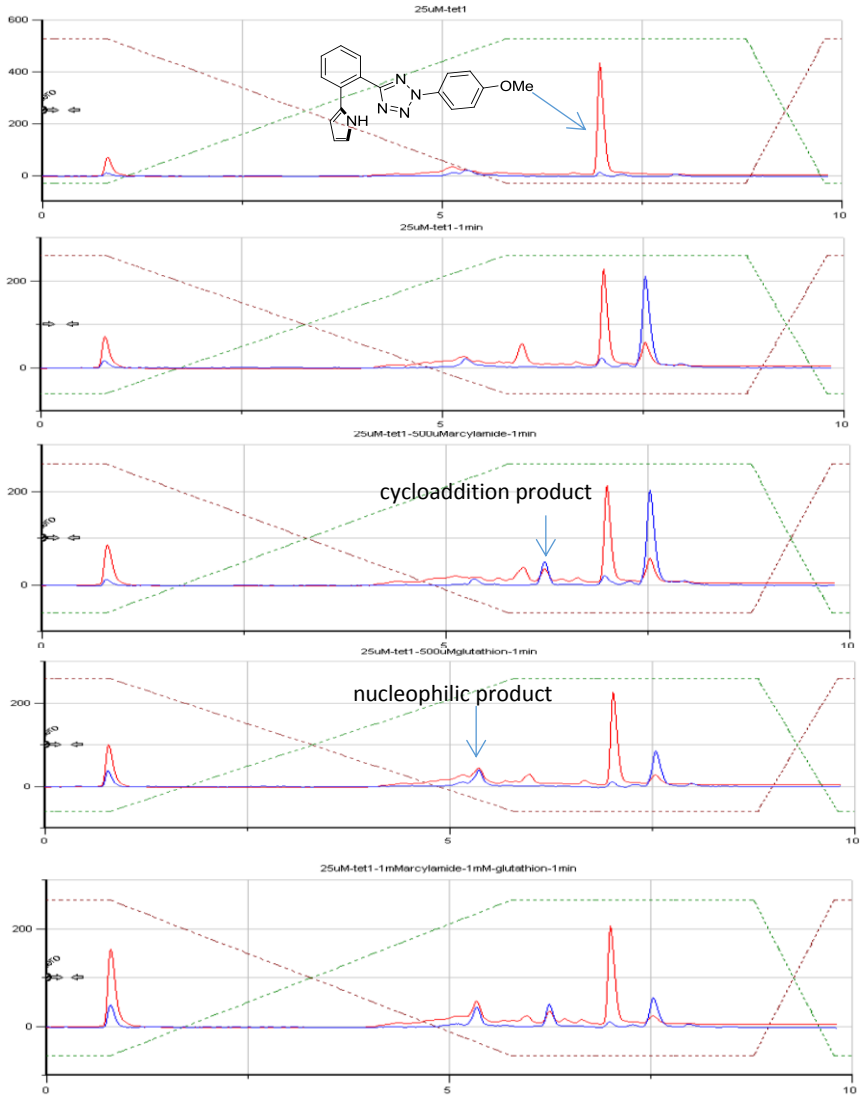

Based on HPLC chromatograms, only trace amounts of acrylamide cycloaddition and glutathione addition products were detected.

Table S1, entry 24:

Tetrazole

PB/ACN only

500 μM acrylamide

500 μM glutathione

500 μM acrylamide + 500 μM glutathione

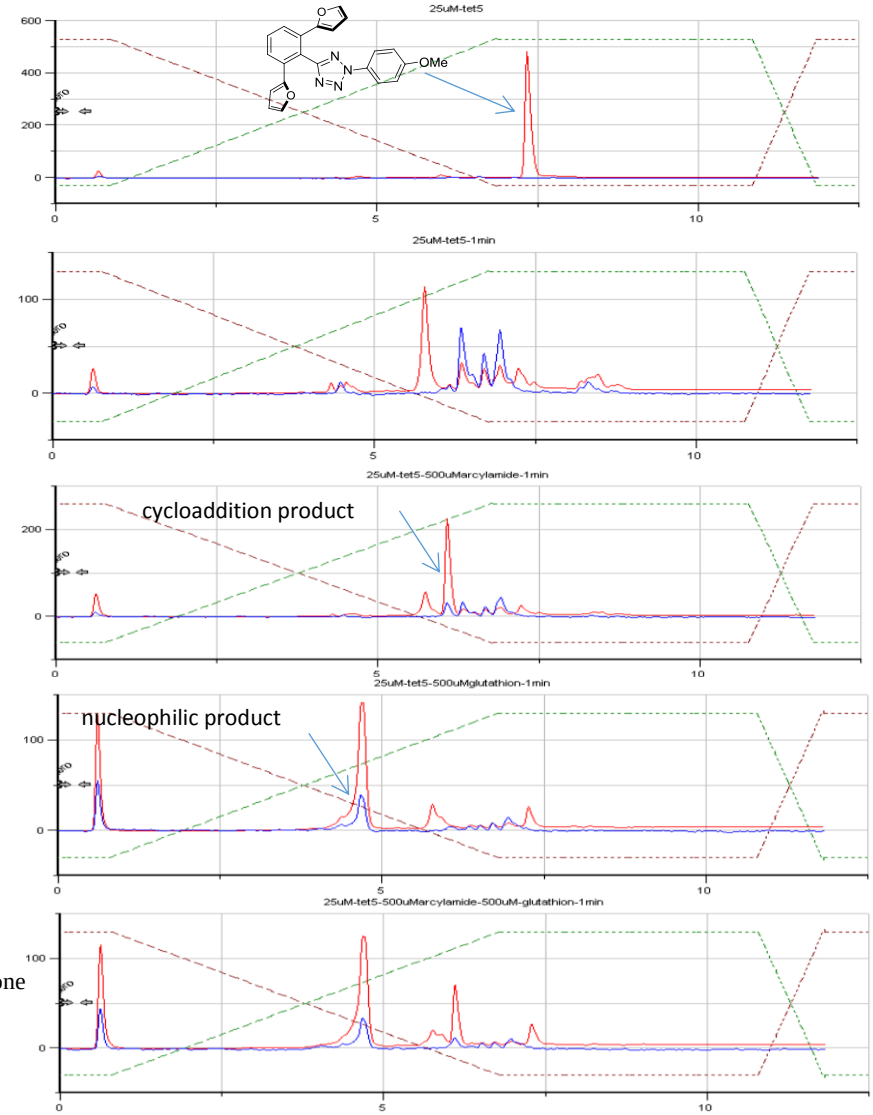

Based on the integration, the ratio of glutathione addition product over the acrylamide cycloaddition product was determined to be 0.59:0.30.

Table S1, entry 25:

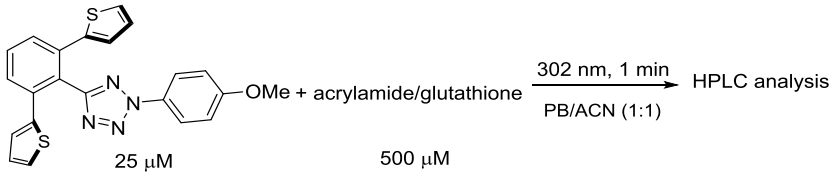

Tetrazole

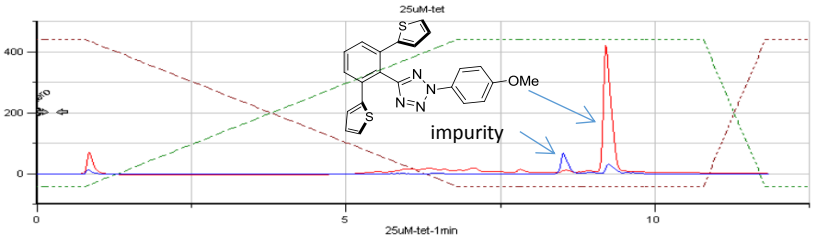

PB/ACN only

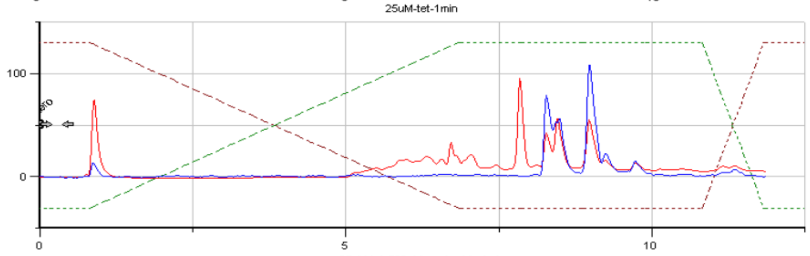

500 μM acrylamide

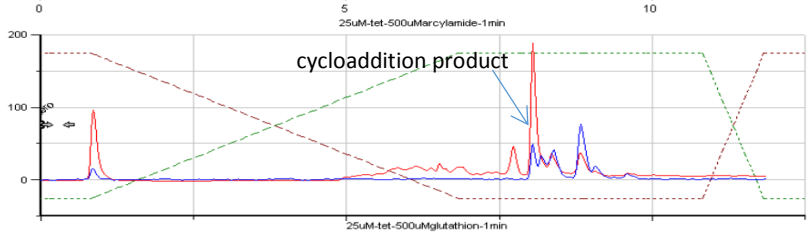

500 μM glutathione

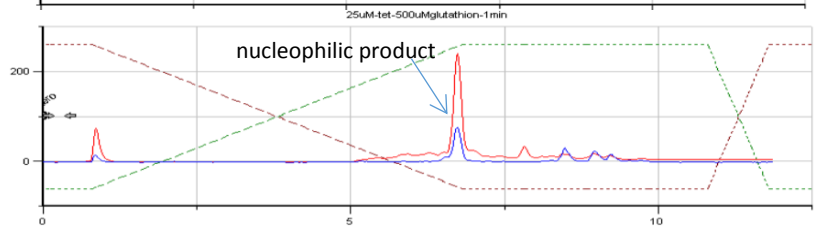

500 μM acrylamide+500μM glutathione

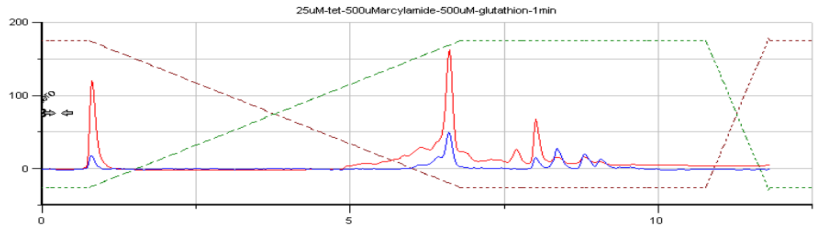

Based on the integration, the ratio of glutathione addition product over the acrylamide cycloaddition product was determined to be 0.63:0.27.

Table S1, entry 26:

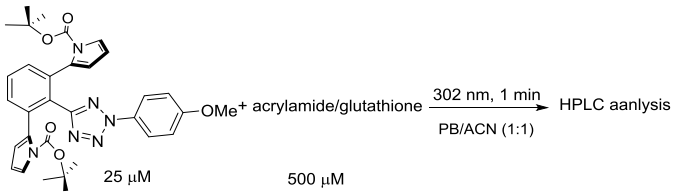

Tetrazole

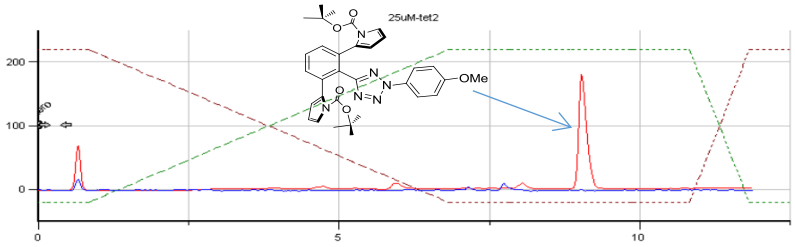

PB/ACN only

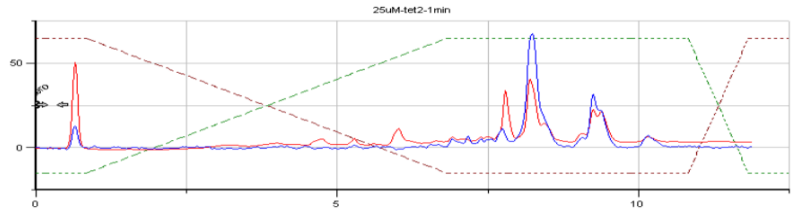

500 μM acrylamide

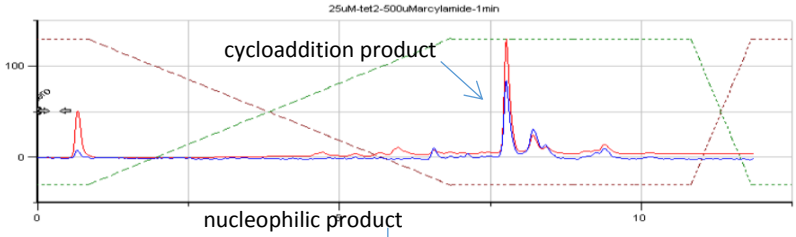

500 μM glutathione

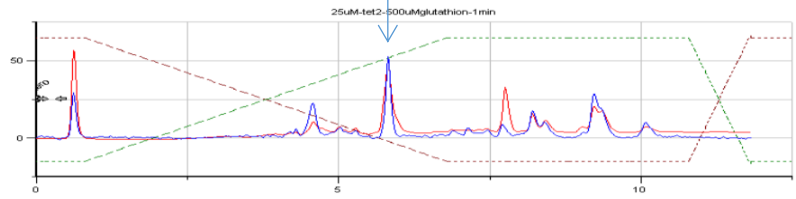

500 μM acrylamide+500 μM glutathione

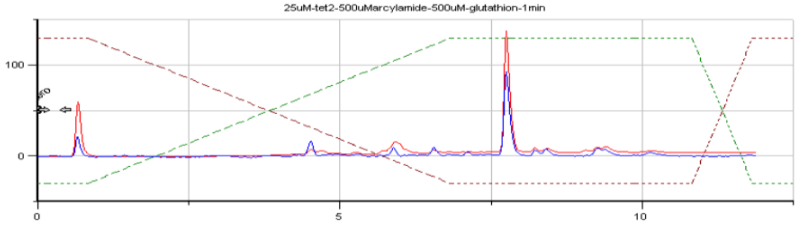

Based on HPLC chromatogram, only trace amount of glutathione addition product was detected. The major product was the acrylamide cycloaddition product (>90%).

Table S1, entry 27:

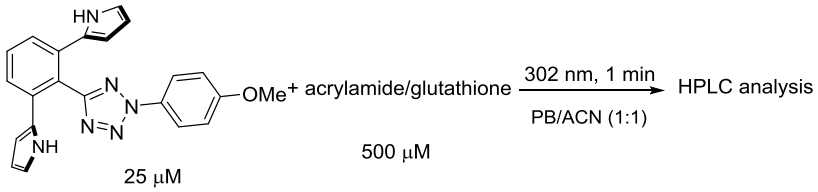

Tetrazole

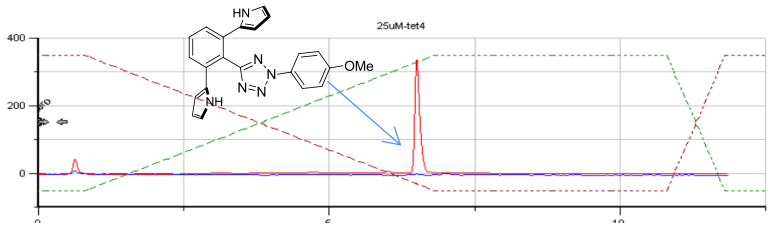

PB/ACN only

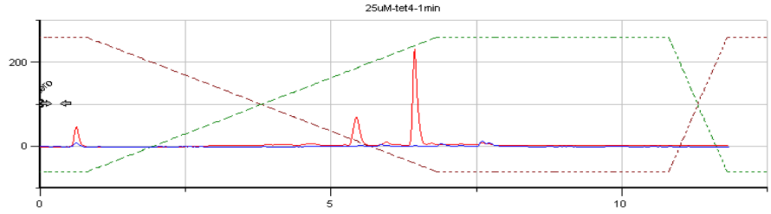

500 μM acrylamide

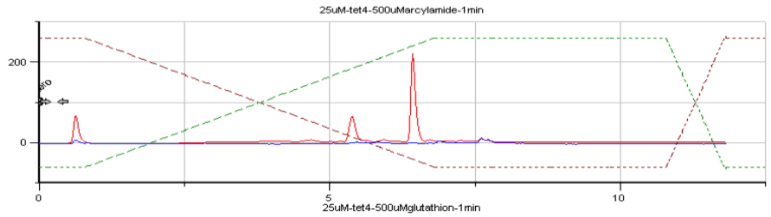

500 μM glutathione

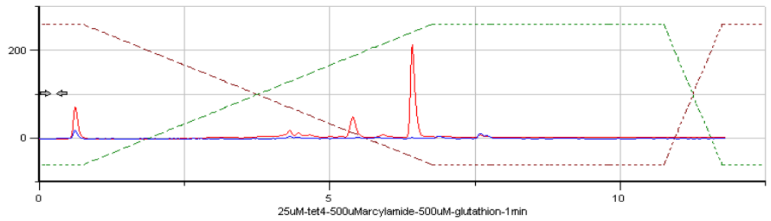

500 μM acrylamide+500 μM glutathione

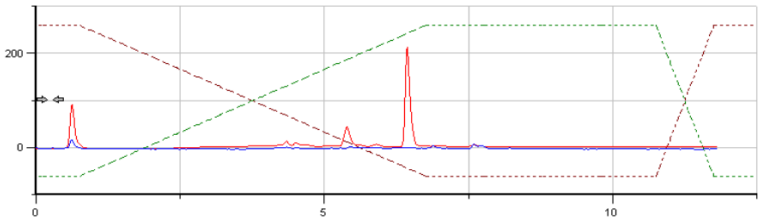

Based on HPLC chromatograms, neither acrylamide cycloaddition product nor glutathione addition product was detected.

Table S1, entry 28:

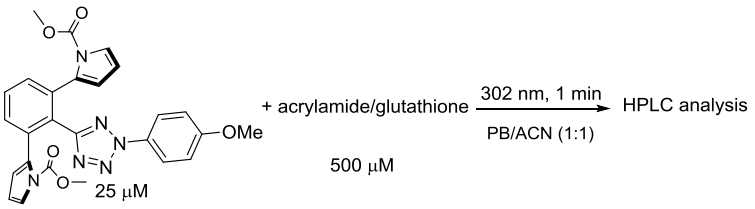

Tetrazole

PB/ACN only

500 μM acrylamide

500 μM glutathione

500 μM acrylamide+500 μM glutathione

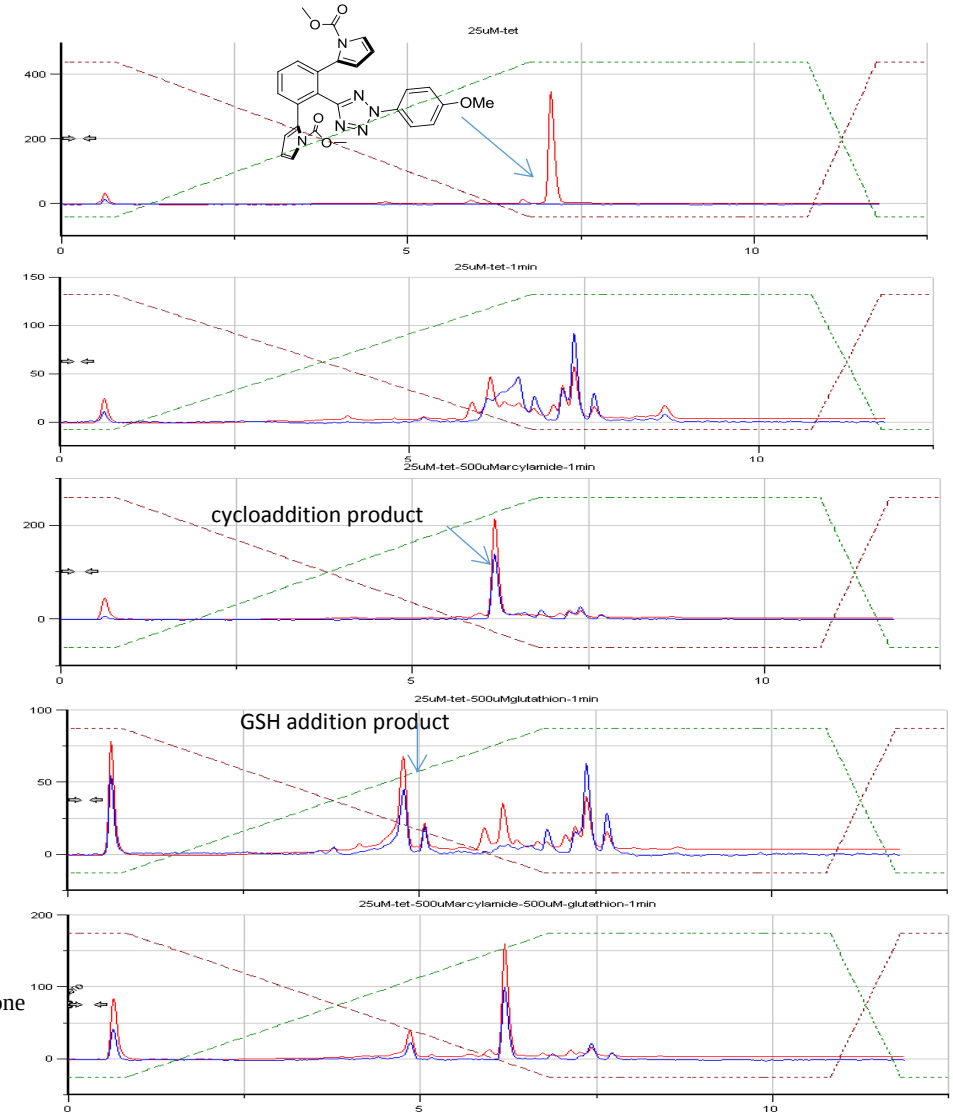

Based on the integration, the ratio of glutathione addition product over the acrylamide cycloaddition product was determined to be 0.20:0.78.

Table S1, entry 29:

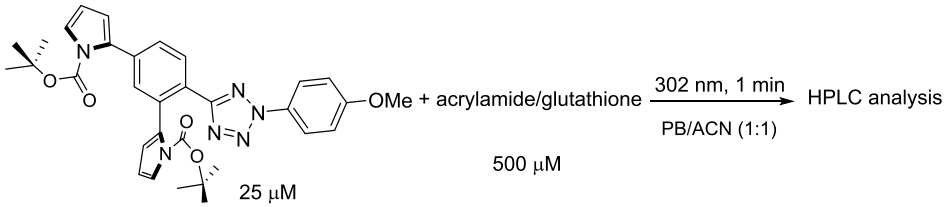

Tetrazole

PB/ACN only

500 μM acrylamide

500 μM glutathione

500 μM acrylamide + 500 μM glutathione

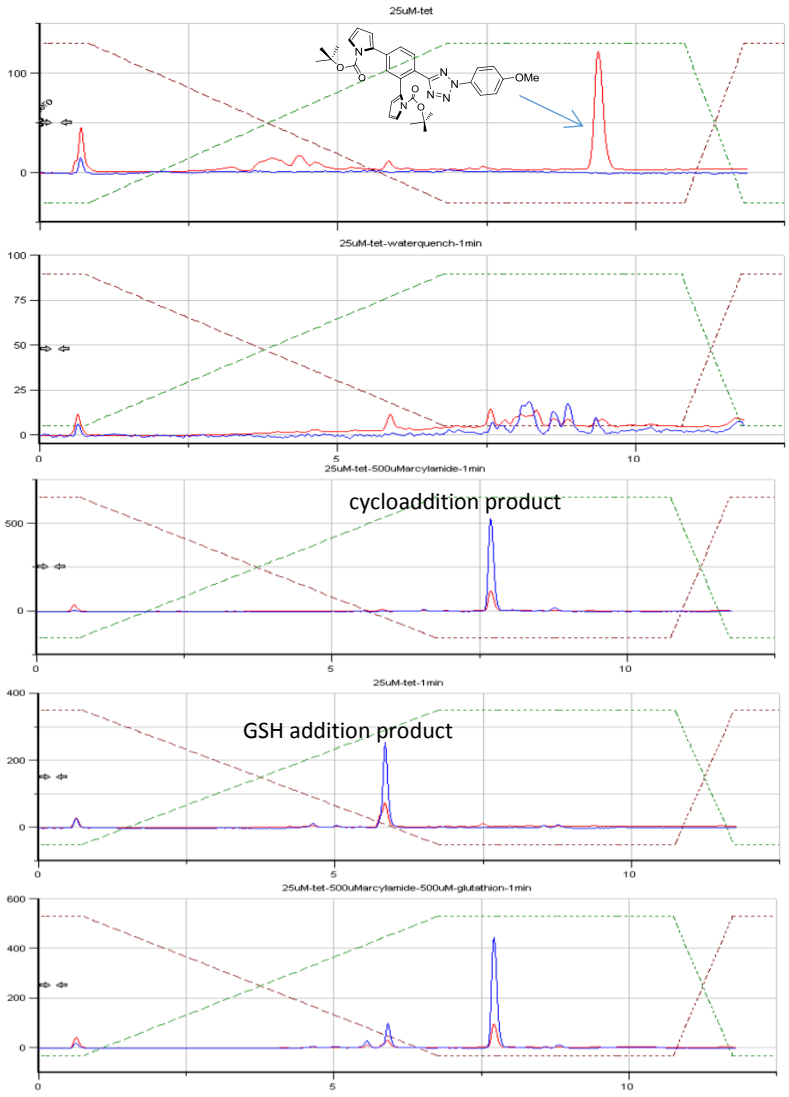

Based on the integration, the ratio of glutathione addition product over the acrylamide cycloaddition product was determined to be 0.24:0.74.

Table 1.

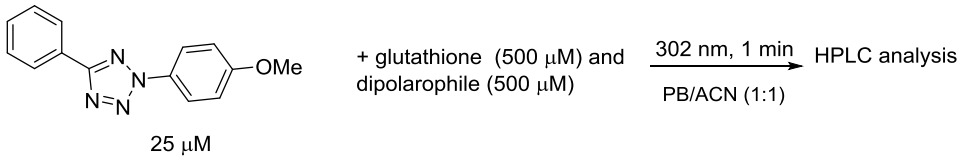

Tetrazole **1**

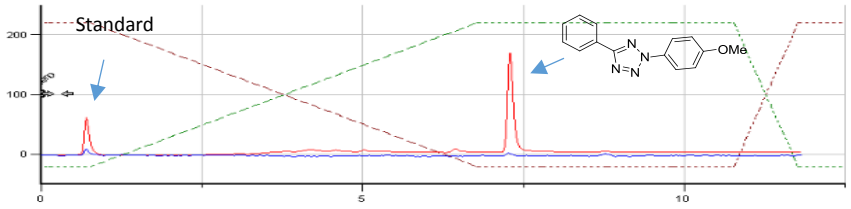

PB/ACN (1:1)

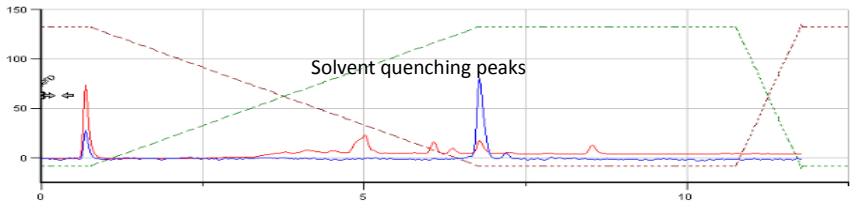

500 μM glutathione

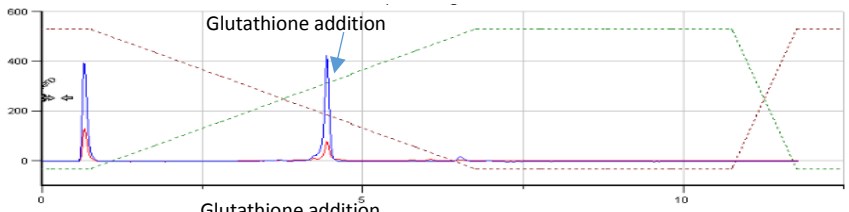

500 μM glutathione + 500 μM Sph

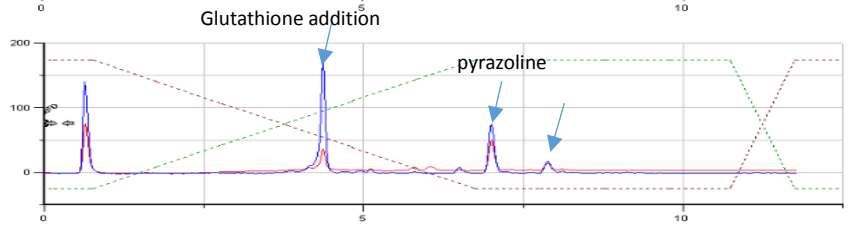

500 μM glutathione + 500 μM 3,3-Cp

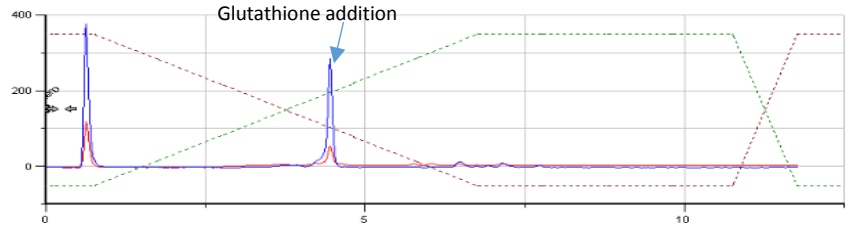

500 μM glutathione + 500 μM 1,3-Cp

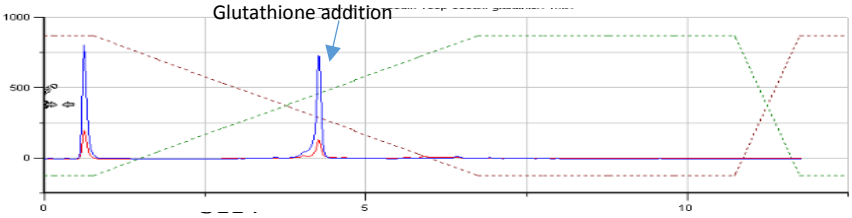

500 μM glutathione + 500 μM norbornene

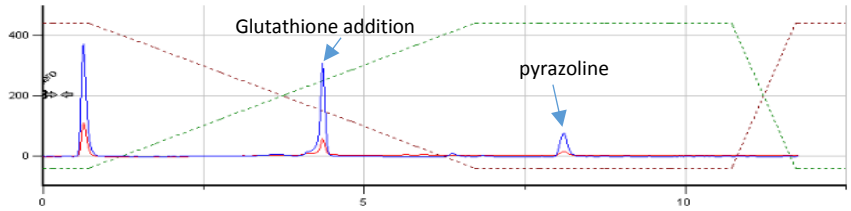

500 μM glutathione + 500 μM TCO

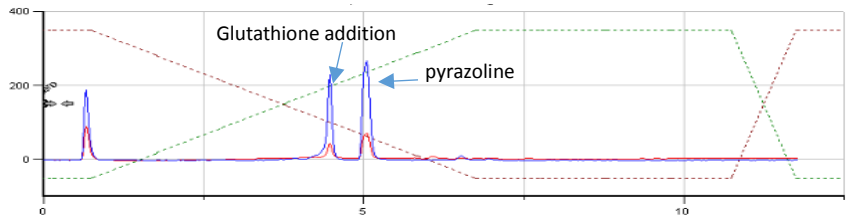

500 μM glutathione + 500 μM dimethyl fumarate

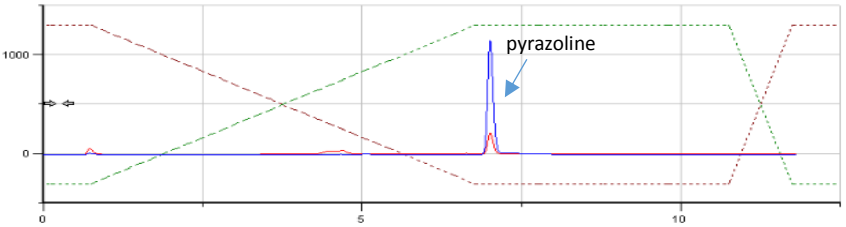

500 μM glutathione + 500 μM styrene

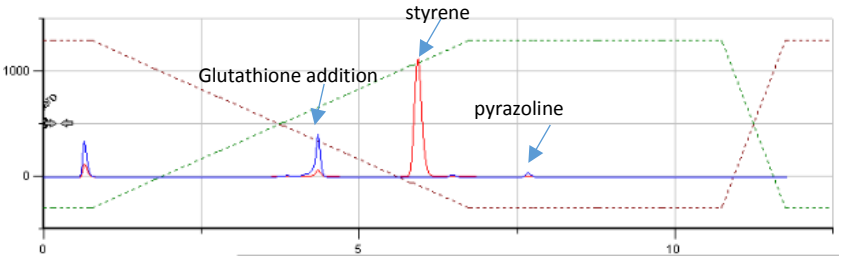

Based on the peak integrations, the glutathione addition products were dominant for most dipolarophiles except dimethyl fumarate. Sph and TCO gave the cycloaddition products at ~60% yield.

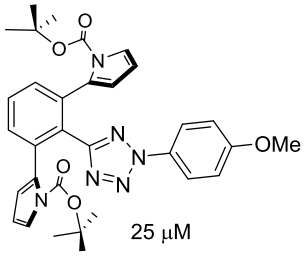

+ glutathione (500 μM) and dipolarophile (500 μM)

302 nm, 1 min

PB/ACN (1:1)

HPLC analysis

Tetrazole **26**

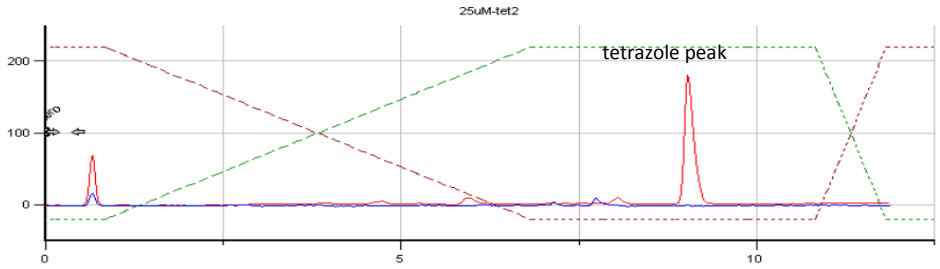

Solvent only

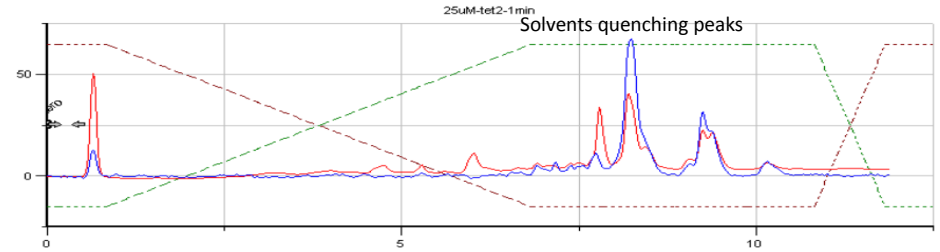

500 μM glutathione + 500 μM 1,3-Cp

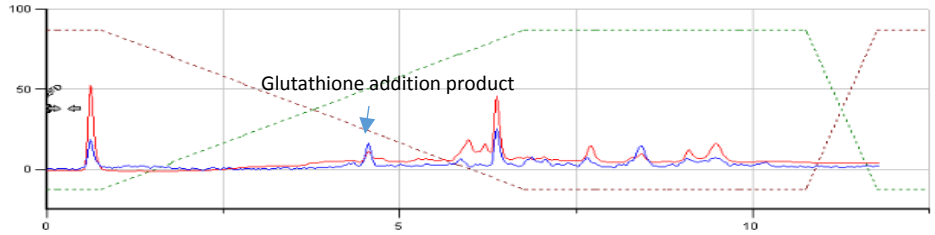

500 μM glutathione + 500 μM norbornene

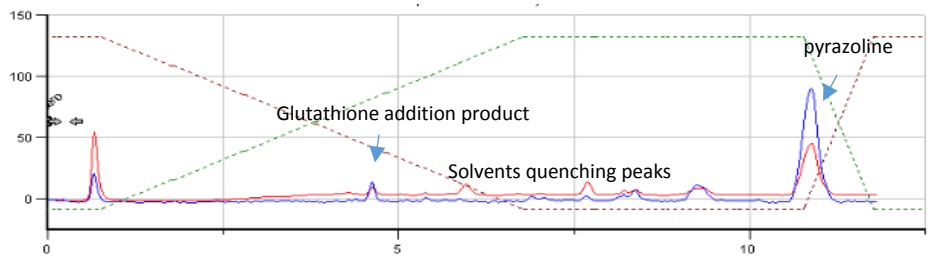

500 μM glutathione + 500 μM styrene

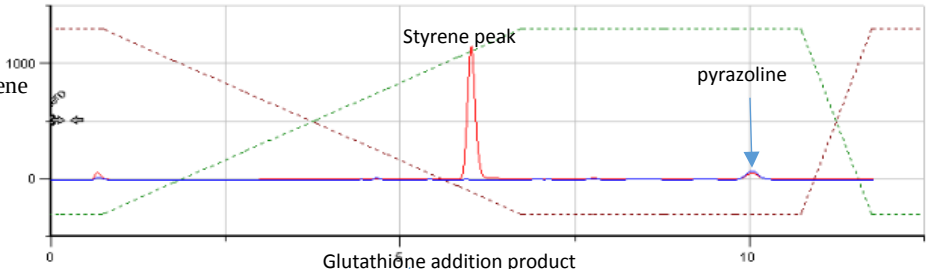

Zoomed-in trace:

500 μM glutathione + 500 μM dimethyl fumarate

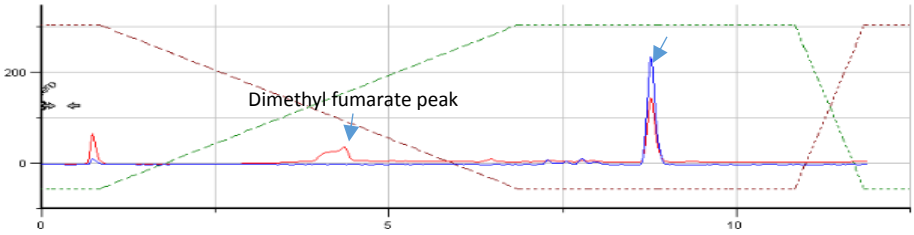

500 μM glutathione + 500 μM 3,3-Cp

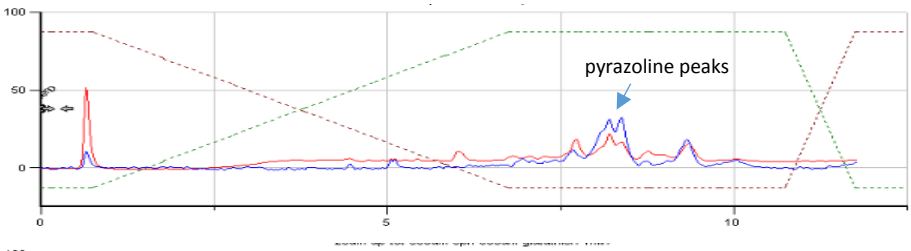

500 μM glutathione +500 μM Sph

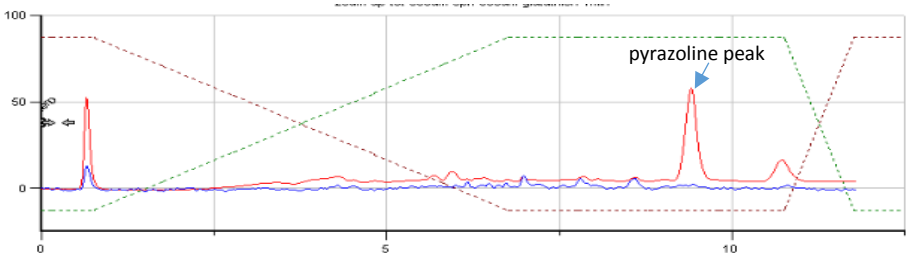

500 μM glutathione + 500 μM TCO-amine

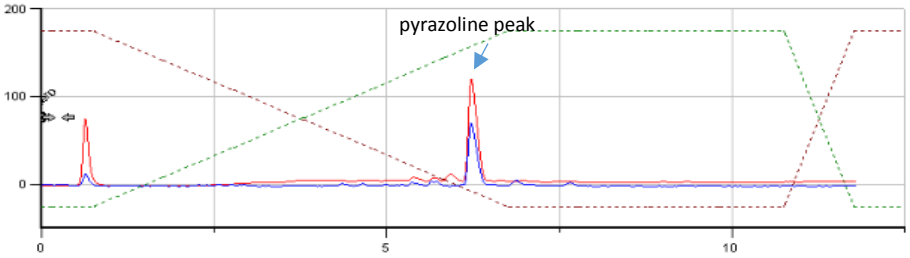

Based on HPLC chromatograms, small amounts of glutathione addition product were detected when 1,3-Cp, styrene, norbornene and 3,3-Cp were used as a dipolarophile. The glutathione addition products were not detected when Sph, dimethyl fumarate, and TCO-amine was used as a dipolarophile.

Cartesian Coordinates

spirohexene

b3lyp-d3 SCF energy in solution: -272.66162297 a.u.
b3lyp-d3 enthalpy in solution: -272.507054 a.u.
b3lyp-d3 free energy in solution: -272.546370 a.u.
wb97xd SCF energy in solution: -272.62411063 a.u.
wb97xd enthalpy in solution: -272.469542 a.u.
wb97xd free energy in solution: -272.508858 a.u.

Cartesian coordinates

ATOM	X	Y	Z
C	-0.224107	1.100113	-0.046043
C	-1.255362	0.000019	-0.447651
C	-0.224263	-1.100211	-0.046035
C	0.855448	-0.000144	0.042395
H	-0.048626	1.906180	-0.769750
H	-0.454341	1.548266	0.930898
H	-1.409921	0.000033	-1.533880
H	-0.048926	-1.906341	-0.769711
H	-0.454553	-1.548307	0.930917
C	-2.599196	0.000097	0.268673
H	-3.191796	-0.887099	0.007867
H	-2.457929	0.000097	1.358017
H	-3.191679	0.887366	0.007851
C	2.182870	0.000103	0.736288
H	2.708463	-0.000138	1.683325
C	2.222813	-0.000035	-0.567811
H	2.800091	0.000293	-1.484428

sme-anion

b3lyp-d3 SCF energy in solution: -438.22587504 a.u.
b3lyp-d3 enthalpy in solution: -438.185307 a.u.
b3lyp-d3 free energy in solution: -438.211902 a.u.
wb97xd SCF energy in solution: -438.22526151 a.u.
wb97xd enthalpy in solution: -438.184693 a.u.
wb97xd free energy in solution: -438.211288 a.u.

Cartesian coordinates

ATOM	X	Y	Z
S	0.000000	0.000000	0.717176
C	0.000000	0.000000	-1.140203
H	0.000000	1.021442	-1.544532
H	0.884595	-0.510721	-1.544532
H	-0.884595	-0.510721	-1.544532

nitrile imine-1

b3lyp-d3 SCF energy in solution: -834.96607471 a.u.
b3lyp-d3 enthalpy in solution: -834.708431 a.u.
b3lyp-d3 free energy in solution: -834.768640 a.u.
wb97xd SCF energy in solution: -834.78917537 a.u.
wb97xd enthalpy in solution: -834.531532 a.u.
wb97xd free energy in solution: -834.591741 a.u.

Cartesian coordinates

ATOM	X	Y	Z
C	5.662651	-0.259102	-0.118023
C	4.374384	-0.791337	-0.194202
C	3.254792	0.036523	-0.002000
C	3.446748	1.403428	0.265149
C	4.737033	1.929688	0.340438
C	5.849125	1.101620	0.149367
H	6.520658	-0.908715	-0.268448
H	4.237185	-1.847489	-0.402892
H	2.589712	2.052345	0.415995
H	4.873815	2.987438	0.548633
H	6.853022	1.513496	0.209051
N	0.780552	0.190503	0.054305
N	-0.165541	-0.736502	-0.085568
N	0.319601	-1.958179	-0.294944
N	1.627685	-1.841651	-0.287249
C	1.902228	-0.524184	-0.079177
C	-1.563731	-0.456884	-0.019493
C	-2.439363	-1.436092	0.465909
C	-2.038420	0.785000	-0.439484
C	-3.799414	-1.162418	0.521732
H	-2.060023	-2.393430	0.806109
C	-3.404916	1.063829	-0.374189
H	-1.352562	1.531981	-0.824270
C	-4.289756	0.087509	0.106669
H	-4.495347	-1.904447	0.900817
H	-3.759051	2.031805	-0.706980
O	-5.643248	0.258362	0.212711
C	-6.207306	1.522772	-0.172345
H	-7.278172	1.434095	0.015810
H	-5.790895	2.335797	0.432962
H	-6.032771	1.718929	-1.236389

nitrile imine-26

b3lyp-d3 SCF energy in solution: -1944.67711127 a.u.
b3lyp-d3 enthalpy in solution: -1944.015954 a.u.
b3lyp-d3 free energy in solution: -1944.129252 a.u.
wb97xd SCF energy in solution: -1944.27325314 a.u.
wb97xd enthalpy in solution: -1943.612096 a.u.
wb97xd free energy in solution: -1943.725394 a.u.

Cartesian coordinates

ATOM	X	Y	Z
C	1.721800	0.425994	0.543684
C	3.027702	0.003082	0.201507
C	1.530970	1.239373	1.688014
C	3.343883	-0.800956	-0.998925
C	4.115859	0.412168	0.986740
C	0.205962	1.671499	2.186960
C	2.639341	1.609456	2.463516
N	2.911668	-2.111655	-1.290106
C	4.106691	-0.385557	-2.063884
H	5.112621	0.082165	0.710281
C	3.926898	1.207627	2.114378
N	-0.733655	2.489127	1.527070
C	-0.358113	1.305516	3.386086
H	2.479181	2.233609	3.337351
C	2.163418	-3.020223	-0.518505
C	3.391909	-2.469882	-2.552634
H	4.561488	0.593590	-2.142983
C	4.129270	-1.429251	-3.045255
H	4.777357	1.510265	2.718848
C	-0.651584	3.150339	0.288722
C	-1.880261	2.586132	2.318443
C	-1.670977	1.874862	3.467287
H	0.114883	0.653196	4.108913
O	1.889313	-2.534612	0.677164
O	1.847553	-4.117701	-0.960856
H	3.177869	-3.447508	-2.955683
H	4.636213	-1.409387	-4.001360
O	0.562675	3.071780	-0.220562
O	-1.621231	3.723702	-0.191209
H	-2.716848	3.182157	1.988161
H	-2.374899	1.767925	4.282531
C	1.096772	-3.295531	1.698196
C	0.949889	3.729377	-1.510934
C	0.953088	-2.264972	2.815114
C	1.919160	-4.499300	2.146982
C	-0.268940	-3.678866	1.131705
C	2.371807	3.210460	-1.709570

C	0.924021	5.239670	-1.300079
C	0.037391	3.267344	-2.645140
H	1.935142	-1.919565	3.154902
H	0.430543	-2.721713	3.661860
H	0.375688	-1.402406	2.473237
H	2.053525	-5.220686	1.337115
H	1.396766	-4.998877	2.970379
H	2.902838	-4.178485	2.506963
H	-0.759988	-2.807222	0.689216
H	-0.198489	-4.468527	0.381314
H	3.002449	3.465319	-0.851265
H	2.801334	3.667918	-2.606734
H	2.372236	2.124219	-1.836515
H	-0.090082	5.599475	-1.106438
H	1.297757	5.731090	-2.205165
H	1.569315	5.521689	-0.461045
H	-0.051991	2.177630	-2.643093
H	0.489622	3.572484	-3.595284
H	-0.959109	3.707781	-2.579851
H	-0.893788	-4.040172	1.955943
C	0.570865	0.023996	-0.281396
N	-0.661452	-0.165405	0.200238
N	-1.356190	-0.476891	-0.888918
N	0.604792	-0.187799	-1.628740
N	-0.616120	-0.497348	-1.997569
C	-2.758070	-0.735409	-0.868602
C	-3.562652	-0.033576	0.028225
C	-3.303384	-1.679922	-1.745315
C	-4.936725	-0.275521	0.059614
H	-3.124095	0.704679	0.691767
C	-4.672481	-1.913195	-1.721063
H	-2.663585	-2.230503	-2.426804
C	-5.494653	-1.215650	-0.819451
H	-5.552188	0.278025	0.758292
H	-5.119520	-2.643644	-2.388298
O	-6.827449	-1.521779	-0.873249
C	-7.724770	-0.827092	0.007888
H	-8.716702	-1.222101	-0.215856
H	-7.476425	-1.027137	1.056427
H	-7.703816	0.251450	-0.185108

ts1

b3lyp-d3 SCF energy in solution: -998.06351660 a.u.
b3lyp-d3 enthalpy in solution: -997.663709 a.u.
b3lyp-d3 free energy in solution: -997.739871 a.u.

wb97xd SCF energy in solution: -997.89369749 a.u.
wb97xd enthalpy in solution: -997.493890 a.u.
wb97xd free energy in solution: -997.570052 a.u.
Imaginary frequency: -353.7511 cm-1

Cartesian coordinates

ATOM	X	Y	Z
O	5.044498	-1.476987	-1.103621
C	1.431687	-1.006955	0.967700
C	1.475891	-1.493210	-0.354088
H	0.555389	-1.757412	-0.866645
C	2.693049	-1.638153	-1.010033
H	2.728382	-2.014860	-2.028638
C	2.636739	-0.689329	1.609696
H	2.612729	-0.315351	2.629716
C	3.893097	-1.299508	-0.365826
C	3.862266	-0.823469	0.951929
H	4.773586	-0.557346	1.474932
C	6.298633	-1.175145	-0.477660
H	6.352951	-0.117226	-0.194717
H	7.062198	-1.393330	-1.226185
H	6.458083	-1.805645	0.405152
C	-1.906373	-0.509304	0.714490
N	-0.847060	-0.974051	1.065296
N	0.242509	-0.800847	1.700083
C	0.089124	1.750374	-0.716856
C	-0.065073	3.199508	-1.266763
C	-0.234593	3.721832	0.192035
C	-0.421793	2.258901	0.652790
H	-0.495525	0.964640	-1.207447
H	1.139181	1.432945	-0.681393
H	-1.009998	3.299677	-1.815868
H	-1.068056	4.409009	0.386819
H	0.690208	4.171374	0.581156
C	1.080531	3.765519	-2.094710
H	0.925268	4.829673	-2.318080
H	2.032006	3.671185	-1.554077
H	1.183087	3.233117	-3.049901
C	-0.321949	1.688792	2.024596
H	0.272209	1.669808	2.926990
C	-1.541241	1.716996	1.494566
H	-2.590491	1.864839	1.715228
C	-3.163619	-0.920377	0.142512
C	-4.362931	-0.281670	0.508116
C	-3.184319	-1.941547	-0.832598
C	-5.567539	-0.676911	-0.076345
C	-4.391787	-2.315886	-1.419115

H	-6.491286	-0.187285	0.219671
C	-5.586871	-1.689177	-1.041938
H	-4.400896	-3.102046	-2.169432
H	-6.525703	-1.987234	-1.500602
H	-2.255745	-2.425719	-1.120846
H	-4.349278	0.509673	1.250497

ts2

b3lyp-d3 SCF energy in solution: -2107.78624098 a.u.
b3lyp-d3 enthalpy in solution: -2106.982750 a.u.
b3lyp-d3 free energy in solution: -2107.108579 a.u.
wb97xd SCF energy in solution: -2107.48401284 a.u.
wb97xd enthalpy in solution: -2106.680522 a.u.
wb97xd free energy in solution: -2106.806351 a.u.
Imaginary frequency: -309.9561 cm-1

Cartesian coordinates

ATOM	X	Y	Z
O	6.059802	-2.474338	-0.701904
C	1.993409	-2.182673	0.242947
C	2.622288	-1.275703	-0.629841
H	2.052652	-0.465777	-1.067349
C	3.972379	-1.403717	-0.925550
H	4.453667	-0.706693	-1.606207
C	2.752267	-3.216235	0.807570
H	2.274400	-3.920202	1.483570
C	4.729655	-2.434918	-0.347350
C	4.115307	-3.343760	0.525666
H	4.677261	-4.149230	0.984265
C	6.868434	-3.535014	-0.175811
H	6.917716	-3.487459	0.918465
H	7.864707	-3.381185	-0.593949
H	6.484375	-4.512957	-0.489542
C	-0.777886	-0.232965	0.240764
N	-0.059110	-1.193207	0.061601
N	0.633028	-2.103523	0.615266
C	2.077514	0.814963	1.987887
C	2.345785	1.825608	3.142220
C	1.606981	0.872485	4.127432
C	1.039660	0.122168	2.902331
H	1.716608	1.214212	1.034790
H	2.955158	0.185443	1.794887
H	1.752862	2.735776	2.993377
H	0.877563	1.321020	4.814231
H	2.307244	0.255134	4.708272

C	3.792194	2.192194	3.441707
H	3.871608	2.803227	4.350951
H	4.398429	1.288278	3.589620
H	4.236665	2.762023	2.614564
C	0.365772	-1.204830	2.846488
H	0.402106	-2.209719	3.242476
C	-0.409568	-0.139932	2.631932
H	-1.377140	0.285822	2.846703
C	-1.687275	0.592536	-0.520291
C	-2.928890	0.995217	0.036052
C	-1.297011	1.083374	-1.792585
C	-3.417247	0.482892	1.324856
C	-3.709700	1.939791	-0.641849
C	-0.076436	0.613196	-2.487486
C	-2.107478	2.021798	-2.442391
N	-3.457869	-0.874011	1.701203
C	-3.803828	1.213665	2.427596
H	-4.658431	2.241440	-0.207798
C	-3.294719	2.469606	-1.863124
N	1.101002	1.375527	-2.627280
C	0.078997	-0.504576	-3.271211
H	-1.796469	2.398956	-3.412470
C	-3.336409	-2.034271	0.901390
C	-3.844023	-0.961166	3.037884
H	-3.824335	2.295232	2.466630
C	-4.072550	0.307737	3.501980
H	-3.908910	3.204747	-2.375128
C	1.462715	2.563006	-1.963925
C	1.973585	0.711841	-3.490353
C	1.368288	-0.446106	-3.896622
H	-0.670447	-1.274597	-3.397753
O	-3.543650	-1.753677	-0.370608
O	-3.106485	-3.126216	1.399309
H	-3.957466	-1.926468	3.507610
H	-4.388123	0.566350	4.504366
O	0.689123	2.770920	-0.917546
O	2.394797	3.253686	-2.354223
H	2.952286	1.120646	-3.690873
H	1.799650	-1.186495	-4.557847
C	-3.492685	-2.783954	-1.461400
C	0.649900	4.069407	-0.172559
C	-3.744468	-1.928942	-2.700229
C	-4.617836	-3.788922	-1.234858
C	-2.113591	-3.433129	-1.509293
C	-0.379136	3.769818	0.915164
C	0.155348	5.151632	-1.127043
C	2.022881	4.379850	0.419214

H	-4.731876	-1.457524	-2.651052
H	-3.703256	-2.560901	-3.593287
H	-2.985326	-1.145471	-2.788822
H	-4.435336	-4.408292	-0.353475
H	-4.684355	-4.443867	-2.110547
H	-5.575974	-3.271329	-1.117142
H	-1.333123	-2.677760	-1.626779
H	-1.908944	-4.023924	-0.614214
H	-1.347940	3.518614	0.471325
H	-0.502029	4.653888	1.549050
H	-0.054181	2.932768	1.540599
H	0.862086	5.318805	-1.944728
H	0.045532	6.089515	-0.571643
H	-0.819011	4.877402	-1.545283
H	2.437560	3.498713	0.914851
H	1.910980	5.173080	1.166562
H	2.726621	4.720388	-0.342943
H	-2.078853	-4.099964	-2.377918

ts3

b3lyp-d3 SCF energy in solution: -1163.63005119 a.u.
b3lyp-d3 enthalpy in solution: -1163.344957 a.u.
b3lyp-d3 free energy in solution: -1163.415201 a.u.
wb97xd SCF energy in solution: -1163.49894422 a.u.
wb97xd enthalpy in solution: -1163.213850 a.u.
wb97xd free energy in solution: -1163.284094 a.u.
Imaginary frequency: -50.0117 cm-1

Cartesian coordinates

ATOM	X	Y	Z
O	5.743244	-1.037619	-0.283678
C	1.942065	0.692025	0.217317
C	-2.425819	-0.777862	-0.105612
C	-2.213059	-1.905667	0.717589
C	-3.615001	-0.671118	-0.848955
C	2.111466	-0.660767	-0.147835
H	1.243191	-1.293866	-0.310257
C	3.386285	-1.199425	-0.303818
H	3.510749	-2.241287	-0.587503
C	3.091649	1.470902	0.426319
H	2.980262	2.514457	0.709685
C	4.524864	-0.407930	-0.099924
C	-4.577888	-1.676132	-0.769020
H	-5.496392	-1.585251	-1.342454
C	4.373363	0.934826	0.269977

H	5.234318	1.572524	0.436764
C	-3.180421	-2.908211	0.783347
H	-3.012371	-3.774996	1.416910
C	-4.364304	-2.796529	0.043545
H	-5.117015	-3.578275	0.101338
C	6.929174	-0.239714	-0.189913
H	6.913820	0.573990	-0.925438
H	7.758838	-0.914915	-0.407598
H	7.049817	0.173987	0.818729
C	-1.391161	0.211304	-0.215938
N	-0.317435	0.598080	0.101887
N	0.692774	1.325913	0.389303
H	-1.293448	-1.986192	1.289889
H	-3.770929	0.210393	-1.461289
S	-3.098776	2.852177	-0.298509
C	-4.617217	2.174977	0.518745
H	-5.107579	2.934465	1.141723
H	-5.354902	1.826267	-0.215458
H	-4.375257	1.322781	1.167246

ts3′

b3lyp-d3 SCF energy in solution: -1163.62995247 a.u.
b3lyp-d3 enthalpy in solution: -1163.344867 a.u.
b3lyp-d3 free energy in solution: -1163.414341 a.u.
wb97xd SCF energy in solution: -1163.49781786 a.u.
wb97xd enthalpy in solution: -1163.212732 a.u.
wb97xd free energy in solution: -1163.282206 a.u.
Imaginary frequency: -97.6315 cm-1

Cartesian coordinates

ATOM	X	Y	Z
O	-5.415362	-1.171807	0.628080
C	-1.704067	0.489711	-0.443961
C	2.683200	-0.762734	-0.042681
C	2.309863	-2.085324	-0.374176
C	4.014430	-0.487569	0.315624
C	-1.806403	-0.675084	0.346978
H	-0.907315	-1.176354	0.695497
C	-3.053203	-1.196570	0.683018
H	-3.127018	-2.094389	1.291211
C	-2.890410	1.102525	-0.879587
H	-2.829616	2.001469	-1.487842
C	-4.229065	-0.574507	0.240514
C	4.959369	-1.514319	0.329433
H	5.988010	-1.291325	0.600498

C	-4.143970	0.582192	-0.545363
H	-5.034951	1.086934	-0.901344
C	3.260964	-3.104542	-0.345364
H	2.966481	-4.118946	-0.601493
C	4.588631	-2.823918	0.002237
H	5.327386	-3.620850	0.017352
C	-6.639451	-0.599702	0.152552
H	-6.765911	0.425925	0.520371
H	-7.435811	-1.230149	0.552349
H	-6.679590	-0.608243	-0.943642
C	1.667168	0.260863	-0.039938
N	0.560099	0.504996	-0.401332
N	-0.489132	1.094127	-0.828019
H	1.280640	-2.298945	-0.648160
H	4.282254	0.533958	0.565453
S	3.054121	2.923245	-0.031331
C	1.530739	3.527601	0.829158
H	1.019470	2.705253	1.344679
H	1.773685	4.289885	1.580870
H	0.815702	3.972721	0.125658

ts4

b3lyp-d3 SCF energy in solution: -2273.34900771 a.u.
b3lyp-d3 enthalpy in solution: -2272.660544 a.u.
b3lyp-d3 free energy in solution: -2272.779766 a.u.
wb97xd SCF energy in solution: -2273.08420149 a.u.
wb97xd enthalpy in solution: -2272.395738 a.u.
wb97xd free energy in solution: -2272.514960 a.u.
Imaginary frequency: -127.9307 cm-1

Cartesian coordinates

ATOM	X	Y	Z
O	-6.443980	-2.433525	-0.080547
C	-2.971459	-0.399108	1.152670
C	-3.008604	-1.190246	-0.015361
H	-2.120069	-1.289793	-0.628483
C	-4.175254	-1.847063	-0.394720
H	-4.192083	-2.454487	-1.296376
C	-4.143008	-0.305045	1.923857
H	-4.134729	0.295400	2.830195
C	-5.337566	-1.740799	0.381807
C	-5.316876	-0.965484	1.548932
H	-6.198134	-0.864633	2.172624
C	-7.629912	-2.412474	0.722120
H	-7.439254	-2.831337	1.717844

H	-8.355572	-3.035610	0.196048
H	-8.025600	-1.394017	0.818842
C	0.314636	0.305565	0.495564
N	-0.825003	0.270970	0.827508
N	-1.835002	0.279169	1.620108
C	1.324927	0.653121	-0.458263
C	2.091883	1.838271	-0.308710
C	1.539094	-0.192315	-1.573814
C	1.847190	2.795203	0.781505
C	3.105442	2.109051	-1.235105
C	0.671756	-1.366167	-1.820650
C	2.532386	0.135455	-2.502567
N	0.593933	3.372994	1.074823
C	2.722744	3.227716	1.748615
H	3.691650	3.015756	-1.115992
C	3.332387	1.264101	-2.323285
N	0.771827	-2.615540	-1.173886
C	-0.401144	-1.442207	-2.675010
H	2.684366	-0.516384	-3.357850
C	-0.568179	3.437831	0.277939
C	0.713509	4.141877	2.234453
H	3.754023	2.908575	1.826684
C	2.012315	4.072756	2.661075
H	4.116091	1.496809	-3.038467
C	1.807247	-3.118319	-0.359718
C	-0.254722	-3.443442	-1.635575
C	-0.982665	-2.748807	-2.561108
H	-0.752776	-0.624043	-3.290145
O	-0.298703	3.141417	-0.980559
O	-1.647960	3.767249	0.748914
H	-0.135612	4.694752	2.606884
H	2.416827	4.565839	3.535671
O	2.817984	-2.273497	-0.291543
O	1.724419	-4.221662	0.164121
H	-0.344045	-4.453783	-1.267355
H	-1.850003	-3.119441	-3.091904
C	-1.346973	3.044307	-2.047456
C	4.150727	-2.641900	0.292903
C	-0.506838	2.679096	-3.268495
C	-2.020434	4.402836	-2.222357
C	-2.326584	1.928635	-1.698771
C	4.960532	-1.374005	0.034939
C	4.715417	-3.827305	-0.485288
C	4.007492	-2.912363	1.786333
H	0.208906	3.475667	-3.498715
H	-1.164456	2.539480	-4.132575
H	0.045741	1.750841	-3.093765

H	-2.675765	4.645384	-1.383164
H	-2.623918	4.378614	-3.136510
H	-1.268227	5.192189	-2.328844
H	-1.799389	0.980339	-1.574360
H	-2.888498	2.146184	-0.787691
H	5.039428	-1.173871	-1.038493
H	5.968582	-1.499359	0.443544
H	4.491414	-0.511497	0.519037
H	4.159081	-4.746935	-0.288866
H	5.755513	-3.983358	-0.178664
H	4.700559	-3.622033	-1.561350
H	3.550188	-2.050131	2.282840
H	5.007478	-3.070888	2.206345
H	3.405969	-3.803033	1.979425
S	1.709603	-0.023087	3.005915
C	0.876829	-1.673119	3.076620
H	1.523077	-2.438050	3.526415
H	-0.049427	-1.635984	3.664780
H	0.611085	-2.023917	2.071064
H	-3.038181	1.819204	-2.524737